FOSSIL FUEL ECONOMICS

Christian W. Knudsen
Paul O. Hedman

Office of Engineering, Economics and Standards
Fossil Energy
U.S. Department of Energy
Washington, D.C. 20545

College of Engineering Sciences and Technology
Brigham Young University
Provo, Utah

ABSTRACT

A large number of fossil energy processes are now in various stages of research and development around the world to produce substitute fuels for conventional oil and gas. Process design and cost estimation of new processes is an invaluable part of the development process to guide R&D to the most promising processes and to place experimental emphasis on technical problems of greatest priority. Types of design and cost estimation are described as well as the uncertainties involved in the resulting estimates as they depend on data quality and the level of estimate detail. Project and process contingencies are given which have been found to be appropriate to account for the expected underestimation.

Cost evaluations are described for coal gasification processes taken from the recent C.F. Braun & Co. report which compares new process developments with commercial Lurgi coal gasification. Costs of approximately $5 per million Btu are indicated. Coal liquefaction costs for processes currently at the pilot plant stage of development are discussed. Liquid product costs are indicated between about $3.50 and $5.00 per million Btu. Power generation is examined on the basis of near-term new and retrofitted plants as well as the longer range potential of combined cycle technology.

INTRODUCTION

Preliminary design and cost estimating of fossil energy processes is the principal means of determining the practical advantages and disadvantages that a given process has compared with others which produce similar products. The results of such comparisons are of particular importance to research and development. They not only indicate those processes which offer promise of technical and economic feasibility in a future market, but also those sections of a process flow scheme which should receive the greatest attention during further development. It becomes quickly apparent that certain unit operations create the heaviest economic burdens on plant investment and product selling price. These areas then become prime targets for innovative engineering.

Successful process-related companies rely greatly on such process analysis to guide their development efforts and to point to new research projects. Inventors pay close attention as well since the royalty they will receive on a new patent will be negotiated as a portion of the savings created relative to the next best alternative.

U.S. Government research and development activities in fossil energy have grown beyond $500 million annually and decisions about program and project direction are strongly influenced by process analyses.

PROCESS DEVELOPMENT AND ANALYSIS

New heavy-industry process development is an expensive and risky enterprise usually conducted by large companies and governments, sometimes in joint venture. The 15 to 20 year development time to first commercialization which has been estimated for new coal conversion processes, for example, practically mandates government-industry cost sharing.

An example of liberal government cost sharing with industry to induce steady development of new coal conversion processes is illustrated by Figure 1. It represents a logical developmental sequence for a hypothetical case. Although no specific case would necessarily follow this example closely, perhaps the composite of a number of cases would be reasonably close.

The example indicates that after conceptual work, exploratory research follows to test scientific feasibility in a unit capable of about one ton of daily coal throughput. Over a period of one to four years for this phase, $10 million or more may be consumed. Next, a process development unit (PDU) is shown to gather the necessary physical, chemical and engineering data. About five years and $20 to $30 million is required for this phase. A large pilot plant is typically the next phase of development and requires about seven years to complete. Project cost for a 100 ton per day plant may approach $100 million. Finally, the last two stages shown by Figure 1 represent successively larger commercial prototype plants in final preparation for a full-sized 50,000 barrel per day plant (or its thermal equivalent if the product is other than oil). This development scheme is admittedly conservative and perhaps for some cases the exploratory research and PDU phases could be combined. Likewise the pilot plant and demonstration plant phases might be accomplished jointly by a plant size of several hundred tons per day capacity. Nevertheless, the time to reach commercialization would still be almost 15 years.

Guiding process development by design and cost engineering analysis is very important, but complicated by the need to compare estimates taken from various sources. Engineering design and cost estimating procedures and data will differ somewhat when different process groups have been involved. Any significant differences usually can be resolved when the material is well documented. However, two other factors must be considered when two or more estimates are to be compared. The first concerns the degree of engineering effort expended in the design and costing of each estimate. Greater engineering effort generally produces more accurate than that taken from smaller units such as PDU-sized equipment. The second concerns the quality or reliability of the data being used for the design. Data from the demonstration or commercial development phase is obviously more accurate than that taken from smaller units such as PDU-sized equipment.

These two sources of inconsistencies in estimates can be resolved by means of project and process contingencies. These are allowances to account for differences in the level of engineering effort and in data reliability, respectively. Application of these contingencies adjusts an estimate to a value equivalent to the completion of development when full data is available for all sections of the plant and an accurate detailed estimate can be made.

Project and process contingencies which are being used to compare and resolve process estimates in the Fossil Energy Program, U.S. Department of Energy, are shown in Figure 2. The process contingency is calculated as a percentage of the onsite portion of the plant and represents the additional investment necessary to improve or expand process equipment to reach design conditions, since data taken while developing a process tend to be optimistic. Project contingency is calculated as a percentage of the total onsite (including process contingency) and offsite investment and is then added to obtain the final investment. It allows for errors in cost estimating due to design assumptions, labor productivity and rate assumptions, late delivery of construction materials, and the like. Therefore, it

reflects only the uncertainty of constructing a given plant for a given cost and does not depend on the uncertainty of the technical data. It does depend on the type of estimate made as shown in the figure. Typical engineering costs of producing these estimates for a 50,000 barrel per day coal conversion plant are given in parentheses.

The contingency figures shown in Figure 2 resulted from discussions with large U.S. processing firms over the last two years and are based on their process development and plant construction experience. Major contribution was received from Exxon Corporation.

A better understanding of various levels of cost estimates and the accuracy which can be expected from them can be gained by considering Figures 3, 4 and 5. Together these figures describe the basic differences between preliminary, definitive and detailed estimates.

The first step in developing an estimate is setting the design basis. All three estimate types require the same type of design basis information, with the exception that the site specification for the three differs. For example, a detailed design including detailed mechanical drawings requires specification of an actual site and core drillings may be necessary to determine foundation design.

The next step in process estimating is the process design itself (Figure 4). Differences in estimate accuracy are most obvious from consideration of the varying efforts expended in this step. In a preliminary design the effort ends with an equipment list, while in a definitive design detailed specifications are prepared, including piping and instrumentation specifications. This additional information requires a great deal more engineering effort to develop, but it is important to accuracy since process plants contain piping and instrumentation that may represent up to 40 percent of the plant capital investment. A detailed design includes the latter elements plus detailed engineering drawings and plans which may require hundreds of thousands of man-hours to produce. Of course, this effort is appropriate only when actual construction is planned.

The last step is the cost estimating process itself. For preliminary estimates, cost curves, experience factors, and rules of thumb are used, whereas for a definitive estimate, a more detailed estimating procedure is required. Vendor quotes, specific cost indexes, and projected financial conditions are appropriate. For a detailed study, one seeks vendor bids, finances under actual conditions, and studies actual labor rates and productivity for the area in question. Actual labor costs and productivity are extremely important factors which are generally overlooked. The availability of skilled craftsmen and the specifics of union rules vary in different parts of the United States and can have a large effect on the final plant cost.

Reconsidering Figure 2, it is clear that a final investment estimate varies a great deal as a result of the contingencies applied to it. Consider, for example, a coal liquefaction plant producing 50,000 barrels of product oil daily. Onsite investment might be roughly $750 million and offsite investment about $250 million. If these investments had been calculated using data of PDU quality by a preliminary type of estimate, process and project contingencies would be taken as 25 and 20 percent, respectively. Applying these contingencies results in a total investment estimate of $1,425 million or an increase of about 43 percent above the investment base of $1,000 million without contingencies.

COAL GASIFICATION ESTIMATES

Consistent cost estimates for coal gasification processes which are now under development have been made by C.F. Braun & Co. using western U.S. subbituminous

coal with 250 million standard cubic feet per day of substitute natural gas production assumed as the standard plant size. The study examines the investments, operating costs, and the resulting prices of the HYGAS, BI-GAS, CO_2 Acceptor and Synthane processes compared with similar figures for the presently-commercial Lurgi gasification technology. Another phase of the same study which will soon be published examines the same processes using eastern U.S. coals.

Figure 6 is a plot of product costs for the various processes calculated by Braun for western coal, assuming 100 percent equity financing, 12 percent discounted cash flow (DCF) rate of return, and 1976 constant dollars. Braun used a 15 percent project contingency for all of these cases, but included no process contingencies in the onsite investments. Note that product costs can be plotted as straight lines when annual operating costs are plotted against total capital requirement.

From the figure one sees that the HYGAS case with the residual char gasified using a steam-oxygen gasifier appears to be the most attractive process at approximately $4.25 per million Btu of product cost. The Lurgi process is about $5.50 per million Btu as is the case for Synthane where excess char is sold outside the plant and slurry coal feeding to the gasifiers is used. BI-GAS and CO_2 Acceptor approach the low-cost HYGAS case. However, the HYGAS case with residual char gasified using a steam-iron gasifier is less attractive than LURGI, as are two Synthane cases which export electrical power for sale outside the plant.

The type of cost estimate performed by the Braun study is equivalent to a preliminary study and the 15 percent project contingency used is reasonable. However, no process contingencies were used to reflect the differing data quality available for the individual estimates. Given the PDU and pilot data quality of all of the data except Lurgi, process contingencies of 15 to 25 percent are indicated. A value of five percent is suitable for the Lurgi estimate. Application of these additional factors to Lurgi and the three estimates on the figure which are lower cost than Lurgi narrows their cost advantage over Lurgi by about 50 cents per million Btu. This has the result that only the HYGAS process retains an apparent advantage over Lurgi technology. Other processes appear marginal or higher cost compared with Lurgi technology.

COAL LIQUEFACTION ESTIMATES

At present several coal liquefaction processes are under development. These include such processes as Exxon Donor Solvent (EDS), H-Coal, and Solvent Refined Coal (SRC). Each of these processes makes liquid fuels with different physical properties. However, each of the processes has some flexibility to operate over a range between a heavier boiler fuel type of primary product and a lighter synthetic crude primary product, depending on liquefaction reactor space velocity.

A recent paper by Gulf (2) concerning the SRC process operated to produce a synthetic crude (although they view its best use as fuel to a boiler) indicates a price of $3.21 per million Btu assuming 100 percent equity financing, 12 percent DCF and 1976 constant dollars. A 20 percent project contingency is included, but no process contingency was applied. Including a 20 percent process contingency increases the cost to about $3.60 per million Btu. This is equivalent to about $22 per barrel.

Preliminary estimates of other liquefaction processes within Fossil Energy indicate prices of $30 per barrel and greater when using this same economic basis to produce a synthetic crude. However, since the various designs and cost estimates have been made by different concerns, it is not clear whether these cost differences are due to true process differences or merely to design philosophy differences among the various firms involved. This matter is currently under study.

POWER GENERATION ESTIMATES

New electric generation facilities can be based on a number of liquid and solid alternative fossil fuels. Figures 7 and 8 contrast various base load alternatives, showing the capital, operation and maintenance (O&M), and fuel components of total cost expressed as mills per kilowatt-hour of power generated. These power costs were derived from recent work done by Gilbert Associates (3) which determined capital and O&M costs for various alternatives. The fuel component was added to these by choosing recent cost ranges for the basic fuels used (Table I). An 800 megawatt electric plant size operating at 70 percent capacity factor is assumed and the basis is utility economics equivalent to a 10 percent DCF rate of return in 1975 constant dollars. A 15 percent project contingency was used in all cases with no process contingency.

In Figure 7, the No. 6 fuel oil case shows a variation in power cost of 28 to 33 mills per kilowatt-hour (the variation in the fuel component of this and all other cases represents the range shown in Table I). The natural gas case is less, but this fuel is now in scarce supply in the United States. SRC hot liquid refers to the Solvent Refined Coal liquefaction process operated so as to make a heavy liquid product which would solidify if cooled. This case and that for heavy synthetic coal liquid both indicate a significant cost increase compared to No. 6 fuel oil. The dashed area is added to emphasize the relative uncertainty of these estimates. Finally, medium Btu gas made off site and bought by the power plant at the range shown by Table I is also relatively expensive. Note that the capital and O&M components for all of these liquid cases are substantially the same and only the fuel components vary.

The solid fuel cases shown in Figure 8 show some interesting variations. Low sulfur coal without flue gas desulfurization (FGD) is very attractive and compares favorably with the use of natural gas on the previous figure. The high sulfur coal case with FGD illustrates the fact that the additional capital and O&M components due to the FGD equipment are not offset by the lower fuel cost of high sulfur coal. Similarly, installation and operation of an on site low Btu gas plant using high sulfur coal is not offset by the cheaper fuel.

The solid SRC case without FGD has the same low capital and O&M components as the low sulfur coal case but the expensive fuel prices this alternative well above the others. Next, cleaned high sulfur coal without FGD appears competitive with low sulfur coal. Finally, the two high sulfur coal cases using fluidized bed combustion and a low Btu gas, combined cycle system both look very competitive.

Retrofit of base load electric utilities is illustrated by Figure 9 using the same economic basis as before. Here the incremental cost of modifying solid and liquid fuel plants is shown by the three cost components. FGD adds only about 10 mills per kilowatt-hour but solid SRC adds over 20 mills. Among alternatives for retrofitting solid fuel plants, cleaned high sulfur coal adds the least or about five mills. For liquid plants, the heavy synthetic coal liquid and the medium Btu gas off site cases add about 10 mills per kilowatt-hour or more. The low Btu gas on site case adds nothing because the savings in fuel cost by using high sulfur coal to generate the gas offsets the capital and O&M components. The coal oil slurry case indicates a reduction, since the needed capital and O&M are not large and the savings in No. 6 fuel oil substituted by less expensive low sulfur coal more than offsets them.

The economics of steam generation by fluidized bed combustion (FBC) have recently been studied (4). Figure 10 contrasts FBC with conventional firing (CF) for both high and low sulfur coal; conventional firing with low sulfur fuel oil is shown for comparison. These costs show capital, O&M and fuel components (see Table I) calculated in 1975 constant dollars at a 10 percent DCF rate of return for

a 100,000 pound per hour boiler. No process contingency was assumed, but a 20 percent project contingency was used.

For high sulfur coal, the FBC case is definitely lower cost than conventional firing with FGD. There is no relative improvement when using low sulfur coal, however. Note that the capital and O&M costs for a boiler based on low sulfur fuel oil is much less than the other cases. Of course, this is fully offset by the relatively higher cost of the fuel oil.

SUMMARY

Consistent process design and cost estimating procedures play an important role in guiding research and development. Application of proper process and project contingencies is a key element in obtaining realistic and comparable estimates.

Preliminary estimates have been made for many of the coal conversion and power generation alternatives now under development in the United States. Coal gasification and power generation economics are presently the most fully developed, but a number of studies are planned to better define the prospects for coal liquefaction.

REFERENCES

1. Detman, R., "Factored Estimates for Western Coal Commercial Concepts - Interim Report," prepared for the U.S. Energy Research and Development Administration and the American Gas Association by C.F. Braun & Co., October 1976.

2. Schmid, B.K. and Jackson, D.M., "Recycle SRC Processing for Liquid and Solid Fuels," presented at the Fourth Annual International Conference on Coal Gasification, Liquefaction and Conversion to Electricity, Univertisy of Pittsburgh, Pittsburgh, Pa. (August 2-4, 1977).

3. "Assessment of Fossil Energy Technologies for Electric Power Generation," Vol. 1, prepared for the Office of Program Planning and Analysis, Fossil Energy, by Gilbert Associates, Inc., October 1976.

4. Farmer, M.H., Magee, E.M., and Spooner, F.M., "Application of Fluidized Bed Technology to Industrial Boilers," prepared for U.S. FEA/ERDA/EPA by Exxon Research and Engineering Company, Linden, N.J., January 1977.

TABLE I

FUEL COST TO POWER GENERATION

	Dollars per Million BTU
Liquid Fuels	
No. 6 Fuel Oil	2.12 - 2.86
Natural Gas	0.52 - 2.00
SRC Hot Liquid	3.00 - 5.00
Heavy Synthetic Coal Liquid	3.00 - 5.00
Medium BTU Gas	3.00 - 4.00
Solid Fuels	
Low Sulfur Coal	1.00 - 1.25
High Sulfur Coal	0.75 - 1.00
Solid SRC	3.00 - 5.00

Purpose, Size, Cost of Individual Coal Conversion Units

	Concept	Exploratory Research	Process Development Unit(PDU)	Pilot Plant	Demonstration Plant	Commercial Demo.
Purpose:	Discovery	Scientific Feasibility	Technical Feasibility	Economic Feasibility	Commercial Feasibility	Resolve Investment Uncertainties
Information:	Theory	Concept Proof	Physical, Chemical, Engineering Data	Engineering Parameters of Scale-up	Validate Process Economics, and Environmental/ Socioeconomic Impacts	Capital and Other Resource Requirements, Marketability of Products
Typical Size: 1/ (Tons/Day)	0 to 0.1	1.0	10	100	1,000	10,000
Capital Cost: 1/ (1976 Million $)	N.A.	$3 to $5	$10 to $15	$20 to $30	$100 to $200	$400 to $800
Annual Operating Cost, 1/ (1976 Million $)	N.A.	$3 to $5	$5 to $10	$10 to $15	$25 to $50	$80 to $160
Government Share: 1/ (Percent)	N.A.	100%	100%	66%	50%	0 to 50% (Cost if Venture Fails)

1/ Typical Values; each process is different & must be individually estimated.

Figure 1

PROJECT AND PROCESS CONTINGENCIES*

TYPE OF COST ESTIMATE

DEVELOPMENT PHASE	STUDY ($2–5 x 10^4)	PRELIMINARY ($2–5 x 10^5)	DEFINITIVE ($2–5 x 10^6)	DETAILED ($2–5 x 10^7)
PDU	25 / 50	20 / 25		
PILOT	25 / 25	20 / 15	15 / 10	
DEMONSTRATION	25 / 15	20 / 10	15 / 5	10 / 5
COMMERCIAL	25 / 5	20 / 5	15 / 5	10 / 5

(PROJECT % / PROCESS %)

*PROCESS CONTINGENCY IS APPLIED TO ONSITES; OFFSITES ARE THEN ADDED AND PROJECT CONTINGENCY IS APPLIED TO THE TOTAL

Figure 2

DESIGN BASIS

PRELIMINARY ($0.2-0.5 X 10^6)	DEFINITIVE ($2-5 X 10^6)	DETAILED ($20-50 X 10^6)
• PRODUCT SPECS	• DO	• DO
• FEED SPECS	• DO	• DO
• DESIGN ASSUMPTIONS	• DO	• DO
• PROCESS DESCRIPTION	• DO	• DO
• UTILITY SPECS	• DO	• DO
• GENERAL SITE	• HYPOTHETICAL SITE	• ACTUAL SITE

Figure 3

PROCESS DESIGN

PRELIMINARY ($0.2-0.5 X 10^6)	DEFINITIVE ($2-5 X 10^6)	DETAILED ($20-50 X 10^6)
• FLOW DIAGRAM	• DO	• DO
• MATERIAL BALANCE	• DO	• DO
• ENERGY BALANCE	• DO	• DO
• OPERATING CONDITIONS	• DO	• DO
• PLOT PLAN	• DO	• DO
• ENVIRONMENTAL ASSESSMENT	• DO	• ENVIRONMENTAL IMPACT STATEMENT
• MAJOR EQUIPMENT SIZED	• ALL EQUIPMENT SIZED	• DO
• EQUIPMENT LIST	• EQUIPMENT LIST AND DETAILED SPECS	• DO
	• P AND I DIAGRAMS	• DO
	• PIPING SPECS	• DO
	• PROCESS RELATED STRUCTURAL SPECS	• COMPLETE STRUCTURAL DRAWINGS
		• DETAILED ENGINEERING DRAWINGS
		• PLANT ELEVATION DRAWINGS
		• PROCUREMENT AND CONSTRUCTION PLAN

Figure 4

PROCESS ECONOMICS

PRELIMINARY ($0.2-0.5 × 10⁶)	DEFINITIVE ($2-5 × 10⁶)	DETAILED ($20-50 × 10⁶)
• COST CURVES	• DO	• VENDOR BIDS
• EXPERIENCE FACTORS	• VENDOR QUOTES ON MAJOR ITEMS	• ACTUAL LABOR COSTS AND PRODUCTIVITY
• RULES OF THUMB	• EXPERIENCE FACTORS BASED ON MORE DETAILED DRAWINGS	• DETAILED ENGINEERING EVALUATION
• GENERAL COST INDEXES	• SPECIFIC COST INDEXES	• FINANCING UNDER ACTUAL CONDITIONS
• ASSUMED FINANCIAL CONDITIONS	• PROJECTED FINANCIAL CONDITIONS	

Figure 5

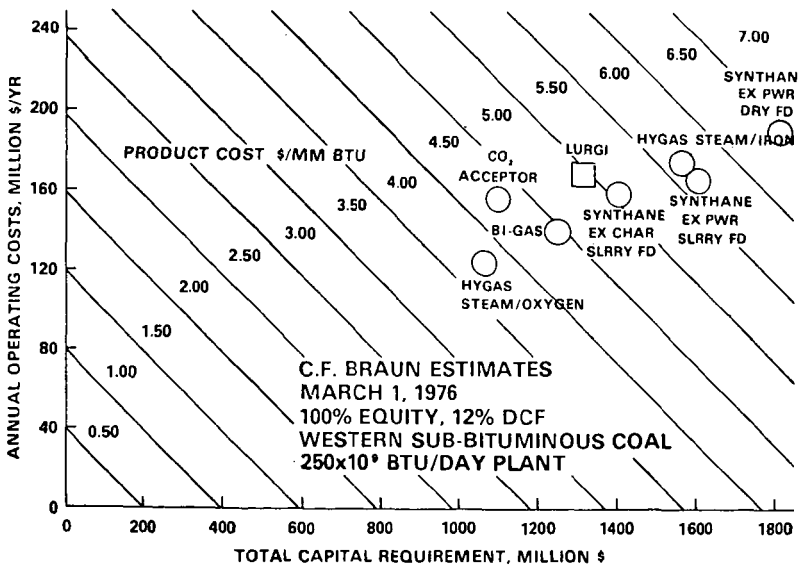

Figure 6

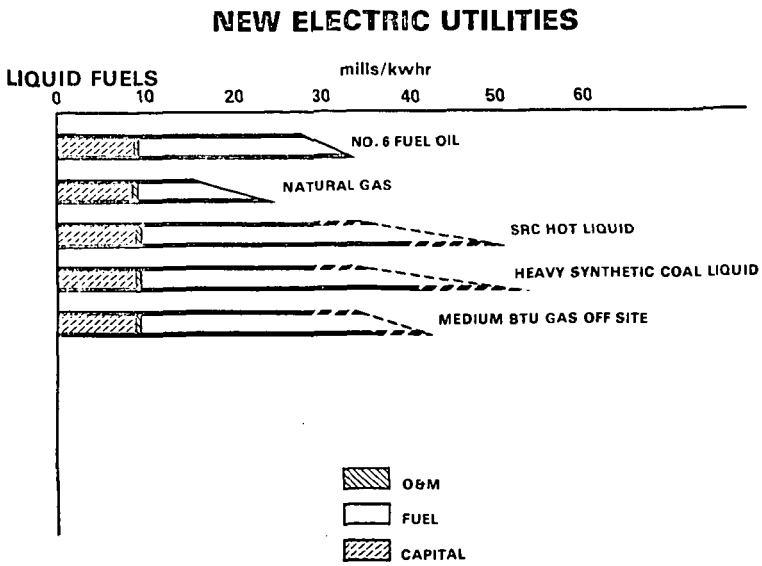

Figure 7

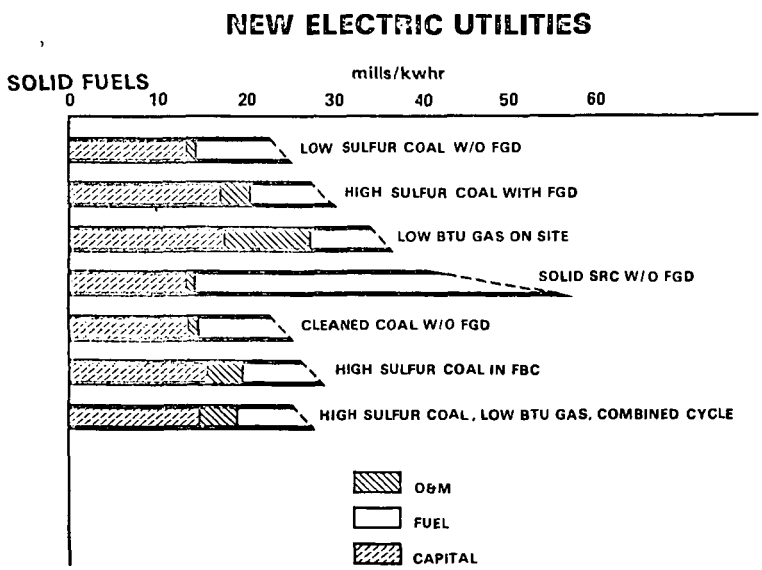

Figure 8

RETROFIT OF ELECTRIC UTILITY

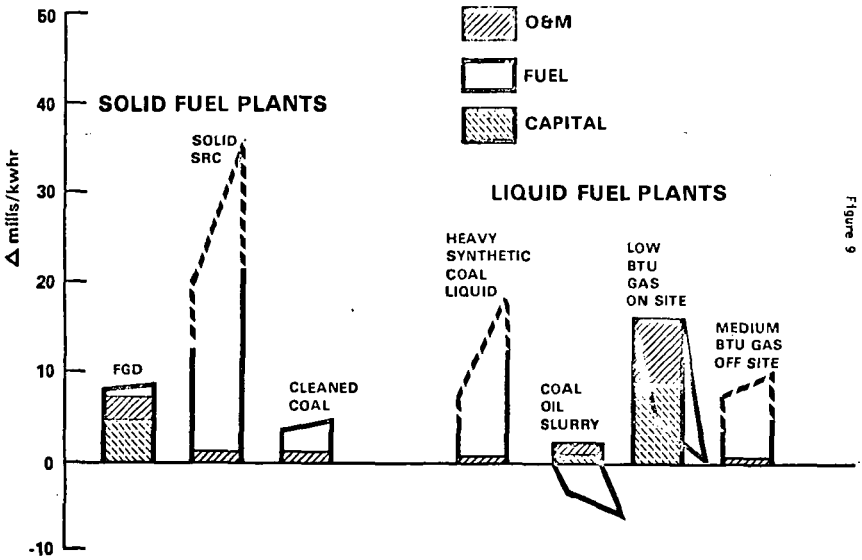

Figure 9

NEW INDUSTRIAL BOILERS

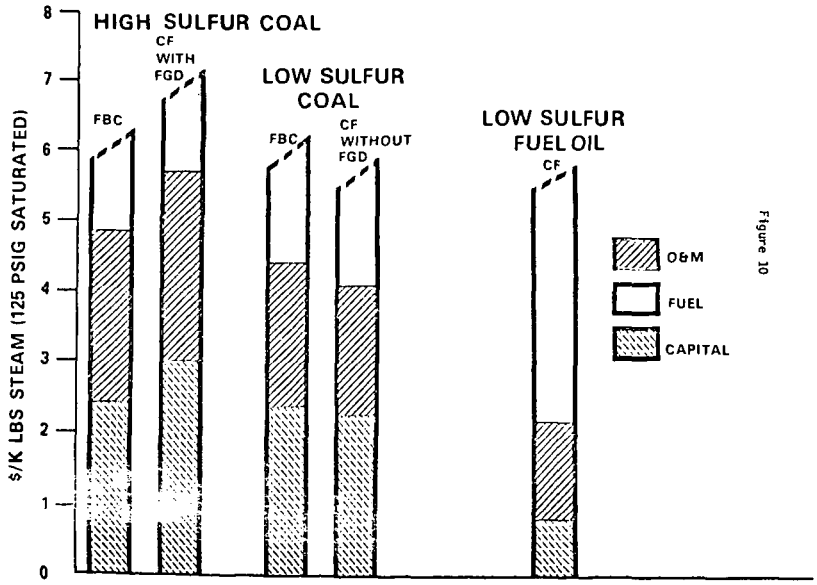

Figure 10

ECONOMICS OF THE KOPPERS K-T GASIFICATION PROCESS FOR SYNTHETIC GAS AND CHEMICAL MANUFACTURE

John F. Kamody and J. Frank Cannon

Koppers Company, Inc.
Engineering and Construction Group
Pittsburgh, PA 15219

INTRODUCTION

The commercially proven Koppers K-T gasification process is employed for the gasification of coal and other carbonaceous fuels to produce a carbon monoxide and hydrogen rich gas. The process involves the entrainment reaction of the fuel with oxygen and steam at high temperature.

Since 1952 a total of 39 gasifiers have been installed at 13 locations in the Eastern Hemisphere. An additional plant at Talcher, India, is scheduled for start-up sometime during 1978. Almost exclusively the plants have been utilized for the production of ammonia from coal. However, the latest commissioned plant in Modderfontein, South Africa, produces 65 metric tons per day of methanol as well as 1000 metric tons per day of anhydrous ammonia.

Inherent features of the K-T process result in the production of a gas which is extremely well suited for chemical synthesis applications. These favorable characteristics of the gas include:

- Tars, phenols, and other condensible hydrocarbons are totally absent from the raw gas. Aside from the obvious environmental advantages of this feature, problems are avoided with gas purification and with catalytic processing of the gas.

- The gas typically contains 85-90 volume percent (dry basis) carbon monoxide plus hydrogen. The third principal constituent is carbon dioxide which, of course, is recoverable or otherwise does not interfere in chemical processing. Sulfur in the fuel is converted predominantly to hydrogen sulfide and carbonyl sulfide, both of which are readily recoverable from the gas. Inert compounds, such as nitrogen and argon, are typically present at only 1 volume percent (dry basis).

- Negligible methane is produced, thus avoiding the need for employing costly steam reforming in applications such as hydrogen or ammonia production.

- The gas can alternatively or simultaneously be employed as an excellent industrial fuel gas, thereby adding to versatility in operation.

- Unlike natural gas, hydrogen to carbon monoxide ratios of 1:1 or lower are readily obtainable without the need for external utilization of excess hydrogen or importation or carbon dioxide. This feature can make the K-T process more practically suited than natural gas for growing applications in oxo-synthesis, methanol production, or Fischer-Tropsch technology.

An additional major advantage to the process is its ability to handle a variety of feedstocks, including all ranks of coal, char and petroleum coke. In addition, liquid feedstocks, such as heavy residuals or tars, can be processed. This advantage is important in contracting for an economical fuel supply or in switching to alternate fuels during the life of the plant. Presently designed units can process a maximum of 850 tons per day of solid carbonaceous fuel.

PROCESS DESCRIPTION

For the sake of brevity and due to the fact that many people are now reasonably familiar with the basic features of the K-T process very little discussion herein is made on the process description. Further information and performance data can be found in other Koppers publications.

The gasifier employs the low pressure partial oxidation of pulverized coal in suspension with oxygen and steam. Reaction temperature ranges from 3500°F at the burners to 2700°F at the gasifier outlet. The gasifier is a steam-jacketed, refractory lined carbon steel vessel. A four-headed gasifier employs four burner assemblies situated 90° apart, while a two-headed gasifier employs a pair of burner assemblies located 180° apart. Characteristically, the gas produced contains 50-55% carbon monoxide and 30-35% hydrogen, both on a dry basis. Carbon dioxide, sulfur compounds (H_2S and COS), and nitrogen principally make up the balance.

Heat is recovered from the gas leaving the gasifier by means of a waste heat boiler where up to 1500 psig saturated steam is generated. Gas from the waste heat boiler is scrubbed of particulates and is then compressed as necessary for the intended application. Sulfur compounds are removed from the gas and ultimately converted to sulfur by a variety of means which are selected based on gas application.

GENERAL ECONOMIC CONSIDERATIONS FOR COAL GASIFICATION

While it is not the intent of this paper to compare the K-T process to competitive coal gasification processes, it is safe to conclude that all applications of coal gasification will be more expensive than presently available sources of oil and natural gas. Paradoxically, however, there is growing evidence that the cost of coal gasification is similar, if not less, than the cost of developing some new sources of natural gas. The high cost of new natural gas today tends to be disguised by the lower cost of old gas production. This situation is gradually shifting with the advent of the fuel cost adjustment and of course the situation will be dramatically changed with inevitable gas deregulation. However, with gas from coal there are presently few well-defined institutional mechanisms for equitably distributing the cost. Consequently there is reluctance from private sectors to invest in coal gasification.

Synthesis gas is presently produced by reforming natural gas or by partial oxidation of oil. It is strictly a matter of time before the supply situation or governmental policy will restrict or prohibit such use of natural gas. Earlier emphasis on coal gasification was directed toward SNG, or high methane content gas. However, it often is illogical to produce SNG whenever industrial users are still reforming or burning natural gas. Thus, the production of CO-H_2 rich gas for industrial use is being favored as a more efficient and economical approach to coal gasification. In addition to the many synthesis gas applications, this gas has excellent properties as an industrial fuel.

Table 1 compares the investment of a fully integrated Koppers K-T plant producing intermediate btu fuel gas with investment required for several projects involving production of natural gas, SNG, and electricity. The K-T fuel gas plant would deliver 140 billion btus per day of 300 btu per cubic foot gas (intermediate Btu gas) at elevated pressure to a number of industrial users.

Although the actual costs of some of the new natural gas or SNG projects can be debated, the intent of presenting the table is merely to indicate that the costs of new sources of gas are much higher than in the past. Furthermore it is apparent that production of intermediate btu gas should be regarded as an equally viable venture. All of the efforts by the gas industry to increase production are important, and there are many areas such as residential markets, where methane is difficult to replace. Industrial fuel or synthesis gas production will ease the burden of supply. Presently industrial usage accounts for over 60% of natural gas consumption.

TABLE 1

Example of Capital Requirements for Gas Production

	Production Billion Btu/Day	Investment $MM 1977	1977 Investment $/Annual MM Btu
Current Embedded Investment in Gas Industry	58,900 (21.5 TCF/yr.)	52,000 1/	2.40
SNG from Liquids	60 (60 MM SCF/Day)	56.7 1/	2.85
LNG Imports (includes foreign investment)	1,000 (365 BCF/Yr.)	4,150 1/	11.35
Alaska Natural Gas Pipeline	2,400 (2.4 BCF/Day)	10,000 2/	11.40
SNG from Coal	250 (250 MM SCF/Day)	1,370 1/	16.60
Heat from Electricity (Nuclear Power)	---	($1,250/kw)	41.80
Intermediate Btu (300 btu/scf) Fuel Gas from Fully Integrated Koppers K-T plant	140	390	8.45

Table 2 presents examples of projected prices of intermediate btu gas with costs of existing natural gas and projected costs of new sources of natural gas. Again, cost of intermediate btu gas from coal compares favorably with the projected prices of new gas.

TABLE 2

Example of Gas Prices

	$/MM Btu (HHV), 1978
Present Natural Gas (Industrial)	2.00 - 2.50 3/
LNG (Existing Massachusetts Terminal)	2.37 4/
LNG (Current Applications for Import)	3.00 - 4.50 4/
Gas from Alaska Natural Gas Pipeline	3.65 - 5.35 5/
SNG from Coal	4.10 - 7.10 6/
Heat from electricity @ 2¢/kw - hr	5.85
@ 4.5¢/kw - hr	13.15
Intermediate Btu Fuel Gas from Fully Integrated Koppers K-T Plant (60% debt financing)	
- with coal @ $15/ton (64¢/MM Btu)	3.35
- with coal @ $30/ton ($1.28/MM Btu)	4.50

In cases where gas is employed for synthesis applications it is important to recognize that natural gas or SNG must be first reformed, which is not a cost requirement for the intermediate btu gas. In the case of a fully integrated, free-standing ammonia plant, about 15% more natural gas (HHV basis) is required than intermediate btu gas, as shown in Table 3.

TABLE 3

Btu Requirement Per Ton of Ammonia

Basis: Gas supplied to ammonia plant battery limits at 500 psig.

(MM Btu/Ton NH_3)	Natural Gas	Intermediate Btu Gas
Synthesis Gas Required *	18.5	23.6
Fuel Requirements:		
Reforming	9.7	---
Utility Support	10.1	8.8
Tail Gas Credit	-1.8	-1.3
Net Fuel Required	18.0	7.5
Total Gas Required	36.5	31.1

* Based on 97% reforming of methane; 94.5% conversion of H_2 to NH_3.

Table 4 shows that for a fully integrated methanol plant over 20% more natural gas is required than intermediate btu gas. Table 4 is based on 95% reforming of methane and does not employ CO_2 addition from an external source. Conversion of CO and CO_2 is 95% within the synthesis loop.

TABLE 4

Btu Requirement Per Ton of Methanol

Basis: Gas supplied to methanol plant battery limits at 500 psig.

(MM Btu/Ton Methanol)	Natural Gas	Intermediate Btu Gas
Synthesis Gas Required	26.0	24.9
Fuel Requirements:		
Reforming	13.3	0.0
Utility Support	0.0	0.8
Tail Gas Credit	-9.9	-1.9
Net Fuel Required	3.4	-1.1
Total Feedstock Required	29.4	23.8

An important, yet often overlooked, advantage of coal gasification is that the mining of coal can be performed with relatively stable capital productivity. This means that once a mine is opened a relatively uniform output of coal can be maintained over the economic life, particularly in view of the fact that coal deposits are well identified. On the other hand, oil and natural gas production is usually characterized by declining capital productivity. For instance, as well head pressure begins to fall, output declines until a point is reached where additional investment is required for secondary or tertiary recovery methods. Thus, capital cost per unit of output tends to increase significantly during the economic life of oil and gas production. This is a major reason why the cost of coal mining is expected to be less subject to price escalation than with natural gas production, particularly in cases where the mine is captively associated with the gasification plant. Of course, coal mining is more labor intensive, although this is less of a case with newer mines or strip mines. The effects of inflation are briefly discussed later in this paper.

FUEL CHARACTERISTICS OF K-T GAS

The K-T gas has excellent fuel characteristics, and is well suited for industrial applications as a so-called "intermediate" btu gas. A more detailed discussion of gas combustion properties can be found in other Koppers' papers. However, the most basic fuel characteristics are herein presented.

In comparison to natural gas, the nominal 300 btu/scf heating value of K-T gas necessitates an increased volumetric usage of fuel for a given heat duty. However, the air required for combustion of K-T gas is substantially reduced. As a consequence, the weight of combustion products is comparable to that produced upon combustion of the more conventional fuels. Table 5 compares overall firing characteristics of a furnace at typical levels of excess air for coal, fuel oil, natural gas, and K-T gas. For this example the K-T gas is humid and supplied at low pressure. Schemes are available for drying the gas if desired.

TABLE 5

Overall Furnace Performance

	Coal WT. %		No. 6 Fuel Oil WT. %		Natural Gas VOL. %		K-T Gas VOL. %
C	70.5	C	87.8	CH_4	83.0	CO	50.7
H	5.0	H	11.0	C_2H_6	16.0	CO_2	7.8
N	1.3	N	0.2	CO_2	0.5	H_2	34.5
S	2.5	S	0.5	N_2	0.5	N_2+Ar	1.2
O	7.5	O	0.5			H_2S+COS	0.1
Ash	10.1	Ash	Nil		100.0	H_2O	5.7
H_2O	3.1	H_2O	Nil				
							100.0
	100.0		100.0				

Gross Heating Value, Btu/Lb	12,809	18,500	---	---
Btu/Scf	---	---	1,128	277
Typical % Excess Air Used	15	5	10	15
Lb. Air Used/MM Gross Btu (60°F wet bulb)	867	793	792	653
Lb. Combustion Gas/MM Gross Btu	937	847	835	840

In retrofitting an alternate fuel to an existing furnace or boiler, the permissible draft loss is ordinarily a limiting consideration. Since K-T gas yields a favorable amount of combustion gas per unit of heat input there are minimal restrictions in retrofitting existing equipment. In addition, use of K-T gas results in a unit efficiency comparable, and often better, than that of more conventional fuels.

The K-T gas offers these additional fuel advantages to the chemical process industry:

- Equilibrium adiabatic flame temperature of the K-T gas with ambient temperature air is approximately 3750°F, compared to typically 3550°F for natural gas. This is important in high temperature processes, such as those involving radiant tube burners.

- The gas can be completely desulfurized and is free of ash constituents or alkali metals. This advantage is particularly important in certain chemical process applications such as firing of Dowtherm boilers, where oil often cannot be used due to its ash, sulfur, or vanadium content.

- The wide flammability limits of the gas promote good combustion efficiency and permit safe control of combustion temperature by use of a relatively high amount of excess air. The wide flammability limits permit reduced nitrogen oxide emissions by means of staged combustor firing.

- The versatile K-T fuel gas can be used as a fuel or as a synthesis gas, without the necessity of a reforming operation.

Within most industries, a reliable fuel supply is important. The K-T process has a proven history of reliability. Gasifier outages, such as those which occur during annual plant turn around, can be compensated by use of spare gasifier capacity or by the temporary use of alternate fuels. If natural gas is used as a back-up fuel, systems can be designed whereby air-ballasted natural gas is automatically used without necessitating burner alterations.

ECONOMICS FOR FUEL GAS OR SYNTHESIS GAS PRODUCTION

It is difficult to generalize the economics of producing synthesis gas from coal since costs are greatly influenced by a number of variables which are specific to each application. These variables include site selection, plant size, availability of off-site facilities, and cost of coal. In addition, specific financing variables such as capital structure, rate of return, and interest rates affect gas cost.

As an example of synthesis gas costs, a case is presented for a large plant which produces gas at 170 psig for delivery to industrial customers within a 100 mile radius. The plant consists of fifteen four-headed gasifiers, including one spare, to produce a net output of 140 billion btus per day (HHV) of gas with a gross heating value of 300 Btu/scf. Raw material for the plant consists of 9700 tons per day of 2" x 0" bituminous coal, with 5.7 wt. % moisture content and gross heating value of 11,810 Btu/lb. Gas is desulfurized and dried to a -18°F dew point before entering the distribution system. The plant satisfies its own utility requirements, except for 94 megawatts of imported electricity, by combustion of a portion of gas within an auxiliary boiler. The plant is a "grass-roots" plant and all general facilities and coal handling facilities are included.

Plant investment (mid 1978) would be about $410 MM, while total capital requirements would amount to about $510 MM. The total capital includes the plant investment plus interest during construction, start-up costs, and working capital (60 day cash supply).

Figure 1 is based on this plant and shows the effect of coal cost on gas cost for a debt to equity ratio of 60/40 and a 12 percent discounted cash flow rate of return. The cash flow method of analysis is representative of private investor financing. Figure 2 illustrates the effect of capital structure, or fraction of debt, on gas cost for a coal cost of $22.50/ton (95¢ per MM Btu). Project life is 20 years, with a 10 year (sum of years digits) depreciation schedule. Federal income taxes are taken as 48%. Debt is retired over the 20 year life of the project by a series of annual payments.

APPLICATIONS OF K-T GAS FOR CHEMICAL SYNTHESIS

Generally, there are three categories of chemical synthesis applications of the gas, either for captive or merchant markets. These are:

- Hydrogen Production
- $CO-H_2$ Based Synthesis
- CO Production

Hydrogen Production

The major present commercial use of hydrogen is in captive markets, that is, those areas where the hydrogen is used integrally with the process. Principally this market relates to ammonia production or petroleum refining applications, such as hydrodesulfurization or hydrocracking. Ammonia is, of course, the base material for such important chemicals as caprolactam, acrylonitrile, urea (and resins thereof), nitric acid, and fertilizers.

An important growing captive use for hydrogen will be in the area of coal liquefaction. In typical liquefaction processes hydrogen is generated by gasifying char or residue which is recovered in the processes. In 1975 the K-T process was successfully used to gasify FMC-COED char during tests in Spain. With residue type feedstock the K-T process is well suited for accommodating the high ash content characteristic of such residues.

$CO-H_2$ Based Synthesis

This application is based on direct synthesis of chemicals from the $CO-H_2$ gas. This use is of particular interest to the chemical industry due to the wide range of valuable products which can be made. It is particularly encouraging to observe the progress which is being made in $CO-H_2$ synthesis technology, especially in regard to catalyst improvements which permit improved yields and reduced synthesis pressures.

The modern schemes of synthesis generally require, stoiciometrically, at least a 1:1 ratio of H_2 to CO, as for example in various oxo-synthesis processes. Higher ratios are required in other applications, such as in methanol of Fischer-Tropsch synthesis, where a 2:1 ratio of H_2 to CO is required. Since K-T gas from coal has initially a H_2:CO ratio of typically 0.6, it is straightforward to obtain increased ratios by merely shifting a portion of the gas. On the other hand, reformed natural gas has a 3.0:1 to 4.0:1 ratio of hydrogen to carbon oxides. Thus, to comply stoiciometrically with certain synthesis applications it is necessary with natural gas based $CO-H_2$ to remove or otherwise utilize as fuel the excess hydrogen in tail gas. Conversely, CO to CO_2 could be added somewhere in the process schemes. Hence at times the practicality, cost, or energy involved in synthesis based on natural gas can be restrictive.

Methanol from coal is being considered for use as a direct fuel. Methanol has the advantage of being easily stored. Present economics do not justify the use of methanol as a fuel unless coal is inexpensive. With coal at $10 per ton, methanol by the K-T process would cost 35-55¢ per gallon depending on plant financing and other factors. Methanol also has traditional important chemical applications, such as, in the production of formaldehyde, methyl methacrylate, acetic acid, and isoprene rubber. Mobil Oil Corporation is developing a process for production of gasoline from methanol. Additional technology is under development for production of olefins, such as propylene, from methanol. These olefins can be used in oxo-synthesis. Oxo-synthesis is the process whereby aldehydes and other oxygenated compounds are produced by catalytic reactions of CO and H_2 with olefins. Products include paints, laquers, butyraldehyde, detergents, solvents, and plasticizers. Recent developments in oxo-synthesis technology by Union Carbide, Davy Power Gas and Johnson Matthey have led to practical use of low pressure technology and improved catalyst selectivity for at least one application (butyraldehyde).

CO Production

For carbon monoxide production the K-T gas is well suited due to its high CO content. Pure CO can be produced from the gas either cryogenically or by selective absorption methods such as the Cosorb process developed by Tenneco Chemicals, Inc. Recent developments in CO recovery technology are expected to greatly increase markets for CO. A major market for CO lies in direct ore reduction. Chemical synthesis applications include phosgene, toluene diisocyanate, and synthetic acids. Developments are aimed at extending CO use to production of terephthalic acid and p-cresol, and to use it as a co-monomer in thermoplastics.

ECONOMICS FOR ANHYDROUS AMMONIA PRODUCTION

An example of costs for anhydrous ammonia is given for a 2000 ton per day plant. The plant is completely integrated and includes coal receiving facilities and all general facilities, except raw water treatment. Four 4-headed gasifiers are used and no spare gasification capacity is provided. A total of 2845 tons per day of as-received bituminous coal is required for gasification. Additional coal is used for firing an auxiliary boiler to meet all plant utility requirements, except for the importation of about 17.5 megawatts of electricity. Coal is the same as that used in the economics of synthesis gas discussed previously. Flue gas from the auxiliary boiler is treated (Wellman-Lord Process) with recovered SO_2 sent to the Claus plant, along with H_2S from the gasification portion of the plant. Plant investment (mid 1978) is approximately $250 MM, while total capital is about $310 MM.

Figure 3 illustrates the effect of coal cost on ammonia selling price. Bases are representative for private financing and include:

- 12% Return on equity
- 9% Interest on debt
- 60/40 Debt to equity ratio
- 10 Year depreciation (sum of years digits)
- 20 Year debt retirement (annual payments)
- 48% Federal income tax.

Figure 4 shows the effect of capital structure, i.e., the extent of debt financing on ammonia price. All coal conversion processes are capital intensive, and it will probably be necessary to adopt non-conventional methods of financing to make coal derived products more competitive with those from oil and natural gas. Many of the recent discussions concerning synfuel projects have, therefore, touched upon concepts such as government loan guarantees, leveraged-leasing arrangements, tax free bonds, and even 100% government ownership as a means of reducing the financial burden of synfuel energy cost.

ECONOMICS OF HYDROGEN PRODUCTION

The economics of hydrogen are briefly discussed here since a more thorough discussion appears in a recent Koppers Company presentation.[7/] Table 6 presents a summary of hydrogen cost whenever bituminous coal cost is $20 per ton (81¢ per million btu).

TABLE 6

Cost of Producing 100 MMSCFD of Hydrogen

	Battery Limits Plant	Fully Integrated Plant
Plant Investment, $MM	185.0	288.0
Total Capital, $MM	229.0	352.5
Selling Price,		
¢/MSCF	1.79	2.27
$/Million Btu (HHV)	5.50	7.00

Bases for cost estimation include 75% debt at 9% interest rate and 25% equity at 12% discounted cash flow rate of return over the 20 year project life.

Hydrogen produced is 97.4 vol. % purity and is available at 500 psig. The principal impurities consist of methane, nitrogen, and argon. Residual carbon monoxide is about 5 ppmv, while molecular sieves are employed to control total carbon dioxide and water content at about 3 ppmv. Technology exists for producing 99.9 + vol. % hydrogen, however, the cost of so doing would be higher than those shown above.

Again, as is characteristic of a capital intensive project the extent of debt financing has an important effect. For instance, when producing hydrogen within a battery limits plant, costs would rise sharply from $5.50/million Btu (see Table 6) to $7.45/million Btu whenever 25% equity financing is replaced by 100% equity financing at 12% discounted cash flow rate of return.

EFFECTS OF INFLATION

In today's inflation dominated economy any cost analysis is incomplete unless the projection of future energy prices is considered. Long term predictions of energy cost are difficult to make, however, it is certain that costs will continue to climb. It is likely in fact that energy costs will be a major contributor to inflationary forces, and hence it would not be surprising if the rate of price escalation of conventional fuels becomes higher than the general inflation rate.

There are a number of reasons why it is expected that costs for alternate fuels will escalate more rapidly than costs from a coal gasification plant, particularly in cases where the coal mine is captively associated with the gasification plant. These reasons include:

- Oil and gas production is characterized by declining capital productivity, whereas the mining of coal is much less subject to such declines.
- Present price regulations on oil and gas production are expected to eventually be eliminated or diminished to a point where oil or gas prices are more representative of true market forces. Inherently, the convenience of conventional fuels should command a much higher free market price than coal.
- Projects involving new oil and gas production are very costly, and some of these projects could in fact be more expensive than the coal gasification options.
- Price of coal is less directly influenced by foreign pricing.

Figure 5 illustrates how the cost of fuel gas or synthesis gas might compare to cost of No. 2 fuel oil over the 20 year plant life, whenever inflation or price escalation occurs at an average rate of 8 percent per year. The 1978 price of the oil was taken as 37.2¢/gal. ($2.65/MM Btu), which is the reported wholesale price of this commodity according to U.S. Department of Labor recent statistics. Price of coal was taken at $22.50 per ton (95¢ per million Btu). The fuel gas plant depicted in Figure 5 is the same large plant (140 billion Btu per day) for which economics were presented earlier in this paper.

Once the gasification plant is built the capital associated charges are not escalated. In determining future cost of gas from the K-T plant it was assumed that all operating costs are subjected to inflation, except for coal, where it was assumed that only about 60% of the coal cost is subject to inflation. This 60% value appears to be representative of non-capital associated costs (such as labor) which are involved in coal mining. Naturally if coal were purchased on the open market, rather than by long-term contract, the full cost of coal would demand escalation.

As Figure 5 illustrates, a point is reached (in this case at about nine years) where the cost of fuel oil exceeds the price of K-T gas. More thorough analysis involving different inflation rates has usually indicated that the average cost of K-T gas or the present worth cost of K-T gas turns out to be lower than the cost of alternate fuels over the 20 year period. This more detailed analysis is beyond the scope of this paper. As previously mentioned this type of long term analysis is difficult and the intent of presenting Figure 5 is merely to show relative effects of price escalation which are difficult to generalize, yet important to consider. The implication is that strictly from a cost standpoint there can be sound financial basis for present investment in a gasification plant.

FIGURE 1

EFFECT OF COAL COST ON GAS COST

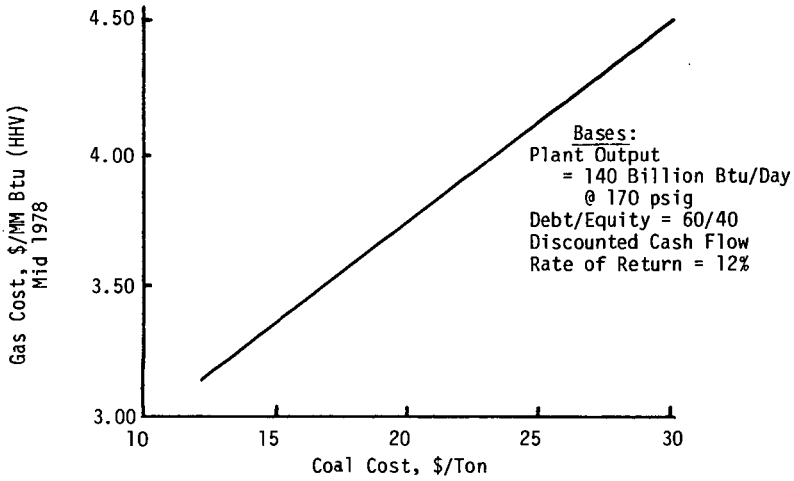

FIGURE 2

EFFECT OF CAPITAL STRUCTURE ON GAS COST

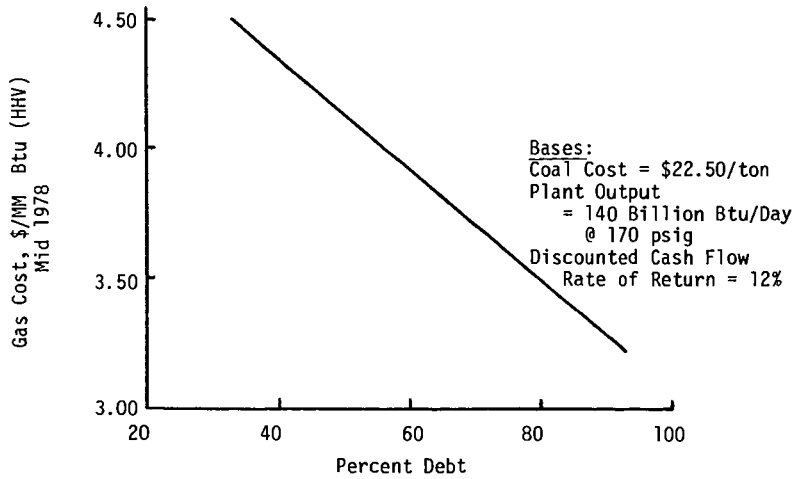

FIGURE 3

EFFECT OF COAL COST
ON AMMONIA COST

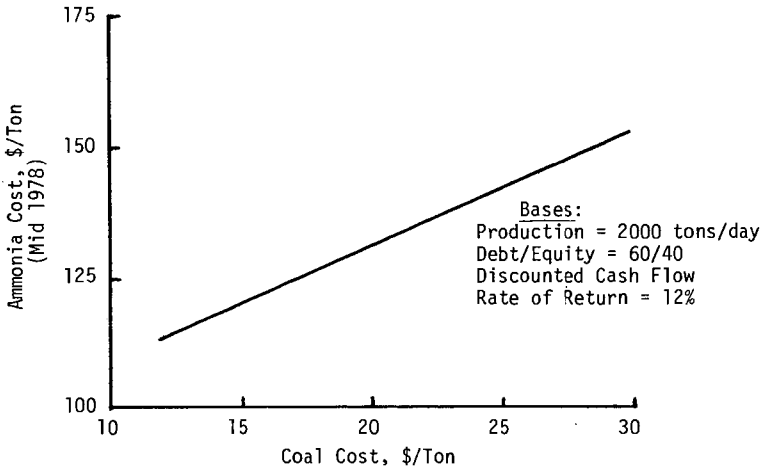

FIGURE 4

EFFECT OF CAPITAL
STRUCTURE ON AMMONIA COST

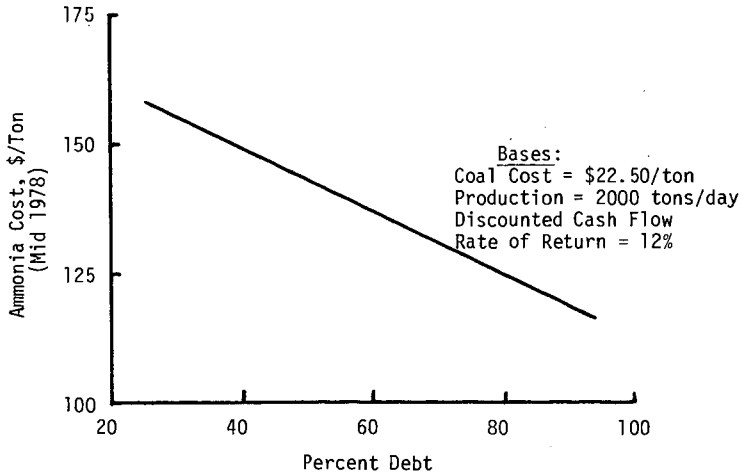

FIGURE 5

EFFECT OF PRICE ESCALATION
ON FUTURE FUEL COSTS

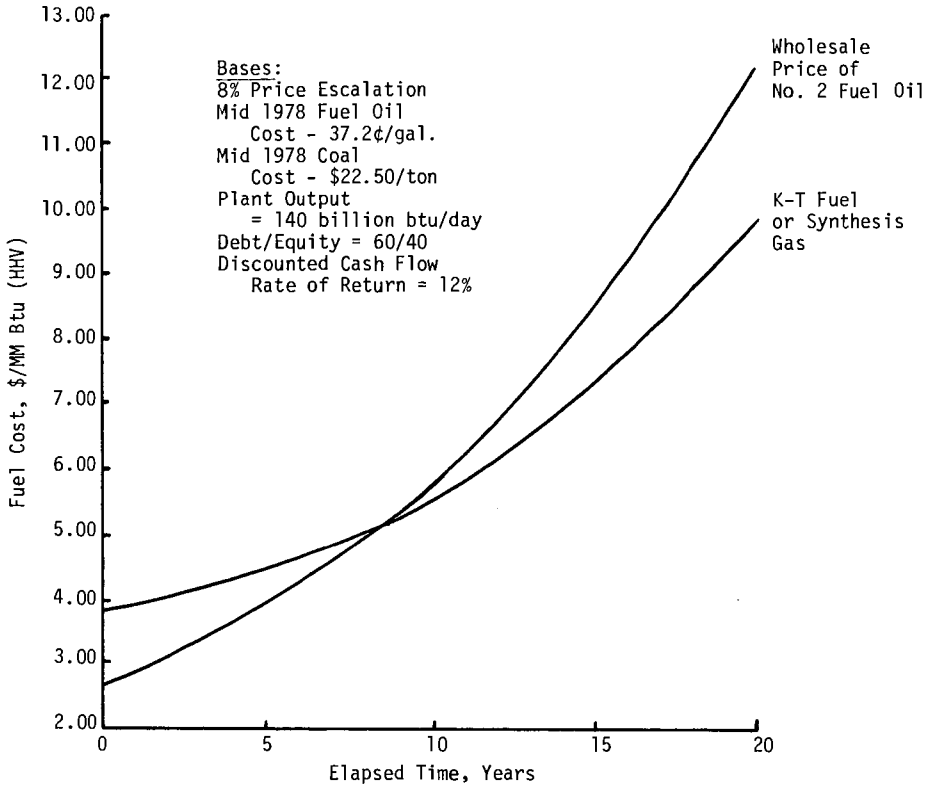

References:

1/ "Forecast of Capital Requirements of the U.S. Gas Utility Industry to the year 2000," A.G.A. Monthly, April, 1978.

2/ "Alaska Gas Pipeline," Wall Street Journal, March 6, 1978.

3/ Koppers Co. survey of industrial customers.

4/ "LNG Projects Approved; Policy Debated," Oil & Gas Journal, January 9, 1978.

5/ A.G.A. Monthly, February, 1978, p. 4.

6/ "How Six Coal Gasification Processes Compare Economically," Pipeline & Gas Journal February, 1977. Based on study by C.F. Braun & Co.; Costs are escalated at 6% to 1978 basis.

7/ Michaels, H.J., Leonard, H.F., "Hydrogen Production Via the K-T Process: Current Economic and Technological Aspects," AICHE 85th National Meeting, Philadelphia, June 4-8, 1978.

ECONOMICS OF THE H-COAL® PROCESS

John G. Kunesh, Michael Calderon, Gabriel A. Popper,
Marvin S. Rakow

Hydrocarbon Research, Inc.
P.O. Box 6047
Lawrenceville, New Jersey 08648

INTRODUCTION

The escalating cost of energy in the U.S. has stimulated an intensive interest in alternate sources. However, even if major breakthroughs are made in such areas as magneto-hydrodynamics, fusion and solar power, the need for liquid and gaseous fuels for transportation, home heating and existing power plants will be with us until well past the year 2000.

Coal liquefaction offers the potential of substantially reducing the balance of payments deficit while utilizing the enormous U.S. coal reserves which are otherwise environmentally unacceptable. HRI's H-Coal® Process is on the verge of being economically competitive with imported oil, particularly in the central portions of the United States. The studies reported herein start from two basic overall plant integration schemes and then examine the sensitivity of the required fuel oil price to some of the more probable expected variations in process and financial parameters.

H-COAL

The H-Coal Process developed by Hydrocarbon Research, Inc., a subsidiary of Dynalectron Corp., is a direct catalytic hydroliquefaction process. It has been under development since 1963 and has accumulated over 53,000 hours of experimental operation in 25 lb/day bench units and a 3 ton/day Process Development Unit. A 600 ton/day Pilot Plant is currently under construction in Catlettsburg, Kentucky adjacent to the Ashland Oil Co. Refinery. The Pilot Plant project is sponsored by the U.S. Department of Energy, The Electric Power Research Institute, Standard Oil Co. (Indiana), Mobil Oil Corp., Conoco Coal Development Co., Ashland Oil, Inc. and the Commonwealth of Kentucky.

In the H-Coal process, crushed and dried coal is slurried with recycle oils, mixed with hydrogen and liquefied in direct contact with catalyst in an ebullated bed reactor. The reactor effluent is separated into recycle and net product streams in conventional processing equipment. Conversion and yield structure are determined by reactor conditions, catalyst replacement rate and recycle slurry oil composition. The studies reported in this paper are based on an operating severity which produces an all-distillate product. This mode of operations produces a product slate which meets current EPA sulfur specifications without further hydrotreating. Plant size was set at 25,000 TPD coal to the liquefaction section to be consistent with other previously published studies.(1)

In optimizing the overall process flow scheme, the means by which the required hydrogen is manufactured is a very important variable. The two primary alternates are steam reforming of the

light gases made in the liquefaction step (a proven process) and partial oxidation of the mixture of ash, unconverted coal and residuum which comes from the bottom of the H-Coal vacuum distllation unit (under development). A second key factor is whether the liquefaction facility purchases power or generates its own. A final significant item is whether there is a customer for the net product gas.

In the present study, two base cases were generated. These are summarized in Table I. Both cases assume on-site power generation. In Case I, the operating severity is adjusted such that the vacuum bottoms, when fed to partial oxidation, put the plant into hydrogen balance. Plant fuel comes from internal streams and net gas is assumed saleable at $2.50/MM Btu. In Case II, the bottoms are carbonized and the resultant coke is fed to the power plant. Excess coke is gasified to prouce a low Btu fuel gas for use in the plant. H_2 is produced by steam reforming. As may be seen, the partial oxidation case has a slight economic advantage for the assumptions used. Table II gives the product properties for the two cases. The net gas produced via Case I does not meet interstate pipeline interchangeability specifications. For purposes of this study, the gas was assumed saleable as-is to an industrial customer. If this is not possible, the net gas can be sent to cryogenic purification with C3 and C4 being recovered as saleable liquid products, and a net interchangeable gas being produced with some hydrogen being recycled to the process. The effect of this additional processing can be accounted for in the value assigned to the mixed off-gas as opposed to final product values. This also applies to product gas transporation cost.

SENSITIVITY TO CAPITAL COST ESTIMATE

Because of the many assumptions required for studies of this type, a series of single variable senstitivty analyses were run. The first, and most obviously needed, is the sensitivity to error in the capital investment. Figure I shows the required fuel oil selling price to yield 10% DCF on equity versus percentage change in total capital investment. With gas at $2.50/MM Btu inflation from 1976 to the present appears to give the edge to steam reforming. If net gas can be sold for $3.50/MM Btu, reforming is always the more expensive alternative. This is based on the assumption that bottoms must be utilized on site, by gasification if necessary.

SOURCE AND COST OF POWER

Most of the commercial studies to date have assumed that power must be generated on site. The cases presented herein adhere to this position. There are two main reasons for including power generation in the facility:

1. It is generally assumed that the plant will be located adjacent to a new coal mine. It may, therefore, be impractical, or at least inordinately expensive, to bring in the required power.

2. This facility is estimated to require about 200 megowatts. Even in an industrialized area, this may be more than the local utility can supply.

In order to evaluate the effect of purchased versus generated power, the following assumptions were made:

1. If power can be purchased, gas can be sold.

2. If power can be purchased, carbonized bottoms can be sold. The value of the coke was set using the AGA-DOE guidelines for gasifier chars as 75% of the fuel value of the feed coal: in this case, $0.50/MM Btu.

Figure 2 gives the results of this comparison. The required oil selling price to yield a 10% DCF on equity is plotted against cost of the purchased power at various selling prices for net gas. The horizontal lines represent on-site power generation. As may be seen, reforming with bottoms coke sold at 50¢/MM Btu and partial oxidation with gas worth $2.50/MM Btu both have about the same break even point with purchased power at about 4-1/4¢/Kwh. At $2.50/MM Btu for gas, if power costs less than 4-1/4¢/Kwh, it is always economically attractive to purchase if it is available. If partial oxidation is chosen for H2 generation and the net gas is worth $3.50/MM Btu, purchased power is preferred even if its cost is above 5¢/Kwh.

EFFECT OF PRODUCTS PRICE STRUCTURE

The choice of hydrogen generation processes as well as the decision as to which internal streams should be used as plant fuel are obviously very dependent on the relative value of the various product streams. In Figure 3, the required fuel oil selling price for a 10% DCF return on equity is plotted against naphtha selling price. In addition to the steam reforming case, partial oxidation cases are shown for product gas valued at $2, $2.50 and $3.00/MM Btu, respectively. If the by-product gas is saleable at $2.00/MM Btu or less, steam reforming is the more economical route. With gas valued at $2.50/MM Btu, partial oxidation is preferred to steam reforming when the naphtha value is equal to or greater than the fuel oil.

EFFECT OF COAL PRICE

Coal price is a direct pass through to product price. Because slightly different final product slates (in terms of total barrels per ton) are obtained from the partial oxidation and reforming schemes, coal prices does not affect the two cases in exactly the same manner. Figure 4 shows the required oil selling price versus coal cost for the reforming case and the partial oxidation case with gas valued at both $2.50 and $3.50/MM Btu. With gas at $2.50/MM Btu, reforming becomes preferable at a coal cost at or above $20/ton. With gas valued at $3.50/MM Btu, partial oxidation is preferred.

ECONOMIC MODEL

Because coal liquefaction is very capital intensive, the economic model, in terms of debt/equity ratio, interest rates, DCF and other financial fctors, has a tremendous effect on the required fuel oil selling price. All computations done to this point have used a 55/45 debt/equity ratio, an 8% interest on debt and a 10% DCF return on equity. Figure 5 gives the effect of the debt equity ratio on the required fuel oil selling price. As

would be expected, increasing debt ratio decreases the fuel oil price. The quantitative effect is quite pronounced in that a change from 40 to 80% debt decreases the fuel oil price by about $2.50/Bbl. Figure 6 shows the effect of required DCF[3] return on equity on fuel oil selling price. Again the effect is significant and expectably almost linear. An increase of 2% in the required return on equity at the 45% equity level raises the required oil selling price by about $1.50/Bbl. These computations reinforce the assertions made by many that the construction of the liquefaction plants is sensitive to the terms and conditions of financing and to taxation policy.

CONCLUSION

These studies show the economic effect of a number of factors which are site specific. Thus, the overall plant confirguration cannot be finally optimized until a reasonably firm location is selected.

COMMERCIALIZATION

A 600 ton per day H-Coal Pilot Plant is currently under construction in Catlettsburg, Kentucky. Operation is scheduled to begin in the first quarter of 1975. The normal commercialization process might wait until Pilot Plant operations were completed before moving ahead. However, the operations on the 3 TPD Process Development Unit have confirmed the operability of the basic process and the real function of the Pilot Plant is equipment testing and fine-tuning of the engineering. Therefore, the commercialization process can be accelerated by immediately beginning such activities as site selection, permit acquisition and preliminary process design. Changes to the yield structure due to the scale difference between the PDU and Pilot Plant will probably not be much greater than the yield variation observed in different batches of coal from the same seam. Therefore, preliminary engineering can begin immediately; this would reduce the commercialization timetable by as much as two years. If such a procedure is followed, a commercial H-Coal plant could be onstream by 1983.

ACKNOWLEDGMENTS

The authors wish to express their appreciation to the Department of Energy, the Electric Power Research Institute, Ashland Oil, Inc., Standard Oil Company of Indiana, Conoco Coal Development Company, Mobil Oil Corporation and the Commonwealth of Kentucky, and to the Dynalectron Corporation for support and assistance in the development of the H-Coal Process.

REFERENCES

1. "H-Coal® Commercial Evaluation", by Fluor Engineers and Constructors, Inc., ERDA Contract No. 49-18-2002.

FIGURE 1. SENSITIVITY TO CHANGES IN CAPITAL

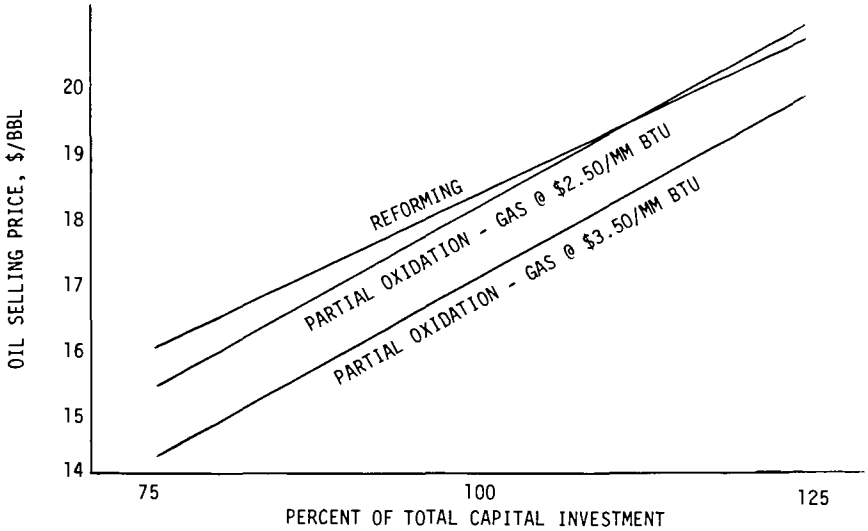

FIGURE 2. EFFECT OF PURCHASED POWER COST

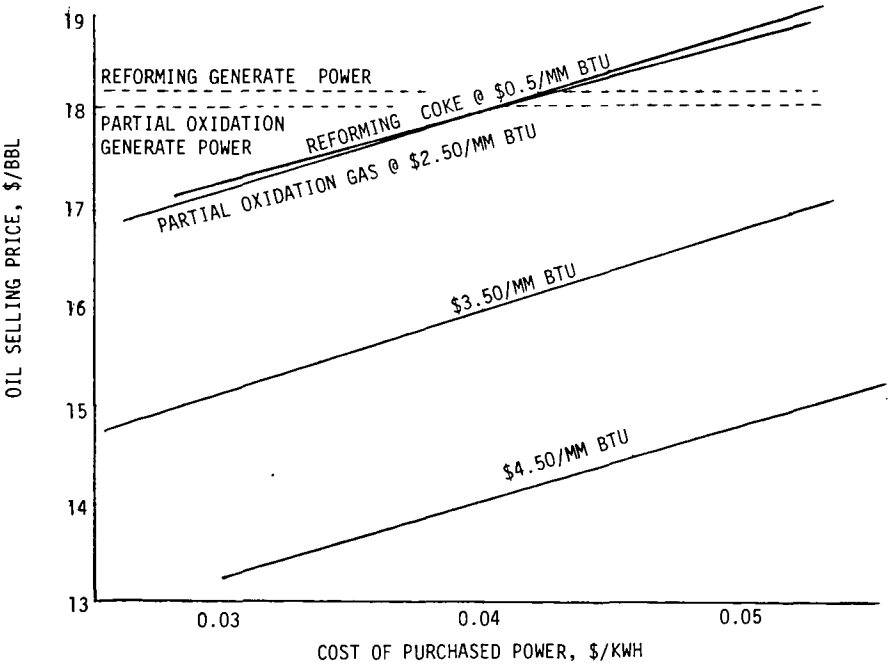

FIGURE 3. EFFECT OF NAPHTHA PRICE AND BY-PRODUCT GAS ON THE ECONOMICS OF DISTILLATE PRODUCTION

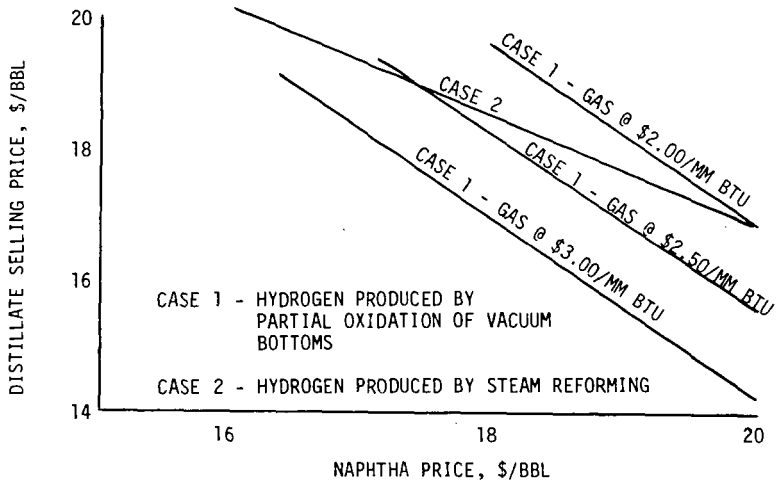

FIGURE 4. EFFECT OF COAL PRICE

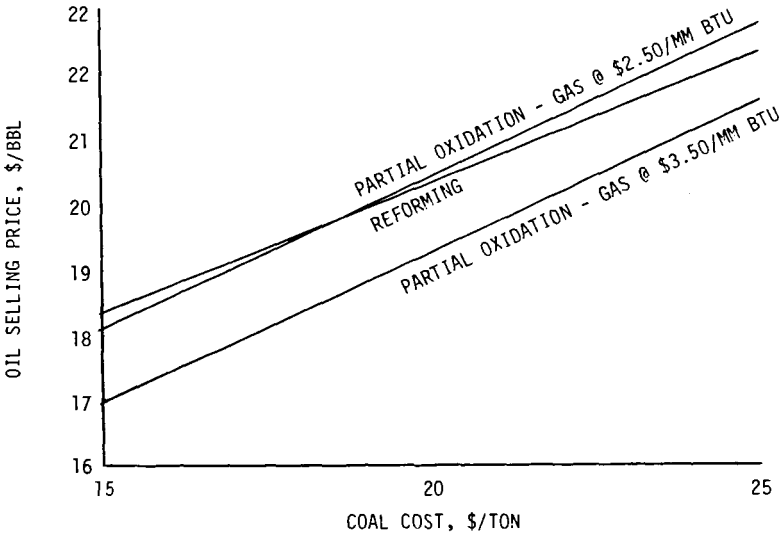

FIGURE 5. EFFECT OF DEBT/EQUITY RATIO

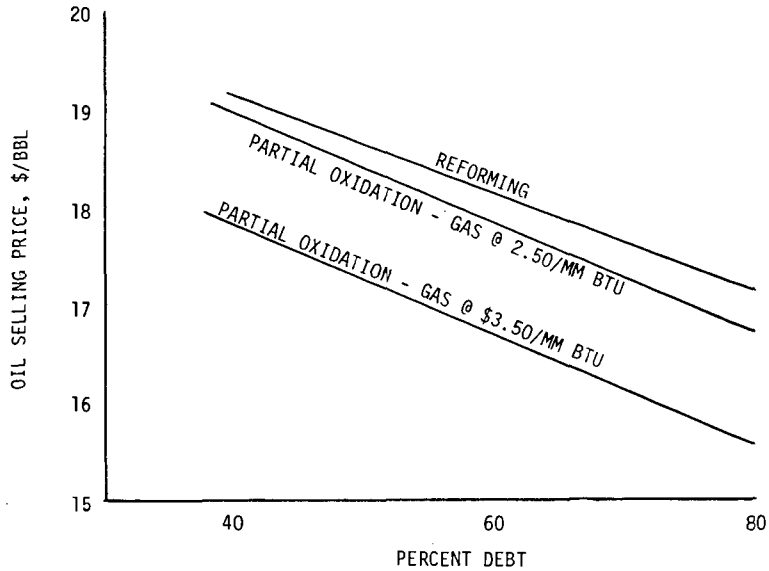

FIGURE 6. EFFECT OF DCF RATE OF RETURN

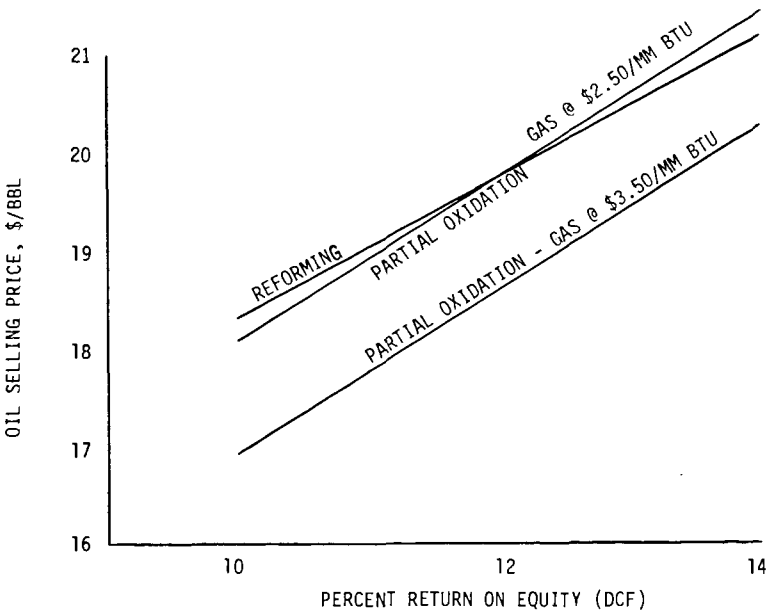

TABLE I

RESULTS TO DATE OF ALL-DISTILLATE

PRODUCTION CASES

Basis: 25,000 T/D coal to hydrogenation
Coal price = $15/Ton, as-received
10% DCF return on equity, 8% interest on debt
Debt/Equity = 55/45
Naphtha value = fuel oil value
By-product gas value = $2.50/MM Btu
Power generation on site
1976 prices used for capital estimates

	Case 1	Case 2
Hydrogen produced by	Partial Oxidation	Steam Reforming
Plant Products		
Naphtha, B/D	35,700	32,200
Distillate fuel oil, B/D	27,200	39,400
Gas, MMM Btu/D (HHV)	70	---
Total depreciable capital investment, $MM	1180	1160
Anhydrous NH_3, ST/D	245	245
Lump sulfur, LT/D	690	708
Thermal efficiency, HHV, %	68.5	67.0
Contribution to Total Oil Selling Price, $/Bbl		
Coal	6.74	5.92
River water	.12	.09
Catalyst and chemicals	.74	.66
Labor, supervision and overhead	.66	.63
Maintenance	1.80	1.56
Insurance and taxes	1.57	1.35
Total Operating Cost	11.63	10.21
Capital-related expense	9.95	8.64
By-product credit	- 3.51	- .59
Total Oil Selling Price	18.07	18.26

TABLE II

SUMMARY OF PRODUCT PROPERTIES IN CASES STUDIED TO DATE

	Case 1 Partial Oxidation	Case 2 Steam Reforming
IBP-400 F Naphtha		
°API	47.0	49.6
Higher Heating Value, MM Btu/Bbl	5.53	5.50
400-975 F Distillate		
°API	21.3	13.5
Wt % Sulfur	0.08	0.12
Higher Heating Value, MM Btu/Bbl	6.13	6.31
Volume %		
400-650 °F	89.6	63.5
650-975 °F	10.4	36.5
Gas		
Higher Heating Value, Btu/SCF	1114.0	
Composition, Vol. %		
H_2	28.8	
N_2	2.9	
C_0	2.1	
C_1	37.7	
C_2	16.0	
C_3	7.8	
C_4+	4.7	
	100.0	

RECENT DEVELOPMENTS ON THE SMALL GASIFIER

ROBERT W. CULBERTSON
STANLEY KASPER

DRAVO CORPORATION
ONE OLIVER PLAZA
PITTSBURGH, PENNSYLVANIA 15222

During the years prior to World War II, thousands of gas producers of the Wellman-Galusha type were utilized in the United States to convert coal to low BTU gas. These so called "small gasifiers" produced gas for all types of utility and industrial applications.

After World War II, the gas transmission system was expanded bringing low cost natural gas to eastern markets. The small gasifier could no longer compete and these installations were closed until only three still operate.

The energy bill presently being worked on by Congress includes provisions to deregulate the price of natural gas. It therefore appears that the small gasifier may once again become competitive and could provide a substantial volume of industrial fuel gas for use by American industry.

In the spring of 1976, DOE initiated a program to demonstrate the utilization of low BTU gas in industrial applications. A total of six (6) projects were undertaken with partial funding by the Federal Government. Four commercially available small gasifiers are being utilized:

1.	The Wellman-Galusha	Three (3) Projects
2.	The STOIC	One (1) Project
3.	The Wellman-Incandescent	One (1) Project
4.	The IGI	One (1) Project

The coals include anthracite as well as bituminous from Wyoming, Utah and Eastern Kentucky. The applications are:

1. Fuel for brick kilns.
2. Boiler feed for space heating of campus buildings.
3. Boiler feed for heating and cooling of housing, shopping centers, schools, industrial park, etc.
4. Boiler feed for process steam and spray drying of milk whey.
5. Fuel for tunnel kilns and dryers.
6. Fuel for an industrial park.

The range of gas clean-up for these projects is:

1. Hot raw gas (no treatment after leaving gasifier).
2. Gas that has tar and particulates removed.
3. Gas with complete clean-up including desulfurization.

In addition to these federally funded projects several privately funded commercial projects have gotten underway.

Let's take a detailed look at the "small gasifier":

Figure 1 shows the Wellman-Galusha gasifier.

In addition to the types mentioned above, other small gasifiers include Wilputte and Riley Morgan.

This equipment is a self-contained unit and requires no investment for a boiler plant when producing low BTU gas. Adequate provision for steam for gas making is included in the engineering design of the plant. Ample fuel and ash storage bins are provided as an integral part of the unit. This fixed bed gasifier operates at atmospheric pressure.

A two compartment fuel bin forms the top of the machine. The upper section is a storage bin and is usually filled by a bucket elevator. The lower compartment is separated from the upper compartment by disc valves through which fuel is fed as required. Similar valves cover the entrance of each of the

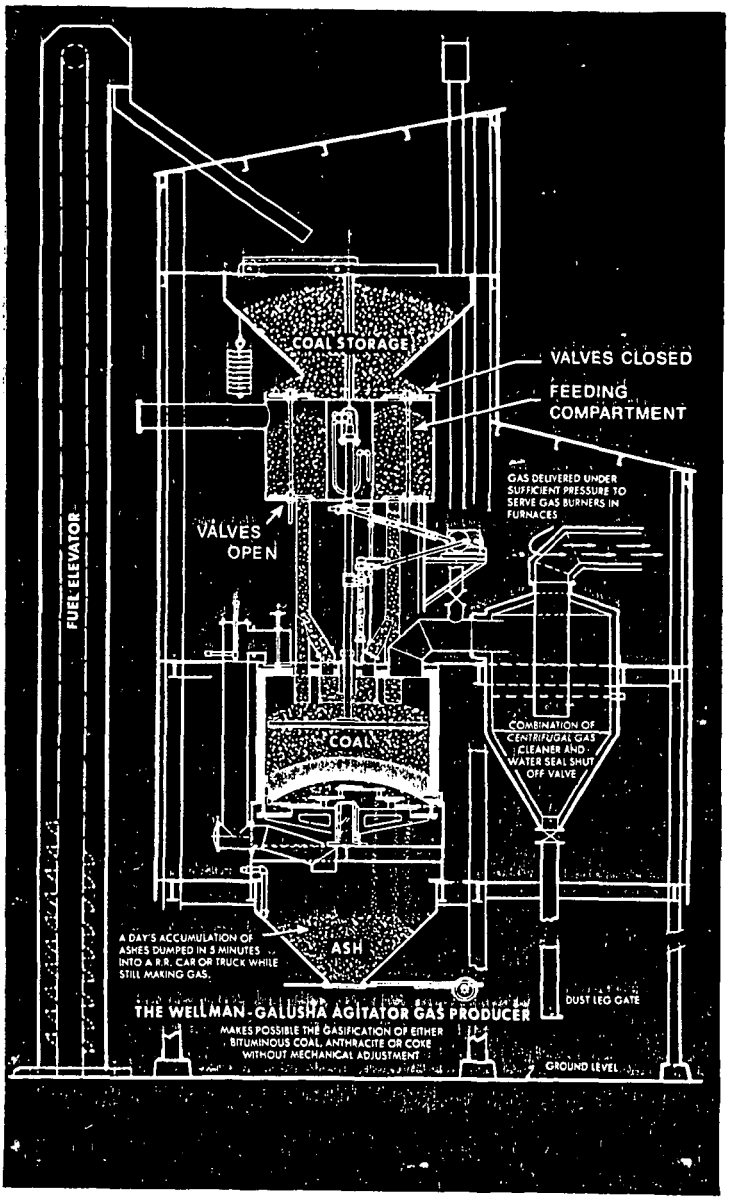

FIGURE 1. *Wellman-Galusha Agitator Type Gas Producer*

heavy steel pipes connecting the lower bin to the fire chamber. Fuel from the lower bin flows continously through these feed pipes to fill the fire chamber.

Fuel feed pipe valves are normally open, but for brief intervals they are closed, during which time the upper valves in the lower compartment are open in order to fill the feeding compartment with fuel. A simple interlocking mechanism prevents the opening of the upper valves unless all lower valves are tightly closed. It also prevents opening any lower valves while any top valve is open. This prevents the escape of gas from the gas making chamber through the coal compartments to the atmosphere.

The gas making chamber is completely water jacketed. Waste heat in the water jacket generates steam required for making gas. Steam and air are introduced at the bottom of the bed. The bed is supported by revolving grates through which dry ash is continously ejected to the ash hopper.

A slowly revolving water cooled horizontal arm, which also spirals vertically below the surface of the fuel bed, retards channeling and maintains a uniform fuel bed. This facilitates the production of uniform quality gas.

Raw gas containing particulates, tars, oils, hydrogen sulfide, etc., leaves the gasifier at a temperature of between 800°F and 1250°F.

These small gasifiers are designed to produce either low BTU gas or intermediate BTU gas. Low BTU gas has a heating value of approximately 150 BTU/SCF and is produced by using air in the gasifier. Intermediate BTU gas has a heating value of approximately 300 BTU/SCF and is produced by using oxygen in the gasifier. For comparison purposes, natural gas of pipeline quality has a heating value of approximately 1000 BTU/SCF.

Figure 2 is a simplified flow diagram showing the various processing steps in the manufacture of clean gas from receipt of coal through sulfur removal.

Table 1 summarizes the capital costs and operating costs of small gasifier systems. There are sixteen (16) cases considered: 1A, 1B, 1C and 1D; 2A, 2B, 2C and 2D; 5A, 5B, 5C and 5D; 10A, 10B, 10C and 10D. The numbers indicate the number of gasifiers in the plant - one, two, five or ten. The letters A, B, C and D refer to the type of gas produced and the type and cost of coal used. Cases A and B are air-blown gasifiers which produce low BTU gas - about 150 BTU per cu. ft. Cases C and D are oxygen-blown gasifiers which produce medium BTU gas - about 300 BTU per cu. ft. In cases A and C high sulfur coal at $25 per ton is utilized while in cases B and D low sulfur coal at $35 per ton is used.

The second line of Table 1 shows the Coal Feed to the system in tons per day of sized coal (2" x 1-1/4"). Several things should be noted: the effect of modules and the effect of the use of oxygen. The coal usage in the 2, 5, and 10 gasifier cases is 2, 5 and 10 times that of the comparable single gasifier cases. When oxygen is used instead of air, the coal feed (and resultant BTU conversion) is substantially increased - 132 tons per day versus 78 tons per day for the single gasifier cases.

The information relevant to Gas Production is shown on the next three lines of the Table: millions of standard cubic feet per day produced; the heating value of the gases produced (158 BTU per cu. ft. air-blown and 285 BTU per cu. ft. for oxygen-blown); and the total BTU produced in billions per day.

You will note that almost 40% more BTU are produced for a given number of gasifiers by using oxygen instead of air.

The next line shows the land area required. These land requirements are based on storing 30 days coal supply.

The line "Total Plant Investment" in current dollars, includes coal storage and handling, gasification, particulate removal, tar removal, ash disposal, and waste water treatment and disposal.

For Cases A and C (High Sulfur Coal), sulfur removal facilities are also included. Cases C and D (Oxygen-blown Gasifier), oxygen plants are required. In all cases, Total Plant Investment includes an Administration and Maintenance

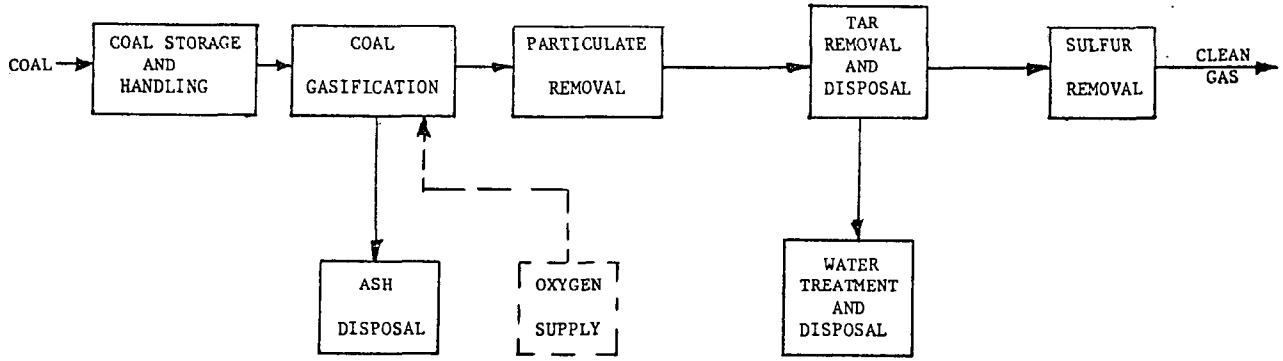

FIG. 2 COAL GASIFICATION (LOW AND INTERMEDIATE BTU GAS)

TABLE 1

SMALL GASIFIERS COST INFORMATION

CASE	1A	1B	1C	1D	2A	2B	2C	2D	5A	5B	5C	5D	10A	10B	10C	10D
GASIFIER (10' Dia.) Qty.	1	1	1	1	2	2	2	2	5	5	5	5	10	10	10	10
COAL FEED (2" x 1 1/4") T/Day	78	78	132	132	156	156	264	264	390	390	660	660	780	780	1320	1320
GAS PRODUCTION																
SCF/DAY (DRY) MM	10.09	10.38	7.84	7.96	20.46	20.76	13.67	15.93	50.44	51.9	39.20	39.8	100.88	103.8	78.41	79.6
HEATING VALUE (DRY BTU/SCF	158	158	285	285	158	158	285	285	158	158	285	285	158	158	285	285
BTU/Day x 10^9	1.59	1.64	2.23	2.27	3.23	3.28	4.47	4.54	7.97	8.2	11.17	11.35	15.94	16.4	22.35	22.7
AREA REQUIRED ACRES	3.2	2.8	3.6	3.3	3.2	2.8	3.6	3.3	6.0	5.5	6.6	6.1	7.4	6.5	8.9	8.0
TOTAL PLANT INVESTMENT MM$	4.77	3.07	7.92	5.73	7.02	4.63	12.39	9.53	11.89	8.62	22.35	18.22	18.28	13.92	36.92	31.47
ADJUSTED PLANT INVESTMENT MM$	4.06	2.24	6.81	4.63	5.99	3.66	10.80	7.98	9.84	6.58	18.72	14.62	15.00	10.68	30.98	25.56
EST. GAS COST (PRICES)																
(1) Total Investment, Utility Financing	4.09	3.62	5.35	5.11	3.18	3.15	4.61	4.67	2.66	2.75	3.97	4.23	2.37	2.57	3.70	4.04
(2) Adjusted Plant Investment ** Utility Financing	3.93	3.45	5.17	4.93	3.07	3.04	4.44	4.55	2.56	2.66	3.85	4.11	2.29	2.50	3.59	3.94
(3) Total Investment 100% Equity 20 Yr. Depreciation No Profit	3.35	3.14	4.45	4.44	2.63	2.77	3.86	4.11	2.27	2.46	3.44	3.78	2.06	2.32	3.25	3.64
(4) Adjusted Plant Investment ** 100% Equity 20 Yr. Depreciation No Profit	3.28	3.06	4.37	4.37	2.58	2.72	3.80	4.06	2.23	2.42	3.39	3.73	2.03	2.29	3.21	3.60

BASIS

Case A - High (3%) Sulfur Coal @ $25/ton with Air-Blown Gasifier
Case B - Low (0.7%) Sulfur Coal @ $35/ton with Air-Blown Gasifier
Case C - High (3%) Sulfur Coal @ $25/ton with Oxygen-Blown Gasifier
Case D - Low (0.7%) Sulfur Coal @ $35/ton with Oxygen-Blown Gasifier

**Administration Building and Waste Water Treatment Facilities Deleted

Building, but excludes land costs. For all cases, it is assumed that needed utilities will be purchased. Therefore, no capital costs are included for cooling water, steam generation and compressed air facilities.

It is expected that Small Gasifier Facilities will be generally located near an existing industrial facility. Therefore, in many cases waste water treatment facilities will exist as well as suitable office space for administration and maintenance facilities. The line Adjusted Plant Investment reflects the deletion of these items from Total Plant Investment.

The last group of numbers, Estimated Gas Costs, are most significant to anyone considering building a coal gasification facility. They have been calculated on four different bases. The first line, (1), results from use of the Utility Financing Method as outlined in ERDA's Gas Cost Guidelines. The costs stated are average gas costs and entail use of the following parameters:

1. 20-year project life.
2. 20-year straight-line depreciation on plant investment, allowance for funds used during construction and capitalized portion of start-up costs.
3. Debt-equity ratio of 75/25.
4. Percent interest on debt of 9 percent.
5. Percent return on equity of 15 percent after taxes.
6. Federal income tax rate of 48 percent.

ERDA maintenance costs are proportional to the plant section investment

1. 6 percent for coal feed preparation, coal gasification, gas quench and solids removal.
2. 3 percent for sulfur recovery, product gas compression and drying, oxygen plant, liquid and solid effluent treating and water treating.
3. 1 percent for all other offsites.

We used 3 percent of total plant investment as a simplification.

Included in the total capital requirements are:

1. Estimated installed cost of both onsite and offsite facilities.
2. Project contingency at 15 percent of the estimated cost of the facilities.
3. Initial charge of catalyst and chemicals.
4. Paid-up royalties.
5. Allowance for funds used during construction.
6. Start-up costs.
7. Working capital.

Operating costs are based on a 90 percent plant service factor. Included in operating costs are:

1. Purchased utilities.
2. Raw materials
3. Catalysts and chemicals.
4. Purchased water.
5. Labor.
6. Administration.
7. Supplies.
8. Local taxes and insurance.
9. Ash disposal.

No credit is taken for byproducts such as sulfur, tars, oils, etc. As stated above, it is assumed that power, steam and water will be purchased. The cost of power is 2.7¢ per KW hour. Steam cost is assumed to be $3.14 per 1000 pounds. Cooling water is 3.8¢ per 1000 gallons and make-up water 40¢ per 1000 gallons.

The gas costs resulting from these calculations range from $2.37 per million BTU for the 10 air-blown gasifier system to $5.35 for the single oxygen blown gasifier system. These gas costs are based on the Utility Financing Method and are slightly different from the costs which result from incorporating

commercial financing considerations and private investor return requirements.

The same parameters and method of calculation were used to determine the gas costs shown on the next line, (2), Adjusted Plant Investment, Utility Financing. As indicated above, the Adjusted Investment refers to the deletion of the Administration Building and Waste Water Treatment Facilities from the Gasifier System. Costs for comparable cases are slightly reduced as expected.

Providing 100% equity with zero return on investment results in substantially lower gas cost as shown on line (3) - the range of costs is from $2.06 per million BTU to $4.45 per million BTU.

With adjusted investment, these gas costs are reduced even further as shown on line (4).

Some general conclusions can be drawn from the gas cost calculations:

1. The larger the plant, the lower the cost of the gas produced.
2. The cost of 150 BTU gas is less than the cost of 300 BTU gas.
3. The cost of producing gas by this small gasifier system is lower than any other known technology. This has been substantiated by studies performed by Dravo on facilities up to approximately 25 billion BTU per day. Indications are that the small gasifier is competitive for facilities of considerably higher capacities.

All of the costs discussed so far have been applied to the battery limits of the gasifier facility.

When an existing plant is converted from use of natural gas to either 300 BTU gas or 150 BTU gas changes must be considered in burners, fuel gas piping, instruments, flue gas piping, compressors, forced and induced draft fans, exhaust stocks, etc. This is necessitated by the changes in fuel gas volume, flue gas volume and flame temperatures.

Special precautions must be taken with respect to the toxicity of the gas produced. Both 150 BTU gas and 300 BTU gas contain large percentages of carbon monoxide which is colorless and odorless. The toxic effects of this gas depend on the concentration level and time of exposure. The distribution system, therefore, should include valving and alarms as well as the use of an odorant.

The feasibility study for a given application should include not only the costs of producing the fuel gas, but also the costs of adapting the existing plant to its use. The small gasifier should not be considered the answer to every coal gasification problem. As the size of the facility increases other processes such as Lurgi, Koppers-Totzek and Babcock and Wilcox must be considered. When second generation technology has been proven those processes also must be considered.

At the present time, however, the small gasifier is a realistic answer for many industrial plants. The distribution and retrofit costs and the applications of the gas along with the battery limits costs will determine whether the gas produced should be 150 BTU or 300 BTU. The degree of "clean-up" of this gas will depend upon environmental regulations, process requirements and the coal used.

THE ECONOMICS OF ELECTRICITY AND SNG FROM IN SITU COAL GASIFICATION

W. C. Ulrich, M. S. Edwards, and R. Salmon*

Abstract

Conceptual process designs and cost estimates are presented for two potential applications of underground coal gasification: a 900 MW(e) combined-cycle electric generating plant fueled by low-Btu gas, and a substitute natural gas (SNG) plant producing 155 MMscfd of 954 Btu/scf gas. Designs were based on experimental data obtained at the Laramie Energy Research Center on subbituminous coal using the linked vertical well in situ gasification process. Respective capital investments were estimated to be $395 and $351 million in first-quarter 1977 dollars. Product prices were calculated as a function of the debt/equity ratio, the annual earning rates on debt and equity, the cost of coal, and plant factor (onstream efficiency). Using a debt/equity ratio of 70/30, an interest rate on debt of 9%, an after-tax earning rate on equity of 15%, and a coal feed cost of $5/ton, product prices were 24 mills/kWh for electricity at 70% plant factor and $2.89/10^6 Btu for SNG at 90% plant factor. Calculated overall thermal efficiencies for the two facilities were 24 and 38% respectively, based on in-place coal.

Introduction

This paper describes two conceptual plants designed for utilizing gas produced from a linked vertical well (LVW) in situ coal gasification process and gives results of economic evaluations based on the designs. The two plants are a 900 MW(e) combined-cycle electric generating plant fueled by low-Btu gas, and a substitute natural gas plant producing 155 MMscf/day of 954 Btu/scf gas.

The facilities are assumed to be located in southern Wyoming. The design coal is subbituminous. Air injection is used for the low-Btu gas case, and a steam/oxygen mixture for the SNG case.

The two cases presented here are not evaluated as competitors with each other, but are intended to represent two possible modes of utilization of underground coal gasification.

This work was done for the Office of Program Planning and Analysis, DOE/Fossil Energy, and reported in ORNL-5341. (1)

Linked Vertical Well Process

There are several modes in which the LVW process can be operated for large-scale gas production. These different operational modes arise

---

* Work performed at Oak Ridge National Laboratory, Oak Ridge, TN 37830.

primarily from variations in the well sequencing patterns used, and the direction in which the coal seam is gasified relative to the direction of injection gas and product gas flow. The system illustrated by Fig. 1 is termed the direct-flow or forward system because the direction of gasification of the coal seam is the same as the direction in which the injection gas and product gas travel. (2) The well sequencing pattern that develops is such that each borehole is used successively for linking, production, and injection.

If air is injected, the product is a low-Btu (100 to 200 Btu/scf) gas. The LVW process is also potentially capable of using an injection gas consisting of a mixture of steam and oxygen, in which case the product would be an intermediate-Btu (200 to 400 Btu/scf) gas.

The procedure shown in Fig. 1 was suggested by researchers at the Laramie Energy Research Center (LERC) to be used for development of the field areas of the conceptual plant designs evaluated in this report. It should be pointed out that large-scale operation of this system has not yet been demonstrated at LERC, although it was used by the Russians at the Podmoskovnaya and Shatskaya underground coal gasification stations. In LERC tests to date, reverse combustion linking has been followed by air injection for forward gasification through the same well used for the linking air injection. Steam-oxygen injection has not yet been demonstrated by LERC, but a three-day injection at Hoe Creek by Lawrence Livermore Laboratory (LLL) subsequent to air injection was successful. LERC and LLL work has been completed thus far only in two-well systems.

Process Descriptions and Flow Diagrams

The plants are divided into three major parts: (1) field development, (2) gas transfer piping, and (3) main plant. Well drilling and gasification operations are carried out in the field development areas. The gas transfer piping systems, which may be a mile or two in length, connect the field development areas with the main plant areas. The main plant areas contain the major gas treating process units, power plants, and utilities systems required to form complete, self-sufficient facilities.

Low-Btu Gas Combined-Cycle Electric Generating Plant Case

For this case, the raw low-Btu gas from the wells is cleaned, compressed, and burned in gas turbines connected to electrical generators. Hot exhaust gases from the turbines are directed to heat-recovery boilers to generate 1000 psig/1000°F steam which drives turbine generators for additional electricity production.

At design throughput [900 MW(e)], 48 producing wells are on-line. These 48 wells are arranged in six parallel trains of eight wells each. Each train requires eight injection wells and eight linking wells, so that a train consists of a total of 24 wells.

Field development plan

Initial production starts with only one train of wells. The remaining five trains are brought on-line at intervals of roughly two weeks. A well has a producing lifetime of about 73 days. As each row of wells is exhausted, the train is moved to the next adjacent row. For a given train, these moves occur at 12-week intervals. Since there are six trains, a move takes place every two weeks. Shortly after the sixth train is brought on stream, the first train is shut down. During the

ensuing 14 days, the field equipment and piping used by the first train are disconnected, moved, and reconnected to the next row of wells, and production from this train is resumed. Each of the six trains follows this same cyclic pattern of relocation.

Process flow description

Figure 2 shows the block flow diagram for the electricity generating case. The facility consists of the following sections:

Plant Section No.	Process Unit
1	Field development area
2	Raw gas gathering and gasification air transfer piping
3	Heat exchange and raw gas scrubbing
4	Stretford sulfur plant
5	Electric generating plant
6	Stack, cooling towers, water plant, waste water treating, and oil recovery plants

Compressed air is piped from the main plant area about one mile to the field development area, where it is injected into the coal seam. Air for the linking process is supplied by a mobile field-located compressor.

Raw gas is piped to the main plant area for cleaning and removal of sulfur-bearing compounds before being burned to generate electricity. The raw gas is cooled by humidification to condense about 90% of the oil, which is transferred to an oil recovery system, and is cleaned of remaining particulate matter and oil in venturi scrubbers. The scrubbed raw gas is cooled before going to Stretford treating plants, where the H_2S content is reduced to less than 100 ppm by volume.

Treated gas (fuel gas) from the Stretford units is compressed, heated by exchange with the raw gas, burned, and expanded through gas turbines which drive the electric generators, combustion air compressors, and fuel gas compressors. About 2/3 of the electric generating capacity is provided by the gas turbine generators. The remaining 1/3 is provided by steam turbines using waste heat from the exhaust gases. Part of the steam is used to drive the gasification air compressors and other auxiliary equipment.

Design of the combined-cycle electric generating plant is based on information appearing in Energy Conversion Alternatives Studies (ECAS) reports. (3)(4) This was supplemented by information supplied for a similar system which was proposed for use with low-Btu gas. (5) The resulting combined-cycle plant developed for this evaluation was assumed to have a net efficiency of 42%.

Substitute Natural Gas (SNG) Production Case

In the SNG case, raw intermediate-Btu gas from the wells is cleaned, compressed, and fed to CO shift reactors to adjust the CO/H_2 ratio for the methanation reaction. After shifting, H_2S and CO_2 are removed. The resulting sweet gas is methanated, compressed, and dried to final product specifications.

At design throughput (155 MMscf/day of 954 Btu/scf gas) 60 producing wells are on line. These are arranged in six parallel trains of 10 wells each. Each train also requires 10 injection wells and 10 linking wells, so that a train consists of a total of 30 wells. The arrangements of trains in a field development area and of the injection, linking, and producing wells for a single train are similar to those of the electricity generating case. Field development also is similar.

Process flow description

Figure 3 shows the block flow diagram for the SNG case. The plant consists of the following sections:

Plant Section No.	Process Unit
1	Field development area
2	Raw gas gathering, oxygen, and steam transfer piping
3	Heat exchange and raw gas scrubbing
4	CO shift
5	Oxygen plant
6	Benfield HiPure plant
7	Methanation
8	Fuel gas treating
9	Stretford sulfur plant
10	Oil recovery and waste water treating
11	Steam generator and offsites

Oxygen and steam are piped separately from the main plant to the field. The oxygen and steam are mixed at the wellheads for injection into the coal seam.

Raw gas is piped to the main plant area, cooled by heat exchange, humidified, and scrubbed as in the previous case.

After scrubbing, the raw gas is separated into two streams. One stream goes to a DEA treating unit for acid gas removal and subsequent use as a fuel gas. The other stream is cooled and compressed to 450 psia for further processing into SNG product.

After compression, the gas is heated by exchange with the raw gas and sent to the CO shift unit, where it is shifted to an H_2/CO ratio of about 3. After heat recovery and cooling the shifted gas goes to the Benfield HiPure unit. Acid gas from the Benfield unit is piped to the Stretford sulfur plant.

Treated gas from the Benfield unit is heated and proceeds through zinc oxide guard beds, which remove the last traces of H_2S.

Methanation is carried out in a series of three fixed-bed catalytic reactors. Reaction temperature is controlled by a combination of heat recovery and hot product gas recycle.

After methanation, the gas is cooled, compressed, and dehydrated in a triethylene glycol drying unit to meet pipeline gas specifications.

Utilities Systems

The major utilities systems for the two plants include steam, electric power, fuel gas and oil, and cooling water. Utilities generation and consumption are summarized in Table 1.

Table 1. Utilities summary

	Electricity generation case[a]	SNG case
Steam (lb/hr)	1,032,500	3,668,700
Electricity (kW)	21,000	47,000
Fuel gas and oil (MMBtu/hr)	-	3,710
Purchased water (gpm)	4,350	5,430
Air cooling load (MMBtu/hr)	550	2,260

[a]Utilities consumed in the combined-cycle generating portion of the facility are not included here.

In the electricity generating case, the gasification air compressors consume about 10% of the total energy produced by the facility. An additional 5% is used to meet other plant requirements. Plant electricity requirements were estimated to be about 21 MW.

In both cases, fresh water (raw water) is assumed to be purchased. All other utilities required by the facilities are generated on site. Process cooling is provided both by air and water cooling. Wet cooling towers were used based on the assumption that adequate water supply (about 5000 gpm) would be available. During start-ups when fuel gas will not be available, oil will be used.

Overall Thermal Efficiencies

Overall thermal efficiencies for the conversion of coal to electricity and SNG are shown in Table 2. Efficiencies were calculated as the higher heating value of the products divided by the higher heating value of the in-place coal. In the low-Btu gas combined-cycle case, the electricity produced was credited at 3413 Btu/kWh. The heating value for SNG was taken at 60°F. No thermal credit was taken for by-product sulfur.

Table 2. Overall thermal efficiencies

Product	Overall thermal efficiency (%)
Electricity	24
SNG	38

Basis for Design and Process Assumptions

The design basis for the linked vertical well (LVW) process was developed from experimental results obtained at the Laramie Energy Research Center (LERC). Field test Hanna II, Phase II was used as the basis for operating conditions and yields for the electricity generating case. This test was conducted in the Hanna No. 1 seam of subbituminous coal at Hanna, Carbon County, Wyoming. Because of the lack of published experimental data for the steam-oxygen injection process, the basis for operating conditions and yields for this mode of gasification was a linear permeation mathematical model of forward combustion which was developed at LERC. (6-8) Table 3 shows the process design parameters developed for the two cases.

Table 3. LVW gasification process design parameters

Parameters common to low-Btu and SNG cases	
Type of coal	Subbituminous (Hanna No. 1 seam)
Seam thickness	30 ft
Depth of seam	300 ft
Well pattern and spacing	Square; 150 ft x 150 ft
Gasification reaction zone advance rate	2 ft/day
Process sweep efficiency	80%
Process thermal efficiency	80%
Overall process efficiency	64%
Raw gas wellhead temperature	640°F
Linking air injection pressure	1 psig/ft of depth
Linking air injection rate	33,000 scf/ft of link
Reverse combustion linking rate	7 ft/day
Parameters applicable to low-Btu gas case	
Single well production rate	30 MMscfd
Air injection requirement	73,570 scf/ton maf coal
Dry gas produced/air injected	1.45 scf/scf
Parameters applicable to SNG case	
Single well production rate	17 MMscfd
Steam/oxygen injection gas composition	60/40 mole %
Steam + O_2 injection requirement	23,270 scf/ton maf coal
Dry raw gas produced/steam + O_2 injected	1.92 scf/scf

Capital Investments

Estimated total capital investments for the two conceptual facilities are summarized in Table 4. The capital investments do not include the cost of the coal (or land and mineral rights) required for the facilities. Coal is charged to the facilities as a raw material as part of the operating costs. The cost, in $/ton, is treated as a variable in the economic calculations.

Table 4. Capital investment summary

Capital investment for plant sections	Capital Investment, 10^6 900 MW(e) plant	SNG plant
Site development	1.8	2.1
Initial drilling costs	1.3	1.6
Field gas treating plant	8.6	11.1
Field piping system	11.3	20.3
Raw gas treating plant	17.2	19.0
CO shift plant	-	28.5
Oxygen plant	-	81.5
Benfield plant	-	17.9
Methanation plant	-	28.1
Fuel gas treating plant	-	6.7
Stretford plant	6.5	4.8
Electric generating plant	255.7	-
Tankage, offsites, utilities	10.6	43.5
Total for plant sections	313.0	265.1
Capital investment for facility		
Engineering	8.1	12.9
Construction overhead	7.6	16.5
Contingencies	32.7	29.3
Contractor's fee	9.8	8.8
Special charges	23.8	18.7
Total for facility	82.0	86.2
Total capital investment	395.0	351.3

Initial well drilling and preparation work which occurs during the plant construction period is included in plant capital costs. After the plant is started up, this cost is included as an operating charge.

All costs given here are referenced to first quarter 1977 and are expressed in first quarter 1977 dollars.

Operating Costs

Operating costs include raw materials, catalysts and chemicals, water, other operating supplies and materials, maintenance materials and labor, operating labor and supervision, and general and administrative overhead. They do not include depreciation (recovery of capital), interest on debt, return on investment, or taxes, which are accounted for internally by the overall economics program. Marketing and distribution costs were not included.

The in-place coal cost, in $/ton, was treated as a variable and was varied parametrically from 0 to $10/ton.

Field equipment moving expenses are based on moving each train of wells once per quarter. The moving cost was estimated from material and labor costs for the initial installation. Additional quarterly costs for labor and equipment used in moving field systems were $120,000 and $135,720 in the electricity generating and SNG cases, respectively.

Operating cost bases are summarized in Table 5. Other assumptions used are as follows:

- Plant operating lifetime: 20 years
- Construction period (pre-operational period): 2 years
- Working capital is 12% of fixed capital investment.
- Maintenance is 4% of depreciable capital per year.
- Plant factor (operating factor) is 70% for electric generating plant, 90% for SNG plant.
- Direct labor rate is $8.25/hr.
- Labor burden is 35% of direct labor.
- Supervision is 15% of labor plus labor burden.
- Operating supplies are 30% of direct operating labor.
- Overhead is 135% of labor plus supervision.
- Federal income tax rate is 48%.
- State income tax rate is 3%.
- Local taxes and insurance are 3% of capital per year.

Table 5. Operating cost basis

Coal	Low-Btu Gas	SNG
Coal used (in-place basis) at 100% plant factor:		
tons/day	18,073	22,951
10^6 tons/yr	6.60	8.25
Drilling:		
Depth of holes (ft)	300	300
Drilling cost ($/ft)	30	30
Number of wells/yr[a]	144/212/100	180/270/150
Operating labor:		
Men/shift	48	45
Catalysts and chemicals at 100% plant factor:		
(10^6 $/yr)	0.217	4.235
By-product sulfur:		
(long tons/day)	29	38

[a]Final year of construction/first through next-to-last operating year/last operating year.

Economic Analysis

Prices of electricity and SNG were calculated as a function of coal cost and annual after-tax rate of return on equity capital. This was done by the discounted cash flow procedure for two capital structures, 100% equity and 70/30 debt/equity. Annual after-tax rate of return on equity was treated as a parameter using rates of return of 10, 12, 15, and 17%. Annual interest rate on debt was assumed to be 9%. By-product credit was included for sulfur at $60/long ton. A computer program was used for these calculations. (9)

The resulting product prices are highly dependent on the capital structure and plant factor. Typical examples are shown in Table 6 and Fig. 4.

Table 6. Estimated product prices[a] at 15% return on equity[b] and 9% annual interest rate on debt

Coal Price ($/ton)	Product price for electricity from low-Btu gas[c] (mills/kWh)		Product price for SNG[d] ($/$10^6$ Btu)	
	100% equity	70/30 D/E	100% equity	70/30 D/E
0	31.4	19.4	3.34	2.13
5	35.6	23.6	4.11	2.89
10	40.0	27.7	4.87	3.66

[a]Product transportation, distribution, and marketing costs are not included.

[b]Annual after-tax rate of return on equity.

[c]70% plant factor.

[d]90% plant factor.

References

1. W. C. Ulrich, M. S. Edwards, and R. Salmon, Process Designs and Economic Evaluations for the Linked Vertical Well In Situ Coal Gasification Process, ORNL-5341 (to be issued).

2. P. V. Skafa, "Underground Gasification of Coal," UCRL TRANS-10880, pp. 334-42.

3. D. H. Brown, et al., Energy Conversion Alternatives Study (ECAS), General Electric Phase 1, Vol. 2, Part 1. NASA-CR-134948-Vol. 2, Pt. 1, prepared by General Electric Company, February, 1976, p. 49.

4. D. J. Amos, et al., Energy Conversion Alternatives Study (ECAS), Westinghouse Phase 1, Vol. 5. NASA-CR-134941-Vol. 5, prepared by Westinghouse Research Laboratories, February 12, 1976.

5. Paul Berman, Westinghouse Electric Corporation, Philadelphia, Pa., personal communication to W. C. Ulrich, June 15, 1977.

6. R. D. Gunn, D. D. Fischer, and D. L. Whitman, "The Physical Behavior of Forward Combustion in the Underground Gasification of Coal," presented at the 51st Annual Technical Conference, Society of Petroleum Engineers, New Orleans, October 3-6, 1976.

7. R. D. Gunn, LERC, personal communication to W. C. Ulrich, May 12 and May 17, 1977.

8. R. D. Gunn, LERC, personal communication to R. Salmon, July 5, 1977.

9. R. Salmon, "PRP - A Discounted Cash Flow Program for Calculating the Production Cost (Product Price) of the Product from a Process Plant," ORNL-5251, March 1977.

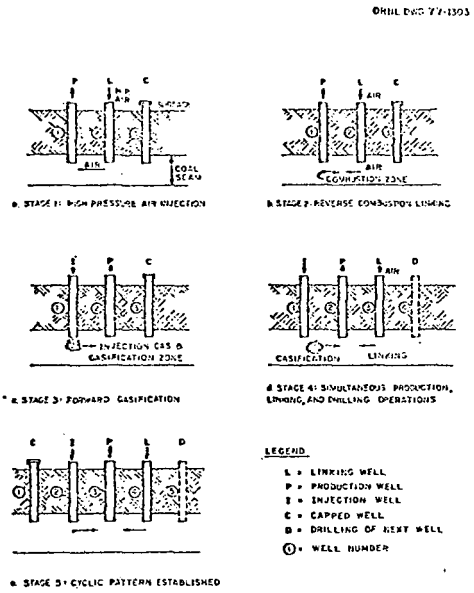

Fig. 1. Stages in the field development of the linked vertical well process

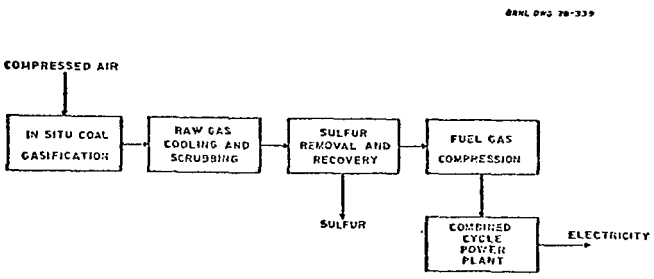

Fig. 2. Block flow diagram for electricity generating case

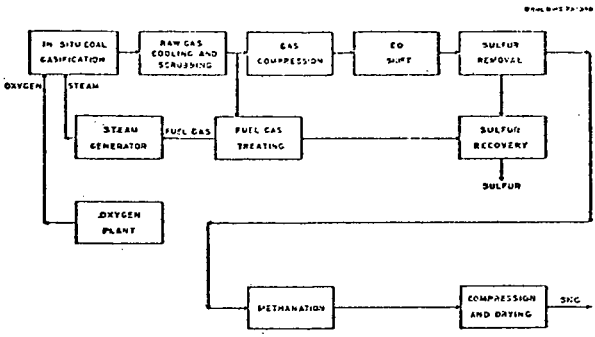

Fig. 3. Block flow diagram for SNG case

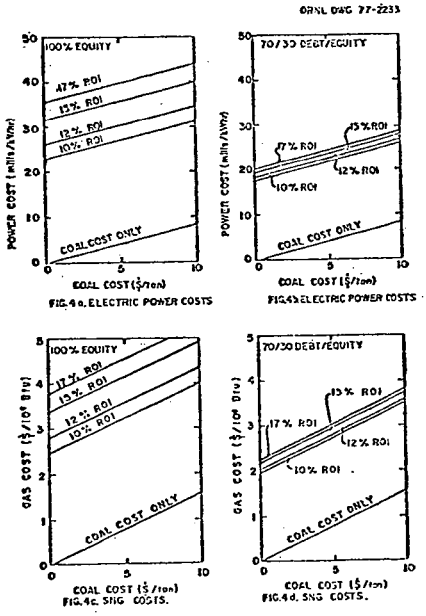

Fig. 4. Electric power and SNG costs

ECONOMICS OF PRODUCING AMMONIA FROM COAL BY PRESSURIZED ENTRAINED AND KOPPERS-TOTZEK GASIFICATION

William C. Morel and Yong Jai Yim[1]

U.S. Department of Energy
Process Evaluation Office
P.O. Box 863, Morgantown, WV 26505

The demand for fertilizer will steadily increase as the world population continues to grow at a rapid rate. Almost all nitrogen fertilizer is derived from ammonia. Natural gas is the raw material used to produce almost all the ammonia in the United States, but its availability for industrial use will decrease significantly in the future. Domestic consumption of natural gas will have top priority especially during the winter months. By 1990 the present administrations plans to phase out natural gas for industrial use. Therefore, a substitute raw material for ammonia production will be needed to supplement and eventually replace natural gas. Coal, our richest fossil energy resource, will make a strong bid to replace natural gas.

An economic evaluation of ammonia production from coal-derived hydrogen and air-derived nitrogen, based on a 1,000-ton-per-day capacity, is presented. Two coal entrained gasification systems for producing the hydrogen requirement are compared--one that operates at 30 atmospheres,[2] and the other, Koppers-Totzek, a commercially available system, that operates at a slightly higher than atmospheric pressure. Two different coals--Illinois No. 6 and Montana subbituminous--were considered for each system. The estimates are based on January 1977 cost indexes. Average selling prices of the ammonia were determined by using discounted cash flow (DCF) rates of 12, 15, 20 percent at various coal costs. No inflation factors are included during the life of the plant. Pollution abatement considerations have been incorporated. Some of the economic and technical details are included for the two systems.

ENTRAINED GASIFICATION AT 30 ATMOSPHERES

In the system, hydrogen required in the ammonia synthesis with nitrogen is prepared from synthesis gas produced by coal entrained gasification at 30 atmospheres. (1) (2) Figure 1, a flow diagram of the process, includes the following steps:

1. Coal preparation, which includes crushing, screening, and sizing of the run-of-mine coal to 70 percent through 200-mesh.
2. Entrained oxygen-coal gasification at 30 atmospheres with a 2,200° F outlet temperature. The synthesis gas is cooled to 750° F by water injection.
3. A dust removal unit removes entrained dust from the synthesis gas with cyclone separators followed by electrostatic precipitators for residual dust removal.
4. First stage shift conversion of the clean synthesis gas to a H_2:CO ratio of 2.3:1 in the presence of a sulfur-resistant catalyst. Part of the 50 psig saturated steam required in the purification unit is produced in the first heat recovery system.
5. First stage purification unit utilizes a hot potassium carbonate solution to reduce the CO_2 content to 2.0 percent and remove essentially all of the H_2S and COS. (3) Char towers are provided for removal of residual sulfur compounds.
6. Second stage shift conversion unit increases the H_2:CO ratio of the synthesis gas to 281.5:1 in the presence of a low-temperature catalyst. Additional 50 psig saturated steam is produced in the second waste heat recovery unit.
7. The CO_2 content of the shifted gas is reduced to 0.1 percent in the second purification unit which is similar to the first stage purification unit.
8. The remaining carbon oxides are converted to methane in the presence of a nickel catalyst. The product gas is cooled to 100° F and then mixed with sufficient

[1]Mr. Yim has resigned from the Department of Energy, and is located with Bechtel Corporation, 50 Beale Street, San Francisco, CA 94119.

[2]Based on U.S. Bureau of Mines research in the 1950's with full commercial development incomplete.

nitrogen from the oxygen plant to yield a synthesis gas having a $H_2:N_2$ ratio of 3:1 which is compressed to 2,000 psig.

9. The makeup gas mixes with cooled recycle gas and is then cooled to 0° F in a refrigeration-type condenser to reduce the NH_3 content to 1.5 percent. The condensed ammonia removes the last traces of water.

10. Eighty-five percent of the gas stream is heated to 706° F by product gas in a heat exchanger located below the catalyst bed prior to entering the catalyst bed. The remaining 15 percent is divided into three quench streams for control of catalyst temperature.

11. The product gas is cooled to 47° F in a series of heat exchangers. The gas stream is separated from the condensed ammonia, recompressed to 2,000 psig, and then recycled to mix with the makeup stream.

12. A small portion of the recycle stream is purged from the system to prevent buildup of methane. To increase the ammonia yield, the purge stream is cooled to -12° F before being vented.

13. The liquid ammonia product is cooled to -12° F, and then the pressure is reduced to 200 psig to remove the dissolved gases. The product is stored in low temperature atmospheric pressure storage tanks.

It is assumed that 15 percent [4] of the total H_2 and N_2 entering the converter is synthesized to ammonia. The design of the ammonia synthesis vessels was based on a gas space of 20,000 scf synthesis gas/ft^3 catalyst/hr. The thermal efficiency of the overall plant is 31.4 percent, based on gross heating values in Btu per pound of 10,700, 9,800 and 3,990 for coal, ammonia, and sulfur, respectively.

KOPPERS-TOTZEK ENTRAINED GASIFICATION

Hydrogen required in this system is prepared from synthesis gas produced by coal entrained gasification in Koppers-Totzek units which operate at 0.5 atmosphere. [5] [6] Figure 2 is a flow diagram of the process and includes the following steps:

1. Coal preparation is the same type of unit described in the entrained gasification system at 30 atmospheres.

2. Entrained oxygen-coal gasification at 0.5 atmosphere with a 2,732° F outlet temperature. The synthesis gas is cooled to 2,100° F by water injection. Part of the 800 psig steam used in the steam turbines is produced in the heat recovery unit.

3. A dust removal unit removed the entrained ash and unburned carbon with fixed-orifice washers followed by adjustable orifice washers for removal of fines. The dedusted gas is then compressed to 355 psig.

The remaining steps are the same as those for the other system.

CAPITAL INVESTMENT

The total investment is estimated to be $196 million for the entrained gasification system operating at 30 atmospheres of $49.5 million lower than the investment for the Koppers-Totzek gasification system, using an Illinois No. 6 coal. Using a Montana subbituminous coal, the total investment is reduced 12 percent to $173 million, and 9 percent to $223 million for the pressurized entrained and Koppers-Totzek systems respectively.

Table 1 is a capital requirement comparison of the two systems, and figure 3 shows the distribution of capital requirement for major processes. Detailed cost summaries of the major processing units are not included, but the costs of the individual units are listed. General facilities include administrative buildings, shops, warehouses, railroad spurs, rolling stock, roads, waste water treatment, and fences. The costs of steam and power distribution, cooling water towers, plant and instrument air, fire protection, and sanitary water are included in plant utilities.

OPERATING COST

Table 2 presents the estimated operating cost comparison for the two entrained gasification systems. An assumed 90-percent operating factor allows 35 days for downtime, two 10-day shutdowns for equipment inspection and maintenance and 15 days for unscheduled operational interruptions. With labor at $7.50 per hour, payroll overhead at 35 percent of payroll, and depreciation at 5 percent of the subtotal for depreciation, allowing credit for sulfur recovered at $40 per ton, and with the cost of coal as a variable, the following operating costs are derived:

Annual operating cost, dollars per ton of ammonia					
Cost of coal, per ton	Illinois No. 6 coal		Cost of coal, per ton	Montana subbituminous	
	Entrained at 30 atm.	Koppers-Totzek		Entrained at 30 atm.	Koppers-Totzek
$17	$146.97	$173.41	$7	$113.21	$138.04
20	155.96	182.91	9	120.74	145.72
23	164.95	192.40	11	128.27	153.39

Based on a 330-day operating year for the plant and allowing credit for the sulfur produced, with coal costs and discounted cash flow rates as parameters, the average selling price of the ammonia product per ton for the two systems is shown in the following table: (These are also plotted on figure 4.)

Ammonia selling price, per ton, Illinois No. 6 coal						
Cost of coal, per ton	12-percent DCF		15-percent DCF		20-percent DCF	
	Entrained at 30 Atm.	Koppers-Totzek	Entrained at 30 Atm.	Koppers-Totzek	Entrained at 30 Atm.	Koppers-Totzek
$17	$249.46	$300.37	$284.54	$344.15	$349.53	$425.16
20	258.45	309.87	292.53	353.64	358.51	434.65
23	267.74	319.37	302.51	363.14	367.50	444.15

Ammonia selling price, per ton, Montana subbituminous coal						
Cost of coal, per ton	12-percent DCF		15-percent DCF		20-percent DCF	
	Entrained at 30 Atm.	Koppers-Totzek	Entrained at 30 Atm.	Koppers-Totzek	Entrained at 30 Atm.	Koppers-Totzek
$7	$201.62	$252.27	$232.27	$291.52	$289.03	$364.72
9	209.16	259.69	239.80	299.20	296.56	372.39
11	216.69	267.36	247.33	306.87	304.10	380.07

The DCF computer program takes into account the capital expenditure prior to startup so that interest during construction is deleted from the capital requirement.

UNIT COST SUMMARY

The selling price used to determine the high-cost elements in the process was based on a 15-percent DCF for a 20-year life, with coal at $20 for the Illinois No. 6 and $9 for the Montana subbituminous. A breakdown of the cost elements for the two systems is shown in table 3 and plotted in figure 5.

SUMMARY OF COMPARISON

As shown in table 1, the total investment for the pressurized entrained gasification system, using Illinois No. 6 coal, is $196 million, or about 80 percent of the Koppers-Totzek investment. About 45 percent of the difference is due to the additional compressor investment required for processing the raw gas product leaving the gasification unit at essentially atmospheric conditions. The Koppers-Totzek system also requires a more complex and expensive gasification, an extra heat

recovery unit, and a wet dust removal system that is more expensive than the dry system used in the pressurized system. The capital investment for the pressurized entrained gasification system is reduced about 12 percent when a Montana subbituminous coal is used. About 70 percent of the reduction is due to the elimination of the flue gas processing unit. Differences in capital costs for the two systems are shown in figure 3.

The operating cost for the pressurized entrained gasification system using Illinois No. 6 coal is $48.5 million, or about 85 percent of the Koppers-Totzek cost, as shown in table 2. Increases in maintenance, overhead, and indirect and fixed costs, which are directly related to the capital investment, represent the main difference. By substituting a Montana subbituminous coal, the operating cost of the pressurized system is reduced about 25 percent. The cheaper western coal accounts for about 75 percent of the reduction.

Over the 12 to 20 percent DCF range at varying coal prices ($17 to 23 per ton) for Illinois No. 6 coal, the selling price for the ammonia from the pressurized entrained gasification system is $249.50 to $367.50 per ton or $51 to $77 per ton less than from the Koppers-Totzek system. This represents about a 20-percent decrease. When a Montana subbituminous coal is used in place of Illinois No. 6 coal, in the pressurized system, the selling price is also reduced about 20 percent. About the same percent reduction in selling price is obtained by substituting western coal in the Koppers-Totzek system.

CONCLUSION

Results of this study show that the pressurized entrained gasification system is more economical than the Koppers-Totzek system for production of ammonia from coal. The selling price of the ammonia can be reduced about 20 percent by substituting a western subbituminous coal for an eastern bituminous coal for both of the systems. Although the selling price is $20 to $100 per ton higher than the current price of ammonia at the lowest percent DCF, a substitute for natural gas, presently used as the raw material, will be required in the near future as gas reserves are depleted. Further research on these coal gasification processes will be required to reduce the manufacturing cost of the ammonia product. Various other processes such as the Lurgi, Winkler, and Texaco gasification systems should be considered as alternatives.

TABLE 1. - Capital requirements: Comparison of pressurized entrained gasification system with Koppers-Totzek system ($1,000)

Item	Pressurized entrained system		Koppers-Totzek system		Difference	
					PE-KT	PE-KT
	Illinois No. 6 coal	Montana subbituminous coal	Illinois No. 6 coal	Montana subbituminous coal	Illinois No. 6 coal	Montana subbituminous coal
Coal preparation.....	4,224	4,970	4,316	4,591	-92	+379
Gasification.....	3,455	3,672	4,735	4,519	-1,280	-847
Heat recovery No. 1.....	-	-	1,466	1,317	-1,466	-1,317
Dust removal.....	623	710	1,698	2,084	-1,075	-1,374
Compression No. 1.....	-	-	22,080	23,300	-22,080	-23,300
Shift conversion No. 1...	1,287	1,473	1,305	975	-18	+498
Heat recovery No. 2.....	2,713	2,691	7,001	9,329	-4,288	-6,638
Purification No. 1.....	11,919	12,967	13,949	15,071	-2,030	-2,104
Shift conversion No. 2...	735	735	688	729	+47	+6
Heat recovery No. 3.....	1,186	1,186	592	592	+594	+594
Purification No. 2.....	5,143	5,143	4,293	4,293	+850	+850
Methanation.....	1,467	1,467	1,438	1,438	+29	+29
Compression No. 2.....	15,625	15,625	16,224	16,224	-599	-599
Ammonia synthesis.....	33,656	33,656	33,656	33,656	0	0
Flue gas processing.....	16,352	-	18,350	-	-1,998	-
Sulfur recovery plant....	900	560	900	650	0	-90
Oxygen plant.....	11,170	11,946	12,000	12,200	-830	-254
Steam and power plant....	19,700	19,850	19,809	19,979	-109	-129
Plant facilities.....	9,762	8,749	12,338	11,322	-2,576	-2,573
Plant utilities.....	13,992	12,540	16,450	16,227	-2,458	-3,687
Total construction..	153,909	137,940	193,288	178,496	-39,379	-40,556
Initial catalyst requirement.....	1,002	1,038	802	780	+200	+258
Total plant cost....	154,911	138,978	194,090	179,276	-39,179	-40,298
Interest during construction.....	23,237	20,847	29,114	26,891	-5,877	-6,044
Subtotal for depreciation.....	178,148	159,825	223,204	206,167	-45,056	-46,342
Working capital.....	17,815	12,786	22,320	16,494	-4,505	-3,708
Total investment....	195,963	172,611	245,524	222,661	-49,561	-50,050

TABLE 2. - Annual operating cost: Comparison of pressurized entrained gasification system with Koppers-Totzek system ($1,000)

Cost item	Pressurized entrained system		Koppers-Totzek system		Difference	
					PE-KT	PE-KT
	Illinois No. 6 coal	Montana subbituminous coal	Illinois No. 6 coal	Montana subbituminous coal	Illinois No. 6 coal	Montana subbituminous coal
Direct cost:						
Coal[1]	16,807	8,701	17,759	8,865	-952	-164
Raw water	314	313	570	784	-256	-471
Catalyst and chemicals	949	569	953	463	-4	+106
Methane	703	-	790	-	-87	-
Subtotal	18,773	9,583	20,072	10,112	-1,299	-529
Direct labor	1,248	1,117	1,380	1,248	-132	-131
Direct labor supervision	187	168	207	187	-20	-19
Subtotal	1,435	1,285	1,587	1,435	-152	-150
Maintenance labor	2,880	2,574	3,600	3,312	-720	-738
Maintenance labor supervision	576	515	720	662	-144	-147
Maintenance material and contracts	4,320	3,861	5,400	4,968	-1,080	-1,107
Subtotal	7,776	6,950	9,720	8,942	-1,944	-1,992
Payroll overhead	1,468	1,312	1,772	1,623	-304	-311
Operating supplies	1,555	1,390	1,944	1,789	-389	-399
Total direct cost	31,007	20,520	35,095	23,901	-4,088	-3,381
Indirect cost	5,383	4,812	6,625	6,083	-1,242	-1,271
Fixed cost:						
Taxes and insurance	4,647	4,169	5,823	5,378	-1,176	-1,209
Depreciation	8,908	7,991	11,160	10,309	-2,252	-2,318
Total, before credit	49,945	37,492	58,703	45,671	-8,758	-8,179
Sulfur credit	-1,444	-133	-1,447	-117	+3	-16
Total, after credit	48,501	37,359	57,256	45,554	-8,755	-8,195

[1]Illinois No. 6 coal @ $17/ton; Montana subbituminous coal @ $7/ton.

TABLE 3. - Unit cost comparison

Unit	Cost per ton of product at 15 percent DCF			
	Pressurized entrained system		Koppers-Totzek system	
	Illinois No. 6 coal	Montana subbituminous coal	Illinois No. 6 coal	Montana subbituminous coal
Coal preparation	$13.26	$13.21	$12.55	$13.10
Gasification	77.83	61.11	71.28	54.87
Dust removal	1.01	1.09	4.06	5.23
Compression No. 1	-	-	43.03	42.46
Shift conversion No. 1	7.46	7.95	26.00	24.94
Purification No. 1	29.34	28.96	33.70	32.51
Shift conversion No. 2	11.10	10.08	10.67	9.81
Purification No. 2	11.92	10.90	9.29	10.08
Methanation	3.15	3.05	3.13	3.36
Compression No. 2	48.07	44.02	44.75	42.72
Ammonia synthesis	59.70	57.43	59.37	57.60
Flue gas processing	30.15	-	35.05	-
Sulfur recovery	.54	2.00	.76	2.52
Total	293.53	239.80	353.64	299.20

NOTE:--Coal cost, dollars per ton--Illinois No. 6 is $20 and Montana subbituminous is $9.

REFERENCES

1. Intra-Department Report No. 78-2, "An Economic Evaluation of Ammonia Production via Synthesis of Nitrogen and Hydrogen Using an Oxygen-Coal Pressurized Entrained Gasification System For Hydrogen Production, 1,000-Ton-Per-Day Plant, Illinois No.6 Coal." Process Evaluation Office, U.S. Department of Energy, Morgantown, W. Va., November 1977.

2. Intra-Department Report No. 78-8, "An Economic Evaluation of Ammonia Production via Synthesis of Nitrogen and Hydrogen Using and Oxygen-Coal Pressurized Entrained Gasification System For Hydrogen Production, 1,000-Ton-Per-Day Plant, Montana Subbituminous Coal," Process Evaluation Office, U.S. Department of Energy, Morgantown, W. Va., April, 1978.

3. Wellman, P., and S. Katell. U.S. Bureau of Mines Information Circular 8366, "Hot Carbonate Purification Computer Program," March 1968.

4. Bresler, Sidney A., and G. Russel James. "Questions and Answers on Today's Ammonia Plants," Chem. Eng., June 21, 1965, p. 116.

5. Intra-Department Report No. 78-3, "An Economic Evaluation of Ammonia Production via Koppers-Totzek Coal Gasification System for Hydrogen Production (Illinois No. 6 Coal), 1,000-Ton-Per-Day Plant," Process Evaluation Office, U.S. Department of Energy, Morgantown, W. Va., December 1977.

6. Intra-Department Report No. 78-7, "An Economic Evaluation of Ammonia Production via Koppers-Totzek Coal Gasification System for Hydrogen Production (Montana Subbituminous Coal), 1,000-Ton-Per-Day Plant," Process Evaluation Office, U.S. Department of Energy, Morgantown, W. Va., April 1978.

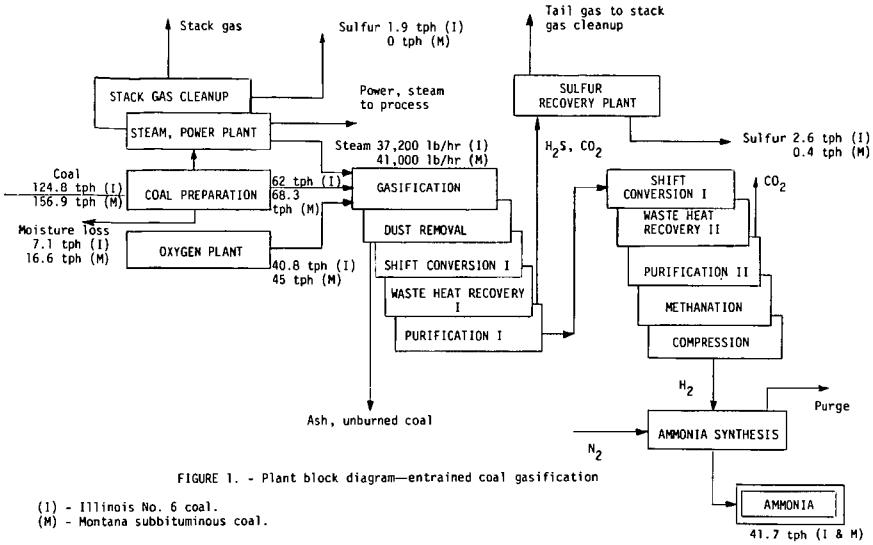

FIGURE 1. - Plant block diagram—entrained coal gasification

(I) - Illinois No. 6 coal.
(M) - Montana subbituminous coal.

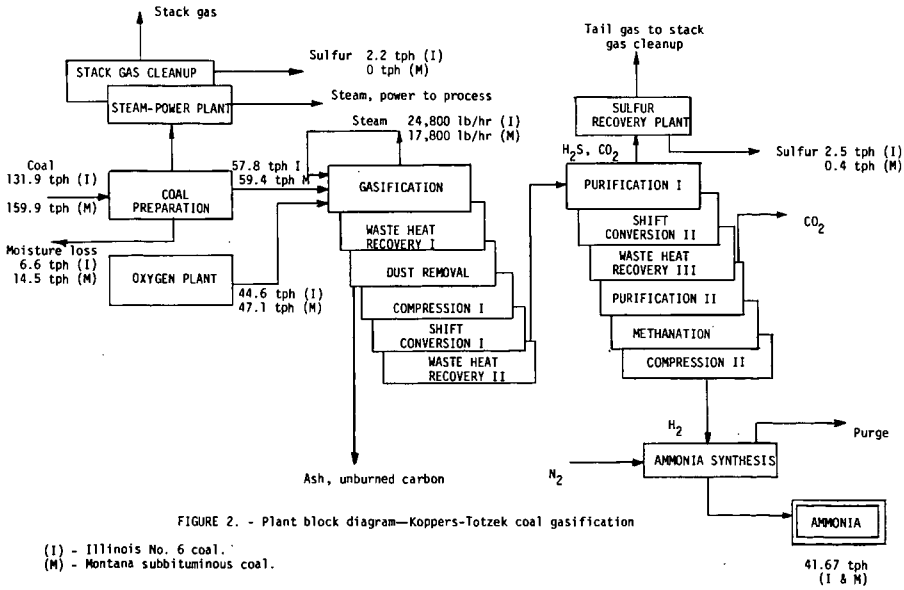

FIGURE 2. - Plant block diagram—Koppers-Totzek coal gasification

(I) - Illinois No. 6 coal.
(M) - Montana subbituminous coal.

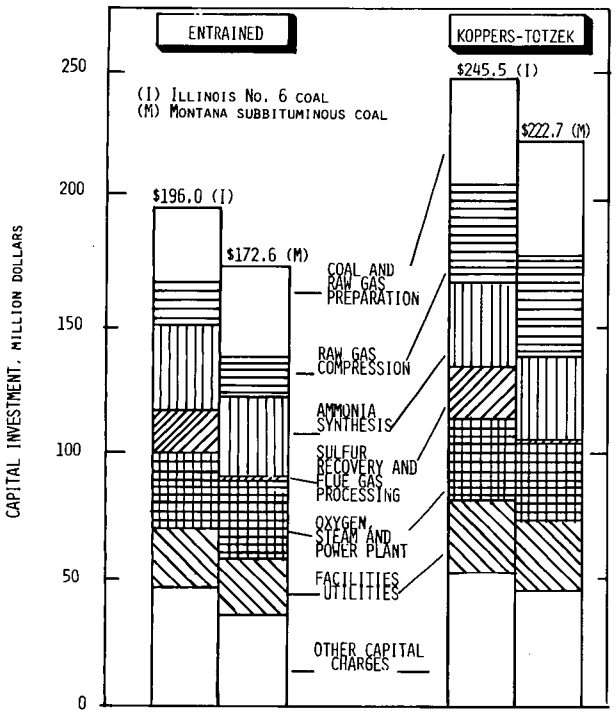

FIGURE 3. - CAPITAL INVESTMENT REQUIREMENTS FOR TWO PROCESSES AND THEIR DISTRIBUTION

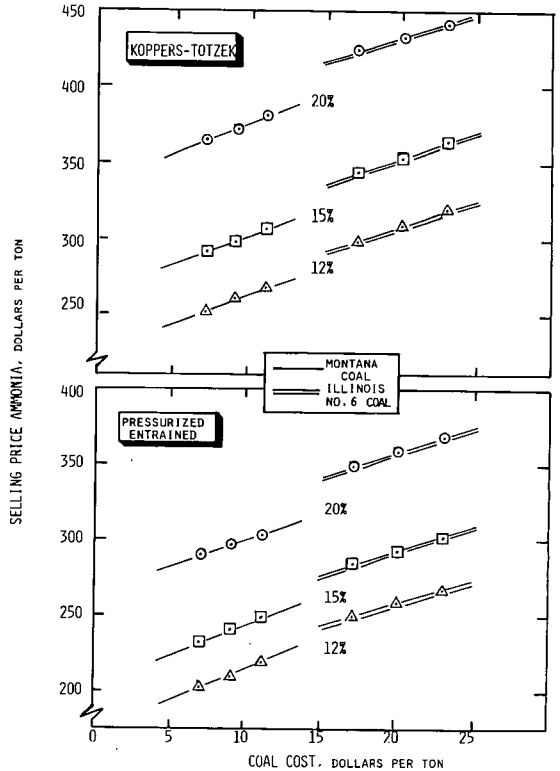

FIGURE 4. - SELLING PRICE OF AMMONIA AT DIFFERENT COAL PRICES WITH DCF RATE OF RETURN AS A PARAMETER

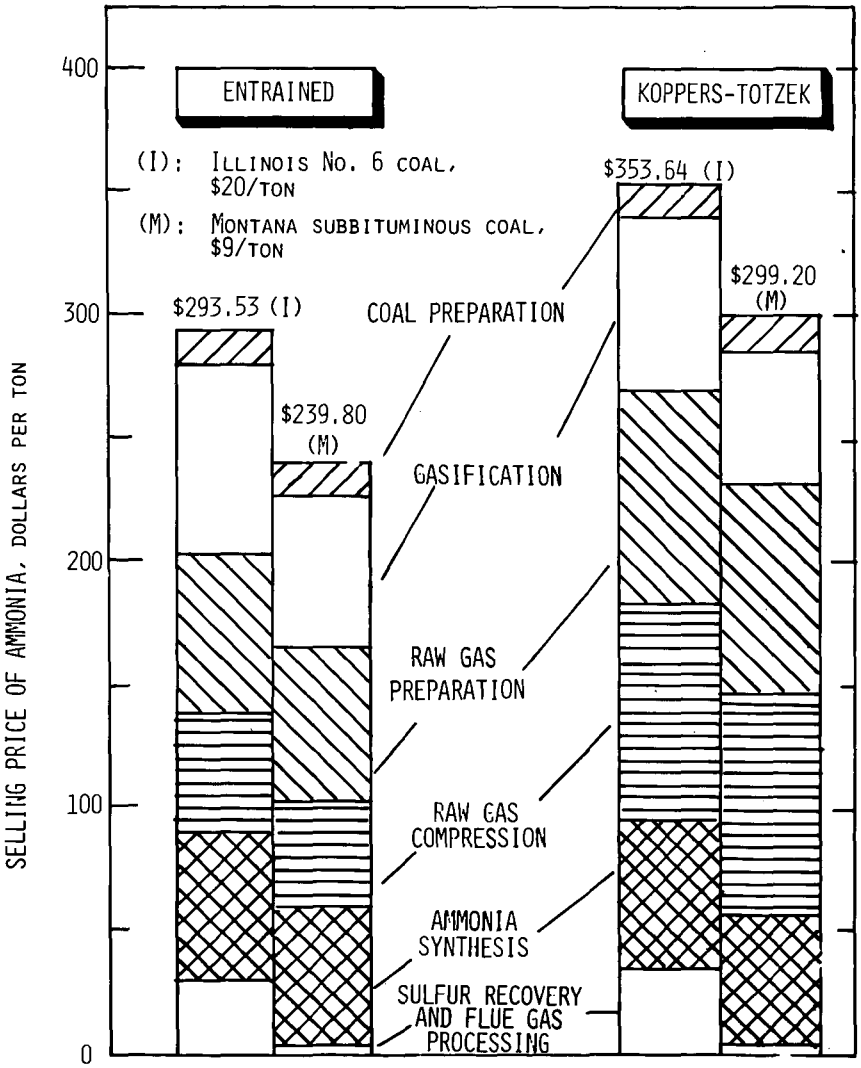

FIGURE 5. - SELLING PRICE OF AMMONIA AND ITS DISTRIBUTION BASED ON UNIT COST PROCEDURE AT 15 PERCENT DCF

THE MODELING OF INITIAL STAGE HYDROGASIFICATION OF VARIOUS RANKED COALS

Edwin J. Hippo
James L. Johnson*

Institute of Gas Technology
3424 S. State
Chicago, Illinois 60616

In the past twenty years, a large effort has been made in the United States to develop commercial coal gasification technology. It has been observed from experimental work that the behavior of coal during the initial stages of coal heat-up, and during a short time interval following heat-up, are crucial to efficiencies of gasification processes. Most carbon oxides, steam, oil and tars, and significant portions of light hydrocarbon gases are evolved during the initial stage. A detailed knowledge of the kinetics of this stage is essential to optimum reactor design.

However, as pointed out previously (1), most studies have been concerned with kinetic correlations of total methane yield after the coal has deactivated to a relatively inert char. On the other hand, this project has been concerned with reactions that take place in the relatively highly reacitve initial stage of transient reactivity, called "rapid-rate methane formation."

Experimental

Details of the reactor system have been presented previously (1). In brief, it is a 1.6 mm diameter, 60 m long helical coiled transport reactor. Nine pairs of electrodes attached along the length of reactor provide an energy source for heating. Temperatures in the nine zones can be adjusted independently to provide constant or linear temperature profiles across the length of the reactor. Coal particles (0.074 to 0.089 mm diameters) are entrained in a gas (hydrogen or helium with less than 0.1% solids by volume) and passed through the reactor. Gas-solid separation occurs in a sintered metal filter (heated to 300°C) at the reactor outlet. Liquids are condensed in a series of cooled traps. The dry gas is analyzed by periodic mass spectrography and by continuous flame ionization. Gases detected have included CO, CO_2, H_2, methane, ethane, and benzene. Proximate and ultimate analyses of coal and chars are determined for each run. Condensible liquids, "heavy hydrocarbons," and steam yields are difficult to determine experimentally because a large surface area is available on which the small yield can condense. Steam yields are determined by oxygen balance, and heavy hydrocarbons are determined by carbon balance.

Isothermal temperatures have varied from 700 to 1040 K, and residence times have been varied up to 13 seconds (depending on the total gas flow rate) for various coals. Maximum temperature for linear temperature profiles range from 700 to 1140 K for constant heating rates of 30, 60, and 80 K/s. A reactor inlet temperature of 590 K was maintained for all constant heating runs. Total operating pressures have ranged from 18 to 52 atmospheres; most runs have been performed at 35 atmospheres.

The gasification kinetics of a Montana lignite, a Montana subbituminous coal, a North Dakota lignite, two Texas lignites, and a Utah subbituminous coal have been investigated. Their proximate and ultimate analyses are included in Table 1. Analyses of coals investigated in other studies (2, 3) are also included. Their gasification behavior will be discussed in terms of the model constructed from the data obtained from the mass transport reactor.

* Deceased.

Table 1. ANALYSES OF THE FEED COALS

Coal	Darco Lignite	Wilcox Lignite	Montana Lignite	North Dakota Lignite	Montana Subbituminous	Illinois No. 6 Bituminous (2)	Utah Subbituminous A	Pittsburg Bituminous (3)	Montana Lignite (3)
Proximate Analysis (Mass %)									
Percentage Ash (Dry)	5.2	25.3	5.15	6.3	8.5	6.0	7.0	11.5	10.6
Percentage Volatile Matter (daf)*	50.8	53.1	45.9	44.9	42.5	39.7	40.9	44.3	44.2
Percentage Fixed Carbon (daf)*	49.2	46.9	54.1	55.1	57.5	60.3	52.1	55.7	55.8
Ultimate Analysis (Dry) (Mass %)									
Percentage Carbon	60.2	47.6	65.13	65.9	67.3	75.45	66.4	68.76	71.2
Percentage Hydrogen	3.49	3.19	4.13	4.19	4.29	5.12	4.14	4.87	5.4
Percentage Nitrogen	0.93	1.14	0.89	0.93	1.07	1.72	1.06	1.32	0.08
Percentage Sulfur (Total)	0.57	1.70	0.57	0.60	1.31	1.32	0.72	5.38	1.32
Percentage Oxygen (By Difference)	29.56	21.01	24.20	22.12	17.58	10.41	20.32	8.21	21.00
	mass %								
O/C (g-atom/g-atom)	0.37	0.33	0.28	0.25	0.20	0.10	0.23	0.09	0.22
H/C (g-atom/g-atom)	0.69	0.80	0.76	0.76	0.74	0.81	0.74	0.85	0.91

* daf = dry ash free.

Typical Results

Typical results for hydrogasification of coals in the mass transport reactor have been reported elsewhere (1). Due to the volume of data collected, only the tentative model for yields of oxygenated species will be discussed in this paper. Models for coal hydrogen evolution have been tentatively proposed and will be presented at a later date.

Previously (4), the evolution of oxygen-containing species during rapid-rate methane formation and devolatilization have been modeled by assuming that a set of reactions occurs to liberate each species. Each set of reactions was represented by a first-order rate equation, but the rate constant had a continuous distribution of activation energies. However, evolved species can arise by different paths. Data scattering and the narrow band of activation energies previously used to fit the data allow a simplifying assumption to be made — namely, that the formation of each species by each route can be represented by a single rate equation containing a single effective activation energy. Thus, the following overall model can be used to fit the data:

$$n_i = \sum_{i,j} \Delta n_{i,j} x_{i,j} \qquad 1)$$

where —

n_i = total amount of species i formed (g-atom of i/g-atom of feed carbon)

$\Delta n_{i,j}$ = maximum amount of species i that can be formed by route j (g-atom of i/g-atom feed carbon)

$x_{i,j}$ = fraction of i converted by route j at any time such that —

$$dx_{i,j}/dt = k_{o_{i,j}} (1 - x_{i,j}) \qquad 2)$$

where —

$k_{o_{i,j}} = k_{o_{i,j}}^{\circ} \exp(-E_{i,j}/RT)$

and —

$k_{o_{i,j}}$ = rate constant for the first order reaction for formation of species i by route j, s^{-1}

$k_{o_{i,j}}^{\circ}$ = pre-exponential factor for the first-order rate equation for the formation of species i by route j

$E_{i,j}$ = activation energy for formation of species i from the coal by route j.

From these assumptions and relationships, the fraction of species i formed can be expressed as —

$$1 - x_{i,j} = \exp\left[- \int_o^{\theta} k_{o_{i,j}}^{\circ} \exp(-E_{i,j}/RT)\, d\theta\right] \qquad 3)$$

for isothermal conversion, and

$$1 - x_{i,j} = \exp\left[-\int_{T_o}^{T_f} \frac{k^{\circ}_{i,j}}{\alpha} \exp\left(-E_{i,j}/RT\right) dT\right] \qquad 4)$$

for a constant heat-up rate condition, where parameters are defined as above and —

T_f = maximum temperature of the coil reactor, K

T_o = entrance temperature of the reactor, K

α = heat-up rate of coal, K/s

Figure 1a reports the carbon dioxide (CO_2) formation and total carbon oxides formation as a function of maximum temperature under constant heat-up and isothermal conditions for Montana and North Dakota lignites gasified in hydrogen. The total carbon oxide yields increase with increasing maximum temperature. CO_2 formation is constant up to 920 K and then decreases with an increase in maximum temperature due to the water-gas shift reaction. The primary CO_2 yield in hydrogen occurs below 755 K, and when corrected for shift, remains constant at higher temperatures. This yield, $n_{CO_2}{}^{H2}$, can be expressed from Equation 1 as —

$$n_{CO_2}{}^{H2} = \Delta n_{CO_2}\, x_{CO_2,0} \qquad 5)$$

where $x_{CO_2,0}$ = 1 for temperatures above 755 K.

The total carbon oxides formed in hydrogen are the sum of the CO and CO_2 formed. Thus, from Equation 1, the total carbon oxides formed in hydrogen can be expressed as —

$$n_{CO + CO_2} = n_{CO_2}{}^{H_2} + n_{CO} \qquad 6)$$

CO formation appears to be derived from one route and the data can be fitted using Equations 3, 4, and 6. The solid lines in Figure 1 represent such a fit for isothermal conditions (line 1) and constant heat-up conditions (line 2).

The total carbon oxides and carbon dioxide yields for the Montana lignite in helium are shown in Figure 1b. Both carbon dioxide and total carbon oxides increase with increasing temperature. In helium, CO_2 formation, $n_{CO_2}{}^{He}$, appears to occur by two paths. One path is described by the model for CO_2 formation in hydrogen; the second path is assumed to be a first-order reaction. Thus, total CO_2 formation can be expressed as:

$$n_{CO_2}{}^{He} = n_{CO_2}{}^{H2} + \Delta n_{CO_2,1}\, x_{CO_2,1} \qquad 7)$$

where $n_{CO_2}{}^{H2}$ has been discussed and $\Delta n_{CO_2,1}\, x_{CO_2,1}$ can be evaluated from the data using Equations 3, 4, and 6. CO formation appears to be the same in helium and in hydrogen. Thus, the total carbon oxide formation in helium can be expressed as:

$$n_{CO + CO_2}{}^{He} = n_{CO_2}{}^{He} + n_{CO} \qquad 8)$$

The solid lines in Figure 1b represent solutions to Equations 3, 4, 7, and 8.

Steam formation can be treated in the same general manner as carbon oxides formation, but data must be corrected for the shift effect. This is done by assuming that primary CO_2 yield in hydrogen is constant above 750 K and that differences between the amount formed by primary gasification and the amount measured are equivalent to the amount of steam formed by the shift reaction. The steam yields for Montana and North Dakota lignites in helium are plotted in Figure 2a, and corrected yields for the two coals in hydrogen are plotted in Figure 2b. A specific amount of steam is formed by one route below 750 K. This "instantaneous" yield can be modeled similar to CO_2 formation below 750 K. This steam yield can be designated $n_{H_2O,o}$. An additional amount of steam is formed in helium by another route above 750 K, such that the total steam yields in helium, $n_{H_2O}^{He}$, are described by —

$$n_{H_2O}^{He} = \Delta n_{H_2O,o}\, x_{H_2O,o} + \Delta n_{H_2O,1}\, x_{H_2O,1} \qquad 9)$$

The lines drawn in Figure 2a were based on the solutions of Equations 3, 4, and 9. Assuming that devolatilization is the same in hydrogen as in helium, it can be seen from Figure 2b that an additional amount of steam formation, beside that predicted by Equation 9, occurs in hydrogen. The amount of oxygen in the additional steam is equal to the amount of oxygen in the increased CO_2 yield in helium. Thus, in hydrogen, a certain fraction of coal-oxygen is evolved as steam by an assumed first-order reaction that inhibits CO_2 formation, which would otherwise occur in an inert atmosphere. Again the additional steam yield is modeled by a first-order rate equation, and the total steam yield in hydrogen can be modeled by —

$$n_{H_2O}^{H_2} = n_{H_2O}^{He} + \Delta n_{H_2O,2}\, x_{H_2O,2} \qquad 10)$$

The solid lines in Figures 2a and 2b are solutions to Equations 3, 4, 9, and 10 for the different coals considered.

The total oxygen evolved from coal can be estimated as the sum of oxygen evolved as CO, CO_2, and H_2O. Curves for predicted coal-oxygen evolution for the Montana and North Dakota lignites in hydrogen under isothermal and constant heat-up conditions are included in Figure 3a. Actual data are also reported to show the close fit. A similar plot of oxygen yield as a function of temperature, shown in Figure 3b, reveals that the model developed for oxygen evolution in helium fits the data for helium gasification of a Montana lignite.

Table 2 lists the kinetic parameters that were used to generate the solid lines in Figures 1 through 3. Note that the parameters are not listed for the "instantaneous" formation of CO_2 and steam (below 750 K) because rate data were not obtained at these temperatures.

Table 2. KINETIC PARAMETERS FOR EVOLUTION OF OXYGENATED SPECIES FROM COALS

Volatile Component	Pre-Exponential Factor k_o°, s^{-1}	Activation Energy E (kcal/mol)
$n_{CO_2,1}$	2.0×10^5	27.83
$n_{H_2O,1}$	5.42×10^9	38.89
$n_{H_2O,2}$	6.45×10^9	44.98
n_{CO}	5.47×10^5	25.80

The evolution of CO, CO_2, and H_2O can be correlated with coal rank. The plots of maximum volatile yields in hydrogen of CO, CO_2, and H_2O, expressed as g-atom oxygen yield per g-atom feed carbon, versus coal rank (expressed as g-atom oxygen per g-atom carbon in the raw coal), are approximately straight lines (Figure 4). These yields are closely related to various functional groups in the coal. For example, CO_2 corrected for shift can be shown to have the following relationship:

$$\Delta n_{CO_2} = n_{carboxyl}(5) = 0 \text{ for } n_o^\circ < 0.1 \qquad 11)$$

$$\Delta n_{CO_2} = 0.4\ (n_o^\circ - 0.1) \text{ for } n_o^\circ \geq 0.1 \qquad 12)$$

where —

Δn_{CO_2} = maximum CO_2 yield (g-atom oxygen/g-atom of feed carbon)

n_o° = total oxygen in raw coal (g-atom O/g-atom carbon)

$n_{carboxyl}$ = total carboxyl oxygen in raw coal (g-atom O/g-atom coal C).

Steam yields can be expressed as —

$$\Delta n_{H_2O} = n_{hydroxyl}(5) = 0.65\ (n_o^\circ) \text{ for } n_o^\circ \leq 0.23 \qquad 13)$$

$$\Delta n_{H_2O} = 0.13 + 2\ (n_o^\circ - .23) \text{ for } n_o^\circ \geq 0.23 \qquad 14)$$

where —

Δn_{H_2O} = maximum steam yield (g-atom O/g-atom feed carbon)

$n_{hydroxyl}$ = hydroxyl oxygen in raw coal (g-atom O/g-atom coal carbon).

Carbonyl oxygen forms CO exclusively, as can be seen in the following correlations:

$$n_{carbonyl}(5) = 0.32\ (n_o^\circ - 0.1)\ n_o^\circ > 0.1 \qquad 15)$$

$$\Delta n_{CO} = 0.31\ (n_o^\circ - 0.1)\ n_o^\circ > 0.1 \qquad 16)$$

where —

Δn_{CO} = maximum CO yield (g-atom O/g-atom feed carbon)

$n_{carbonyl}$ = carbonyl oxygen in feed coal (g-atom O/g-atom feed carbon).

Thus, it appears that volatile yields containing oxygen can be estimated from a single parameter: coal rank expressed as the O/C ratio.

Using the above model and the maximum yields of individual products measured for each coal, yields at the various maximum temperatures can be predicted with the aid of Equations 1-10. These models also predict behavior for hydrogasification of a Illinois No. 6 bituminous coal (2) and pyrolysis of a lignite and Pittsburgh No. 9 bituminous coal (3).

Figure 5 presents a comparison of the predicted total oxygen yields from Equation 1-10 and the actual experimental yields for the various coals gasified under a variety of conditions. Similar plots for carbon oxides in hydrogen, carbon oxides in helium, steam in hydrogen, and steam in helium, can be made. The correlations are adequate in predicting yields of oxygenated species for given temperature histories in most cases.

In summary, even though the hydrogasification is not completely understood, it can be seen that significant strides have been made in identifying individual reaction paths that contribute to the gasification phenomena.

References Cited

1. Johnson, J. L., "Kinetics of Initial Coal Hydrogasification Stages," ACS Fuel Abstracts 22, No. 1, 17-37 (1977) March.

2. Feldmann, H. F., Mina, J. A. and Yavorsky, P. M., "Pressurized Hydrogasification of Raw Coal in a Dilute-Phase Reactor," Adv. Chem. Ser. 131 (1974).

3. Suuberg, E. M., "Rapid Pyrolysis and Hydropyrolysis of Coal," Ph.D. Thesis, Massachusetts Institute of Technology, August 1977.

4. Johnson, J. L., "Kinetics of Devolatilization and Rapid Rate Methane Formation," 1975 Annual Report to A.G.A. from Institute of Gas Technology, Project IU-4-11.

5. Van Krevelen, D. W., Coal Science, Elsevier, Amsterdam, 1961.

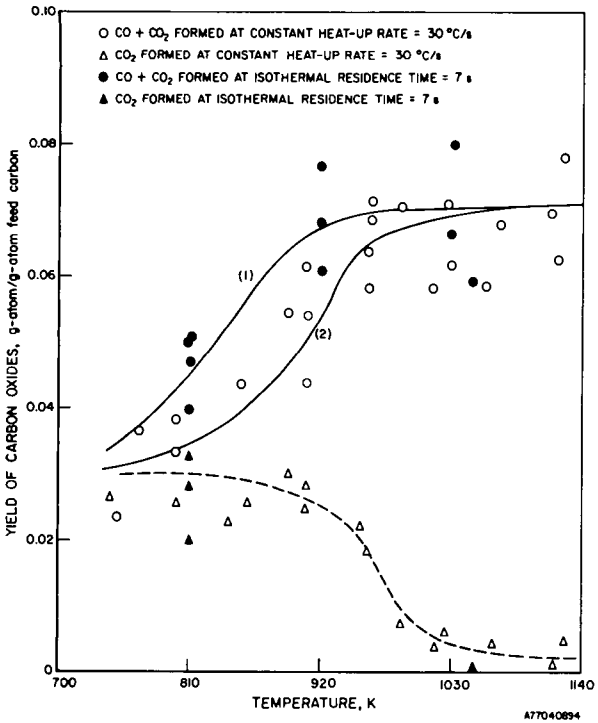

Figure 1a. Yields of Carbon Oxides for Montana and North Dakota Lignites in Hydrogen

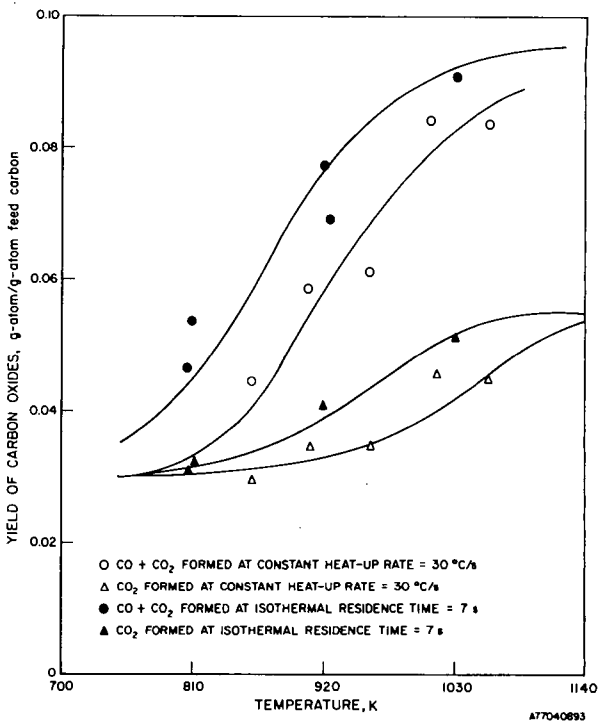

Figure 1b. Carbon Oxides Yields for Montana Lignite in Helium

Figure 1. PREDICTED AND ACTUAL CARBON OXIDE YIELDS FOR MONTANA AND NORTH DAKOTA LIGNITES

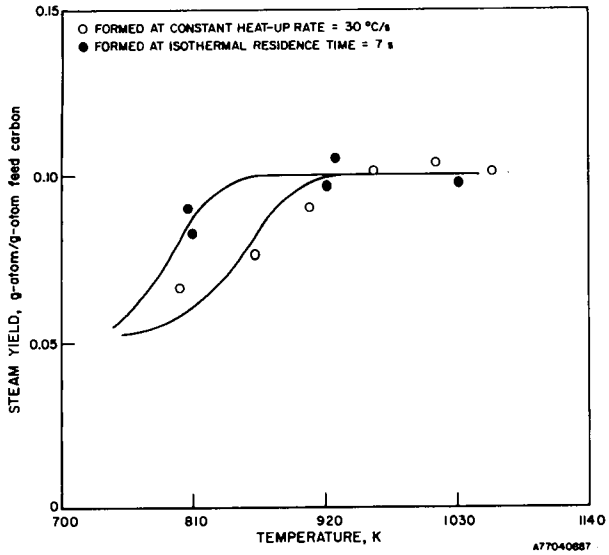

Figure 2a. Steam Yields for Montana and North Dakota Lignites in Hydrogen

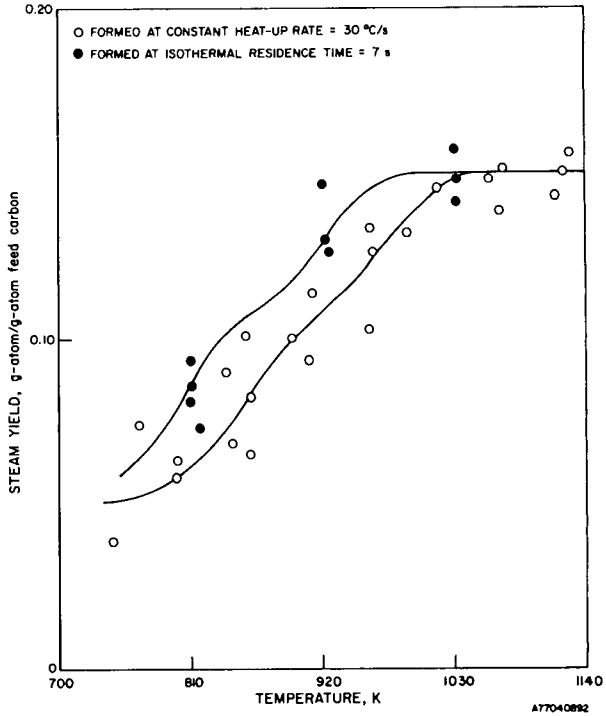

Figure 2b. Steam Yields for Montana Lignite in Helium

Figure 2. PREDICTED AND ACTUAL STEAM YIELDS FROM MONTANA AND NORTH DAKOTA LIGNITES

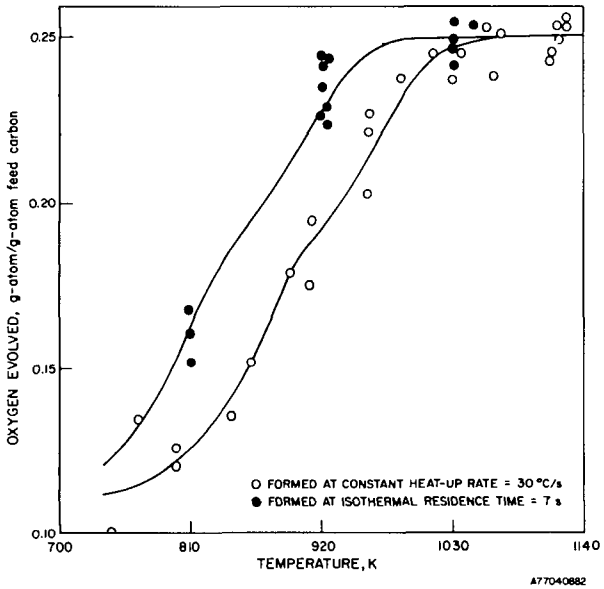

Figure 3a. Total Oxygen Evolved From a Montana and a North Dakota Lignite in Hydrogen

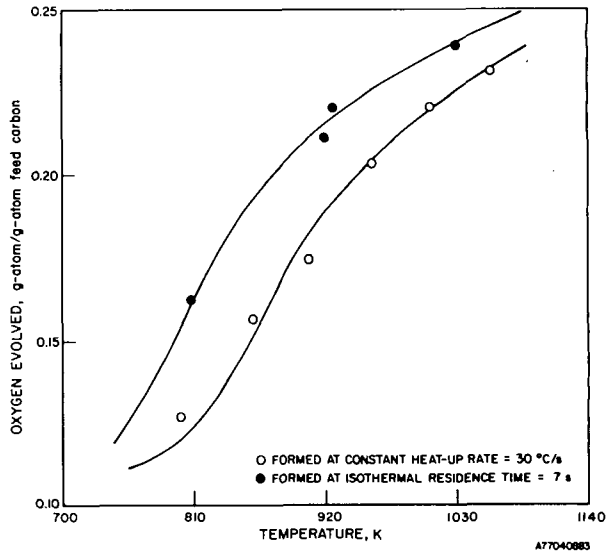

Figure 3b. Oxygen Evolved From Montana Lignite in Helium

Figure 3. PREDICTED AND ACTUAL COAL OXYGEN GASIFIED FROM MONTANA AND NORTH DAKOTA LIGNITE

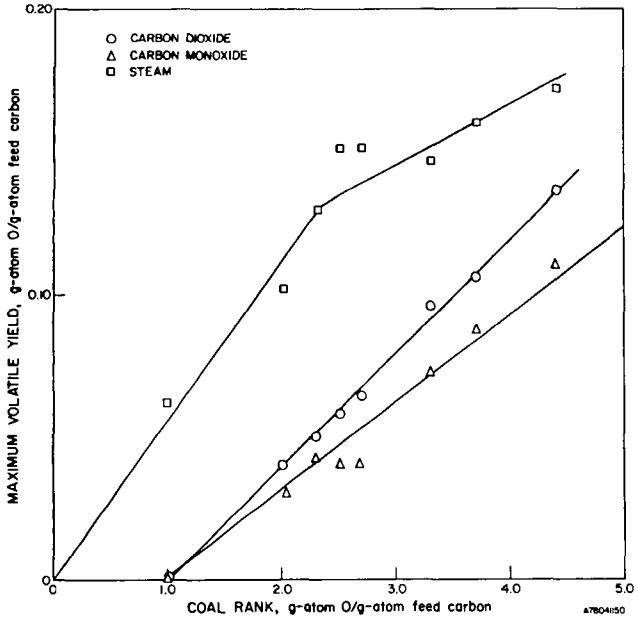

Figure 4. CORRELATION BETWEEN COAL RANK AND VOLATILE YIELDS

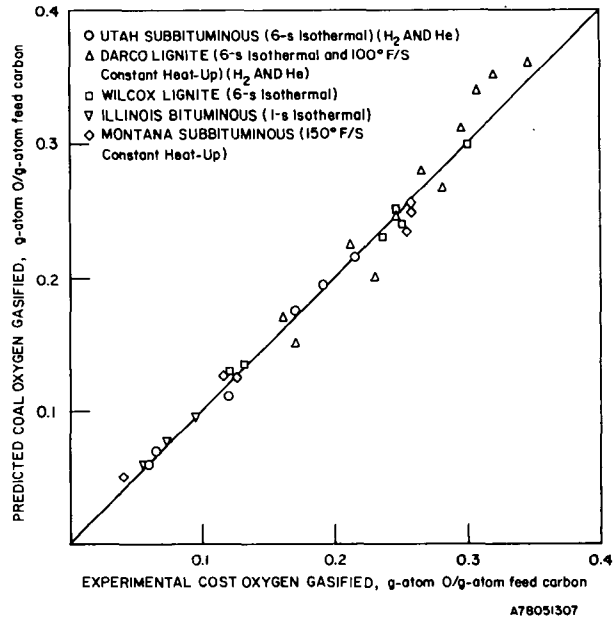

Figure 5. COMPARISON OF PREDICTED AND EXPERIMENTAL YIELDS OF TOTAL COAL OXYGEN GASIFIED FROM VARIOUS COALS UNDER A RANGE OF CONDITIONS

DETERMINATION OF THE KINETICS OF HYDROGASIFICATION OF CHAR USING A THERMOBALANCE

S. P. Chauhan and J. R. Longanbach

Battelle's Columbus Laboratories
505 King Avenue
Columbus, Ohio 43201

INTRODUCTION

The gasification of coal with fairly pure hydrogen, referred to as "direct hydrogasification", is considered to be an attractive approach for the production of substitute natural gas (1,2). Conceptually, direct hydrogasification processes involve two stages of gasification, one for hydrogasification of the coal and another for steam-oxygen gasification of the char from the first stage as shown in Figure 1. The hydrogen required by the hydrogasification stage is produced in the steam-oxygen gasification stage. About 85-95 percent of the methane in the final product gas is formed directly in the gasifier (3,4). Thus, the requirement for catalytic methanation is greatly reduced compared to single-stage steam-oxygen processes. Process analyses indicate several technical advantages, which add up to a significant economic advantage, of direct hydrogasification processes over single-stage steam-oxygen processes (1-6). Some examples of the direct hydrogasification processes under development are: (a) the Hydrane process (1,3) being developed by the Pittsburgh Energy Research Center (PERC), (b) the Rocketdyne Process (7), and (c) a catalytic hydrogasification process being developed by Battelle's Columbus Laboratories (4,8,9).

In support of the hydrogasification processes under development, it is necessary to obtain accurate kinetic and yield data for design and scale up. These data should properly take into account the suppressing effect of the primary product of reaction, namely, CH_4, on the rate of conversion of coal. Unfortunately, however, there is only a limited amount of data presented in literature (10,11) on the kinetics of hydrogasification in the presence of CH_4 present at levels representing commercial design. The bulk of the available data are for gasification with essentially 100 percent hydrogen. Another problem with available data is that most if it have been obtained using preoxidized coal while all the direct hydrogasification processes under development do not employ preoxidation.

In this paper we provide kinetic data on the hydrogasification of coal char, produced by partial hydrogasification of raw, caking bituminous coal, with mixtures of H_2 and CH_4. The data are correlated employing a combination of kinetic models proposed by Johnson (11) and Gardner, et al (12). Although the data were obtained for the Hydrane process, general applicability to other direct hydrogasification processes is suggested. In the Hydrane process, which operates at a total pressure of about 1000 psig, the required carbon conversion for the hydrogasification stage is about 50 percent for achieving balanced operation, i.e., to avoid excess H_2 or char from the steam-oxygen step. The hydrogasification stage itself consists of two countercurrent stages as shown in Figure 2. In the first hydrogasification stage, raw coal is contacted in a free fall, dilute phase with a mixture of primarily H_2 and CH_4 (greater than about 40 percent of each) to hydrogasify about 25 percent of the carbon. The char from the first hydrogasification step is further hydrogasified in a fluid bed with essentially pure H_2 and the resulting product gas is fed to the first hydrogasification stage (3). It is this second stage of hydrogasification for which the kinetic data reported in this paper were obtained (13).

EXPERIMENTAL DETAILS

The hydrogasification experiments were carried out in a thermobalance reactor described elsewhere (8,13). By continuously recording the mass of a sample held in a wire-mesh basket the progress of a reaction can be easily monitored in such a system. The operation is essentially isothermal and the gas conversion is limited to a few percent. A typical experiment in the thermobalance involves bringing the reactor to operating conditions first and then lowering the sample basket, measuring 0.63 inch O.D. and containing a 0.5 to 1.0 gram sample of char, at the rate of about one inch per second until it reaches the desired position in the reactor (I.D. = 0.75 inch). Thus, there is no weight trace for about the first 0.15 minute during which the sample is exposed to the reactive atmosphere. An additional minute or so is required for the sample to reach operating temperature. The temperature is measured by a thermocouple placed 1/4-inch below the sample basket.

The eight char samples employed in this study were produced at PERC in a dilute phase hydrogasifier operated at a nominal feed rate of 10 lb/hr of coal. The chars were derived from a Pittsburgh No. 8 hvAb and an Illinois No. 6 hvCb coal each processed in the dilute phase reactor at four temperatures: 725 C, 800 C, 850 C, and 900 C. Typical analyses of chars from the two types of coal are shown in Table 1. The raw coal

TABLE 1. TYPICAL ANALYSES OF CHARS FROM DILUTE PHASE HYDROGASIFIER

Analysis, wt %	Coal Source: Pittsburgh No. 8 hvAb	Coal Source: Illinois No. 6 hvCb
Proximate, as received		
Moisture	2.5	1.5
Ash	7.5	16.4
Volatile matter	9.2	9.7
Fixed carbon (by difference)	80.8	72.4
TOTAL	100.0	100.0
Ultimate, dry		
Carbon	84.4	75.8
Hydrogen	2.4	2.1
Nitrogen	1.5	1.3
Sulfur	1.0	1.3
Ash	7.7	16.6
Oxygen (by difference)	3.0	2.9
TOTAL	100.0	100.0
Particle Size Distribution,[a] U.S. series mesh size		
+10	70.7	2.9
-10+12	7.0	2.3
-12+16	8.7	9.0
-16+30	9.0	33.0
-30+50	3.2	31.9
-50	1.4	20.9
	100.0	100.0

(a) The chemical analyses above correspond to the +50 mesh fraction.

was -50+100 mesh (U.S. sieve series) but the char particle size was much larger, as shown in Table 1, due to swelling during hydrogasification. The average carbon conversion during dilute phase hydrogasification was 26 percent and the resulting chars had an average volatile matter content of about 10 percent. The variation in proximate and ultimate analyses of various chars was small. However, the mean particle diameter of the chars from Pittsburgh No. 8 coal was about three times (about 1800 μm) that of chars from Illinois No. 6 coal due to the higher FSI of Pittsburgh No. 8 seam coals.

Each of the eight char samples were hydrogasified at a fixed total pressure of 1000 psig (69 atm) at several different temperatures ranging from 700 C to 1000 C and employing three feed gas compositions: (a) 100 percent hydrogen, (b) 74 percent H_2-26 percent CH_4, and (c) 48 percent H_2-52 percent CH_4. To contain the samples in the 100 mesh screen basket, only the +50 mesh fraction, which nearly represented the bulk of the samples, was used. These experiments were preceded by studies on the effect of char particle size and gas velocity, employing chars produced at 800 C, to determine the influence of mass transfer on rate of hydrogasification.

In some experiments some carbon was deposited on the sample basket due to cracking of methane present in the feed gas. A correction was made for this deposition on the basket so as to obtain true char hydrogasification rate data.

RESULTS AND DISCUSSION

General Observations and Definitions

It is well recognized that bituminous coals exhibit an initial, transient period of extremely high hydrogasification reactivity followed by a rather slow rate of hydrogasification regime. The initial, high-reactivity period, which is generally over in a few seconds at temperatures above 850 C, consists of gasification of the volatile matter as well as some fixed carbon, the amount of which depends on the partial pressure of hydrogen (2). In the thermobalance, this regime lasts longer because of limitations on rate of heating of coal.

The rate of hydrogasification in the first kinetic regime is so much higher than the rate for the second regime that a "knee" is apparent in the curves showing fractional conversion, X, versus time as shown in Figure 3. The definition of X is

$$X = \frac{-\Delta W}{W_o} \qquad 1)$$

where $-\Delta W$ is the weight loss of as-received char due to gasification and W_o is the initial weight. Because of the heat up effects during the first minute the thermobalance is not suitable for determining the rate of hydrogasification in the rapid-hydrogasification kinetic regime. However, it is quite suitable for determining the onset of the slow-hydrogasification kinetic regime which is made possible by noting the "knee" in the X versus time curves. This boundary or "cut-off point" between the two regimes, designated as X_{CP}, was determined for each hydrogasification run. The cut-off reaction time was found to be as much as about 2.5 minutes at 700 C and as short as about 0.5 minutes at 1000 C. Johnson (11) used 2 minutes as the cut-off time for hydrogasification runs at temperatures of 850 C or higher.

The thermobalance data were correlated in terms of the conversion of base carbon which is that portion of the total carbon in char which is not associated with the ASTM volatile matter (10,11). The fractional conversion of base carbon is defined as

$$X_{BC} = \frac{X-V}{1-A-V} \qquad 2)$$

where V is the ASTM volatile matter (including moisture) and A is the ash content of char, each expressed as weight fraction of as-received char. As mentioned above, a portion of the base carbon is hydrogasified in the rapid-hydrogasification regime. The total amount of this "rapid base carbon" is represented as X^R_{BC}. The remaining base carbon can be termed "slow base carbon". Now another fractional conversion term can be defined based on the slow base carbon content of char:

$$X_{SC} \equiv \frac{X_{BC}-X^R_{BC}}{1-X^R_{BC}} = \frac{X-X_{CP}}{1-X_{CP}-A} \qquad 3)$$

It was assumed in writing Equations 2 and 3 that all volatile matter, including moisture, is hydrogasified during the rapid-hydrogasification regime and that the rate of carbon conversion relative to the rate of ash-free char conversion is constant after devolatilization. Both of the assumptions were found to be quite reasonable as determined by ultimate and proximate analyses data for chars hydrogasified to various levels of conversion.

Rapid Hydrogasification Regime

The effects of gas-film and pore diffusion on the yield of rapid base carbon conversion, X^R_{BC}, were investigated by varying the gas velocity and particle size, respectively. All experiments were performed at 1000 C temperature using a feed gas containing only H_2. Increasing the superficial gas velocity from 0.04 to 0.23 ft/sec resulted in only a slight increase in X^R_{BC} as shown in Figure 4. And increasing the mean particle diameter from 450 to 2100 μm did not affect X^R_{BC} as shown in Figure 5. Anthony, et al, on the other hand, reported a significant increase in the yield of rapid base carbon with decreasing particle diameter. One explanation for this difference may be that Anthony, et al, worked with rather dense particles compared to the char particles used in this study which had a popcorn-like consistency in which case the internal surfaces of particle may be equally accessible to H_2 for particles of varying outer diameters.

The +50 mesh samples denoted by closed symbols in Figure 5 were employed for determining the dependence of X^R_{BC} as a function of temperature, pressure, and feed gas composition as well as the char preparation (dilute phase hydrogasification) temperature. The char preparation temperature did not appear to affect X^R_{BC} for either type of coal.

Since the variation among the individual values of X^R_{BC} was small enough, the average values of X^R_{BC} for the eight chars were used to determine the effect of temperature and partial pressure of H_2 and CH_4. The average X^R_{BC} values were found to depend on temperature and p_{H_2} but not on p_{CH_4}. Furthermore, temperature seemed to affect X^R_{BC} only below 800 C. The data were correlated using the following equation which is similar to the one given by Johnson (11) for temperatures exceeding about 850 C:

$$-\ln(1-X^R_{BC}) = k_1\, p_{H_2} \qquad 4)$$

where k_1 is a function of temperature. Figure 6 shows the dependence of X^R_{BC} on p_{H_2} for temperatures ranging from 800 to 1000 C. The k_1 values obtained at different temperatures are summarized below:

Temperature, C	k_1, atm^{-1}
700	0.0016
750	0.0023
≥800	0.0030

It should be pointed out that Johnson did not apply Equation 4 for temperatures below about 850 C.

The effect of temperature was found to be qualitatively similar to that observed by others (2,10,14,15), i.e., X_{BC}^{R} increases with temperature until about 850 C and then levels off. Actually, the relationship between X_{BC}^{R} and temperature may be quite complex as shown by Pyricioch, et al (10), and Anthony, et al (2). At temperatures exceeding 850 C, Johnson found the value of k_1 to be 0.0092 for air pretreated Ireland mine coal char, containing 28.4 percent volatile matter, as opposed to 0.0030 for this study. The difference in these k_1 values is because some rapid base carbon is hydrogasified during dilute phase hydrogasification in the Hydrane Process.

Slow Hydrogasification Regime

It is necessary that a significant portion of the base carbon be gasified in the slow hydrogasification regime if the following conditions are to be met for a process involving the direct hydrogasification of high-volatile bituminous coal together with steam-oxygen gasification of char: (a) process operates at a total pressure of 1000 psig or lower, (b) the heat content of gas after methanation of the CO produced in the direct hydrogasification stage is equal to or greater than 950 Btu/scf, (c) there is no excess char produced. Therefore, the thermobalance data were analyzed to determine the kinetic parameters for the slow hydrogasification regime.

Rate Expression

The slow hydrogasification reaction has been studied by a number of researchers (10-12,15-19) and a number of rate expressions have been employed for the same. Most of these rate expressions can be written in the following generalized form:

$$-\frac{dX_{SC}}{dt} = k_2'(1-X_{SC})^{n_1} \exp(n_2 X_{SC})^{n_3} \qquad 5)$$

where X_{SC} is the fraction of the base carbon that remains in the char after the rapid hydrogasification stage is complete, and k_2', n_1, n_2, and n_3 are parameters that depend on reaction conditions. Following are some specific forms of Equation 5 that appear in literature:

$$-\frac{dX_{SC}}{dt} = k_2''(1-X_{SC}) \qquad 6a)$$

$$-\frac{dX_{SC}}{dt} = k_2'''(1-X_{SC})^{2/3}\exp(-\alpha X_{SC}^2) \qquad 6b)$$

$$-\frac{dX_{SC}}{dt} = k_2(1-X_{SC}) \exp(-bX_{SC}) \qquad 6c)$$

The first of these is the simplest, but not generally found to be applicable to hydrogasification (11,12). The second equation was used by Johnson who found the value of α to be 0.97. At this value of α, however, Equation 6b can be approximated by Equation 6a since the value of $(1-X_{SC})^{1/3}$ is within 3 percent of the value of $\exp(-0.97\ X_{SC}^2)$ for X_{SC} values up to 0.6 which covers the range of interest. Equation 6c was developed by Gardner, et al, who assumed that bRT was independent of temperature (12), unlike the results of our study, discussed later.

Equation 6a, which is a good approximation for Equation 6b as discussed above, was found to be unsatisfactory for hydrogasification of Hydrane char, particularly at temperatures below 900 C. This is illustrated in Figure 7 which shows the plots of

$\ln(1-X_{SC})$ as a function of time, which are expected to be straight lines for Equation 6a to be valid. However, Equation 6c was found to be applicable at all conditions and was therefore used in this study. The basic hypothesis behind Equation 6c is that there is a continuous, exponential decay in the reactivity of the char as hydrogasification proceeds.

The determination of parameters k_2 and b required rearranging Equation 6c and taking the integral of each side as follows:

$$\int_{o}^{X_{SC}} \frac{-\exp(bX_{SC})}{(1-X_{SC})} = k_2 t \qquad 7)$$

where t is measured from the end of the rapid hydrogasification regime. The integral on the left hand side of Equation 7 was numerically evaluated for various values of b to give the best straight line when plotted against t. Samples of straight lines thus obtained are shown in Figure 8.

Effect of Gas-Film and Pore Diffusion

The effect of gas-film diffusion on the initial rate of hydrogasification, k_2, was found to be significant only below a gas velocity of about 0.15 ft/sec as shown in Figure 9. Wen, et al, similarly found that gas-film diffusion was not an important factor in their experiments with Hydrane char at 0.2 ft/sec (17). The gas velocities used for studying the effects of the variables discussed next were kept high enough so that gas-film diffusion was not a factor.

The effect of particle size on k_2 for Hydrane char was found to be quite different from that found by others for preoxidized coal chars. Specifically, the value of k_2 for Hydrane char was found to increase significantly with mean particle diameter as shown in Figure 10. But, Tomita, et al, found that changing the particle size range of low volatile coal char from -40+100 to -200+325 U.S. mesh resulted in a 1.6-fold increase in the hydrogasification rate at 400 psig and 980 C (19). Johnson, on the other hand, used a rate expression which assumed the rate to be independent of particle size (11). The reason for the peculiar behavior of the Hydrane char is yet unknown. It is suspected that the variation in internal surface properties with particle size will explain this peculiar behiavor. Variation in the ash content was not found to be large enough to explain it.

Effect of Char Preparation
Conditions and Coal Type

The char preparation temperature was not found to affect the initial rate of hydrogasification, k_2. However, the Pittsburgh No. 8 seam chars were found to be more reactive than Illinois No. 6 seam chars as shown in Figure 10. The difference in the reactivities of the +50 mesh fractions, which nearly represented the entire char sample as shown in Table 1, was even more pronounced due to the difference in the mean particle diameter. On the average, the +50 mesh Pittsburgh No. 8 chars were about 25 percent more reactive than the +50 mesh Illinois No. 6 chars. Johnson, on the other hand, using preoxidized chars found the Pittsburgh No. 8 chars to be about 10 percent less reactive than Illinois No. 6 chars (20). Again this difference is unexplained but is suspected to be due to variation in surface properties. For one thing, the bulk density of Pittsburgh No. 8 chars was found to be considerably lower than that of Illinois No. 6 chars.

In order to determine the effect of preoxidation on reactivity, the k_2 values for Hydrane char from our study were compared with those reported in literature for other chars. The comparison, which was complicated due to variation in coal sources

and kinetic expressions used to determine rate constants, did not conclusively show that Hydrane char is more reactive than chars produced by preoxidation. For example, the k_2 value for Pittsburgh No. 8 Hydrane char at 900 C using H_2 only was found to be 0.074 hr^{-1} atm^{-1}. On the other hand, Johnson (11) and Gardner, et al (12) reported 0.021 and 0.117 hr^{-1} atm^{-1}, respectively, for preoxidized chars from similar coals. Also, we found that the k_2 value for preoxidized Synthane char was 0.037 hr^{-1} atm^{-1} for the same coal (13).

Effect of Pressure and Temperature

Since the char preparation temperature did not significantly affect the k_2 values, these were averaged over the four types of chars for each coal source. Thus, for each set of temperature and pressure, two k_2 values, one for each coal source, were obtained.

The back reaction of methane to form carbon on char was found to make a very significant contribution at higher temperatures and methane partial pressures. In fact, the value of k_2 was found to be nearly zero at about 850 C when the partial pressures of H_2 and CH_4 were 33.1 and 35.9 atm, respectively. A simplified form of the following correlation, developed by Johnson, was used:

$$k_2 = \frac{k_3 \, p_{H_2}^2 \left[1 - \frac{p_{CH_4}}{p_{H_2}^2 K^E}\right]}{1 + k_4 \, p_{H_2}} \qquad 8)$$

where k_3 and k_4 are constants that depend on temperature only and K^E is the equilibrium constant for the formation of CH_4 by reaction of H_2 with β-graphite. However, at the conditions used in this study, $k_4 \, p_{H_2}$ is expected to be large compared to one (11). Thus, Equation 8 can be simplified as follows:

$$k_2 = k_5 \left[p_{H_2} - \frac{p_{CH_4}}{p_{H_2} K^E}\right] \qquad 9)$$

But, k_5 is expected to show an Arrhenius type dependence on temperature. Thus,

$$k_2 = k_o \exp(-E_o/RT) \left[p_{H_2} - \frac{p_{CH_4}}{p_{H_2} K^E}\right] \qquad 10)$$

Figure 11 shows that Equation 10 is applicable for Illinois No. 6 chars only above about 850 C. Below 850 C, k_2 does not appear to be too sensitive to temperature. Similar results were found for Pittsburgh No. 8 chars. For this range of applicability the following values of k_o and E_o were determined for the two coal sources:

Coal Source	k_o, min^{-1} atm^{-1}	E_o, kcal/mole
Pittsburgh No. 8 seam	106.2	26.5
Illinois No. 6 seam	1067.1	32.5

In Figure 11, the data points for higher CH_4 partial pressures appear to fall somewhat below those at lower CH_4 pressures. This suggests that the value of K^E for Hydrane char is somewhat higher than the value for β-graphite. This is also supported by the fact that the value of k_2 for Hydrane char at 850 C, p_{H_2} and p_{CH_4} values of 33.1 and 35.9 atm, respectively, was positive, though nearly zero, while it is expected to be negative for β-graphite at temperatures above 840 C for the same partial pressures of H_2 and CH_4.

It is easy to see from Equation 6c and 10 that E_o corresponds to the activation energy for hydrogasification at X_{SC} equal to zero. As X_{SC} increases, the effective activation energy, E_1, increases since bRT is positive and Equations 6c and 10 can be combined as follows:

$$\frac{dX_{SC}}{dt} = k_o(1-X_{SC}) \exp(-E_1/RT)[p_{H_2} - \frac{p_{CH_4}}{p_{H_2} E^K}] \qquad 11)$$

where

$$E_1 = E_o + (bRT)X_{SC}. \qquad 12)$$

Equation 12 shows that the char becomes less reactive as X_{SC} increases. Gardner, et al, assumed but did not show that bRT is independent of temperature and pressure. However, bRT for Hydrane char was found to depend both on temperatures and partial pressure of H_2 and CH_4 as shown in Figure 12. The bRT values plotted in Figure 12 are average values based on eight chars since the coal source and char preparation temperature did not significantly affect bRT. Three things are to be noted in Figure 12. First, bRT decreases with temperature, i.e., higher temperatures help maintain the reactivity. Second, the bRT is more or less independent of temperature above 850 C which is the regime that Gardner, et al, operated in. And third, bRT decreases with increasing p_{H_2}. In other words, higher p_{H_2}, just as higher temperature, impedes decay of reactivity with increasing X_{SC}.

The value of bRT at 850 C or higher for 100 percent H_2 case was found to be 3.6 kcal/mole. For these conditions one can write the apparent activation energy as a function of X_{SC} for Pittsburgh No. 8 chars as

$$E_1(\text{kcal/mole}) = 26.5 + 3.6\ X_{SC}. \qquad 13)$$

Gardner, et al, on the other hand, found the following relationship for preoxidized Pittsburgh No. 8 char

$$E_1 = 29.3 + 2.43\ X_{MAF} \qquad 14)$$

where X_{MAF} can be approximated by X_{SC}. Thus, the initial activation energy, E_o, and rate of deactivation are not affected much on preoxidation of coal. This suggests that the kinetic data for the slow hydrogasification regime reported in this paper are generally applicable to direct hydrogasification processes whether they employ preoxidation or not.

Although the results on bRT are preliminary and somewhat sketchy, they provide important insight into the factors responsible for deactivation of chars during hydrogasification.

Conditions for Achieving Required Carbon Conversion

As mentioned earlier, about 50 percent of the carbon present in raw coal needs to be hydrogasified in the dilute phase and fluid bed stages for balanced operation. The conditions required to achieve this level of carbon conversion were therefore determined by combining the dilute phase and thermobalance data. Figure 13 shows the total carbon conversion, including 26 percent for dilute phase hydrogasification, as a function of time, temperature, and gas composition for Pittsburgh No. 8 char. The curves in Figure 13 are applicable when the second-stage hydrogasification takes place in a fluid bed reactor with perfect backmixing of gas. Under such conditions the product gas composition for the second-stage reaction is to be used to determine the appropriate curve in Figure 13. Note that the data for 100 percent H_2 case are not plotted since the CH_4 concentration in the gas from the fluid bed stage will be between

25 and 50 percent, probably greater than 40 percent.

CONCLUSIONS

Kinetic data were obtained on a thermobalance (TGA) for hydrogasification of chars produced in a dilute phase hydrogasifier, for designing a scaled-up, direct, fluid-bed hydrogasification reactor for the Hydrane process. Two distinct kinetic regimes were observed at any set of conditions. The first regime corresponded to rapid hydrogasification of volatile matter as well as some base carbon and was over in less than 2.5 minutes in the TGA. For this regime the yield of base carbon conversion, X^R_{BC}, was found to be practically independent of gas velocity, particle size, and char type. The yield of X^R_{BC} increased continuously with p_{H_2} which was the most important variable. The yield of X^R_{BC} was found to be independent of p_{CH_4}. Apparently the rate of the forward reaction between coal carbon and H_2 was much higher than the rate of cracking of CH_4 at all conditions. Increasing the temperatures resulted in an increase in X^R_{BC} until about 800 C, after which it did not change.

The second kinetic regime corresponded to the slow hydrogasification of base carbon. A kinetic model was employed that properly accounted for the fact that there was continuous deactivation of char with increasing fractional conversion. The rate of deactivation was found to be lower at higher temperatures and p_{H_2}. Again, the char preparation temperature did not affect the reactivity. But, there were two unexpected results. First, the initial rate of hydrogasification, k_2, increased with particle size. And second, the Pittsburgh No. 8 chars were found to be more reactive than Illinois No. 6 chars rather than the opposite. It is possible that these two unexpected results can be explained on the basis of differences in surface properties such as surface area, average pore size, etc. Although the surface properties of Hydrane char may be different from those of preoxidized chars, the initial activation energy and rate of deactivation with level of conversion are not. Also, it cannot be conclusively shown that initial rate of gasification of Hydrane chars is higher than that of pre-oxidized coal chars.

ACKNOWLEDGMENTS

This work was supported by the Energy Research and Development Administration (now DOE). The technical assistance provided by Drs. Jim A. Gray and Mike Baird of PERC and Mr. Herman Feldmann of Battelle is greatly appreciated.

REFERENCES

(1) Feldmann, H. F. and Yavorsky, P. M., Proceedings of the Fifth Synthetic Pipeline Gas Symposium, A.G.A. Catalog No. L5 1173, 1974, p 287.

(2) Anthony, D. B. and Howard, J. B., AIChE Journal, 22 (4), 625 (1976).

(3) Gray, J. A., Donatelli, P. J., and Yavorsky, P. M., Preprints of Fuel Chemistry Division, ACS, 20 (4), 103 (1975).

(4) Feldmann, H. F., Chauhan, S. P., Longanbach, J. R., Hissong, D. W., Conkle, H. N., Curran, L. M., and Jenkins, D. M., "A Novel Approach to Coal Gasification Using Chemically Incorporated CaO", Phase II Summary Report to ERDA, Battelle Report No. BMI 1986 (UC-90c), November 11, 1977, p 33.

(5) Wen, C. Y., Li, C. T., Tscheng, S. H., and O'Brien, W. S., "Comparison of Alternate Coal Gasification Processes for Pipeline Gas Production", paper presented at 65th Annual AIChE Meeting, New York, November 26-30, 1972.

(6) Hottel, H. C. and Howard, J. B., New Energy Technology, MIT Press, Cambridge, Mass., 1971.

(7) Gray, J. A. and Sprouse, K. M., "Hydrogasifier Development for the Hydrane Process", First Quarter Report, FE 2518-4 (UC-90c), June, 1977.

(8) Chauhan, S. P., Feldmann, H. F., Stambaugh, E. P., and Oxley, J. H., Preprints of Fuel Chemistry Division, ACS, 20 (4), 207 (1975).

(9) Chauhan, S. P., Feldmann, H. F., Stambaugh, E. P., Oxley, J. H., Woodcock, K., and Witmer, F., Preprints of Fuel Chemistry Division, ACS, 22 (1), 38 (1977).

(10) Pyrcioch, E. J. and coworkers, IGT Res. Bull. No. 39, Chicago, November, 1972.

(11) Johnson, J. L., Coal Gasification, Advances in Chemistry Series No. 131, Ed. by L. G. Massey, American Chemical Society, Washington, D.C., 1974, p 145.

(12) Gardner, N., Samuels, E., and Wilks, K., *ibid*, p 217.

(13) Longanbach, J. R. and Chauhan, S. P., "Study of Hydrogasification Rate of Reaction for Hydrane Char by the Thermobalance Method", Phase III Summary Report to ERDA, Battelle Report No. BMI-X-680, May 5, 1977.

(14) Feldmann, H. F., Mima, J. A., and Yavorsky, P. M., Coal Gasification, Advances in Chemistry Series No. 131, Ed. by L. G. Massey, American Chemical Society, Washington, D.C., 1974, p 108.

(15) Wen, C. Y. and Huebler, J., I&EC Proc. Des. & Dev., 4 (2), 142 (April, 1965).

(16) Wen, C. Y. and Huebler, J., *ibid*, p 147.

(17) Wen, C. Y., Mori, S., Gray, J. A., and Yavorsky, P. M., Preprints of Fuel Chemistry Division, ACS, 20 (4), 155 (1975).

(18) Feldmann, H. F., Chemical Reaction Engineering Reviews, Advances in Chemistry Series No. 148, Ed. by H. M. Hulbert, American Chemical Society, Washington, D.C., 1975, p 132.

(19) Tomita, A., Mahajan, O. P., and Walker, P. L., Jr., Preprints of Fuel Chemistry Division, ACS, 20 (3), 99 (1975).

(20) Johnson, J. L., Preprints of Fuel Chemistry Division, ACS, 20 (4), 85 (1975).

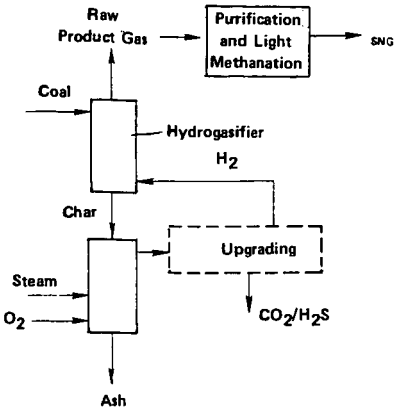

FIGURE 1. SCHEMATIC FLOWSHEET FOR DIRECT HYDROGASIFICATION OF COAL

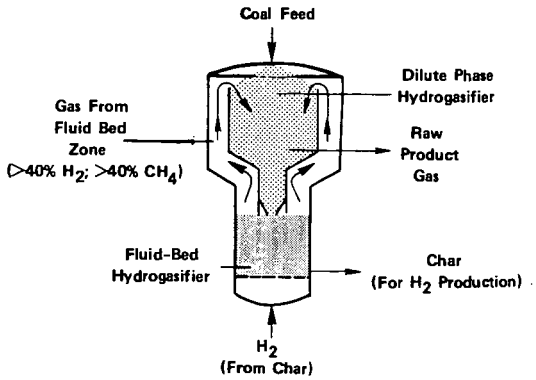

FIGURE 2. SCHEMATIC OF TWO-STAGE HYDROGASIFIER FOR THE HYDRANE PROCESS (Ref. 17)

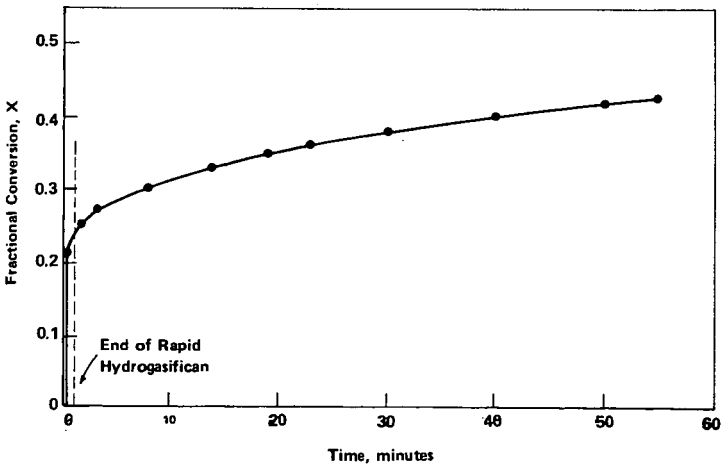

FIGURE 3. TYPICAL THERMOBALANCE DATA FOR HYDROGASIFICATION OF CHAR

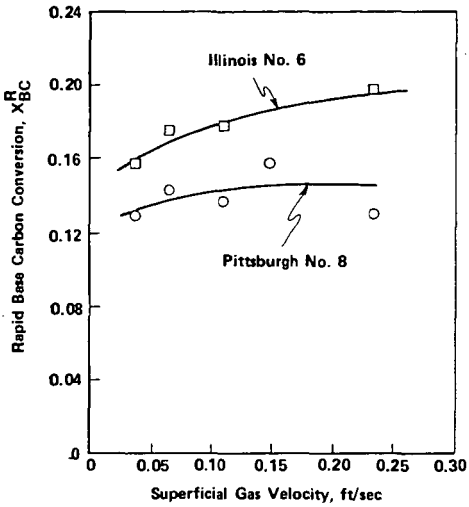

FIGURE 4. DEPENDENCE OF X^R_{BC} ON GAS VELOCITY FOR HYDROGASIFICATION OF -18+35 MESH CHAR AT 1000 C, 69 ATM, 100% H_2

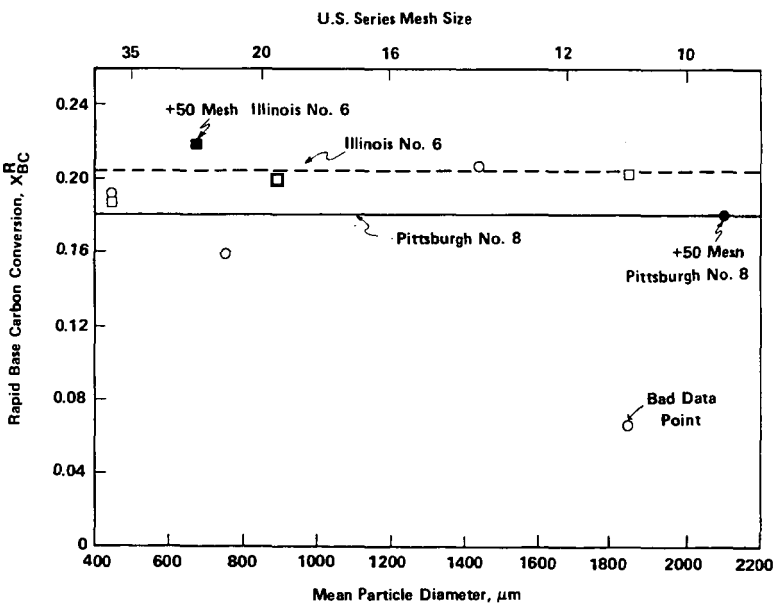

FIGURE 5. DEPENDENCE OF X^R_{BC} ON CHAR PARTICLE SIZE FOR HYDROGASIFICATION AT 1000 C, 69 ATM, 100% H_2

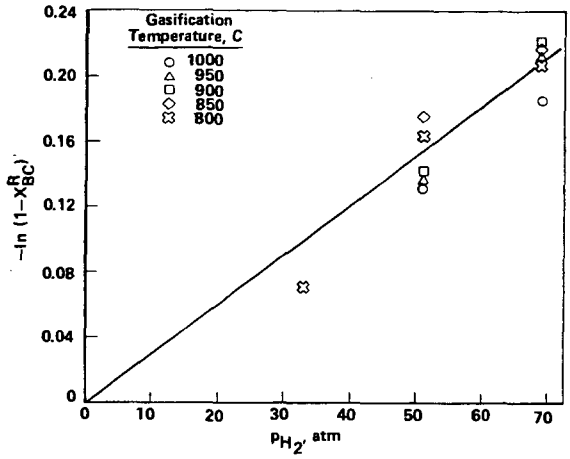

FIGURE 6. CORRELATION OF X^R_{BC} WITH HYDROGEN PARTIAL PRESSURE

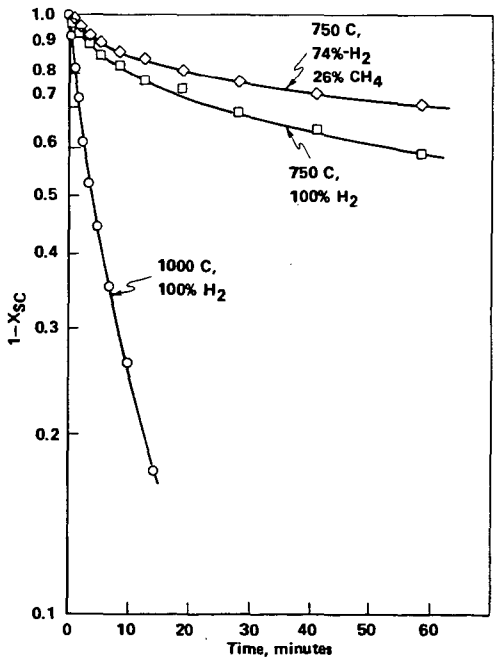

FIGURE 7. $(1-X_{SC})$, PLOTTED ON A LOGARITHMIC SCALE, VERSUS TIME FOR HYDROGASIFICATION OF PITTSBURGH NO. 8 CHAR AT 69 ATM TOTAL PRESSURE

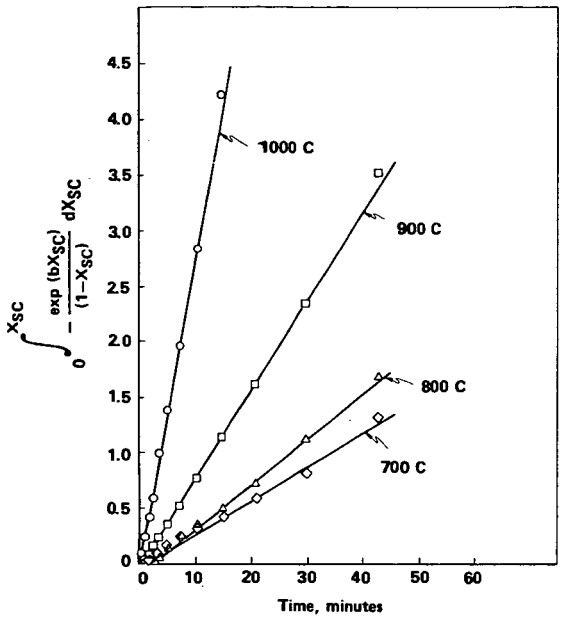

FIGURE 8. $\int_0^{X_{SC}} \frac{-\exp(bX_{SC})}{(1-X_{SC})} dX_{SC}$ VERSUS TIME FOR HYDROGASIFICATION OF PITTSBURGH NO. 8 CHAR AT 69 ATM, 100% H_2

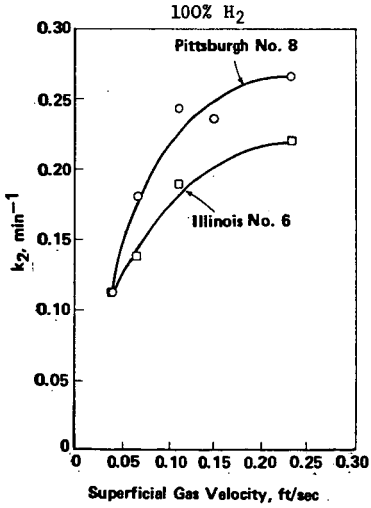

FIGURE 9. DEPENDENCE OF k_2 ON GAS VELOCITY FOR HYDROGASIFICATION OF -18+35 MESH CHAR AT 1000 C, 69 ATM, 100% H_2

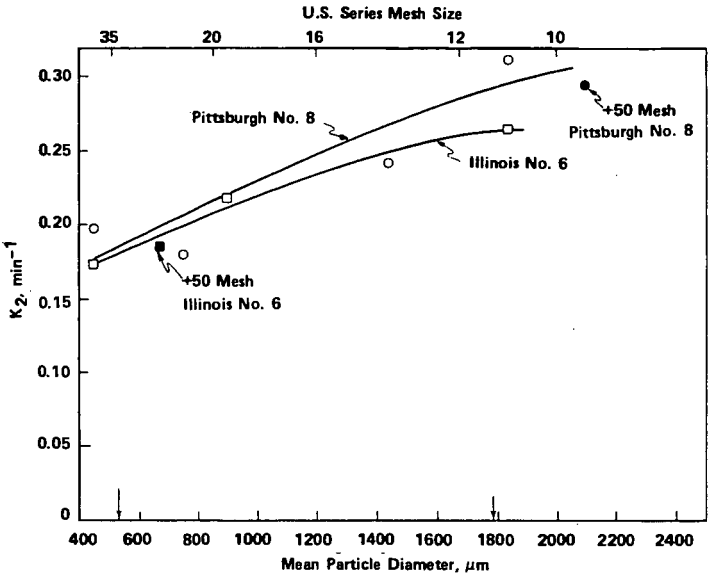

FIGURE 10. DEPENDENCE OF k_2 ON CHAR PARTICLE SIZE FOR HYDROGASIFICATION AT 1000 C, 69 ATM, 100% H_2

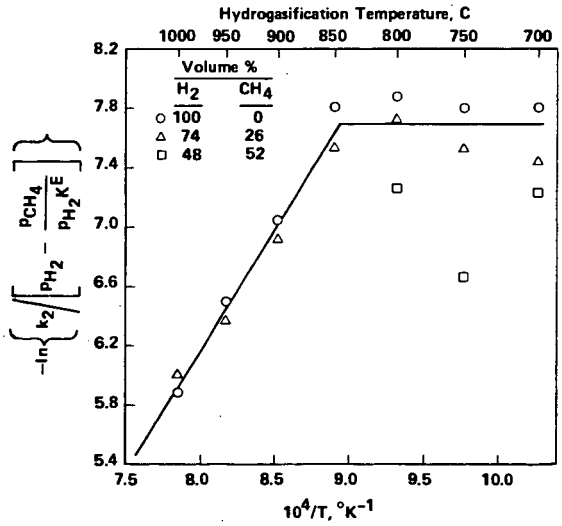

FIGURE 11. CORRELATION OF k_2 WITH HYDROGASIFICATION CONDITIONS FOR CHARS DERIVED FROM ILLINOIS NO. 6 COAL. TOTAL PRESSURE = 69 ATM

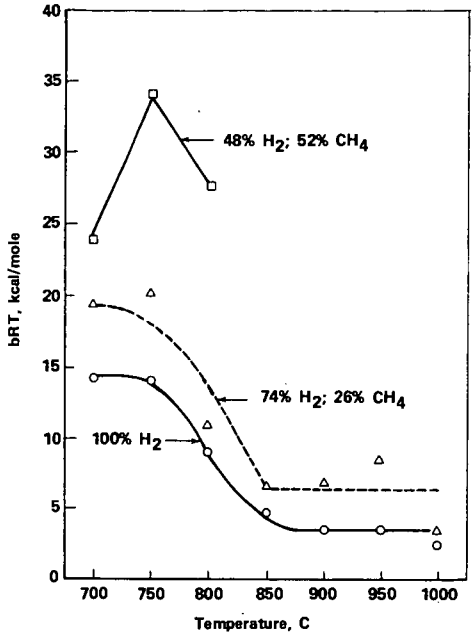

FIGURE 12. DEPENDENCE OF bRT ON REACTION CONDITIONS. TOTAL PRESSURE = 69 ATM

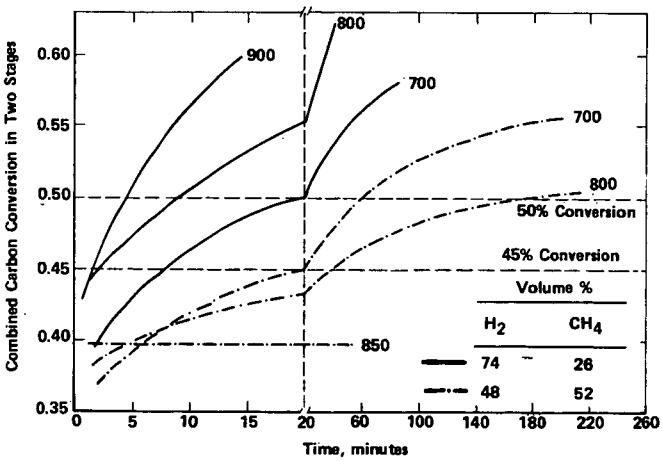

FIGURE 13. COMBINED CARBON CONVERSION IN FIRST STAGE (DILUTE PHASE) AND SECOND STAGE AS A FUNCTION OF TIME AT 69 ATM TOTAL PRESSURE FOR CHARS DERIVED FROM PITTSBURGH NO. 8 COAL

KINETICS OF POTASSIUM CATALYZED GASIFICATION

Charles J. Vadovic and James M. Eakman

Coal Research Laboratory
Exxon Research and Engineering Company
P. O. Box 4255
Baytown, Texas 77520

INTRODUCTION

The Exxon Catalytic Coal Gasification Process(2) is based upon a new combination of processing steps which avoid thermodynamic constraints inherent in the previous art. The use of the catalyst in the reaction step and the manner in which the reactor is integrated into the overall process are the keys to this concept. The goal of the work reported here is the formulation of a kinetic relationship for catalytic gasification which can be used in developing a model for the fluid bed reactor used in this process. This model is needed to correlate pilot unit conversion data and as a design tool for commercial scale units. This paper reports on the work which culminated in the successful formulation of the required kinetic expression.

Alkali metal gasification catalysts increase the rate of steam gasification(3,4,5) promote gas phase methanation equilibrium,(2,5) and minimize agglomeration of caking coals.(1) The catalytic gasification process uses an alkali metal gasification catalyst (K_2CO_3) with a novel processing sequence which maximizes the benefits of the catalyst. The process combines a relatively low gasifier temperature (1300°F) and high pressure (500 psig) with the separation of syngas ($CO + H_2$) from the methane product. The syngas is recycled to the gasifier so that the only net products from gasification are CH_4, CO_2, and small quantities of H_2S and NH_3. The resulting overall gasification reaction can be represented as follows:

$$\text{Coal} + H_2O \rightarrow CH_4 + CO_2$$

Since this reaction is essentially thermoneutral, major heat input to the gasifier at high temperature is not required. Thus, as discussed by Nahas and Gallagher(5), second law constraints on thermal efficiency inherent in other processes are avoided.

A simplified flow plan for the process is shown in Figure 1. Coal is impregnated with catalyst, dried and fed via a lockhopper system to a fluidized bed gasifier which operates at about 1300°F and 500 psig. The coal is gasified with a mixture of steam and recycled syngas. The major gasifier effluents are CH_4, CO_2, CO, H_2, and unconverted steam. No tars or oils are produced. The gaseous products are cooled and the unconverted steam is condensed. The dry product gas is treated in a series of separation steps including acid gas scrubbing to remove CO_2 and H_2S, and cryogenic fractionation to separate methane from syngas. The syngas is combined with feed steam and recycled to the gasifier at approximately 150°F above the gasification temperature. Although there is no net heat required for the gasification reactions, some small amount of heat input is required to heat up the feed coal, to vaporize residual water, and to provide for gasifier heat losses.

Ash/char residue from the gasification step is sent to a catalyst recovery unit in which a large fraction of the catalyst is leached from the residue using countercurrent water washing. The recovered catalyst, along with some makeup catalyst, is reimpregnated on the coal to complete the catalyst recovery loop.

EXPERIMENTAL

Design of the gasifier for this process requires a quantitative description of the kinetics of the catalytic gasification reaction. Bench scale studies were conducted in a fixed bed reactor to provide the necessary data for the development of the rate equation.

Apparatus

The high pressure apparatus used in this study is shown in Figure 2. The main components of the system are the fixed bed reactor, water pump and steam generation equipment, pressure and temperature control systems, unreacted steam condenser, a gas chromatograph and a dry gas flow measurement system. Provisions were included for the optional use of an inert or reactant gas (such as H_2 + CO) as a feed supplementing steam.

A high pressure pump was used to supply H_2O at a constant rate to the steam generator which consisted of 1/4" stainless steel tubing coiled around the fixed bed reactor. Both the steam generator and the reactor were mounted vertically in a split tube furnace. The reactor temperature was measured and controlled at the center of the bed of char. The product gas stream, consisting primarily of H_2, CO, CH_4, CO_2 and unreacted H_2O, was filtered and then depressurized through the pressure control valve. The unreacted H_2O was condensed and the gas stream was further dried by calcium sulfate. The dry gas stream passed through a gas chromatograph sampling system, which provided automatic sampling at 15-minute intervals. The dry gas flow was measured by a wet test meter connected to a pulse generator. The signals from the pulse generator were accumulated as a measure of total gas volume produced.

The fixed bed reactor was constructed from 1-inch Schedule 80 stainless steel pipe and was approximately 30 inches in length. The reactor was filled to a depth of 15 inches by 1/8-inch mullite beads which supported the bed of char.

Procedure

Samples were prepared by soaking 30 to 100 mesh Illinois coal No. 6 in a solution containing the desired weight of catalyst, typically between 10 and 20 gms K_2CO_3/100 gms of coal (referred to as 10 and 20% K_2CO_3). Normally, the weight ratio of water to coal was slightly greater than one. The samples were then dried overnight in a vacuum oven. A scanning electron microscope study showed a fairly even dispersion of potassium throughout the coal particle. The impregnated coal samples were then devolatilized at atmospheric pressure for 30 minutes in a muffle furnace under a nitrogen atmosphere at 1200°F. The samples were allowed to cool to room temperature and then stored in bottles under nitrogen.

A run was made by loading the reactor with a 20 gram char sample. The reactor was purged with helium and the temperature was raised to the desired level. At that point the pressure in the reactor was raised to operating conditions by manually injecting water through the pump. When the run pressure was achieved, the pump was set in the automatic mode. If syngas was used, the supplementary gas valve was also opened at the start of the run. Steam and syngas (if used) were then fed to the reactor. At the end of a run, the feed was shut off and the unit depressured.

During the run, gas analyses and cumulative dry gas volumes were obtained. From this data the carbon gasified is calculated. Assuming that the oxygen content of the char is small in relation to the oxygen content of the steam fed, the steam conversion is obtained from the oxygen content of the dry product gases.

Runs were made in the fixed bed reactor with Illinois coal catalyzed with 10% and 20% K_2CO_3 with steam as the gasifying medium. Temperatures of 1200°F and 1300°F were used and pressures varied from 0 to 500 psig. Steam flows ranged from 3 to 100 gm/hr. With these conditions, steam conversions from 10% to 80% and total carbon conversions from 50% to 100% were obtained. Material balances on hydrogen were used to check the consistency of the data. The balance closures ranged from 100% to 105% for typical runs.

Results

During the runs it was observed that the steam gasification rate was independent of pressure. The gasification rate was found to increase with an increasing rate of steam fed to the reactor. Additionally, at high steam flow rates, or low steam conversions, the gasification rate was directly proportional to the catalyst loading. One explanation for these observations is that the kinetics are controlled by a strong product inhibition. This suggests that a kinetic expression in the classical Langmuir-Hinshelwood form may be used to fit the data. It was further seen that methane and carbon dioxide were in chemical equilibrium with the other gas phase components for the conditions studied, i.e., the methanation and shift reactions are at equilibrium.

DATA INTERPRETATION

Fixed Bed Reactor Model

A mathematical model for the fixed bed reactor was developed based upon the observed behavior. Plug flow of gas through the bed is assumed. It is also assumed that strong product inhibition results in a high rate of gasification over a very short distance of the bed followed by a slower rate over the remaining length of the bed where higher partial pressures of products exist. This assumption leads to a simplified picture for the fixed bed reactor shown in Figure 3. In this model the reaction proceeds so as to form a sharp "carbon burnoff front." If little or no carbon is present, gasification will not take place. Therefore, the potassium catalyst which is left behind this "burnoff front" does not contribute to the reaction rate.

The equation describing conversion in the plug flow reactor is

$$\int_0^V \frac{dV}{N^o_{H_2O}} = \int_0^x \frac{dx}{-r_G} \tag{1}$$

where V is the reactor volume, $N^o_{H_2O}$ is the molar rate of steam fed to the reactor, r_G is the molar rate of the carbon-steam gasification reaction per unit volume and x is the extent of reaction defined as moles carbon gasified per mole steam fed. The sharp burnoff front model provides a relationship between the carbon remaining in the bed and the effective fixed bed reactor volume,

$$n_c = C_c\ V \tag{2}$$

where n_c is the instantaneous moles of carbon in the bed, V is the effective reactor volume, and C_c is the proportionality constant with the dimension moles carbon per unit volume. Based upon initial bed conditions C_c will have a value of approximately 0.045 gmole/cc. Substitution of Equation (2) into Equation (1) provides

$$\frac{n_c}{N^o_{H_2O}\ C_c} = \int_0^x \frac{dx}{-r_G} \tag{3}$$

This model may now be used for the identification of acceptable forms for the rate, r_G, and to obtain best fit values for the parameters in these expressions.

A Langmuir-Hinshelwood type expression for heterogeneous catalytic kinetics as applied to the carbon-steam reaction may be written in the generalized form.

$$r_G = \frac{k[p_{H_2O} - p_{CO}\ p_{H_2}/K_G]}{1 + \sum_i (b_i p_i + \sum_j b_{ij} p_i\ p_j)} \tag{4}$$

where p_{H_2O}, p_{CO}, p_{H_2}, etc. represent the partial pressures of these components, k is the kinetic rate constant for the carbon-steam reaction, K_G

is the equilibrium constant for this reaction, and the b's represent the adsorption constants, no more than four of which will be allowed to be nonzero in any one model being tested.

Equation (4) when substituted into Equation (3) gives

$$\theta = \frac{n_c}{N^{\circ}_{H_2O}} = \frac{C_c}{k}\int_0^x \frac{dx}{R_G} + \sum_i \frac{b_i C_c}{k}\int_0^x \frac{p_i}{R_G}\,dx + \sum_i\sum_j \frac{b_{ij} C_c}{k}\int_0^x \frac{p_i p_j}{R_G}\,dx \qquad (5)$$

where the reaction driving force term in the denominator of each of the integrals is given by

$$R_G = -[p_{H_2O} - p_{COP_{H_2}}/K_G] \qquad (6)$$

For a given conversion,the shift and methanation equilibrium relationships are sufficient to calculate the partial pressures of all components (H_2, CO, CH_4, CO_2, H_2O) in the gas phase. Using a closely spaced series of incremental values for x, the partial pressures were accurately mapped over a range of conversions. This needed to be done only once. These partial pressures were then substituted as required into the expressions under the integrals shown in Equation (5). The values of these integrals for any specified conversion are then obtained by a Simpson's rule numerical integration of the expression under the integrals.

The data collected in the fixed bed steam gasification experiments described above were used to calculate and tabulate conversion, x, moles carbon gasified per mole steam fed as a function of holding time, θ, moles instantaneous bed carbon per molar steam flow rate. The "carbon burnoff front" model for fixed bed potassium catalyst gasification requires that the data for x as a function of θ collected for different steam flow rates must all mesh together to give a single curve for any fixed temperature, pressure, and catalyst loading. A plot of data collected for steam gasification over a range of steam flowrates at 1300°F, 500 psig and 20% K_2CO_3 on Illinois coal is provided in Figure 4. For each experimental run the initial data points are at the right and move to the left as carbon is depleted from the bed. The flat region in the data at the upper right of Figure 4 represents the equilibrium limit for the carbon steam reaction. This limit corresponds to a carbon activity of about twice that of β-graphite. The region at the lower left of the diagram shows the carbon conversions limited by the rate of reaction. The data points at the different steam rates overlap in the required manner over three orders of magnitude of residence time. Thus, the experimental observations are consistent with the postulated model. This reactor model was then used as the basis for the analysis of the reaction data.

Parameter Estimation

The coefficients in front of the integrals in a series of particular forms of Equation (5) were estimated by regression analysis. The regression data base used consisted of the results of the steam gasification runs at 500 psig described above as well as runs at 0, 100 and 250 psig at steam rates of 6, 12 and 24 gm H_2O/hr. Two additional series of runs were conducted at 500 psig and the same three steam rates. The first was at 1200°F and 20% K_2CO_3 and the second was at 1300°F and 10% K_2CO_3. The data from these runs were used to assess the effect of temperature and catalyst loading on gasification rate.

Numerous kinetic models were formulated and tested by regression for the constants in Equation (5). These models consisted of all combinations of from one to four terms involving the partial pressures of H_2, CO, and H_2O and the cross products of the partial pressures of H_2 and CO, and H_2 and H_2O. Those which gave negative coefficients on regression were discarded as being physically unreal. Four additional models were discarded because they gave an infinite rate in the limit of zero steam conversion. The three models which remained are

(A)
$$r_G = \frac{k(p_{H_2O} - p_{CO}\, p_{H_2}/K_G)}{p_{H_2} + b_1\, p_{H_2O}} \tag{7}$$

(B)
$$r_G = \frac{k(p_{H_2O} - p_{CO}\, p_{H_2}/K_G)}{p_{H_2} + b_1\, p_{H_2}\, p_{CO} + b_2 p_{H_2O}} \tag{8}$$

(C)
$$r_G = \frac{k(p_{H_2O} - p_{CO}\, p_{H_2}/K_G)}{p_{H_2} + b_1\, p_{CO} + b_2\, p_{H_2O}} \tag{9}$$

All are independent of pressure. The variance of the residuals around the regression line for these are A: 0.0556, B: 0.0519, and C: 0.0562. Since Model B has a smaller variance than A or C, it was chosen as the basis for further analysis. However, further studies should be done to better discriminate between these and possibly other kinetic expressions. The coefficients obtained by regression of Model B are

$$\frac{C_c}{k} = 1.603 \text{ hr}$$

$$\frac{b_1 C_c}{k} = 0.3371 \text{ hr/atm}$$

$$\frac{b_2 C_c}{k} = 0.0954 \text{ hr}$$

These coefficients were used in Equation (5) to compute the values of θ required to achieve the various measured conversion levels. These calculated values are compared to the actual holding times in Figure 5. While there is scatter to the data, it is seen that the model provides a reasonable fit over the broad range of pressures (0-500 psig) and flowrates (3-100 gm/hr) considered.

Using the approximate value of C_c = 0.045 gmole/cc, the values for the parameters at 1300°F and 20% K_2CO_3 loading may be expressed as

$$k = 0.0281 \ \frac{\text{gmole C}}{\text{hr}\cdot\text{cc}}$$

$$b_1 = 0.210 \ \text{atm}^{-1}$$

$$b_2 = 0.0595$$

It was found by comparing the 1200°F and 1300°F data that the rate constant, k, has an activation energy of 30 kcal/gmole in the Arrhenius expression. Furthermore, its value at the 10% K_2CO_3 loading was approximately half that at the 20% K_2CO_3 level. Hence, within this range k may be expressed as

$$k = k_o C_K \exp(-E/RT). \tag{10}$$

where k_o is the frequency factor, C_K is the moles of catalytically active potassium per unit volume, E is the activation energy, R is the universal gas constant and T is the absolute temperature. For 20% K_2CO_3 on Illinois coal the value of C_K for the fixed bed of char is typically

$$C_K = 0.0021 \ \text{gmole/cc}$$

On this basis the value of the frequency factor may be computed as

$$k_o = 6.80 \times 10^7 \ \text{gmole C/hr}\cdot\text{gmole K}$$

for

$$E = 30 \ \text{kcal/gmole.}$$

The ratio of holding times necessary to attain a given conversion level, x, at two different temperatures and catalyst levels is given by

$$\frac{\theta_1}{\theta_2} = \frac{k_2}{k_1} = \frac{C_{K_2}}{C_K} \quad \exp\left[-\frac{E}{R}\left(\frac{1}{T_2} - \frac{1}{T_1}\right)\right] \tag{11}$$

This assumes that the temperature difference does not significantly affect the equilibrium calculation for the partial pressures. Equation (11) allows the definition of an "equivalent residence time," θ^*, which can be used to combine data collected at different temperatures and catalyst levels. The quantity θ^* is defined as the holding time at T^* and C_K^* which will give the same conversion as that obtained with a holding time θ at temperature T and catalyst concentration C_K. Specifically,

$$\theta^* = \theta \frac{C_K}{C_K^*} \exp\left[-\frac{E}{R}\left(\frac{1}{T} - \frac{1}{T^*}\right)\right] \tag{12}$$

This relationship was tested for its ability to correlate 500 psig fixed bed reaction data collected at 10% K_2CO_3-1300°F and 20% K_2CO_3-1200°F with the data base collected at 20% K_2CO_3-1300°F. The result is given by the data points shown in Figure 6 where conversion, x, is plotted as a function equivalent residence time, θ^*, with all data adjusted if needed to 1300°F and 20% K_2CO_3. It is seen that the data appear uniformly correlated by this expression.

Generalized Fixed Bed Model

The above kinetic relationships apply to a pure steam feed. In order to apply them to the synthesis gas recycle case, they must be generalized for mixed gas input to the fixed bed. This may be done by writing the differential equations describing the molar flow of each molecular species through the bed and numerically integrating these over the effective volume. These equations are

$$\frac{d N_{H_2}}{dz} = A\ (-3\ r_M + r_S + r_G) \tag{13}$$

$$\frac{d N_{CO}}{dz} = A\ (-r_M - r_S + r_G) \tag{14}$$

$$\frac{d N_{CH_4}}{dz} = A\ r_M \tag{15}$$

$$\frac{d N_{CO_2}}{dz} = A\ r_S \tag{16}$$

$$\frac{d N_{H_2O}}{dz} = A\ (r_M - r_S - r_G) \tag{17}$$

where N_i is the molar flow rate of component i, z is the distance down the bed, A is the cross-sectional area of the bed, and r_M, r_S and r_G are the

rates of the methanation, shift, and carbon-steam gasification reactions respectively expressed as moles per unit reactor volume per unit time.

The reaction rate expressions used for the shift and methanation reactions are

$$r_S = k_S (P_{CO} P_{H_2O} - P_{CO_2} P_{H_2}/K_S) \tag{18}$$

$$r_M = k_M (P_{CO} P_{H_2}^3 - P_{CH_4} P_{H_2O}/K) \tag{19}$$

where k_S and k_M are the respective rate constants and K_S and K_M are the respective equilibrium constants. These reactions may be forced to equilibrium by assigning arbitrarily large rate constants. The reaction rate expression used for the potassium catalyzed carbon-steam reaction is obtained by combining Equations (8) and (10)

$$r_G = \frac{k_o C_K \exp(-E/RT) [P_{H_2O} - P_{CO} P_{H_2}/K_G]}{P_{H_2} + b_1 P_{CO} P_{H_2} + b_2 P_{H_2O}} \tag{20}$$

The ordinary differential Equations (13)-(17) were numerically integrated by a Runga-Kutta-Fehlberg procedure for a series of cases considering pure steam fed to a fixed bed reactor at 500 psig, 1300°F and C_K = .0021 gmoles potassium per cc (corresponding to 20% K_2CO_3 on Illinois coal). The conversion, x, was determined at various distances, z, down the bed from

$$x = \frac{N_{CO} + N_{CH_4} + N_{CO_2}}{N^o_{H_2O}} \tag{21}$$

The residence time corresponding to each conversion was computed as

$$\theta = \frac{C_c A z}{N^o_{H_2O}} \tag{22}$$

The integrations performed in this manner for various steam flowrates overlapped to give the single correlation line shown in Figure 6. This line is seen to provide a reasonable fit to the data.

Model Verification Experiments

To test the predictive capability of the kinetic model with a mixed gas feed, two fixed bed gasification runs were made with steam plus syngas (H_2 + CO)

at 1300°F. One run was made with 5 liter per hour syngas at 500 psig. The second was made with 15 liter per hour syngas at 100 psig. Both runs were made with 12 grams per hour steam feed. In both cases the syngas composition was 75 mole % H2 and 25 mole % CO. In these experiments the conversion, x, was computed as

$$x = \frac{N_{CO} + N_{CH_4} + N_{CO_2} - \overset{\circ}{N}_{CO}}{\overset{\circ}{N}_{H_2O}} \tag{23}$$

where $\overset{\circ}{N}_{CO}$ is the molar rate of carbon monoxide fed to the reactor. The residence time is computed by Equation (22). A comparison between the predicted and experimental conversions for these two experiments is shown in Figure 7. Good agreement is observed in the 500 psig case. The conversions obtained here are essentially the same as observed above for pure steam feed. At 100 psig with higher syngas flow, the data show a lower conversion than at 500 psig for the same residence time. It is also seen that the model underpredicts the actual conversion. This may be due, in part, to the use of parameters which are derived from pure steam data.

CONCLUSIONS

An empirical Langmuir-Hinshelwood kinetic model for the potassium catalyzed gasification of Illinois #6 bituminous coal has been developed. This model provides a good fit to fixed bed reactor data over pressures ranging from atmospheric to 500 psig and a 30-fold range of steam flow rates. It also predicts conversions for the temperature range 1200°F to 1300°F and catalyst loadings from 0.1 to 0.2 grams K_2CO_3 per gram of coal. For the catalyst levels examined, the gasification rate was proportional to the amount of catalyst present. Additional studies need to be performed over a broader range of catalyst loadings to determine the limits of this relationship. It was also shown that these kinetics can be applied to predict trends in conversion for H_2O, H_2 and CO mixed gas feeds.

The kinetic expression obtained has been shown to have adequate predictive capabilities in the range of interest. It is in a form which can be used directly in the development of models for fluid bed gasification reactors. Thus, the goal for this study has been achieved. Future work will be directed toward formulating a fluid bed reactor model.

ACKNOWLEDGEMENT

This work was supported, in part, by Contract #(49-18)-2369, U.S. Department of Energy.

Nomenclature

A	cross-sectional area of reactor
b	adsorption constant in Langmuir-Hinshelwood rate expression
C_C	carbon concentration, moles C per unit reactor volume
C_K	potassium concentration, moles K per unit reactor volume
E	activation energy in Arrhenius expression for carbon-steam reaction rate constant
k	rate constant for carbon-steam reaction
k_o	frequency factor in Arrhenius expression for carbon-steam reaction rate constant
k_M	rate constant for methanation reaction
k_S	rate constant for shift reaction
K_G	equilibrium constant for carbon-steam reaction, atm
K_M	equilibrium constant for methanation reaction, atm^{-2}
K_S	equilibrium constant for shift reaction
N_i	molar flow rate of component $\underline{i}$
N_i^o	molar flow rate of component $\underline{i}$ fed to reactor
n_C	moles carbon (total in reactor)
p_i	partial pressure of component $\underline{i}$, atm
R	universal gas constant
R_G	driving force for carbon-steam reaction, see Equation (6)
r_G	molar rate of carbon-steam reaction per unit reactor volume
r_M	molar rate of methanation reaction per unit reactor volume
r_S	molar rate of shift reaction per unit reactor volume
V	volume of fixed bed reactor
x	extent of reaction, moles carbon reacted per mole H_2O fed
z	distance from start of fixed bed reactor
θ	residence time in fixed bed, moles bed carbon-hr/mole H_2O fed

References

1. G. F. Crewe, V. Gat, and V. K. Dhir, "Decaking of Bituminous Coals by Alkaline Solutions", Fuel, 54, 20-23 (1975).

2. W. R. Epperly, and H. M. Siegel, "Catalytic Coal Gasification for SNG Production", in "11th Intersociety Energy Conversion Engineering Conference Proceedings, American Society of Mechanical Engineers, N.Y. (1976), pp. 249-253.

3. W. P. Haynes, S. J. Gasior, and A. J. Forney, "Catalysis of Coal Gasification at Elevated Pressure," in L. G. Massey ed., "Coal Gasification", Advances in Chemistry Series No. 131, Amer. Chem. Soc., Washington, D. C. (1974), pp 179-202.

4. W. K. Lewis, E. R. Gilliland, and H. Hipkin, "Carbon-Steam Reaction at Low Temperatures", Ind. Eng. Chem., 45, 1697-1703 (1953).

5. N. C. Nahas and J. E. Gallagher, Jr., "Catalytic Gasification Predevelopment Research", paper presented at the 13th Intersociety Energy Conversion Engineering Conference" (August, 1978).

6. H. S. Taylor, H. A. Neville, "Catalysis in the Interaction of Carbon with Steam and with Carbon Dioxide," J. Am. Chem. Soc., 43, 2065-2071 (1921).

This paper was prepared as an account of work sponsored, in part, by the United States Government. Neither the United States nor the United States DOE, nor any of their employees, nor any of their contractors, subcontractors, or their employees, makes any warranty, express or implied, or assumes any legal liability or responsibility for the accuracy, completeness, or usefulness of any information, apparatus, product, or process disclosed, or represents that its use would not infringe privately owned rights.

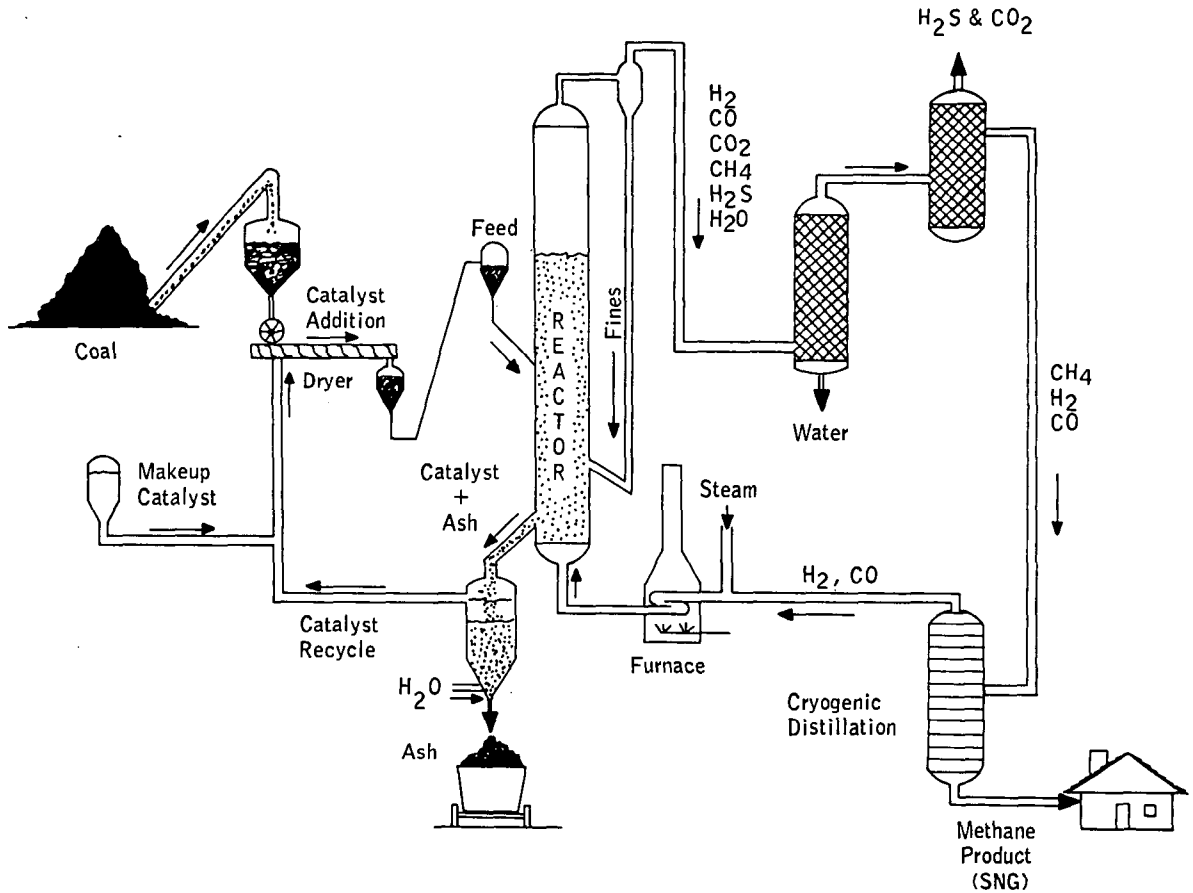

78B-6-5-1

FIGURE 1. OVERALL FLOW PLAN OF THE EXXON CATALYTIC COAL GASIFICATION PROCESS

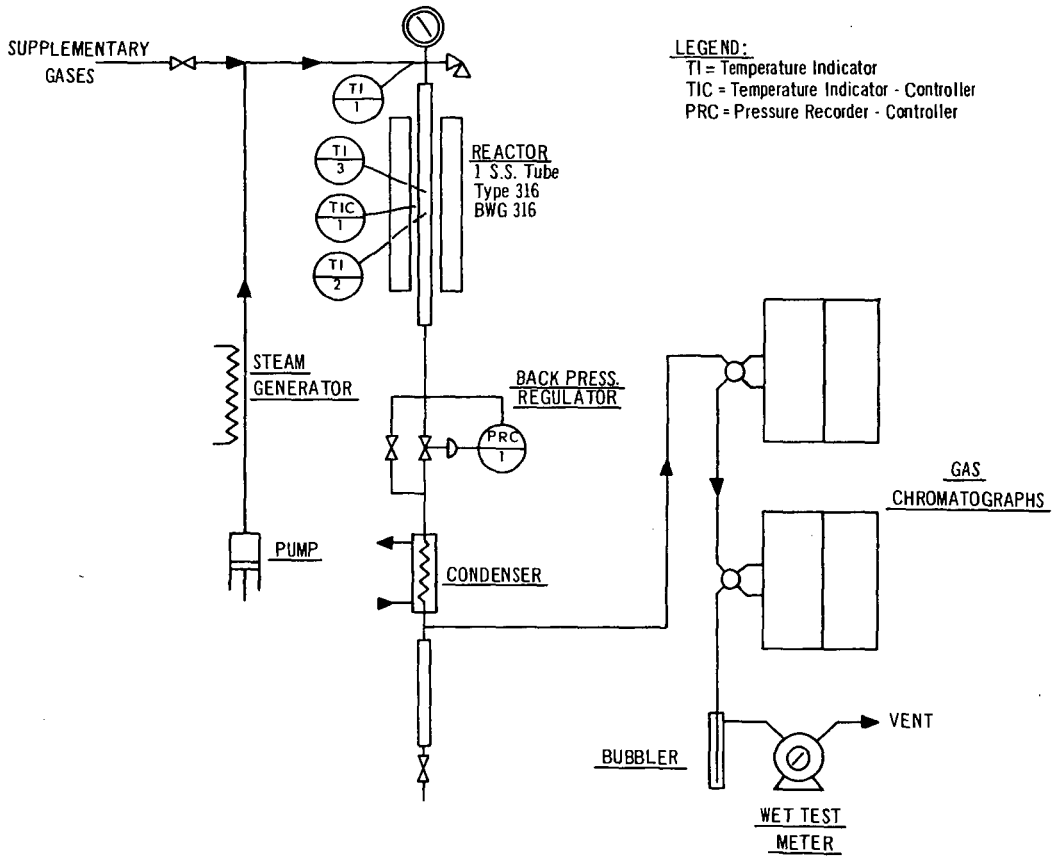

FIGURE 2 SCHEMATIC DIAGRAM OF BENCH SCALE FIXED BED GASIFICATION UNIT

78B-6-4-8

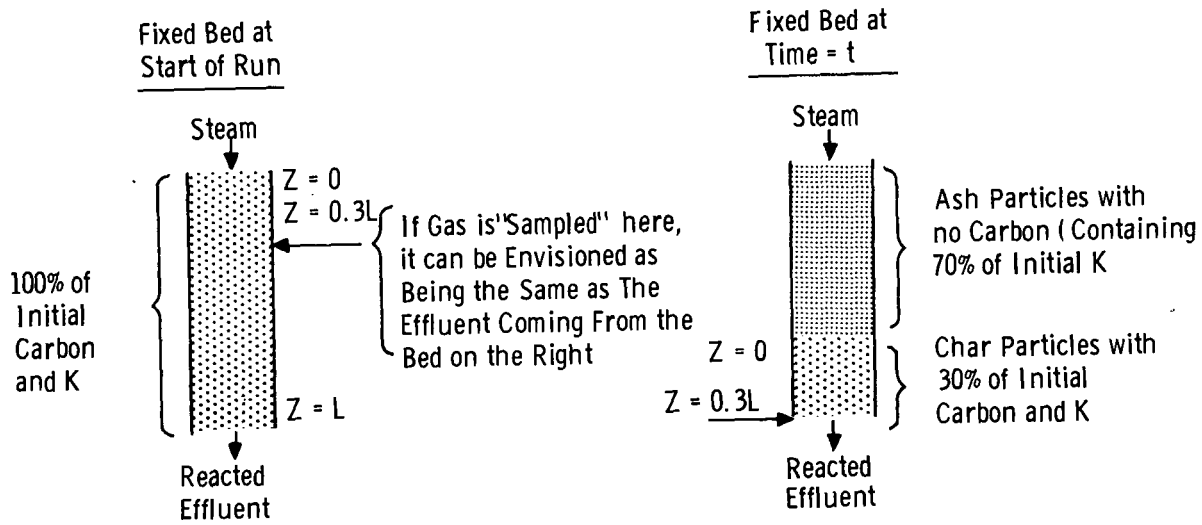

FIGURE 3. SIMPLIFIED MODEL FOR FIXED BED REACTOR IN POTASSIUM CATALYZED STEAM GASIFICATION

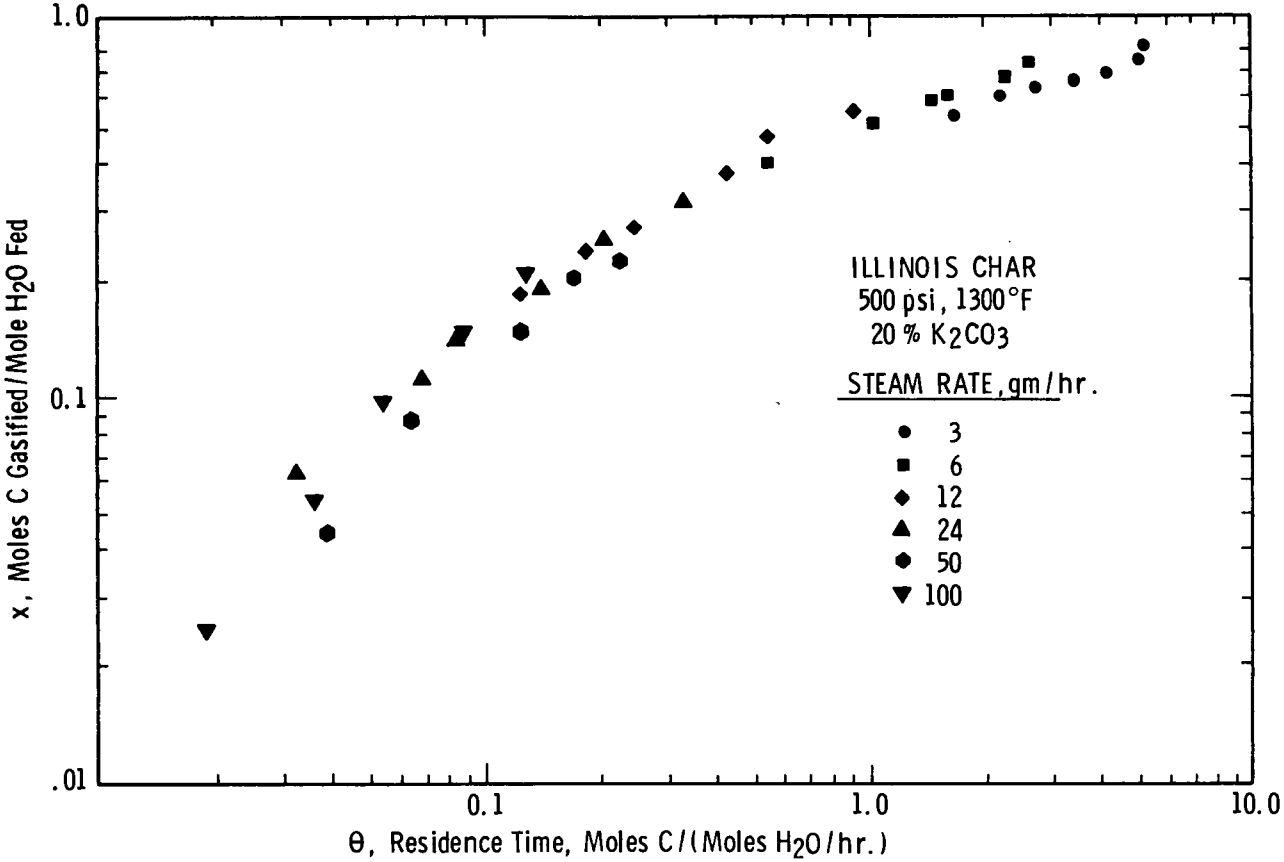

FIGURE 4 EXTENT OF CARBON STEAM REACTION AS A FUNCTION OF RESIDENCE TIME

78B-6-4-10

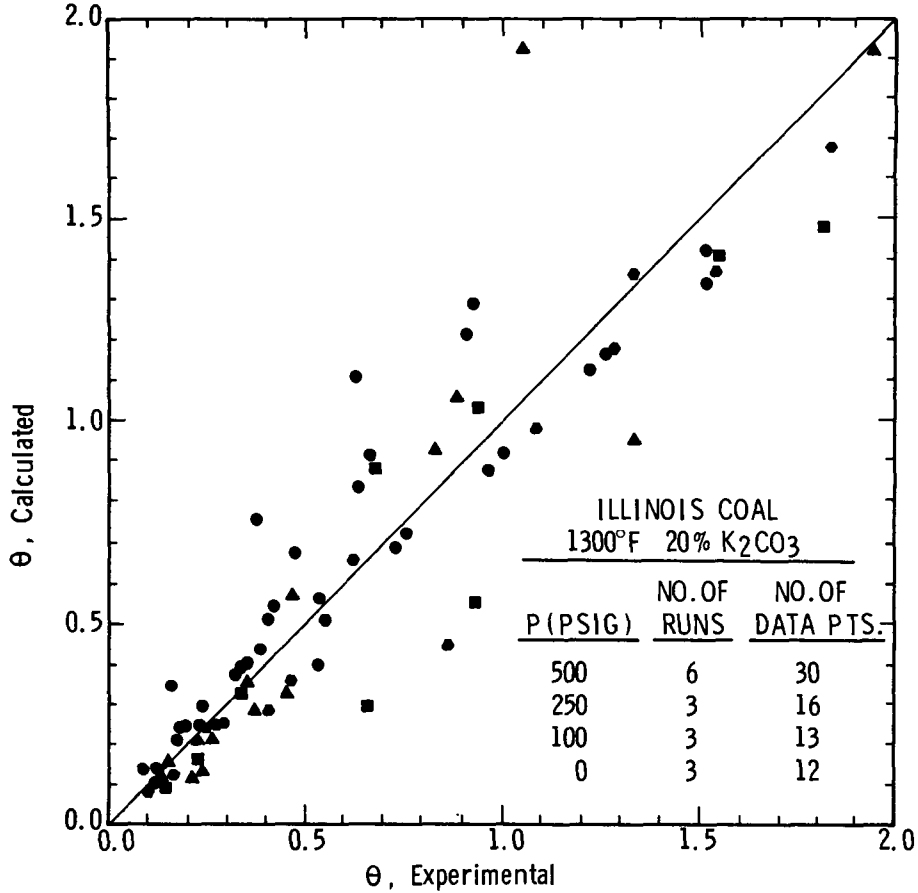

FIGURE 5 COMPARISON OF EXPERIMENTAL AND PREDICTED HOLDING TIME, θ, TO ATTAIN A GIVEN CONVERSION FOR MODEL "B"

78B-6-4-11

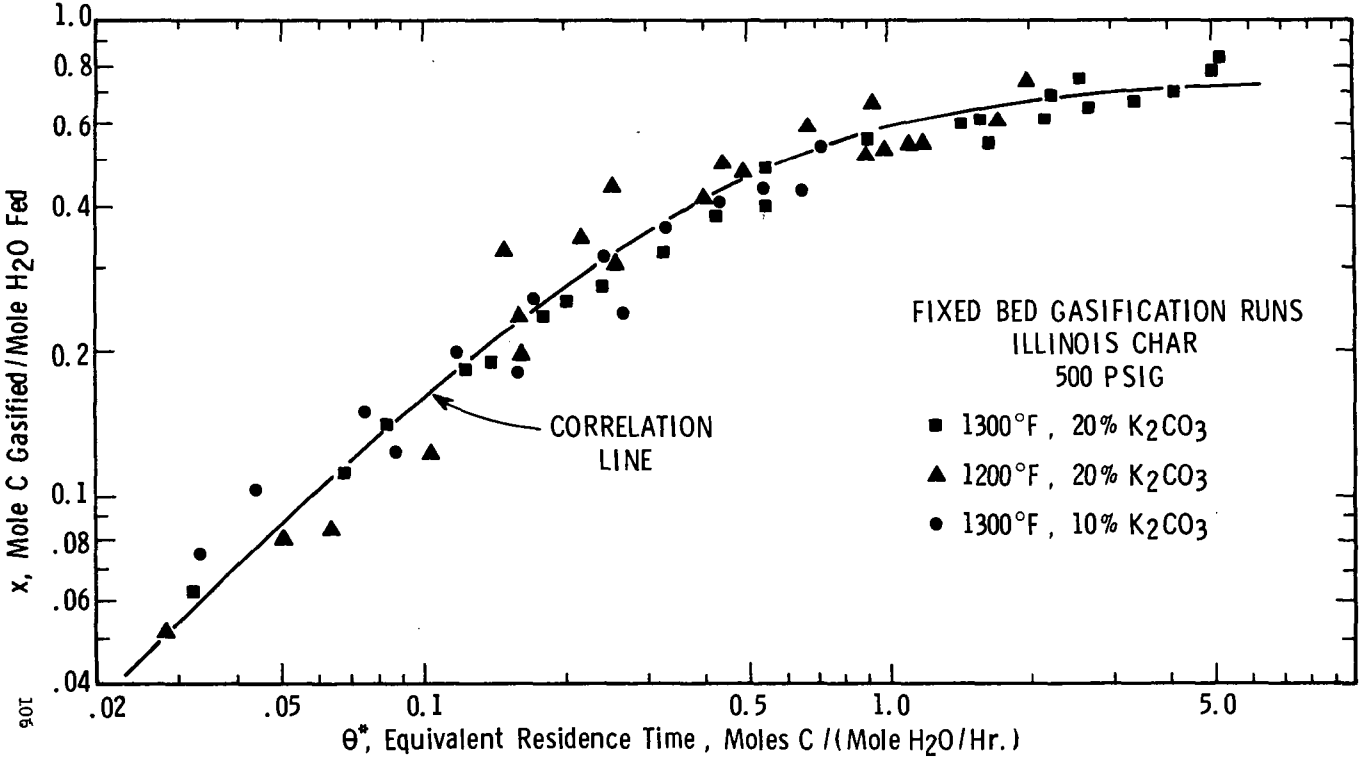

FIGURE 6 COMPARISON OF FIXED BED DATA WITH MODEL PREDICTION FOR STEAM FEED

78B-6-4-12

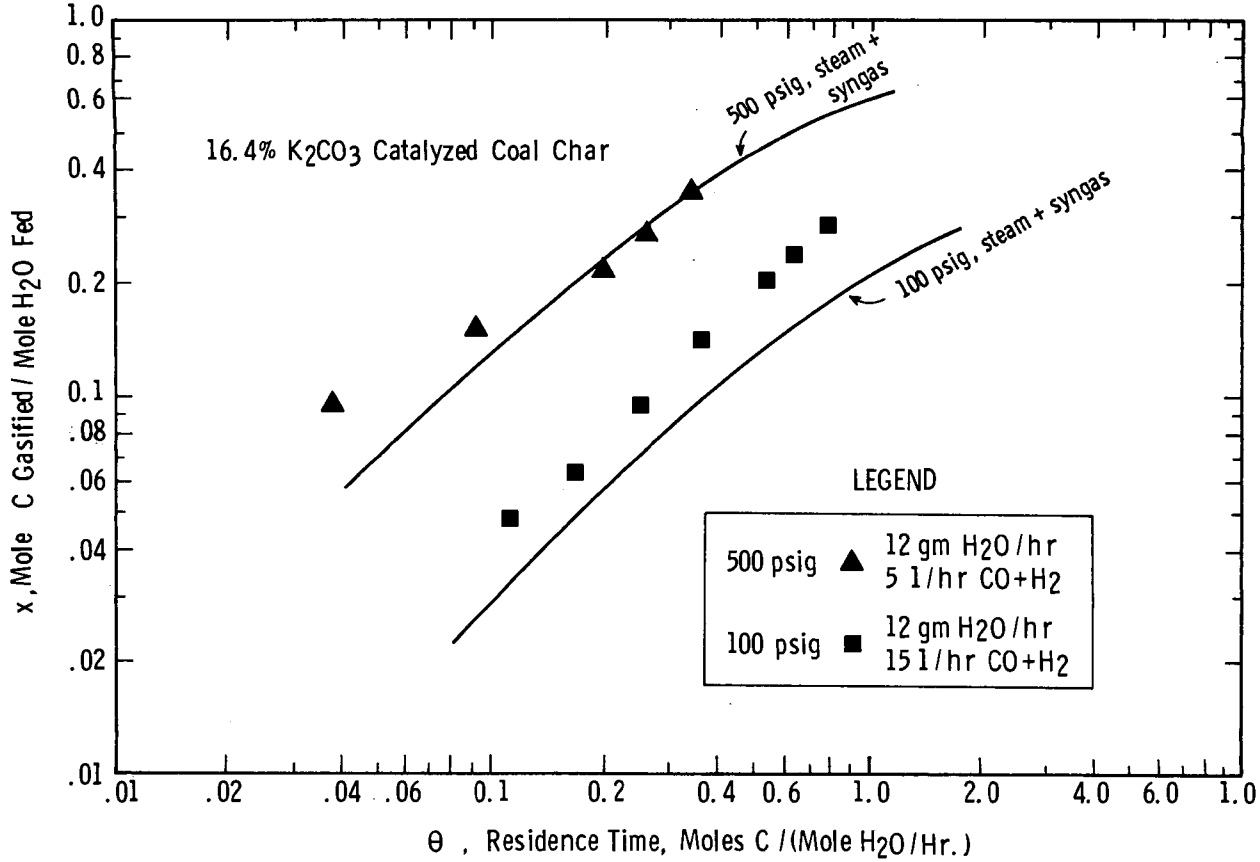

FIGURE 7 COMPARISON OF FIXED BED DATA WITH MODEL PREDICTIONS FOR STEAM/SYNGAS FEED

78B-6-4-13

Reaction Characteristics During *In-Situ* Gasification of Western Subbituminous Coals

J. E. Young and J. Fischer

Chemical Engineering Division
Argonne National Laboratory
9700 South Cass Avenue
Argonne, IL 60439

INTRODUCTION

In-situ gasification of coal offers a number of significant potential advantages which suggest its use both as a supplement to and, in some cases a substitute for conventional mining combined with surface gasification. These include:

- Utilization of coal reserves which cannot be economically recovered by conventional techniques
- Reduction of capital expenditures and operating costs
- Easier and more economic control of pollution problems
- Less stringent feed water quality requirements
- Reduction of the health and safety problems associated with conventional coal processing techniques
- Reduction of socioeconomic impact

In underground gasification, wells are drilled into a coal seam for gas injection and product recovery and are linked by means of any of several techniques including: reverse combustion, hydrofracturing, electro-linking, directional drilling, and explosive fracturing. The linking step facilitates movement of product gas from the reaction zone to the recovery wells.

Maintenance of a high-permeability link between wells is extremely difficult with Eastern coking coals, because of their swelling at high temperatures. In addition, transport of water and reactant gases through Eastern seams is more difficult because of the lower permeability of the coal itself in its natural state. As a result, the greatest success has been with underground gasification of Western subbituminous coals and Texas lignites.

Field studies are currently being carried out by the Morgantown Energy Research Center with Pittsburgh seam coal near Pricetown, West Virginia, but no complete gasification test has yet been completed. Several gasification tests have been completed by the Laramie Energy Research Center at Hanna, Wyoming, and by Lawrence Livermore Laboratory at Hoe Creek, Wyoming. In addition, Texas Utilities Service Company has conducted field tests in Texas lignite deposits, utilizing technology licensed from the Soviet Union.

In underground coal gasification (UCG), three more-or-less well-defined reaction zones can be identified. The zone nearest the product recovery well is the drying and pyrolysis zone, in which water is driven from the coal and the pyrolysis reactions occur. Tars produced in this zone are continually driven forward into the cooler regions of the seam, with a portion being cracked to lighter hydrocarbons. Cracking proceeds until the tars are light enough to be carried with the product gas stream out of the coal seam. Immediately behind the pyrolysis zone is the reducing zone or gasification zone. In this area, the primary reactions are:

$$C + H_2O \rightarrow H_2 + CO \qquad 1)$$

$$C + CO_2 \rightleftarrows 2\,CO \qquad 2)$$

$$C + 2H_2 \rightarrow CH_4 \qquad 3)$$

$$CO + H_2O \rightleftarrows H_2 + CO_2 \qquad 4)$$

$$CO + 3H_2 \rightleftarrows CH_4 + H_2O \qquad 5)$$

The water necessary for reaction 1) is supplied either by injection of steam with the air or oxygen or by natural intrusion of water into the reaction zone if the coal seam is a natural aquifer (as is the case for many Western coal seams). Behind the gasification zone is the combustion zone, which supplies the process heat. Heat is transferred from the combustion zone to the gasification zones primarily by convection of the product gases, rather than by conduction through the solid char and coal.

In experimental studies at Argonne, the kinetics of the reactions occurring in the gasification zone are being measured. The data from these studies are used in mathematical models being developed at other laboratories for each of the field projects. This paper describes the reaction characteristics of coals from the Hanna No. 1 and Wyodak coal seams for reactions 1), 4), and 5). Data for reactions 2) and 3) are not yet complete and are not discussed here.

EXPERIMENTAL

The kinetic experiments were carried out in a differential packed-bed reactor system capable of simulating any of the operating conditions expected in underground gasification. A schematic of this system is shown in Fig 1. The product gas from the reactor is analyzed for H_2, CO, CH_4, and CO_2 by gas chromatography. All operating temperatures, pressures, and gas flows are monitored and recorded on punched paper tape by means of a data logging system. In addition, the data output from the gas chromatograph is recorded on punched tape, permitting rapid computer processing of the large amount of data produced.

In a typical gasification experiment, the coal is crushed to -4 +12 mesh, and a 5 to 20 g sample is placed in the reactor. The coal is then pyrolyzed at a heating rate of 3°C/min in a flow of 1.0 to 2.5 l/min 20% hydrogen in nitrogen. System pressure during pyrolysis is 790 kPa (100 psig). The final pyrolysis temperature is that at which the gasification experiment is to be carried out. When the final pyrolysis temperature is reached, the reactor is flushed with nitrogen at the final temperature for approximately 30 min, and then steam and/or other reactants are introduced.

The product gas composition data are converted to rates of carbon conversion, which are then integrated over time to calculate the extent of carbon converison. Rates and extents of carbon conversion are expressed on an ash-free basis. Following each gasification experiment the char residue in the reactor is burned to determine the final carbon balance for the experiment. Generally, carbon balances are near 100%.

RESULTS AND DISCUSSION

1. Steam-Char Reaction

The product gas from underground gasification consists primarily of hydrogen, carbon monoxide, carbon dioxide, methane, and nitrogen. This mixture constitutes a reducing atmosphere which sweeps through the coal during pyrolysis. In order to obtain a true simulation of these conditions during pyrolysis prior to our study of gasification kinetics, the sweeping gas mixture should contain all of these constituents.

However, the addition of carbon monoxide to the pyrolysis sweeping gas would result in the deposition of carbon, which would be added to the char in the gasification reactor. This additional carbon would be a product of the reverse Boudouard reaction, catalyzed by the coal ash and by the metal components of the reactor:

$$2CO \rightleftarrows C + CO_2$$

Deposited carbon is not quantitatively determinable and must be eliminated or made negligible in order to obtain a carbon balance. Therefore, our pyrolysis reactions have been carried out in a reducing atmosphere consisting of only hydrogen and nitrogen. Our experiments indicate that for Wyodak coal, pyrolysis in a reducing atmosphere (20% H_2, balance N_2) results in recovery of approximately ten percent less char following pyrolysis than when pure nitrogen is used as the sweeping gas. However, the reactivity of the char produced in hydrogen and nitrogen is the same as that for char produced in pure nitrogen.

The rate of reaction of steam with chars prepared from Wyodak coal has been measured in the temperature range, 600-775°C, with a partial pressure of steam of 0.25-0.26 MPa (2.5-2.6 atm), and a total pressure of approximately 0.9 MPa (0 atm). These rates are plotted as a function of reciprocal temperature (Arrhenius plot) for Wyodak coal in Fig. 2. At each temperature, the reaction rates following gasification of 10% of the carbon and also following gasification of 50% of the carbon are shown. The rate at 10% carbon conversion corresponds to the rate for fresh char; the rate at 50% conversion corresponds to that for the more refractory residual char.

The apparent activation energies (E_a) calculated from Fig. 2 are summarized in Table 1. The decrease in E_a as a result of increasing the temperatures is much greater at 10% conversion than at 50% conversion, which is consistent with the expectation that micropore diffusion is a limiting factor for the steam-char reaction under conditions expected in an underground gasifier. By the time 50 percent of the carbon has been gasified, the micropore structure has opened somewhat, resulting in the higher values for E_a at 50% conversion.

Table 1

Apparent Activation Energies for Steam-Char Reaction

	E_a at 10% Conversion	E_a at 50% Conversion
Wyodak		
600°C	182 kJ/mol (43.6 kcal/mol)	235 kJ/mol (56.3 kcal/mol)
775°C	53 kJ/mol (12.8 kcal/mol)	109 kJ/mol (26.1 kcal/mol)
Hanna		
600°C	143 kJ/mol (34.1 kcal/mol)	156 kJ/mol (37.2 kcal/mol)
775°C	89 kJ/mol (21.2 kcalmmol)	110 kJ/mol (26.2 kcal/mol)

In Fig. 3, the temperature dependence of the rate of reaction of steam with chars prepared from Hanna No. 1 coal is shown. The steam partial pressure was 0.25 MPa (2.5 atm). The temperature range was 600-775°C. The apparent activation energies calculated from the curves for Hanna coal are also listed in Table 1. The lower values of E_a at higher temperatures for the Hanna coal are indicative of more severe micropore diffusion limitations with the Hanna char than with the Wyodak coal.

The Wyodak char pyrolyzed under simulated UCG conditions has a nitrogen BET surface area of approximately 1 m^2/g, and the surface area measured by carbon dioxide adsorption is approximately 450 m^2/gm. For the Hanna char, the BET surface is 0.2 m^2/g, and the CO_2 surface area is approximately 550 m^2/g. These data indicate that for both chars, the pore structure of the fresh char is limited to extremely small micropores. The pore structure of the Hanna char, as indicated by CO_2 surface areas, is apparently even smaller on the average than is that for the Wyodak char, an observation consistent with variations encountered in E_a for the steam-char reaction of each of these two chars. The micropores are apparently not accessible to the reactant steam, and must be opened appreciably to attain maximum reaction rates.

Wyodak chars prepared by pyrolysis at 3°C/min in either nitrogen or 20% H_2 in nitrogen were gasified at 700°C with steam at partial pressures of 0.12-0.65 MPa (1.2-6.5 atm). Reaction rate for Wyodak char is plotted as a function of steam partial pressure in Fig. 4. At lower partial pressures of steam, the curve is nearly linear, with a slope of approximately 0.85. This corresponds to a reaction order of 0.85 with respect to steam. At higher steam partial pressures, the reaction order decreases as indicated by the flattening of the curve in Fig. 4. Since underground gasification of coal would generally involve partial pressures of steam at the lower end of this range, the reaction order of 0.85 is probably applicable for use in the mathematical models proposed for this process.

Fig. 5 shows the dependence of the reaction rate on the partial pressure of steam for Hanna char. The reaction rate is plotted for conversions of 10, 30, and 50% of carbon, in the range of 0.1-0.27 MPa (1.07-2.7 atm) steam. In the case of the Hanna char, a series of parellel straight lines can be fitted through the points for the three extents of carbon conversion. The slope of these straight lines corresponds to a reaction order of 0.56 with respect to steam. This value is considerable lower than that obtained for the Wyodak char--undoubtedly due to diffusion of steam being limited by the finer pore structure of the Hanna char.

All gasification runs described up to this point were designed to maintain the partial pressures of product gases at values as low as possible. In runs with very high gasification rates (*e.g.*, at high temperatures or high partial pressures of steam)hydrogen levels were 2-4 mol %. However, in the majority of the runs, hydrogen content of the product was considerably less than 1 mol %. In order to investigate inhibition of the steam-char reaction by product hydrogen, a series of experiments was carried out in which hydrogen was added to the reactant steam. The range of hydrogen partial pressures investigated includes those expected to be encountered in the current low-pressure underground field tests (*i.e.*, up to approximately 0.1 MPa (1 atm)).

In Figs. 6 and 7 are shown the inhibitive effects of hydrogen at 600 and 700°C for Wyodak char. At 600°C (Fig. 6), inhibition of the reaction by hydrogen results in a rapid decline in reaction rate as the char is consumed. At 700° (Fig. 7), this inhibition is sufficient to eliminate the effects of diffusion limitations during the early stages of the reaction. At yet higher temperatures, the diffusion limitations are severe enough that they are apparent even in the presence of 0.75 atm hydrogen. At all temperatures,the higher the partial pressure of hydrogen, the earlier in the reaction that the rapid decrease in the reaction rate occurs. Hydrogen exerts a greater inhibitory effect at higher temperatures and as the extent of gasification increases. Similar effects of hydrogen have been observed with the Hanna coal.

2. Catalysis by Coal Ash

Many coals which would be good candidates of UCG have too high an ash content for economical aboveground utilization. This ash would be expected to have a catalytic effect on gasification reactions occurring underground. The ash in Hanna coal has been found to catalyze the water gas shift reaction and the methanation reaction under the conditions expected in UCG.

To investigate reaction 4), the water gas shift reaction, a series of experiments was carried out in which carbon monoxide and steam were reacted at various temperatures over a bed of char prepared from Hanna coal in the following manner. The char was prepared by heating to a temperature of 600°C at a heating rate of 3°C/min. This pyrolysis was carried out in a reducing gas mixture consisting of 20% H_2 in nitrogen. The overall pressure was 0.76 MPa (100 psig). The temperature was limited to 600°C during pyrolysis in order to minimize chemical changes that might occur in the mineral matter of the coal. On the other hand, at 600°C, most of the hydrocarbon decomposition would have occurred, yielding a clean, relatively hydrocarbon-free char to expose to the steam utilized for the reaction study.

Following pyrolysis, the temperature was reduced to the desired value and 0.13 MPa (1.33 atm) steam was introduced to the reactor along with 60 kPa (0.6 atm) carbon monoxide. The balance of the gas was nitrogen, and the total system pressure was 0.76 MPa (7.6 atm). The contact time of the gas mixture in the char bed ranged from 1.1 s at 500°C to 1.6 s at 250°C. Following utilization of the fresh char, 15% of the carbon was steam-gasified away at 600°C and then the shift reaction was studied at the lower temperatures. The purpose of the gasification step was to expose more of the mineral matter at the surface of the char particles. After the shift reaction rates were measured for the char from which 15% of the carbon had been removed, an additional 6% of the char was steam-gasified and the shift rates were measured again.

The results of these studies are shown in Fig. 8. The rates for the shift reaction over fresh char are appreciably lower than for the partially gasified char, but there is little difference between the rates obtained after 15 and after 21% carbon removal. In Fig. 8, the extent of the shift reaction as a function of temperature is compared with the thermodynamic equilibrium curve. Once an appreciable amount of the carbon has been gasified from the char, the reaction approaches thermodynamic equilibrium in the temperature range of 500 to 600°C. The point plotted for Wyodak char at 650°C was calculated from data obtained in an earlier gasification run in which carbon monoxide was observed in the product gas, permitting calculation of an equilibrium value. This point confirms that the reaction is indeed at equilibrium at 650°C, for a contact time on the order of one second.

At expected UCG processing condition, steam has been found to exhibit a synergistic effect with hydrogen for the production of methane. At 700°C, a mixture of 138 kPa (20 psig) hydrogen and 0.33 MPa (3.3 atm) steam was passed over Hanna char and yielded a methane concentration of 300 parts per million (by volume). Reaction at that partial pressure of hydrogen alone gave a methane concentration of only 150 ppm. Since this experiment was carried out under differential conditions, the hydrogen contributed by the steam-carbon reaction did not change the partial pressure of hydrogen in the reactor. Introduction of steam at 0.5 MPa (5 atm) gave a five-fold increase in the rate of methane production.

A probable mechanism for this phenomenon is methanation of the carbon monoxide produced by the steam-carbon reaction, with the methanation catalyzed by the mineral matter in the coal. The methanation of carbon monoxide by hydrogen has been found to occur when only the ash from Hanna coal (formed by low-temperature ashing) is placed in the reactor in the temperature range of 400 to 700°C. Insufficient experiments have been carried out to determine conversion rates for this reaction quantititively.

3. Brackish Water Effects

The water occurring in the aquifers in the Hanna, Wyoming, area is quite brackish. A typical analysis is 600 mg/L sodium, 7 mg/L potassium, 22 mg/L calcium plus magnesium, 1100 mg/L carbonates, 400 mg/L sulfate, 40 mg/L chloride, and a pH of 8.5. There have been numerous reports in the literature that impregnation of coal with alkali or alkaline earth cations sometimes enhances the rates of gasification reactions with coal. Hence the inevitable use of brackish water in UCG may in fact enhance the kinetics of the steam-char reaction.

In a series of experiments to investigate this question, two aqueous solutions were prepared to simulate the brackish water characteristic of the water found in the Hanna aquifers. One solution containing approximately the natural concentrations of contaminants was prepared using calcium chloride, sodium sulfate, potassium carbonate and sodium bicarbonate. The second solution contained about five times the natural concentrations.

A sample of Hanna No. 1 coal was crushed and washed with boiling distilled water several times to remove any soluble salts already in the coal. A portion of this washed coal was gasified to obtain a base-line reaction rate. Ten grams of this washed coal was oven-dried and then impregnated with 1.0 ml of the simulated brackish water solution. The coal completely absorbed this solution; no excess liquid drained off. Likewise, a sample of the washed coal was dried, then impregnated with the solution having a fivefold concentration of contaminants. Each of these impregnated coal samples was then pyrolyzed and gasified.

Our standard gasification reaction conditions were used, *i.e.*, 700°C, 0.25 MPa (2.5 atm) steam after pyrolysis had been carried out in 20% H_2/80% N_2 with a heating rate of 3°C/min to reaction temperature. The results of these runs are summarized in Fig. 9. Impregnation of the washed coal with the simulated brackish water appears to enhance the rate of reaction of steam with the char by ten to fifteen percent. There was little apparent difference between the effects of the standard concentration and the five-fold concentration of contaminants. An enhancement of the reaction rate of this small magnitude may not be significant because of the very small samples of coal gasified in each run. Normal variations in the coal can give this much variance in a measured reaction rate. The fact that the single-fold and the five-fold concentrations show little difference also suggests that the observed enhancement may not be significant.

Brackish water would be expected to have minimal effects on the reaction rate for a coal having the characteristics of Hanna No. 1. The core sample of Hanna coal which we are studying contains 17% ash, on an as-received basis. This means that the char remaining after pyrolysis contains 32% ash. The amount of inorganic material added to a coal with this high an ash content--even by using simulated brackish water having five times the normal concentration of contaminants--would be a rather small percentage of the total inorganic matter in the coal. Nevertheless, the possibility exists that brackish water may have an effect on the rate of reaction of steam with chars that have a lower ash content than does Hanna.

CONCLUSIONS

At high temperatures (700-750°C), the Wyodak char is 50-100% more reactive with steam than is Hanna char, although at lower temperatures (600-650°C), the two have essentially equal reactivities with steam. The lower apparent activation energy observed for the Hanna char indicates that its average pore size is smaller than that of the Wyodak char. The reaction order with respect to steam is greater for the Wyodak char than for the Hanna chars--undoubtedly also because of the differences in pore structure.

Hydrogen severely inhibits the reaction of steam with both chars. The inhibition is greater as a greater fraction of the carbon is gasified.

Mineral matter catalyzes the water gas shift reaction, and thermodynamic equilibrium is reached at approximately 550°C. The ash alone also has been found to catalyze the methanation reactions, but kinetic data have not yet been determined for these reactions.

The alkali and alkaline earth cations present in brackish waters exert a minimal catalytic effect on the steam-char reaction--most likely because the high ash content of the coal already supplies sufficient catalyst for the reaction.

The submitted manuscript has been authored by a contractor of the U. S. Government under contract No. W-31-109-ENG-38. Accordingly; the U. S. Government retains a nonexclusive, royalty-free license to publish or reproduce the published form of this contribution, or allow others to do so, for U. S. Government purposes.

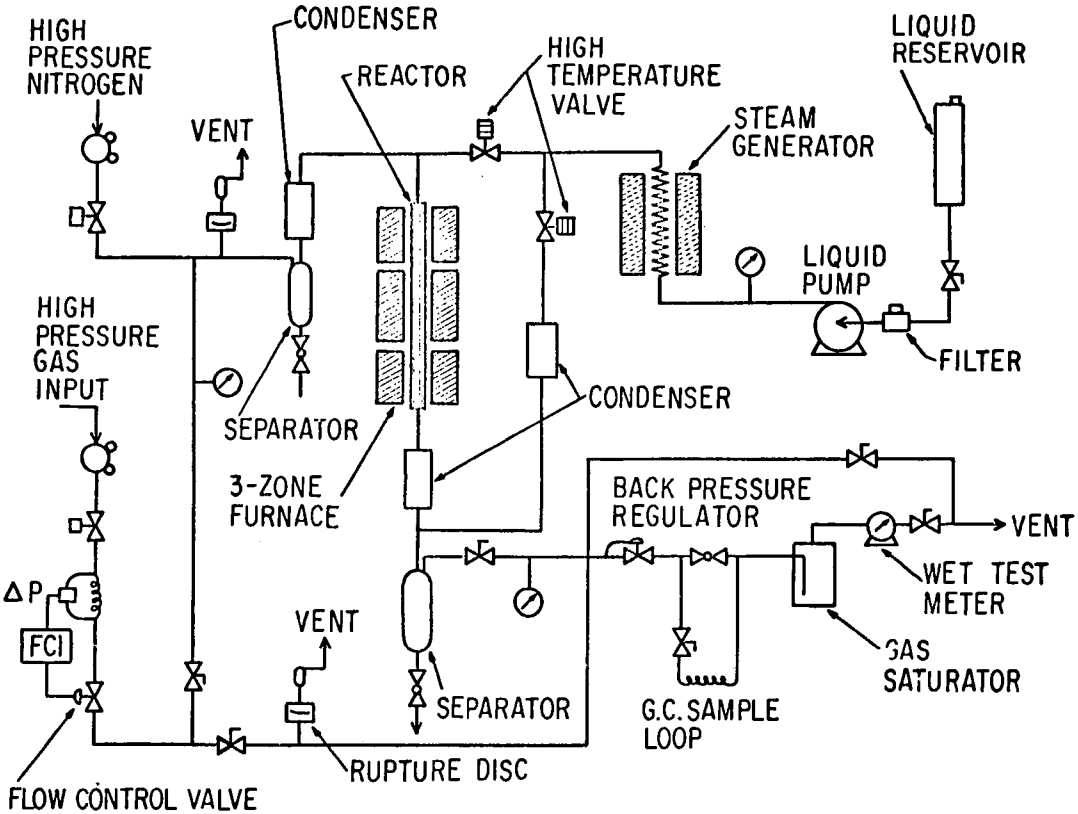

Fig. 1. Schematic of Char Gasification System

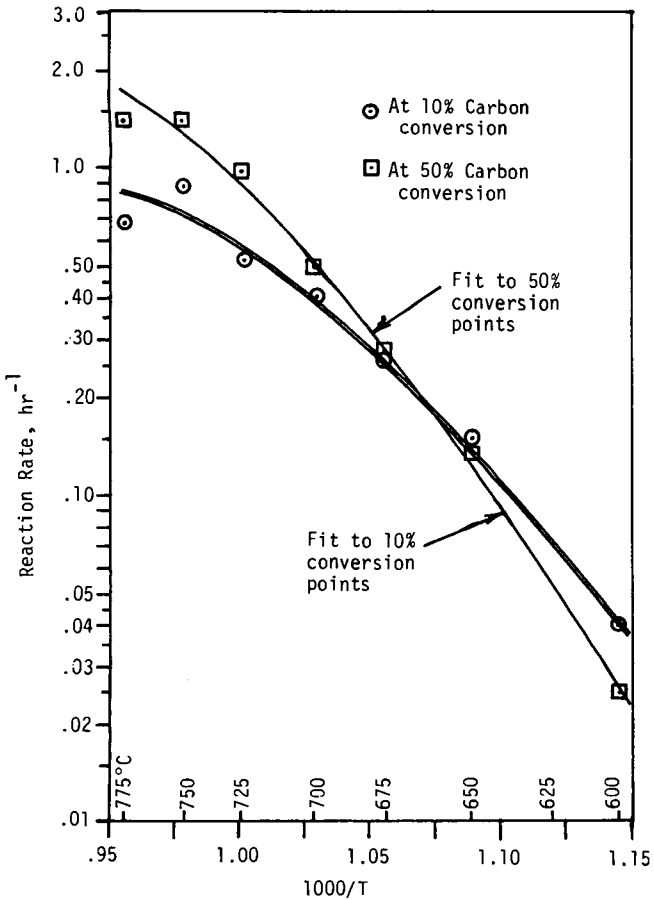

Fig. 2. Temperature Dependence of Steam-Char Reaction Rate. Wyodak Char, 0.25 MPa (2.5 atm) Steam

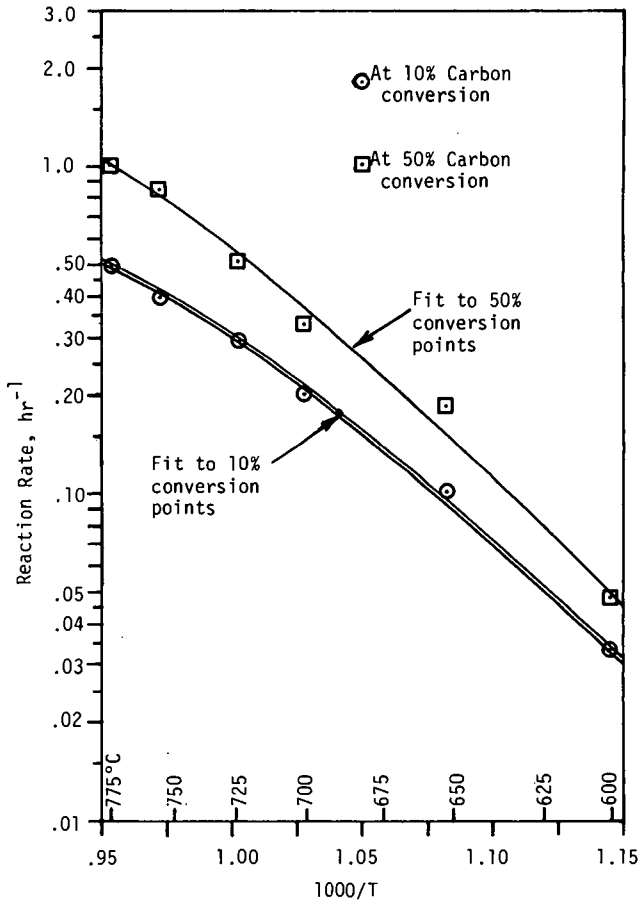

Fig. 3. Temperature Dependence of Steam-Char Reaction Rate. Hanna No. 1, 0.25-MPa (2.5-atm) Steam

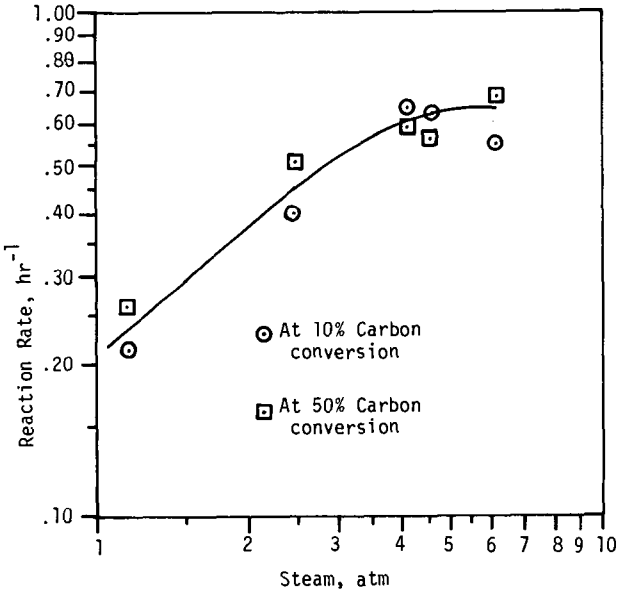

Fig. 4. Dependence of the Steam-Char Reaction Rate on the Partial Pressure of Steam. Wyodak Char, 700°C

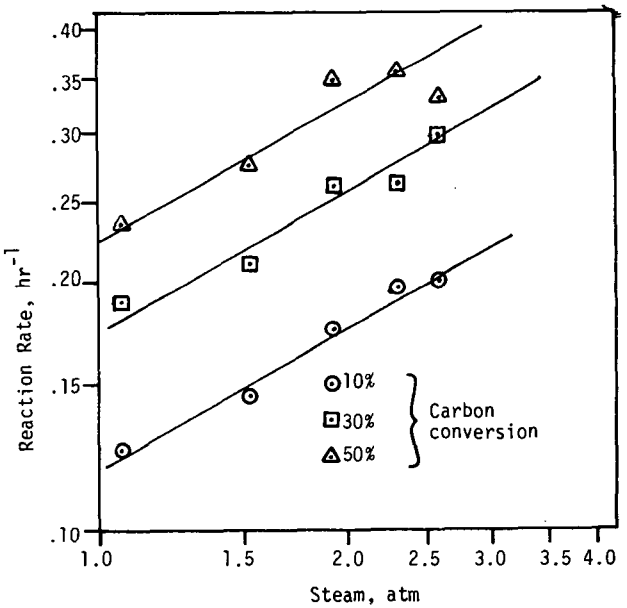

Fig. 5. Dependence of the Steam-Char Reaction Rate on the Partial Pressure of Steam. Hanna No. 1 Char, 700°C

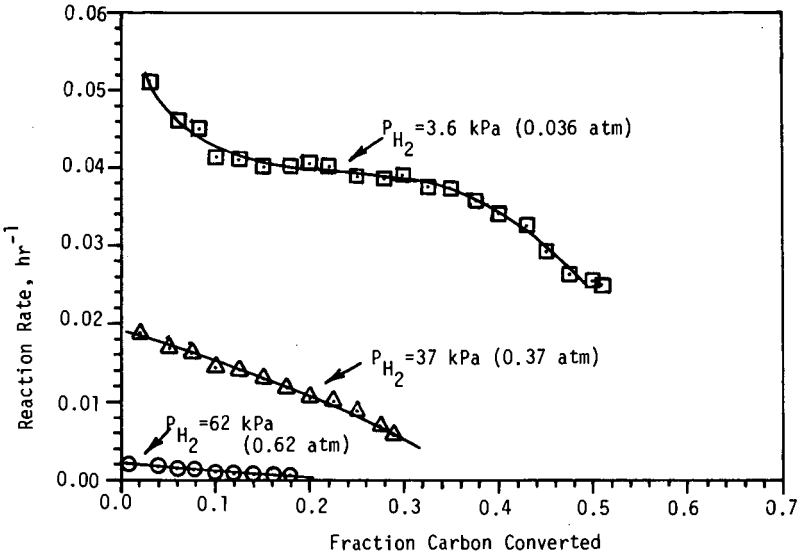

Fig. 6. Hydrogen Inhibition of the Steam-Char Reaction. Wyodak Char, 600°C, 0.25 MPa (2.5 atm) Steam

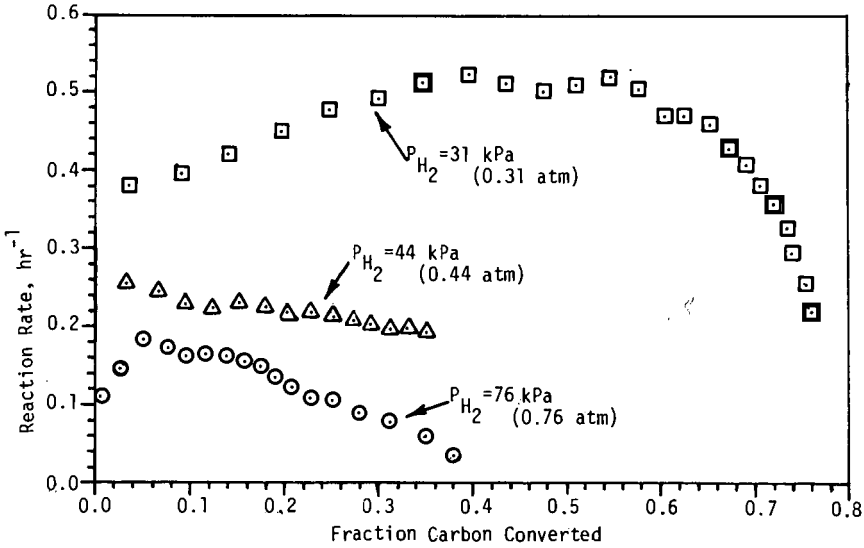

Fig. 7. Hydrogen Inhibition of the Steam-Char Reaction. Wyodak Char, 700°C, 0.25 MPa (2.5 atm) Steam

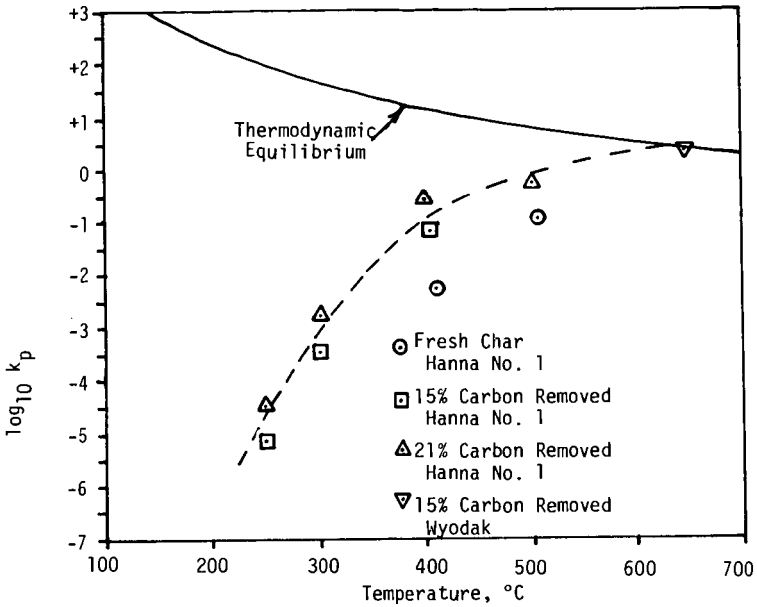

Fig. 8. Water Gas Shift Reaction. 1.0-1.5 s Contact Time

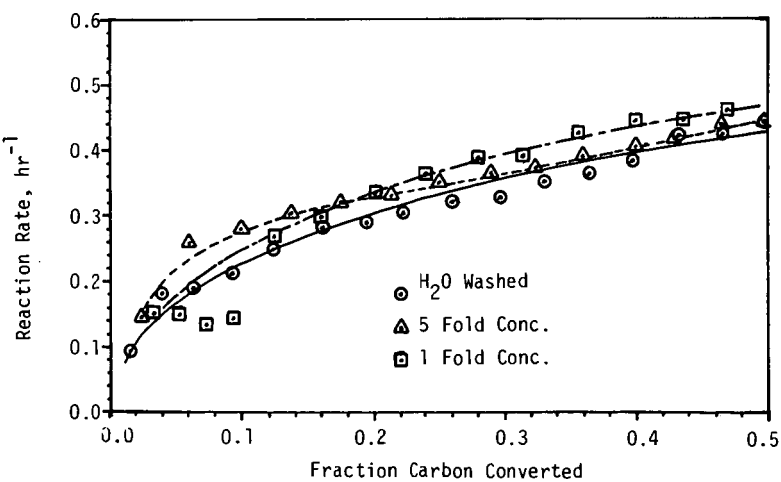

Fig. 9. Effect of Brackish Water on Steam/Char Gasification Rate. Hanna No. 1 Char, 700°C, 0.25 MPa (2.5 atm) Steam

Oxidative Pretreatment of Illinois No. 6 Coal: Material and Energy Balances

F. N. Gromicko, L. Saroff, S. Gasior and J. Strakey

U. S. Department of Energy
Pittsburgh Energy Research Center
4800 Forbes Avenue
Pittsburgh, PA 15213

INTRODUCTION

One of the difficulties encountered when gasifying caking coals is the tendency of the coal to agglomerate. The SYNTHANE process, developed at the Pittsburgh Energy Research Center, incorporates a mild oxidation pretreatment step which destroys the agglomerating characteristic of the coal before entry into the gasifier. The fluidized-bed or entrained pretreater is connected directly to the gasifier and operates at the same pressure. The pretreater products (hot pretreated coal (char) gases, and tar vapors) are fed directly into the gasifier. Consumption of carbon in this step is not detrimental to the process economics. If the oxidative pretreatment were eliminated, additional oxygen would have to be added to the gasifier to heat the coal to the pretreatment temperature. Oxidative pretreatment is presently being studied in entrained-flow and fluidized-bed PDU reactors. Batch fluidized-bed tests have been studied by Forney, et al. (1) and continuous fluidized-bed experiments were described by Gasior, et al. (2). Coal pretreatment tests in an entrained state have been carried out and reported by Saroff, et al. (3).

Experiments have been designed to determine the operating characteristics of entrained-flow and fluidized-bed reactors. Actual experimental data from each reactor are organized and reported as material and energy balances. Operating parameters and process stream compositions are discussed for three sets of data: 40-atmosphere entrained-flow, 40-atmosphere fluidized-bed and 70-atmosphere fluidized-bed. Entrained-flow data has been based on a typical run from a series of 10 similar experiments. Fluidized-bed data are a composite of four similar experiments at each operating pressure. Typical material balances are generated from this data. These balances can be used as a design basis for the pretreatment steps in a gasification plant. Similar balances have been prepared to describe the pretreatment step in the IGT hydrogasification process (4).

EQUIPMENT DESCRIPTION

Entrained Reactor

The entrained pretreatment system, Figure 1, consists primarily of a coal hopper, a process gas heater, a transport line reactor, and a pretreated coal receiver. The reactor is equipped with full instrumentation to permit the measurement of gas flows, operating pressures, pressure differentials, and temperatures at various points in the process. Sample points are provided for the product gas and char. Coal is fed from the hopper by a rotating perforated disc feeder. As each perforation passes the discharge line a synchronized injection of gas forces the coal into a take-off pipe. Coal flow rates are determined by hopper weight losses which are monitored on a tension load cell.

The entrained reactor is a 1/4-inch, 304 stainless steel pipe shaped as an inverted U, 76 feet in length, with auxiliary heaters along its entire length. The heaters are used to minimize heat losses. Temperature measurements are made with chromel-alumel sheathed thermocouples. System pressure is monitored on calibrated bourdon tube gauges.

The product gas exits through a particle disengagement zone. Residual dust particles are filtered from the gas which is then passed through a heat exchanger to remove moisture and any other condensables. The pretreated coal is collected in a vessel equipped with a screw extractor to permit sampling under pressure. A product gas sample point and an exit gas meter complete the unit.

Fluidized-bed Reactor

The fluidized-bed pretreater is shown in Figure 2. In many respects this system is similar to the entrained unit. The coal feed mechanism is identical. Process nitrogen is heated prior to carrying the coal into the pretreater vessel. The pretreatment vessel is a 1" schedule 80, 304 stainless steel pipe approximately 10 feet in length. Electric heaters are provided to insure adiabatic operation. Temperature is monitored by four thermocouples. Pretreated coal exits from the top of the pretreatment vessel and falls into the receiver. Fine dust particles are removed by a filter. Water and tars are condensed from the gas stream which is then sampled. The unit is equipped with instrumentation to permit accurate observation and control of all inlet and outlet process streams.

EXPERIMENTAL PROCEDURE

Entrained Reactor

Experiments were conducted solely with Illinois #6 coal ground to minus 20 mesh, with approximately 30% through 200 mesh. Complete proximate-ultimate, ash, and particle size analyses were carried out for each feed. A typical analysis is shown in Table 1. Coal was weighed and charged to the coal hopper prior to the run, and any residual coal in the hopper at the end of the run was weighed to accurately determine the average coal feed rate.

All of the entrained pretreater tests were run at 40 atmospheres pressure. The coal hopper was pressurized independently of the remaining part of the unit. After sealing the entire unit, the back pressure regulator was set at the desired operating pressure and the unit was pressurized.

The transport gas, nitrogen, was heated to 450° C and adjusted to the proper flow rate. The transport line heaters were set to minimize heat losses along the entire reaction length. The speed of the rotating feeder disc was adjusted to give the desired coal feed rate. Shortly after establishing a consistent coal rate, oxygen, at a predetermined flow rate, was introduced to the system. When stable conditions, as evidenced by constant temperatures, were reached, periodic gas and pretreated coal samples were taken. The gas samples were analyzed for O_2, CO, CO_2, CH_4 and higher molecular weight hydrocarbons. Representative pretreated coal (p.c.) samples were taken at the end of the run and completely analyzed.

Fluidized-bed Reactor

The fluidized-bed unit was operated at both 40 and 70 atmospheres total pressure. The back-pressure regulator was set and pressurization proceeded similar to the entrained process. Nitrogen was heated between 360 and 380° C and adjusted to the desired flow rate. Oxygen was then added down stream of the heater to form the gas mixture that transports the coal to the reaction vessel. Adiabatic settings were maintained on the vessel heaters. Coal feed was initiated and a fluidized-bed was developed in the 10-foot-long vessel.

The exit gas was continuously monitored for oxygen content. Spot samples were analyzed for carbon oxides, CH_4 and higher molecular weight hydrocarbons. Pretreated

coal dropped from the top of the fluidized-bed and was collected in the receiver. Representative samples of this coal were analyzed at the conclusion of the run. Water and tar were collected, sampled, and analyzed.

In all tests, nitrogen was used as the transport medium. For a commercial-scale plant, steam would be used to transport the coal, since it can be easily removed by condensation, and therefore does not dilute the product. Furthermore, in a commercial facility, lower fluidization velocities would be employed.

DISCUSSION OF RESULTS

Material Balances

Actual mass balances for each unit are presented in Figures 3, 4 and 5. In order to facilitate comparisons between the tests, elemental balances were based on 100 pounds of raw coal. Tables 2, 3 and 4 show the input and output as elemental balances. These elemental balances were scaled upward to a 100 lb. basis from the operating parameters given in Figures 3, 4 and 5. The feed coal was subdivided into three components: free moisture, water of hydration and the remaining coal. Free moisture was determined using ASTM analysis procedures. The water of hydration, held by the clay materials in the coal, was estimated to be 8 weight percent of the ash taken on a moisture-free basis, as discussed by Given (5). Hydrogen and oxygen shown in Tables 2, 3 and 4 were appropriately adjusted to account for the changes in the ultimate analysis caused by the water of hydration assumption. Due to the high operating temperatures of these processes, all of the water of hydration was broken free from the clay materials in the char. Therefore, water of hydration does not appear in the output section of the elemental balances. Corrections for the water of hydration will be important in calculating exit temperature from the enthalpy balance. If the water of hydration was ignored, additional water would appear to be formed during the reaction step, thus a higher exit temperature would be predicted.

Exit stream compositions were examined for each test. The entrained reactor had virtually no tar present at the process exit. Typical tar analyses were used for the 40-and 70-atmosphere fluidized-bed tests. Tar production generally ranged from 1 to 3% of the feed coal, with an average of 1.4% for the 40-atmosphere tests. In the 70-atmosphere tests, tar production ranged from 1 to 5% with an average of 3.2%.

Table 5 shows actual exit gas concentrations for the three processes. Oxygen breakthrough occurs in the entrained pretreater, probably due to the short coal residence time which requires a higher initial partial pressure of oxygen in the feed. The fluidized-bed reaction produces a larger variety of gaseous products such as methane and other hydrocarbons. These gas analyses were incorporated into the material balances.

Closure on the overall mass balances, calculated on a nitrogen gas-free basis, ranged from 93.6% in the 40-atmosphere fluidized-bed run to 99.9% in the 70-atmosphere fluidized-bed experiment. Carbon and hydrogen closures are generally good, with the oxygen being furthest from closure. Poor oxygen closures were probably caused by the analysis technique for the coal and char. Oxygen content is determined by difference, thereby incorporating all of the analysis errors into the oxygen term. Volborth, et.al., (6) describe a method for direct determination of oxygen which may lead to better oxygen closure. These actual balances were composites of data from several similar tests.

When presenting a process flow sheet of any reactor system, it is necessary to have input and output mass flow rates that are totally balanced. This has been achieved by making minor adjustments in the typical balances presented to form design-basis material balances. The char is one of the most difficult streams to measure accurately. There are a number of locations in the process, such as the disengagement zone, where char can become trapped and therefore omitted from the complete balance. In addition, truly representative samples of the char may not always be obtained. Thus elemental balances were brought to complete closure by adjusting the ultimate analyses of the char stream. This led to new ultimate analyses which were within the range of results generally seen for the process.

The completed design-basis mass balances are shown in Figures 6, 7 and 8, and the design-basis elemental balances are given in Tables 6, 7 and 8. These balances have been developed using a large number of pretreatment runs and can be viewed as a good approximation of the material that would be fed to a gasifier after the coal pretreatment step has been accomplished.

Energy Balances

Energy balances were completed for both fluidized-bed tests and the entrained reactor test using the material balances based on actual operating data. The calculations were completed by employing Hess' Law. All the reactant enthalpies were calculated at base temperature, 25° C. Process gas inlet temperatures were generally around 450° C for the entrained reactor and between 360° C and 380° C for the fluidized-bed reactor. The raw coal was always fed at 25° C, so no initial enthalpy term for this coal enters into the balance.

A simple group of reactions was used to describe the overall reaction step at 25° C. Table 8 shows the reactions that were considered. The largest enthalpy changes resulted from the formation of carbon dioxide and water. Contributions from the other components were small, mainly due to the low concentrations. The total enthalpy available can be used to predict the process exit temperature.

Determination of exit temperature involves heating all of the process gases present in the outlet stream and heating of the char. The latent heat of vaporization of water from 25° C to the exit temperature was also included. Table 10 shows a comparison of calculated outlet temperatures and the measured exit temperatures. The fluidized-bed tests were carried out at almost totally adiabatic conditions as was planned. Comparing the calculated temperature with the exit temperature for the entrained pretreater indicates that an adiabatic system was not attained. Due to certain material limitations in the experimental equipment, the char receiver cannot be operated at reaction temperatures. Therefore the insulation on the last 25 feet of the transport line was removed to prevent excessive temperatures in the char receiver. In doing this, an appreciable amount of heat is lost, accounting for the non-adiabatic operating conditions and lowered exit temperature.

Supplemental Analyses

Several other parameters were briefly examined to more completely characterize the two pretreatment processes. A measure of the success of the pretreatment process is its ability to destroy the agglomeration tendency of caking coals. The free swelling index, FSI, is often the parameter used to distinguish a raw caking coal from a treated non-agglomerating char. Table 11 gives FSI's for the raw and treated coals that were studied. The 70 atmosphere reactor was the most successful producer of a non-caking, FSI=0, coal. The remaining two tests did not pretreat the coal completely. Fluidized-bed tests at 40 atmospheres pressure have reduced

the FSI of raw coal to less than the value given in Table 11. A higher operating temperature of approximately 420° C is required for this reduction. The test presented here was operated at only 400° C, thus accounting for the higher free-swelling index. However, the material balance for a 420° C fluid-bed pretreater does not change appreciably from a 400° C reactor.

The carbon consumption during the pretreatment reaction is also noteworthy of examination. In this study, the percentage carbon consumption is determined as the ratio of carbon in the exit tar and gas streams to the carbon in the feed coal. For all of the 40-atmosphere tests, regardless of reactor type, the carbon consumption ranged from 1.9 to 3%. However, in the 70 atmosphere fluidized-bed reactor, a carbon consumption of 10.4% was observed. Tar production in the 70-atm. test consumed 6.2% of the feed carbon, while the product gases accounted for the remaining 4.2% of the conversion. Differences in carbon consumption are probably due to the variation in coal residence times.

Table 12 provides the proximate analyses of the coal before and after the pretreatment reaction takes place. In each instance, the volatile matter is decreased in the process. This can lead to some of the tar formation, and is probably a factor in reducing the agglomeration tendency.

The sulfur forms in the coal before and after pretreatment in the entrained reactor are shown in Table 13. The process does not affect the overall sulfur in the coal to any great extent.

CONCLUSION AND SUMMARY

The oxidative pretreatment of Illinois #6 coal has been studied in two types of reactors: a short residence time entrained-flow unit and a longer residence time fluidized-bed unit. The entrained reactor was operated at 40 atmospheres pressure and the fluidized-bed reactor was tested at both 40 and 70 atmospheres pressure. Material balances were constructed using the raw data gathered in both processes. The 70- atmosphere fluidized-bed and the entrained reactor experiments had closures of 95% or better, while a closure of 94% was calculated in the 40-atmosphere fluidized-bed test. Individual elemental balances varied, carbon and hydrogen recovery were excellent and oxygen recovery generally was the poorest. Typical material balances that can be used for design calculations were generated from the data. Energy balances based on these material balances indicated that the fluidized-bed reactor was operated at almost total adiabatic conditions. Some heat loss was seen in the entrained reactor and linked to the cooling of the process stream at the end of the reactor to protect the char receiver.

Both pretreatment schemes were successful in destroying a large portion of the coal's agglomerating tendencies, as indicated by the free swelling index of the treated coal samples. Tar formation in the entrained reactor was found to be negligible. In the fluidized-bed reactor, 1 to 5% of the feed coal was converted to tar compounds. The work completed and described should prove useful in providing an accurate description of input feed compositions to the gasifier which would be encountered in gasifying caking coals.

Table 1. - Typical Illinois #6 Coal Analysis

Proximate-Ultimate

	Coal(as received), wt.%
Moisture	6.2
Volatile Matter	39.3
Fixed Carbon	43.5
Ash	11.0
H	5.3
C	64.3
N	1.2
S	3.4
O	14.8
Ash	11.0

Ash Analysis, %

Silica	47.03
Al_2O_3	18.07
Fe_2O_3	18.46
TiO_2	1.04
CaO	7.29
MgO	1.03
Na_2O	0.86
K_2O	1.83
SO_3^{-2}	4.38

Particle Size

Sieve Size	wt. % Retained on Sieve
20	0
50	9.2
100	30.9
140	14.9
200	18.3
325	25.0
PAN	1.7

Table 2. - Actual Entrained Reactor Elemental Balance, wt.

	H	C	N	S	O	Ash	Total
Input							
Coal	4.26	62.78	1.12	3.63	7.65	12.56	92.0
Moisture in coal	0.78				6.22		7.0
Water of hydration	0.11				0.89		1.0
Oxygen feed					11.18		11.18
Total	5.15	62.78	1.12	3.63	25.94	12.56	111.18
Output							
Pretreater coal, pc	3.64	60.54	1.0	3.74	8.66	13.57	91.15
Moisture in pc	0.41				3.29		3.7
Condensate	0.87				6.96		7.83
Product gas		1.19			2.93		4.12
Total	4.92	61.73	1.0	3.74	21.84	13.57	106.8
Recovery, %	95.5	98.3	89.3	103.0	84.2	108.0	96.1

Table 3. - Actual 40-Atmosphere Fluidized-Bed Elemental Balance, wt.

Input	H	C	N	S	O	Ash	Total
Coal	4.5	64.25	1.22	3.47	8.4	11.07	92.91
Moisture in coal	0.69				5.51		6.2
Water of hydration	0.1				0.79		0.89
Oxygen feed					8.64		8.64
Total	5.29	64.25	1.22	3.47	23.34	11.07	108.64
Output							
Pretreated coal, pc	3.73	56.41	1.0	2.99	7.47	11.37	82.97
Moisture in pc	0.07				0.6		0.67
Condensate	1.12				8.92		10.04
Product gas	0.09	1.96		0.24	4.43		6.72
Tar	0.11	1.04		0.06	0.09		1.30
Total	5.12	59.41	1.0	3.29	21.51	11.37	101.7
Recovery, %	96.8	92.5	82.0	94.8	92.2	102.7	93.6

Table 4. - Actual 70-Atmosphere Fluidized-Bed Elemental Balance, wt.

Input	H	C	N	S	O	Ash	Total
Coal	4.24	63.48	1.11	3.51	7.68	11.46	91.48
Moisture in coal	0.84				6.76		7.6
Water of hydration	0.1				0.82		0.92
Oxygen feed					7.2		7.2
Total	5.18	63.48	1.11	3.51	22.46	11.46	107.2
Output							
Pretreated coal, pc	2.95	54.98	1.07	2.95	7.54	12.45	81.94
Moisture in pc	0.16				1.26		1.42
Condensate	1.1				8.8		9.9
Product gas	0.22	2.64		0.85	5.23		8.94
Tar	0.41	3.92		0.24	0.33		4.9
Total	4.84	61.54	1.07	4.04	23.16	12.45	107.1
Recovery, %	93.4	96.9	96.4	115.1	103.1	108.6	99.9

Table 5. - Exit Gas Compositions on a Volume Percentage Basis

	40-atm. entrained	40-atm. fluidized-bed	70-atm. fluidized-bed
CO_2	1.16	3.18	1.7
CO	0.62	0.6	0.3
CH_4		0.4	0.3
C_2H_4			trace
C_2H_6		trace	0.1
C_3H_6			trace
C_3H_8			trace
H_2		0.2	trace
O_2	0.18	0.1	
H_2S		0.2	0.3
N_2	Balance	Balance	Balance

Trace defined as <0.1 volume %.

Table 6. - Entrained Reactor Design-Basis Elemental Balance, wt.

Input	H	C	N	S	O	Ash	Total
Coal	4.5	64.25	1.22	3.47	8.4	11.07	92.91
Moisture in coal	0.69				5.51		6.2
Water of hydration	0.1				0.79		0.89
Oxygen feed					11.18		11.18
Total	5.29	64.25	1.22	3.47	25.88	11.07	111.18
Output							
Pretreated coal, pc	3.95	63.01	1.22	3.47	12.17	11.07	94.89
Moisture in pc	0.43				3.42		3.85
Condensate	0.91				7.24		8.15
Product gas		1.24			3.05		4.29
Total	5.29	64.25	1.22	3.47	25.88	11.07	111.18

Table 7. - 40-Atmosphere Fluidized-Bed Design-Basis Elemental Balance, wt.

Input	H	C	N	S	O	Ash	Total
Coal	4.5	64.25	1.22	3.47	8.4	11.07	92.91
Moisture in coal	0.69				5.51		6.2
Water of hydration	0.1				0.79		0.89
Oxygen feed					8.64		8.64
Total	5.29	64.25	1.22	3.47	23.34	11.07	108.64
Output							
Pretreated coal, pc	3.89	61.25	1.22	3.17	9.26	11.07	89.86
Moisture in pc	0.08				0.64		0.72
Condensate	1.12				8.92		10.04
Product gas	0.09	1.96		0.24	4.43		6.72
Tar	0.11	1.04		0.06	0.09		1.3
Total	5.29	64.25	1.22	3.47	23.34	11.07	108.64

Table 8. - 70-Atmosphere Fluidized-Bed Design-Basis Elemental Balance, wt.

	H	C	N	S	O	Ash	Total
Input							
Coal	4.5	64.25	1.22	3.47	8.4	11.07	92.91
Moisture in coal	0.69				5.51		6.2
Water of hydration	0.10				0.79		0.92
Oxygen feed					7.20		7.2
Total	5.29	64.25	1.22	3.47	21.9	11.07	107.2
Output							
Pretreated coal, pc	3.4	57.69	1.22	2.38	6.28	11.07	82.04
Moisture in pc	0.16				1.26		1.42
Condensate	1.1				8.8		9.9
Product gas	0.22	2.64		0.85	5.23		8.94
Tar	0.41	3.92		0.24	0.33		4.9
Total	5.29	64.25	1.22	3.47	21.9	11.07	107.2

Table 9. - Formation Reactions Used in Determining Heat of Reaction

$C + O_2 \rightarrow CO_2$	$\Delta H^\circ_{f_{298}}$	$= -94,052$	$\frac{\text{cal}}{\text{gram mole}}$
$C + 1/2O_2 \rightarrow CO$	$\Delta H^\circ_{f_{298}}$	$= -26,416$	"
$C + 2H_2 \rightarrow CH_4$	"	$= -17,889$	"
$2C + 3H_2 \rightarrow C_2H_6$	"	$= -20,236$	"
$S + H_2 \rightarrow H_2S$	"	$= -4,815$	"
$1/2O_2 + H_2 \rightarrow H_2O_{(liq.)}$	"	$= -68,317$	"

Table 10. - Predicted Exit Stream Temperature Determined Through Energy Balances

	Predicted exit temperature	Observed exit temperature
40-atm. entrained	401° C	353° C
40-atm. fluidized	419° C	401° C
70-atm. fluidized	427° C	419° C

Table 11. - Free Swelling Index Before and After Pretreatment

	Raw Coal	Pretreated Coal
40-atm. entrained	4.0	0.5
40-atm. fluidized	4.0	1.0
70-atm. fluidized	4.0	0

Table 12. - Comparison of Proximate Analyses of Pretreated Coals

	Feed coal	Entrained	Fluidized 40-atm.	Fluidized 70-atm.
Moisture	6.2	2.4	0.8	1.7
Volatile matter	39.3	33.7	35.9	26.2
Fixed carbon	43.5	49.0	50.4	57.2
Ash	11.0	14.9	13.6	14.9

Table 13 - Change in Sulfur Distribution During Entrained Pretreatment*

	Raw	Treated
Sulfate	0.43	0.35
Pyritic	1.05	1.3
Organic	2.37	2.32

*values are percentage of coal sample on a moisture-free basis

References

1. Forney, A. J., R. F. Kenny, S. J. Gasior and J. H. Field. Bureau of Mines, Report of Investigation, #6797, 1966.

2. Gasior, S. J., A. J. Forney, W. P. Haynes and R. F. Kenny, AIChE Symposium Series, No. 156, Vol. 72, pp. 117-124, 1977.

3. Saroff, L., F. N. Gromicko, G. E. Johnson, J. P. Strakey, and W. P. Haynes., Coal Processing Technology, Vol. 3, CEP Technical Manual, 1977.

4. Pipeline Gas From Coal-Hydrogenation (IGT Hydrogasification Process), Quarterly Report #3, FE-2434-12, May 1977.

5. Given, P. H. and R. F. Yarzab, Problems and Solutions in the Use of Coal Analyses, Technical Report #1, FE-0390-1, November 1975.

6. Volbroth, A., Miller, G. E., Garner, C. K. and P. A. Jerabek, Fuel, 57, p. 49, 1978.

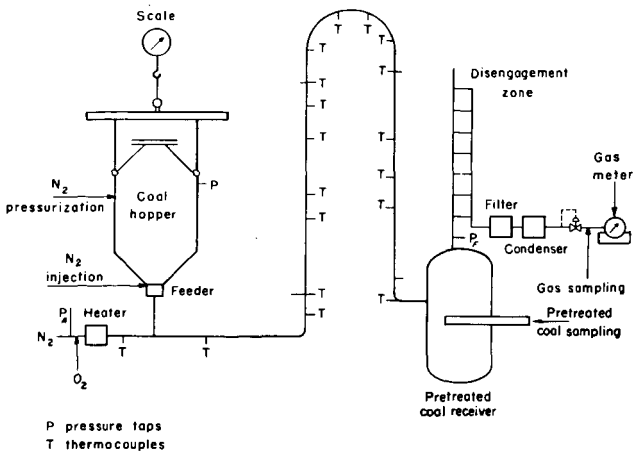

Figure-1 Schematic sketch of entrained pretreater PDU

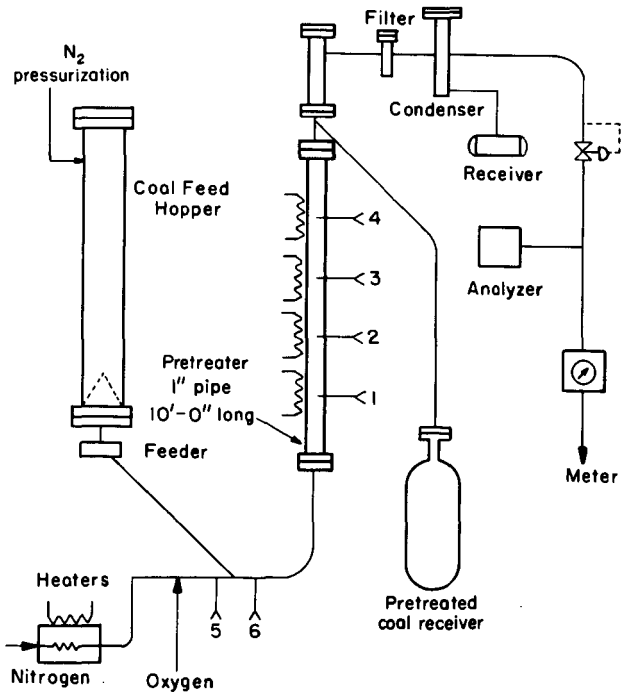

Figure 2 - Schematic sketch of fluidized-bed coal pretreater PDU.

4-28-78 L-16026

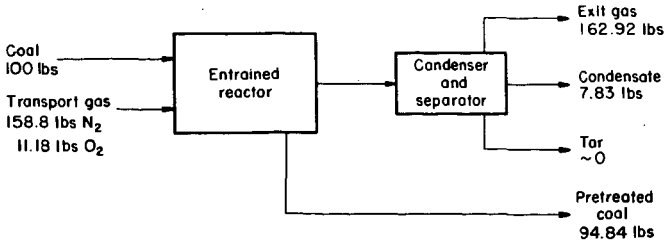

Run parameters

Coal rate = 19.6 lbs/hr

Superficial gas velocity = 12.4 ft/sec

Average operating temperature = 377°C

Maximum operating temperature = 485°C

Figure 3 - Entrained reactor overall mass balance based on actual operating data.

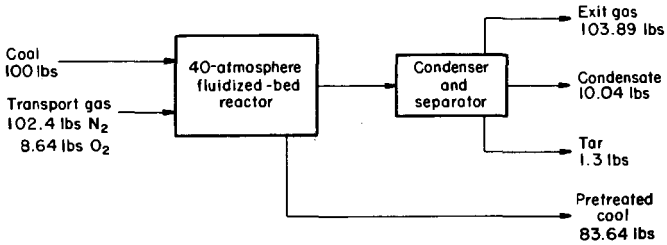

Run parameters

Coal rate = 23.2 lbs/hr

Superficial gas velocity = 1.08 ft/sec

Average operating temperature = 401°C

Figure 4 - 40-atmosphere fluidized-bed reactor overall mass balance based on actual operating conditions.

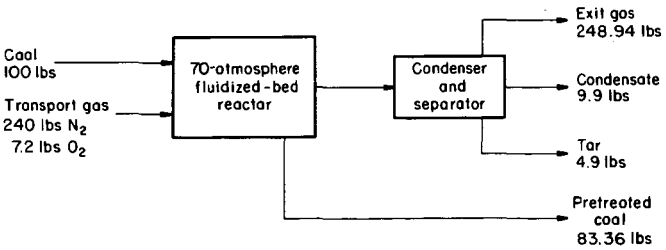

Run parameters

Coal rate = 10.5 lbs/hr

Superficial gas velocity = 0.68 ft/sec

Average operating temperature = 419°C

Figure 5 - 70-atmosphere fluidized-bed reactor overall mass balance based on actual operating conditions.

4-28-78 L-16027

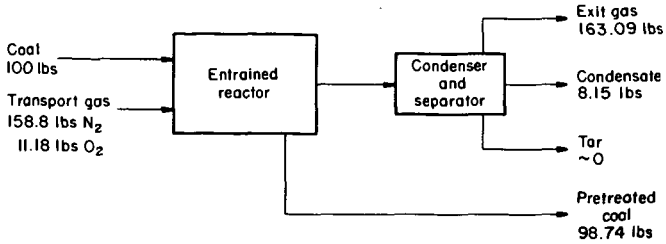

Run parameters
Coal rate = 19.6 lbs/hr
Superficial gas velocity = 12.4 ft/sec
Average operating temperature = 377°C
Maximum operating temperature = 485°C

Figure 6 - Typical, design-basis, entrained reactor mass balance.

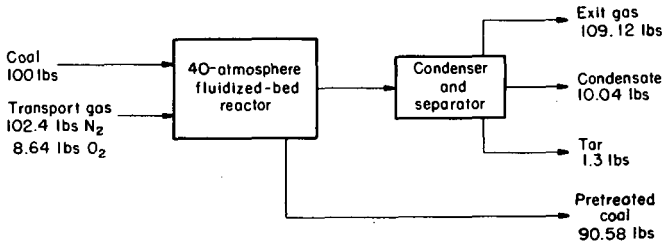

Run parameters
Coal rate = 23.2 lbs/hr
Superficial gas velocity = 1.08 ft/sec
Average operating temperature = 401°C

Figure 7 - Typical, design-basis, 40-atmosphere fluidized-bed reactor mass balance.

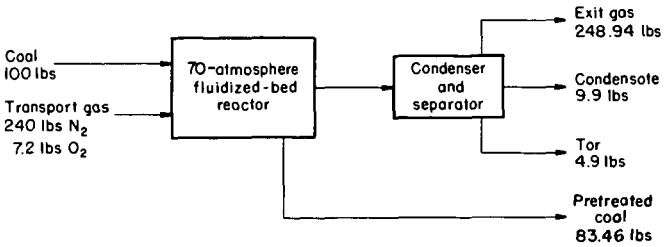

Run parameters
Coal rate = 10.5 lbs/hr
Superficial gas velocity = 0.68 ft/sec
Average operating temperature = 419°C

Figure 8 - Typical, design-basis, 70-atmosphere fluidized-bed reactor mass balance.

4-28-78 L-16028

CARBONIZATION REACTIONS IN THE GRAND FORKS FIXED-BED SLAGGING GASIFIER

Harold H. Schobert,[1/] Bruce C. Johnson,[2/] and M. Merle Fegley[2/]
Grand Forks Energy Research Center, US DOE
Box 8213, University Station
Grand Forks, ND 58202

A coal gasification pilot plant using a fixed-bed slagging gasifier is being operated at the Grand Forks Energy Research Center of the U.S. Department of Energy. The gasifier has a nominal maximum coal feed rate of 1 ton/hour and operates at pressures to 400 psig. Current gasification studies have focused on Western lignite and subbituminous coals; plant modifications are underway to extend operating capability to Eastern caking coals.

The slagging gasification pilot plant was installed during 1958-59, when GFERC was a part of the U.S. Bureau of Mines. The original program was conducted through 1965, to determine operability and maximum capacity. Details of the construction of the gasifier and test results obtained during the 1958-65 period have been reported (1). Operation of the pilot plant was resumed in 1976, and these later results have been reported by Ellman and co-workers (2).

A cross-sectional view of the gasifier is shown in Figure 1. The reactor chamber is about 16-1/2 inches in diameter and has a maximum fuel bed depth of approximately 15 feet. The test coal (nominally sized 3/4 x 1/4 inch) flows by gravity from the coal lock into the gasifier shaft. As the coal descends, drying and devolatilization is accomplished by the countercurrent flow of hot gases from the gasification reactions in the lower section of the gasifier. Gasification occurs at temperatures of 2800-3100° F and is sustained by an oxygen-steam mixture injected through four tuyeres at the bottom of the fuel bed. During the gasification reaction the coal is completely consumed, leaving only the molten ash. The molten ash (slag) drains continuously through a taphole into a water quench bath.

As the coal descends through the gasifier, various reactions occur. A previous publication (3) has shown that a slagging fixed-bed gasifier could be thought to consist of four reaction zones at steady state operation, as shown in Figure 2. This figure is an idealized example, since in actual practice the locations and relative lengths of the indicated zones will vary and overlap depending on the operating conditions and the characteristics of the coal being gasified. Similar conceptual schemes have been given for other gasifiers (4,5).

In the drying zone the incoming coal is heated by the ascending gases to the temperature at which the moisture in the coal is vaporized. After being dried, the coal descends through the devolatilization zone where the tars and oils are vaporized and some product gas is formed. The reaction

$$\text{Coal} + \text{Heat} = \text{Char} + \text{Oils} + \text{Tars} + H_2 + CO + CO_2 + \text{Gaseous Hydrocarbons} + H_2O$$

indicates the changes taking place in this zone. The devolatilized coal (char) then enters a zone in which little carbon is consumed but some gas reactions take place; this has been termed (3) the quasiquiescent zone. Finally, the coal enters the gasification/combustion zone.

1/ Acting Supervisor, Analytical Services.
2/ Chemical Engineer.

One of the major components of the current GFERC gasification pilot plant program is the sampling, analysis, and characterization of effluents produced during the gasification process. The GFERC effluent program has been treated in extensive detail in a recent publication by Paulson and co-workers (6), which describes sampling and analytical methods, and summarizes results on effluent composition. One aspect of this study is the development of mathematical and conceptual relationships between the effluent characteristics and the gasifier operating conditions and coal type.

From a consideration of the gas and coal tar characteristics, the production of organics in the devolatilization zone can be shown to be very similar to a high-pressure, low-temperature carbonization process. The similarity is important since it is then possible to draw on the extensive literature of coal carbonization to help interpret and understand the factors governing the production of tar and volatiles in the GFERC gasifier.

The product gas from the GFERC gasifier contains small quantities of C_{2-4} hydrocarbons; these gases typically being less than 1 pct (by volume) of the total. Analytical methods and production information have been discussed previously by Olson and Schobert (7). Formation of these gases during a carbonization process is considered to be due to thermal cleavage of the peripheral aliphatic and alicyclic portions of the coal "molecule." The relative proportions of the C_{2-4} hydrocarbons in the GFERC product gas is compared in Table 1 to gas from carbonization. The data from the three sources has been normalized to a basis of C_2H_6 = 1. The GFERC data represent average values from two 200 psi pilot plant tests using Baukol-Noonan lignite. Except for ethylene, good agreements exist for the relative quantities of the gases produced.

Gas component	Source		
	GFERC	Reference (8)	Reference (9)
Ethane.....	1.00	1.00	1.00
Propane.....	0.18	0.23	0.35
Butane.....	0.02	0.00	0.10
Ethylene.....	0.74	0.43	0.24
Propylene.....	0.30	0.23	0.23
Butylene.....	0.00	0.07	0.03

Total alkene production decreases with increasing pressure, as suggested (9) for high pressure carbonization processes. Data from pilot plant tests at 125, 200, and 400 psi with Indian Head lignite show alkenes (the sum of ethylene, propylene, and butylene) decreasing from 0.26 $\pm$ 0.01 pct at 125 psi to 0.23 $\pm$ 0.02 pct at 200 psi and then to 0.16 $\pm$ 0.03 pct at 400 psi.

The aromatization index has been proposed (10) as a convenient method for classifying coal tars. The aromatization index, N, is calculated from the relationship

$$N = C_W/3\ H_W$$

C_W and H_W are the weight percent of carbon and hydrogen in the tar. Tar samples are obtained both from an end-of-run composite sample and from side stream samplers described in previous publications (2,6). Analyses were done using the classic combustion train method or a Coleman model 33 carbon-hydrogen analyzer. Data from 17 pilot plant tests were used to calculate average values of N for 12 sets of operating conditions.

Coal	Rank	Pressure psi	Oxygen rate scfh	O_2/Steam ratio	N
Baukol-Noonan	Lignite	200	4,000	1.0	3.20
Do.....	..do.....	200	5,000	1.0	3.25
Do.....	..do.....	400	4,000	1.0	3.27
Indian Head	Lignite	100	4,000	1.0	3.83
Do.....	..do.....	125	4,000	1.0	4.18
Do.....	..do.....	200	4,000	0.9	3.16
Do.....	..do.....	200	4,000	1.0	3.13
Do.....	..do.....	400	4,000	1.0	3.26
Do.....	..do.....	400	6,000	1.0	3.25
Kemmerer	Subbituminous	200	4,000	1.0	2.97
Rosebud	Subbituminous	200	4,000	1.1	3.18
Do.....	..do.....	200	5,000	1.1	3.19

Nine of the 12 values are between 3.13-3.27 and a tenth is 2.97. This agrees reasonably well with a value of 3.05 suggested by Jurkiewicz et al (11) for low temperature carbonization tar from European brown coals.

Increasing pressure has been shown (9) to decrease the concentration of phenol and increase the concentration of high molecular weight aromatics in carbonization tar. Coal tar composition is determined at GFERC by mass spectrometry. For two pilot plant tests at 200 psi the average phenol content of the tar was 18.4 pct; for two other tests in which only the pressure was changed -- to 400 psi -- the phenol content averaged 13.0 pct. The lignite gasified in these tests was Indian Head.

The effect of pressure on the formation of higher molecular weight compounds in the tar was evaluated for five compounds: fluorene, phenanthrene, pyrene, chrysene, and benzopyrene. The same pilot plant data used to determine the effect of pressure on phenol concentration was also used for this comparison. Results are summarized as follows:

Tar component	Gasification pressure, pct 200 psi	400 psi
Fluorene.....	3.4	4.0
Phenanthrene.....	3.0	4.6
Pyrene.....	2.0	2.8
Chrysene.....	2.1	2.1
Benzopyrene.....	2.4	2.2

The quantities of three of the five compounds agree well with the high pressure carbonization model (9), in that the amount of these compounds increased with increasing pressure.

Increasing residence time in the reactor should decrease the yield of tar (9). Two mechanisms are available for changing residence time in the GFERC gasifier. At constant pressure, an increase in the oxygen-steam feed rate will decrease residence time; at identical oxygen-steam rates, increasing operating pressure will increase residence time. Previously published GFERC data (6) show that at 400 psi, tar production at a 6,000 scfh oxygen rate is 71.9 lb/ton maf lignite. Tar production drops to 55.5 lb/ton maf lignite at an oxygen feed rate of 4,000 scfh. At an oxygen rate of 4,000 scfh, tar production, decreases 92.4 lb/ton maf lignite in 100 psi tests to 70.1 at 200 psi and to 55.5 at 400 psi. These results were from tests using Indian Head lignite at a 1.0 oxygen/steam mole ratio.

VanKrevelen and Schuyer (12) provide a detailed kinetic treatment of carbonization processes. Production of char (or devolatilized lignite in the quasi-quiescent zone before gasification/combustion zone) can be determined for the slagging gasifier by sampling the bed after shutdown. Char sampling and analysis have been discussed previously (3). Using data from a 200 psi run, at 4000 scfh oxygen rate and 1.0 oxygen/steam mole ratio with Indian Head lignite, the first-order rate constant for char production was calculated to be 0.014 min^{-1}. The amount of volatile material produced was determined by summing the gaseous hydrocarbon, tar, and aqueous organic material. The first-order rate constant calculated for volatile production for the same run is 0.011 min^{-1}. The good agreement of the two rate constants suggests that the char and volatiles are indeed being produced in a reaction following VanKrevelen's kinetic model of a carbonization process.

The agreement of GFERC pilot plant data on gas, tar, char production with carbonization models shows that it is possible to regard the devolatilization zone in the gasifier as a region of typical coal carbonization reactions. As research continues at GFERC further understanding of devolatilization in the gasifier can be derived from carbonization models.

REFERENCES

1. Gronhovd, G.H., A.E. Harak, M.M. Fegley, and D.E. Severson. Slagging Fixed-Bed Gasification of North Dakota Lignite at Pressures to 400 psig. U.S. BuMines RI 7408 (1970).

2. Ellman, R.C., M.M. Fegley, B.C. Johnson, L.E. Paulson, and H.H. Schobert. Slagging Fixed-Bed Gasification. Presented at 4th International Conference on Coal Gasification, Liquefaction, and Conversion to Electricity, Pittsburgh, August 1977.

3. Johnson, B.C., H.H. Schobert, and M.M. Fegley. The Grand Forks Slagging Gasifier: Gas-Solid Reactions in the Real World. Presented at National Meeting, American Institute of Chemical Engineers, New York, 1977.

4. Grant, A.J. Applications of the Woodall-Duckham Two Stage Coal Gasification. Presented at 3rd International Conference on Coal Conversion, Pittsburgh, August 1976.

5. Agroskin, A.A. Chemistry and Technology of Coal. Israel Program for Scientific Translations, Jerusalem, 1977.

6. Paulson, L.E., H.H. Schobert, and R.C. Ellman. Sampling, Analysis, and Characterization of Effluents from the Grand Forks Energy Research Center Slagging Fixed-Bed Gasifier. Presented at 175th National Meeting, American Chemical Society, Anahiem, March 1978.

7. Olson, J.K., and H.H. Schobert. Production of C_1-C_4 Hydrocarbons in the Gasification of Some North Dakota Lignites. Presented at 70th Annual Meeting, North Dakota Academy of Science, Grand Forks, April 1978.

8. Heilpern, S., and A. Kijewska. Modern Concepts of the Chemical Structure of Coal. In Selected Articles on Chemistry and Structure of Coal. OTS 61-11350 (1963).

9. Altschuler, J., and H. Shafir. Peculiarities of Low-Temperature Carbonization of Solid Fuel Under Pressure. In Chemical Processing of Fuels. Academy of Sciences of the USSR. Moscow, 1957.

10. Jurkiewicz, J., T. Niewiadomski, and S. Rosinski. A Tentative Classification of Coke-Oven Tars, Based on New Theoretical Principles. In Selected Articles on Coal Tars. OTS 61-11344 (1963).

11. Jurkiewicz, J., T. Niewiadomski, and S. Rosinski. New Basis of Coal-Tar Clasification. ibid.

12. VanKrevelen, D.W., and J. Schuyer. Coal Science. Elsevier Publishing Co., New York, 1957.

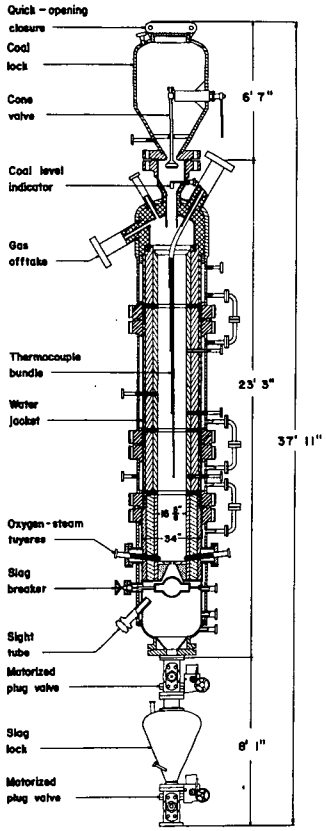

Figure 1

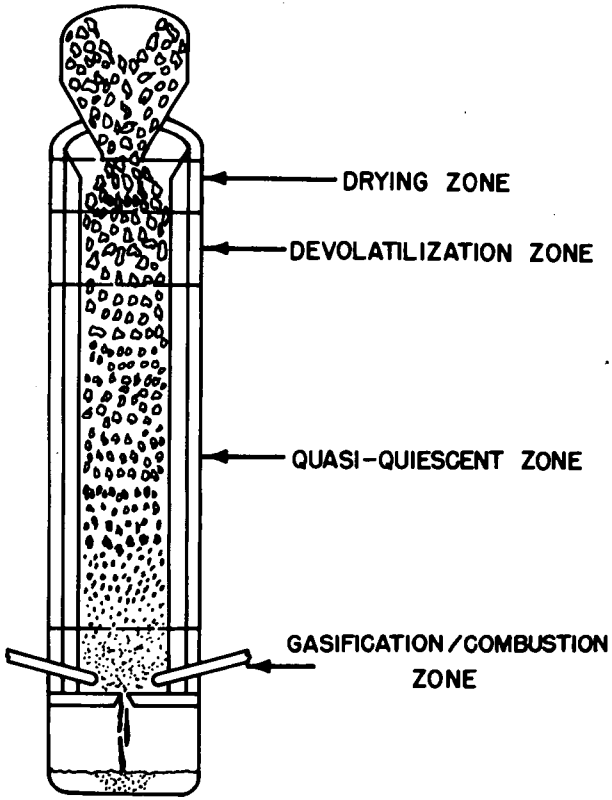

Figure 2

DEVELOPMENT OF AN ADVANCED FLUIDIZED BED COAL GASIFICATION PROCESS

R. E. Andermann, G. B. Haldipur

Westinghouse Electric Corporation
Advanced Coal Conversion Department
Box 158
Madison, Pennsylvania 15663

Introduction

Westinghouse Electric Corporation, under contract with the U.S. Department of Energy, is developing a coal gasification process. The process utilizes a variety of caking or non-caking coals to produce a clean combustible gas. The process was designed to supply a clean, low-Btu gas for electric power generation through a gas and steam turbine combined-cycle plant; however, the process can be used to produce a low-Btu or medium-Btu gas for either industrial fuel gas or synthesis gas. The Westinghouse coal gasification process can also be used for the cogeneration of steam, gas, and power.

The Westinghouse coal gasification system includes two fluidized bed reactors (see Figure 1). The first reactor, the devolatilizer, is used to devolatilize and decake coals as required. Coal is fed from lockhoppers to this reactor through a draft tube into a fluidized bed which operates at 1690 kPa (230 psig) and 870°C (1600°F). Devolatilized char circulates around the draft tube and dilutes the incoming coal, thus preventing the agglutination of coal particles as they pass through the plastic stage during heating. The two product streams from the devolatilizer are a combustible gas and char.

The second reactor, the gasifier, is used to gasify a wide range of feed materials which include coals as well as coal-derived chars. In the gasifier, the feed materials react with steam and air. The carbon-air combustion reaction provides the heat for the entire process and also causes the ash present in the char to agglomerate at about 1095°C (2000°F). These heavier, larger ash particles defluidize and are withdrawn from the bed. The steam-carbon gasification reaction is used to consume the remainder of the carbon not combusted by air. The gasification reaction moderates the reactor temperature and provides the combustible gas which is introduced into the devolatilizer as the fluidizing medium.

Since August 1972, a three-phased effort has been in progress at Westinghouse: bench scale and analytical work; pilot scale development on a 545 kg/hr (1200 lb/hr) Process Development Unit (PDU); and scale-up studies for a commercial scale plant. This paper considers only the work related to the PDU.

Mechanical completion of the PDU was achieved in September 1974. Precommissioning of utilities and process systems was completed by January 1975. The synthesis gas generators were commissioned in early 1975. Shakedown of the generators resulted in their redesign, which was followed by their successful commissioning in September 1975. Testing of the devolatilizer reactor began in October 1975. The tests, which were completed in August 1976, demonstrated the feasibility of the draft tube concept for this portion of the process. The results of these tests are reported elsewhere[1-6].

Testing of the gasifier reactor started in November 1976 and ended in December 1977. During this series of tests, successful operation of the gasifier was demonstrated with a wide variety of feedstocks which included chars produced early in the devolatilizer test series. Controlled tests of 100 to 150 hours were readily achieved during the gasifier tests. Also, the concept of agglomerating the ash in the feed material and the subsequent separation of the agglomerated ash from the fluidized char bed was demonstrated. This paper will discuss the conceptual design of the gasifier and operating results from some of the tests.

Westinghouse Gasifier Description

The gasifier includes two distinct sections (see Figure 1). During gasifier operation, the upper section contains a fluidized bed of coal-derived char particles. In this fluidized bed, the combustion and gasification reactions consume the carbon in the char particles. The agglomeration of the ash remaining in the particles also occurs within the upper section. The physical separation of the char and ash takes place in the lower section of the gasifier which is called the ash annulus.

The upper fluidized bed section of the gasifier is conceptually subdivided into a combustion/agglomeration region and a gasification region. The combustion/agglomeration region is located just above the air tube. The solid feed material (char or coal) which is pneumatically conveyed to the gasifier is injected directly into this region. In this region, char combusts with air, producing the heat necessary to: 1) promote agglomeration of ash rich particles, and 2) drive the carbon-steam gasification reaction. The gasification region of the fluidized bed is the reducing atmosphere region of fluidized bed where the carbon-steam gasification reaction occurs.

The gas flow rates into the upper section of the reactor control the fluid dynamics in this section. Circulation of solids within the fluidized bed is a function of the air tube volumetric flow which can be controlled by adjusting either air mass flow and/or air preheat temperature. The other control on solids circulation in the upper section is at the transition between the ash annulus and the larger diameter fluidized bed section of the gasifier. Gas flow (either steam or recycle gas) is injected into a grid at this transition to insure movement of material in this region.

Gas flow rates to the upper section of the gasifier also control the temperature of the fluidized bed. Air, steam, and to a lesser extent, cold recycle product gas, are used to control temperature. Fluidized bed temperatures can be easily controlled anywhere from 760°C (1400°F) to 1095°C (2000°F).

The lower section of the gasifier, or ash annulus, is where the separation of char and ash particles occur. Both a slugging bed and a fixed bed exist in the ash annulus. The slugging region contains a mixture of char and ash particles. As the char and ash are separated, the larger and heavier ash particles defluidize. The defluidized ash particles make up a moving fixed bed region which is withdrawn from the bottom of the ash annulus. The molar gas flow rate through the ash annulus controls the char/ash separation. Separation of char and ash occurs at relatively low velocities, typically less than 0.75 m/s (2.5 ft/s). The main advantage of the ash annulus is that it divorces the char/ash separation zone from the well-mixed fluid bed.

Test Results for the Westinghouse Gasifier

In 1977, the Westinghouse gasifier was operated on a wide variety of feed materials which included both chars and coals. The chars processed were from the following sources: 1) coke breeze from metallurgical coke production; 2) FMC char from the COED plant in Princeton, New Jersey; and 3) char produced in the earlier tests of the Westinghouse devolatilizer. In addition to the char processed, three types of coals were processed in the gasifier for short time periods. The coals included a non-caking, a mildly caking, and a highly caking coal.

Most of the tests run in 1977 were conducted using char materials which were derived from various coals. The predominate feedstock used in the early design evaluation and operability tests was coke breeze. The origin of the coke breeze is a Pittsburgh seam coal. The FMC chars processed in the gasifier were derived from two coal sources: a Kentucky coal and a Utah coal. Finally, the devolatilizer chars were derived from three coal sources: 1) an Indiana #7 seam; 2) a Pittsburgh seam; and 3) an Upper Freeport seam. Typical feed properties of the chars are given in Table I.

In addition to the chars processed, three coals were fed directly without pretreatment to the gasifier. The coals include a Wyoming sub-bituminous C coal, a mildly caking bituminous coal (Indiana #7), and a highly caking bituminous coal (Pittsburgh seam). Typical properties of the coals processed are given in Table I.

Successful operation of the gasifier was achieved on both chars and coals. The two different configurations used for char or coal feed are shown in Figure 2. Typical operating conditions, feed rates, and product gas and solids compositions for the various runs are given in Table II. Run times in excess of 6 days were achieved on char materials. The important concept of agglomerating the ash in the feed material and the subsequent separation of the agglomerated ash particles from the char bed was successfully demonstrated in the gasifier tests.

Typical particle size distributions for feed material, ash agglomerates, and fines which are carried over in the gasifier off-gas to the cyclone separator are shown in Figure 3. It can be seen that significant particle growth occurs due to ash agglomeration. Table II also shows that the bulk density of the ash product is greater than the feed or the fluidized bed char. Both the increase in particle size and density allows the agglomerated ash to be separated from char material. As for the fines carried over from the reactor, comparing their size distribution with that of the feed material has shown that most fines are simply entrained feed material. The fines are recycled to extinction by reinjection directly into the combustion zone.

During the gasifier tests, it was shown that the agglomerated ash particle size, shape, and physical appearance depends both on gasifier temperature and ash holdup or residence time in the reactor. Figure 5 shows the effect of gasifier temperature on the ash agglomerates. Agglomerates produced at higher reactor temperatures tend to be denser and more spherical. The effect of ash residence time is shown in Figure 6. By forcing the ash particles to remain in the reactor and pass repeatedly through the high temperature zone, the ash particles coalesce and grow in size.

In addition to studying ash agglomeration, the carbon-steam gasification reaction kinetics were analyzed for the PDU gasifier. Based on more detailed carbon-steam reaction kinetics studies being conducted on a bench scale unit at the Westinghouse Research Laboratories, the following equation was used to analyze the PDU data:

$$r_c = C \exp(-E/RT) \, (P_{H_2O})^n \qquad 1)$$

where r_c is the mass rate of carbon consumed per mass of carbon in the bed (min)-1,

C is an empirically determined constant,

E is the activation energy (218,200 j/g mole or 93,800 Btu/lb mole)[7],

P_{H_2O} is the inlet stream partial pressure, psia.

A plot of specific reaction rate ($r_c \exp(E/RT)$) as a function of steam partial pressure for various PDU test points is given in Figure 4. The regressed data for coke breeze gave a steam partial pressure exponent, n, of 0.72. This compares favorably with values of 0.66[7] and 0.63[8] reported elsewhere.

It is worth noting in Figure 4 that the relative reactivity of coke breeze is much less than other chars or coals processed in the gasifier. This apparently low reactivity is probably a result of the severe processing which occurs during coking. Coke is produced at temperatures of 1035-1095°C (1900-2000°F) and has a residence time at these temperatures of between 16-30 hours. The other char materials used during the gasifier tests were typically produced at temperatures between 705-870°C (1300-1600°F) with a residence time at these temperatures of between 1 to 2 hours.

In conclusion, the gasifier test series has been very successful. A wide variety of feed material which includes coal and coal-derived chars have been processed in the Westinghouse gasifier. Controlled operation of the gasifier has been achieved for continuous runs in excess of 6 days. Insights into ash agglomeration and subsequent separation from the char bed has been gained and laboratory scale experiments have proved helpful in analyzing the gasification kinetics for the PDU gasifier.

Acknowledgments

The authors thank the U.S. Department of Energy for its support of this program and all the engineers and staff who contributed to the work performed at the Westinghouse Coal Gasification site at Waltz Mill.

References

(1) "Advanced Coal Gasification System for Electric Power Generation"; Westinghouse Electric Corporation, Contract report to ERDA/DOE:
a) Interim Report No. 4, FE-1514-53
b) Interim Report No. 5, FE-1514-57
c) Quarterly Report (1Q-FY 1977), FE-1514-61

(2) L. A. Salvador, E. J. Vidt, and J. D. Holmgren; "The Westinghouse Fluidized Bed Combined Cycle Process: Status of Technology and Environmental Considerations"; Environmental Aspects of Fuel Conversion Technology II Symposium; December 16, 1975.

(3) R. Shah, P. J. Margaritis, L. K. Rath, P. Cherish, and L. A. Salvador; "Operation of the Westinghouse Coal Gasification Process Development Unit"; Proceedings, Eleventh Inter-Society Energy Conversion Engineering Conference; September 1976.

(4) L. K. Rath, P. J. Margaritis, R. Shah, P. Cherish, and L. A. Salvador; "Operation of the Westinghouse Coal Gasification PDU"; 4th National Conference on Energy and the Environment; October 6, 1976.

(5) P. J. Margaritis, S. S. Kim, P. Cherish, and L. A. Salvador; "Operation of the Westinghouse Fluidized Bed Devolatilizer with a Variety of Coal Feedstocks"; 173rd National Meeting of the American Chemical Society, Division of Fuel Chemistry; March 1977.

(6) L. A. Salvador, J. D. Holmgren, L. K. Rath, and P. J. Margaritis; "Development of the Westinghouse Coal Gasification Process - A Status Report"; 12th Inter-Society Energy Conversion Engineering Conference; August 28 - September 2, 1977.

(7) "Advanced Coal Gasification System for Electric Power Generation"; Westinghouse Electric Corporation, Contract report to ERDA/DOE:
a) Quarterly Report (3Q-FY 1977), FE-1514-69.

(8) L. Seglin, L. D. Friedman, and M. E. Sacks; "The COGAS Process for the Gasification of Coal"; 168th National Meeting of the American Chemical Society, Division of Fuel Chemistry, 19, No. 4; September 1974.

Figure 1. Westinghouse Coal Gasification System

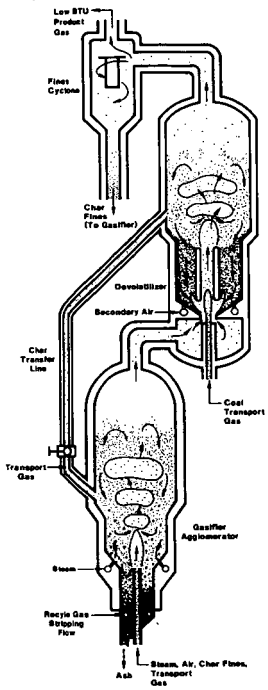

Figure 2. Westinghouse Gasifier Feed Configurations

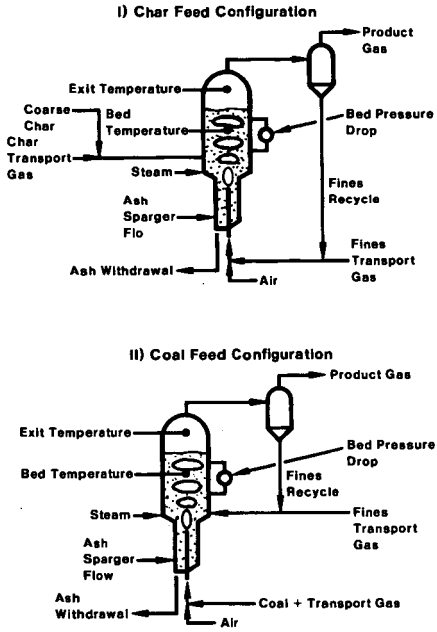

Table 1. Gasifier Feedstocks Properties

	Pittsburgh Coke Breeze (-8 mesh)	PDU Pittsburgh Char	PDU Indiana 7 Char	FMC-COED W. Ky. & Utah Chars	Pittsburgh Coal	Indiana 7 Coal	Wyoming Sub-C Coal
Proximate Analysis, %							
Carbon	83	76	78	75	47	46	36
Volatiles	5	3	3	10	45	40	47
Moisture	1	1	1	2	2	6	13
Ash	11	18	18	13	6	8	2
Size, Microns							
Coarse Feed	800	1,270	1,100	200	820	1,000	1,100
Fines Feed	200	230	210	200	200	200	200
Bulk Density							
kg/m^3	610	370	385	480	736	914	690
lb/ft^3	38	23	24	30	46	57	43
Caking Properties							
Free Swell Index	0	0	0	0	8	2	0
Gaiseler Plasticity	0	0	0	0	28,000	–	–
Heating Value J/g (Btu/lb)	–	–	–	–	32,300 (13,927)	27,900 (12,024)	24,400 (10,505)
Relative Reactivity*	1.0	2.5	9.9	11.8	–	–	12.0
Acid Insoluble Iron, % of Total	34	24	17	8	–	–	–

*Based on lab data for initial rate.

Table 2. Typical Gasifier Results

			Pittsburgh Coke Breeze		PDU Indiana Char		PDU Upper Freeport Char		FMC-COED Char (Utah)		Pittsburgh Coal		Indiana 7 Coal		Wyoming Sub-C Char	
System Pressure	kPa	(psia)	1690	(245)	1690	(245)	1690	(245)	1690	(245)	1690	(245)	1690	(245)	1690	(245)
Exit Gas Temperature	°C	(°F)	960	(1800)	950	(1740)	955	(1750)	955	(1750)	965	(1770)	935	(1720)	935	(1720)
Bed Temperature	°C	(°F)	1020	(1865)	985	(1805)	1000	(1830)	1000	(1835)	1000	(1835)	965	(1770)	960	(1760)
Coal or Char Feed Rate	kg/hr	(lb/hr)	200	(440)	225	(500)	325	(720)	370	(820)	385	(850)	410	(900)	455	(1000)
Char Fines Recycle Rate	kg/hr	(lb/hr)	200	(440)	110	(240)	160	(350)	205	(873)*	130	(285)	245	(540)	315	(700)
Air Rate	kg/hr	(lb/hr)	635	(1400)	575	(1265)	1020	(2250)	960	(2120)	1495	(3300)	1615	(3560)	1290	(2840)
Steam Rate	kg/hr	(lb/hr)	70	(155)	35	(80)	90	(200)	135	(300)	110	(245)	75	(170)	0	(0)
Recycled Product Gas	kg/hr	(lb/hr)	475	(1050)	500	(1105)	610	(1340)	410	(900)	655	(1440)	560	(1230)	460	(1060)
Coal or Char Transport Gas Rate	kg/hr	(lb/hr)	290	(645)	345	(765)	320	(700)	340	(750)	265	(590)	345	(765)	190	(415)
Char Fines Transport Gas Rate	kg/hr	(lb/hr)	375	(830)**	375	(825)**	370	(820)**	350	(775)**	175	(385)	210	(465)	315	(690)**
Ash Withdrawal Rate	kg/hr	(lb/hr)	75	(160)	45	(95)	55	(120)	45	(100)	25	(55)	35	(90)	10	(25)
Average Bed Pressure Drop	Pa/m	(psi/ft)	420	(0.20)	210	(0.10)	210	(0.10)	315	(0.15)	210	(0.10)	210	(0.10)	315	(0.15)
Average Bed Height	m	(ft)	7.6	(25)	7.0	(23)	7.6	(25)	7.0	(23)	8.0	(26)	7.6	(25)	7.6	(25)
Feedboard Velocity	cm/sec	(ft/sec)	60	(1.9)	5.0	(1.7)	8.0	(2.7)	7.5	(2.5)	9.0	(3.0)	9.5	(3.1)	7.6	(2.4)
Ash Annulus Gas Velocity	cm/sec	(ft/sec)	3.5	(1.2)	3.0	(1.0)	4.5	(1.4)	3.0	(1.0)	5.0	(1.6)	4.0	(1.3)	3.5	(1.2)
Bed Ash Content	wt %		20-25		30-35		30-35		30-45		15-25		15-25		15-25	
Ash Withdrawal Ash Content	wt %		45-65		60-70		50-65		40-60		30-45		30-45		30-55	
Bed Bulk Density	kg/m^3	(lb/ft^3)	560	(35)	400	(25)	320	(20)	480	(30)	400	(25)	320	(20)	320	(20)
Ash Withdrawal Bulk Density	kg/m^3	(lb/ft^3)	640	(40)	480	(30)	560	(35)	640	(40)	560	(35)	560	(35)	640	(40)
Product Gas Composition																
CH_4	mol %		0		0		0		0		2.0		0.6		1.1	
CO	mol %		9.8		15.0		13.7		18.4		14.2		10.3		10.9	
H_2	mol %		2.6		2.9		3.3		7.2		10.3		6.0		10.3	
CO_2	mol %		22.1		18.9		21.2		19.3		12.6		21.2		10.9	
N_2	mol %		63.3		62.4		56.6		53.2		55.2		53.4		52.1	
H_2O	mol %		2.3		0.9		5.3		1.9		5.7		8.2		3.9	

*No recycled fines. This feed is FMC char.
**Transport gas for this case is air.

Figure 3. Typical Size Distributions of Gasifier Feeds and Products

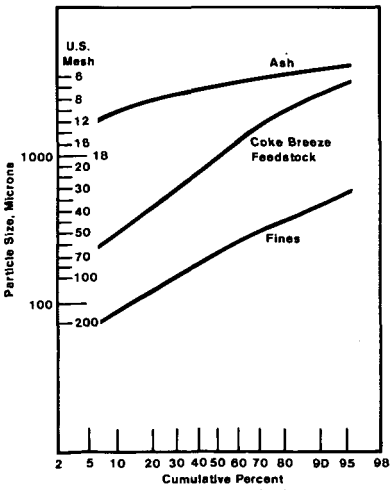

Figure 4. Specific Reaction Rate as a Function of Steam Partial Pressures for Various Gasifier Feed Material

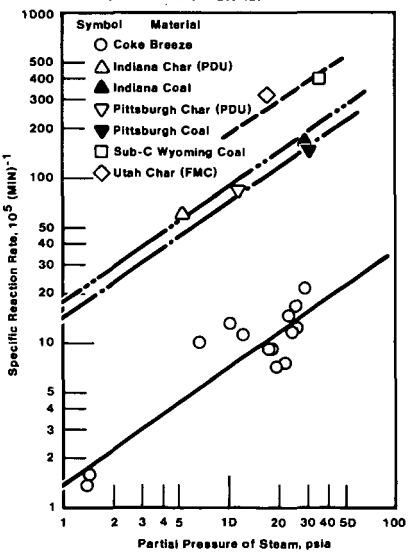

Figure 5. The Effect of Temperature on Ash Agglomerates

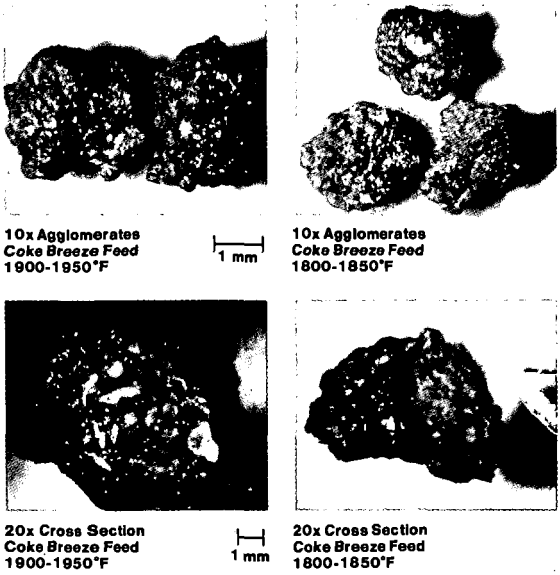

Figure 6. The Effect of Increased Holdup in the Reactor on Ash Agglomerates

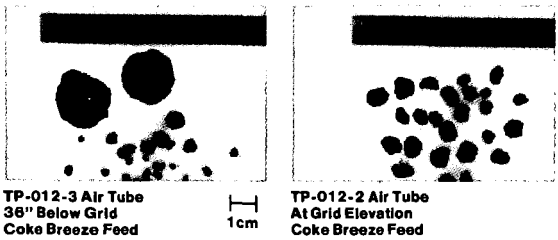

PEAT HYDROGASIFICATION. S.A. Weil, M. Onischak, D.V. Punwani. Institute of Gas Technology, 3424 S. State St., Chicago, IL 60616, and M. J. Kopstein, U.S. Department of Energy, Washington, D.C. 20545.

The hydrogasification of a Reed Sedge peat from Minnesota was studied in a 200 foot by 1/16 inch laboratory-scale reactor and in a 160 foot by 0.8 inch PDU reactor, at pressures up to 1000 psi and temperatures up to 1500°F. In these cocurrent dilute-phase reactors, the hydrogasification of peat yields up to 40% of the carbon as light hydrocarbon gases within 10 seconds. These hydrocarbons appear to be found in several ways. A kinetic description of the process accounting for the light hydrocarbon gases, the carbon oxides, and the liquid products is presented.

PRODUCTION OF SNG BY FREE-FALL DILUTE-PHASE HYDROGASIFICATION OF COAL

Harold F. Chambers, Jr. and Paul M. Yavorsky

U. S. Department of Energy
Pittsburgh Energy Research Center
4800 Forbes Avenue
Pittsburgh, PA 15213

INTRODUCTION

Hydrogasification of coal has been under investigation at PERC since the mid-1950's. Initial experiments were conducted with a 70-inch by 5/16-inch stainless steel, tubular reactor electrically heated to 800° C at 6000 psi and containing an 8-gram sample of 30 x 60 mesh coal (1).

Experiments at PERC in the early 1960's were conducted using downward entrained flow, helical tube reactors 60 feet by 1/8-inch and 20 feet by 5/16-inch. Coal was entrained at a rate of 60 gm/hr in a 2 ft/sec hydrogen stream. Plugging problems due to particle agglomeration were encountered in the 500° to 550° C zone of the helical tube (2, 3).

These experiments led to development of the vertical free-fall, dilute-phase (FDP) reactor with large diameter so that coal particles were dispersed to reduce contact while in the plastic temperature range. Very rapid particle heating in the dilute-phase by mixing with concurrently fed hot hydrogen controlled agglomeration and eliminated the need for oxidative coal pretreatment. The FDP reactor was initially tested as the first stage of the two-stage HYDRANE process (4, 5). Experiments in the HYDRANE series used primarily hvAb coals with hydrogen/methane mixtures in the FDP reactor. However, a limited number of experiments were conducted which demonstrated that the FDP reactor alone could adequately convert lower rank coals and lignite in pure hydrogen. (6)

The basic objective of any gasification process to produce SNG is the conversion of coal, typically $CH_{0.7}$ to methane, CH_4. Hydrogasification uses the approach of direct reaction of coal with hydrogen,

$$\text{Coal} + H_2 \rightarrow CH_4 + \text{Char} \qquad 1)$$

as opposed to formation of synthesis gas followed by methanation,

$$\text{Coal} + H_2O \rightarrow CO + H_2 + \text{Char} \qquad 2)$$

$$CO + 3H_2 \rightarrow CH_4 + H_2O \qquad 3)$$

In the dilute-phase hydrogasification process, coal which has been washed, pulverized and dried is fed directly to the reactor without a requirement of oxidative pretreatment. Pretreatment, to destroy the coal's agglomerating property, may consume 9 pct of the volatile matter and 13 pct of the weight (7). A further advantage of hydrogasification is in the minimum use of the methanation reaction shown in Equation 3. This reaction is highly exothermic, but the heat cannot be used directly in the gasifier because the temperature must be limited to 450° C for protection of catalysts. In the DPH process, typically 65-75 pct of total methane product may be produced directly in the FDP reactor.

A block diagram of the DPH process is shown in Figure 1. Raw pulverized coal and heated hydrogen were fed to the reactor and char and product gas were recovered as products. Char from the reactor may be used either in hydrogen generation or as a fuel for power and steam generation.

EXPERIMENTAL FACILITY

A schematic of the laboratory experimental facility is shown in Figure 2. Coal pulverized to 80 pct minus 200 mesh (U. S. standard sieve series) was initially loaded into a ground-level, low-pressure charging hopper and transferred in the dense phase by nitrogen to the first high-pressure lock hopper. Pressure was equalized between lock hoppers and coal transferred between them by gravity flow. Each lock hopper was 10-inch diameter schedule 120 carbon steel with a stainless steel liner and held approximately a 100 lb coal capacity.

Coal was fed from the second lock hopper by a rotary vane feeder through a water-cooled nozzle, a 0.3-inch tube, to the reactor at rates from 9 to 47 lb/hr. The reactor consisted of an electrically heated 304 stainless steel pipe, 3.26-inch internal diameter and enclosed in a 10-inch carbon steel pressure vessel. Reactor lengths of 5 and 9 feet were used. Hydrogen gas was heated by passing through a helical coil of tubing located in the annulus between the hot reactor wall and pressure vessel. It was injected at the reactor head concurrently downward with the coal. Char and product gas were separated in a disengaging zone below the reactor.

Product gas samples were automatically analyzed by an on-line gas chromatograph at 15 minute intervals. All experimental data, including gas analyses, were stored on a PDP-11 computer.

Char was collected at the base of the facility in two air-cooled, stainless steel receivers which were alternately filled and emptied during a test. Use of dual feed lock hoppers and char recievers allowed continuous operation.

EXPERIMENTAL PROGRAM AND RESULTS

In the present single-stage FDP reactor it was anticipated that only the more reactive lower rank coals would have adequate carbon conversion for SNG production. Therefore, only Illinois #6 hvCb coal and North Dakota lignite have been tested for the DPH process. Objectives of the experimental program were to demonstrate feasibility and operability of the FDP reactor for SNG production through both long and short duration parametric experiments. Data were obtained on yield and distribution of hydrogenation products to determine optimum test conditions and provide a thorough design data base for scale-up to a larger process development unit. Parameters in the test program were coal type, reactor length, hydrogen/coal ratio and reactor throughput.

Results of several experiments are summarized in Table 1 and typical analyses of coal and lignite are presented in Table 2. All tests were conducted at 1000 psig, with the reactor wall at 900° C. No thermocouples were located internally below the coal injection point to eliminate any potential blockage. Feed gas in all experiments was over 99 pct hydrogen. Both coal and lignite were pulverized and screened to 80 pct minus 200 mesh (all minus 100 mesh). Average particle size for lignite and coal was 73.4 and 82.6 μm respectively, determined by screen analysis. Conversion was calculated on the basis of ultimate analysis and actual feed and recovery weights of coal and char, with no forcing to 100 pct carbon or ash balance.

Experiments #124 and #128 were typical of those conducted with Illinois #6 coal using the five-foot heated reactor. Test times were limited by the single coal hopper that was used prior to installation of the dual lock hopper feed system. These experiments represent a 50 pct variation in coal feed rate, with two hydrogen/coal ratios tested at each feed rate. In both experiments carbon conversion and methane yield varied directly with the hydrogen/coal ratio. Char particles from these experiments showed an average diameter of 588 μm by screen analysis, with size independent of test conditions. Neither experiment produced a carbon conversion necessary for balanced plant operation, indicating the necessity for a longer

residence time in the reactor.

Major facility modifications following tests with Illinois #6 coal (dual lock hoppers) permitted extended continuous operation. The five-foot reactor was replaced with a nine-foot reactor having heated lenghts of one to nine feet in two-foot intervals. Testing then resumed using North Dakota lignite.

High moisture and oxygen contents of the lignite led to production of more water and carbon oxides than with hvCb coal. The higher CO content in the product gas stream reduced total methane to typically 75 pct with lignite as compared to 90 pct with bituminous coal.

In experiment #134, the first five-foot section of the reactor was operated at 900° C while the lower four-foot section was only heated to 300° C. This was to minimize the possibility of moisture condensation and char packing by permitting water to be removed through the product gas system. Following this procedure the experiment was conducted for a period of 45 hours at an average lignite feed rate of 12.5 lb/hr. No reactor problems were encountered; however the test was terminated by feeder stoppage due to fine particulates packing around the shaft, causing it to seize. Balanced plant operation was achieved with 44 pct carbon conversion, but product gas hydrogen-to-carbon monoxide ratio was higher than desired for final methanation.

The complete reactor was operated at 900° C in experiment #135 in order to achieve high carbon conversion at low hydrogen/coal ratios. Two hydrogen/coal ratios were tested, resulting in carbon conversion of 44 and 50 pct with low hydrogen/carbon monoxide ratios in product gas. Ratios of 3.36 and 2.8 were obtained as compared to ratios in excess of 7.0 in previous experiments. These values are consistent with requirements for final cleanup methanation with no residual hydrogen separation. Product gases from 135A and 135B had calculated heating values of 939 and 1008 Btu/scf, assuming CO methanation.

Experiment #136 was conducted for 22.6 hours at conditions nearly duplicating test #135B to verify results at these conditions. Figure 3 is typical of methane and hydrogen composition of the product gas for the duration of this test.

Experiment #137 was conducted to determine the effect of throughput on FDP reactor performance. Coal feed rate was varied from 15.9 to 47.0 lb/hr corresponding to a throughput range of 276 to 816 lb/ft^{2}hr. Feed gas rates were varied proportionally to maintain nearly constant hydrogen/coal ratio. Conversion varied inversely with throughput, indicating a requirement for incresed reactor length at high throughput conditions. However, under all test conditions, steady state reactor operation was easily maintained and carbon conversion to methane remained nearly 62.5 pct. No oil formation was detected in either char receivers or liquids traps at any operating conditions.

In experiment #139 data was obtained on the effect of hydrogen/coal variation upon carbon conversion and gas composition at a nominal 25 lb/hr lignite feed rate. A 68 pct change in hydrogen/coal ratio was tested, resulting with a 23 pct increase in methane yield per pound of coal. All other changes were relatively small.

CONCLUSIONS

Dilute-phase hydrogasification has been demonstrated in successful, continuous, long duration experiments. Carbon conversion necessary for balanced plant operation with lignite has been demonstrated at hydrogen/coal ratios producing a high-Btu SNG with no residual hydrogen separation requirement. High carbon selectivity to gas phase products has been demonstrated with no benzene and only trace oil formation. Parametric testing has established effects of throughput upon carbon conversion and product distribution. Steady operation was achieved at a throughput of over

800 lb/ft^2hr. Reproducibility of test results has been demonstrated by duplicated test operation.

REFERENCES

1. Hiteshue, R. W., Anderson, R. B., and Schlesinger, M. D., "Hydrogenating Coal at 800° C", Ind. and Eng. Chem., 49, pp. 2008-10, Dec. 1957.

2. Hiteshue, R. W., Friedman, S., and Madden, R., "Hydrogenation of Coal to Gaseous Hydrocarbons", U. S. BuMines R. I. 6027, 1962.

3. Hiteshue, R. W., Friedman, S., and Madden, R., "Hydrogasification of Bituminous Coals, Anthracite and Char", U. S. BuMines R. I. 6125, 1962.

4. Feldman, H. F., and Yavorsky, P. M., "The Hydrane Process", 5th AGA/OCR Synthetic Pipeline Gas Symposium, Chicago, Illinois, October, 1973.

5. Gray, J. A., and Yavorsky, P. M., "The Hydrane Process", Clean Fuels from Coal II Symposium, IGT, Chicago, Illinois, June, 1975.

6. Feldman, H. F., Mima, J. A., and Yavorsky, P. M., "Pressurized Hydrogasification of Raw Coal in a Dilute-Phase Reactor", Advances in Chemistry Series, No. 131, Coal Gasification, ACS, 1974.

7. Wen, C. Y. et. al., "Optimization of Coal Gasification Processes", NTIC #PB 235 787, 1972.

TABLE 1.-Dilute-phase hydrogasification of coal

Experiment No.	124A	124B	128A	128B	134	135A	135B
Coal Type	Illinois	Illinois	Illinois	Illinois	Lignite	Lignite	Lignite
Time (hr)	4.5	1.43	3.75	4.17	45.0	4.2	8.5
Reactor length (ft).	5	5	5	5	5	9	9
Temperature (° C) ..	900	900	900	900	900	900	900
Pressure (psig)	1000	1000	1000	1000	1000	1000	1000
Coal rate (lb/hr)[a] ..	15.0	15.0	10.03	10.03	12.4	14.8	14.8
Throughput (lb/ft^{2}hr)[a]	260	260	174	174	215	257	257
Feed gas/coal (scf/lb)[a]	9.31	7.93	13.78	12.10	15.6	17.0	10.6
Product gas/coal (scf/lb)[a]	9.75	8.03	14.53	12.17	16.8	18.8	12.3
Product gas comp. (vol%)							
H_2	42.1	32.5	47.4	40.1	54.3	48.0	41.4
CH_4	48.9	58.4	46.1	52.1	30.6	30.5	33.3
C_2H_6	1.5	0.4	-	-	-	-	-
CO	5.3	6.2	5.7	6.3	7.9	14.3	14.8
CO_2	2.0	1.9	0.4	0.6	6.5	6.6	10.0
H_2S	-	-	-	.4	0.3	0.2	0.2
N_2	0.2	0.2	0.3	.3	.3	.3	.3
Conversion (wt%)[b]							
Carbon	31.6	27.2	36.0	29.8	44.2	44.0	50.7
Hydrogen	76.2	72.5	80.8	77.8	83.5	83.3	88.4
Maf coal	40.6	37.0	45.1	39.7	58.1	57.6	63.7
Feed hydrogen consumption (scf/lb)[a]	5.09	4.47	6.84	7.67	6.48	7.98	5.51
Product yield/coal fed							
Methane (scf/lb)[c]	5.28	5.19	7.53	7.11	6.47	8.42	5.92
Char (lb/lb)[b] ...	0.64	0.67	0.60	0.64	0.46	0.47	0.40
Water (lb/lb)[b] ...	.04	.04	.03	.03	.13	.11	.11
Carbon recovery (wt%)	94.4	97.5	97.8	102.0	98.0	100.5	95.0
Heating value (Btu/scf)[d]	803	892	755	852	705	939	1008
CH_4 made in reactor (%)	90.2	90.4	89.0	89.2	79.5	68.1	69.2

TABLE 1-cont.

Experiment No.	136	137-A	137-B	137-C	137-D	139-A	139-B
Coal type	Lignite	Lignite	Lignite	Lignite	Lignite	Lignite	Lignite
Time (hr)	22.6	12.43	12.51	2.19	10.71	7.56	8.01
Reactor length (ft)	9	9	9	9	9	9	9
Temperature (°C)	900	900	900	900	900	900	900
Pressure (psig)	1000	1000	1000	1000	1000	1000	1000
Coal rate (lb/hr)[a]	14.6	15.90	26.29	47.31	14.48	26.11	24.64
Throughput (lb/ft^{2}hr)[a]	253	274	454	816	250	453	428
Feed gas/coal (scf/lb)[a]	9.91	9.59	9.76	11.23	12.13	8.90	14.94
Product gas/coal (scf/lb)[a]	12.3	12.64	12.53	11.86	14.03	11.78	16.07
Product gas comp. (vol%)							
H_2	46.7	45.6	49.5	56.8	53.8	44.9	51.8
CH_4	34.5	34.0	31.1	26.4	30.6	33.5	32.3
C_2H_6	-	0.1	0.1	0.2	-	-	-
CO	11.2	11.6	11.2	9.0	10.3	14.9	12.2
CO_2	7.1	8.2	7.5	7.0	4.9	6.1	3.1
H_2S	0.2	.2	.3	.3	.1	.4	.2
N_2	.3	0.3	0.3	0.3	0.3	0.2	0.3
Conversion (wt%)[b]							
Carbon	48.2	44.1	39.7	30.6	47.1	38.9	40.4
Hydrogen	82.8	83.9	81.3	75.3	80.6	82.3	85.8
Maf coal	56.0	59.3	55.7	46.6	59.9	54.3	55.8
Feed hydrogen comp. (scf/lb)[a]	4.17	3.83	3.56	4.49	4.58	3.61	6.61
Product yield/coal fed[d]							
Methane (scf/lb)	5.62	5.76	5.30	4.20	5.71	5.80	7.14
Char (lb/lb)[b]	0.44	0.46	0.49	0.58	0.44	0.49	0.48
Water (lb/lb)[b]	.13	.13	.20	.28	.14	.08	.12
Carbon recovery (wt%)	95.0	93.1	93.8	99.0	94.8	94.3	99.1
Heating value[d] (Btu/scf)	856	875	823	694	760	1005	834
CH_4 made in reactor (%)	75.5	74.6	73.5	74.6	74.8	69.2	72.5

[a]As received [b]Moisture free [c]Prior to methanation [d]Calculated assuming methanation

Table 2. Typical coal and lignite analysis

	Illinois #6 hvCb Coal	North Dakota Lignite
Proximate (wt pct)		
Moisture	1.0	9.7
Volatile matter	35.2	38.2
Fixed carbon	53.7	42.5
Ash	10.1	9.6
Ultimate (wt pct dry)		
Hydrogen	4.8	4.9
Carbon	71.8	56.9
Nitrogen	1.7	0.7
Oxygen (by difference)	10.1	25.7
Sulfur	1.4	1.2
Ash	10.2	10.6
	100.0	100.0

hvCb from Orient #3 mine, Freeman Coal Co., Waltonville, IL.
Lignite from Beulah seam, North Dakota.

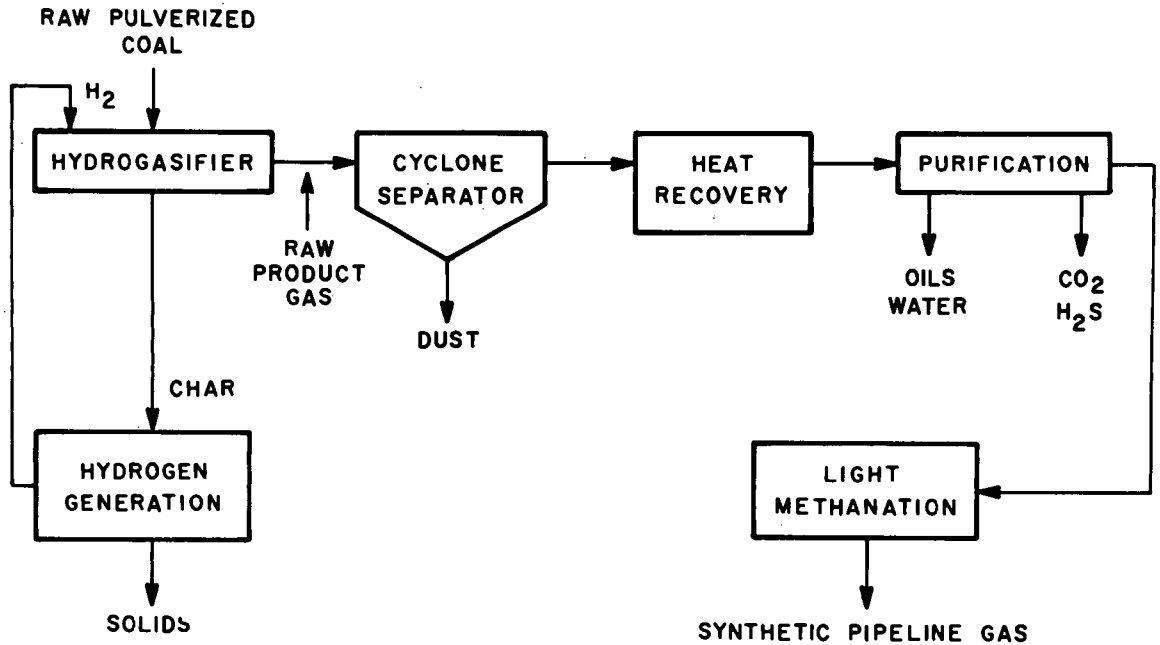

Figure 1 - Dilute phase hydrogasification process

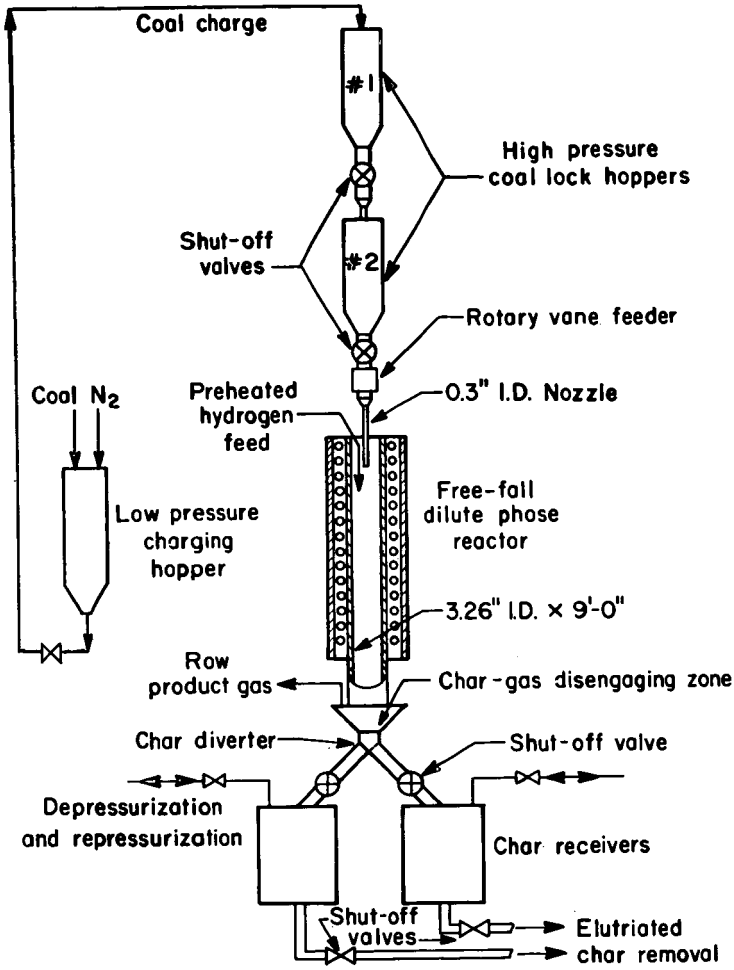

Figure 2– Dilute-phase hydrogosifier

3-15-77 L-15059

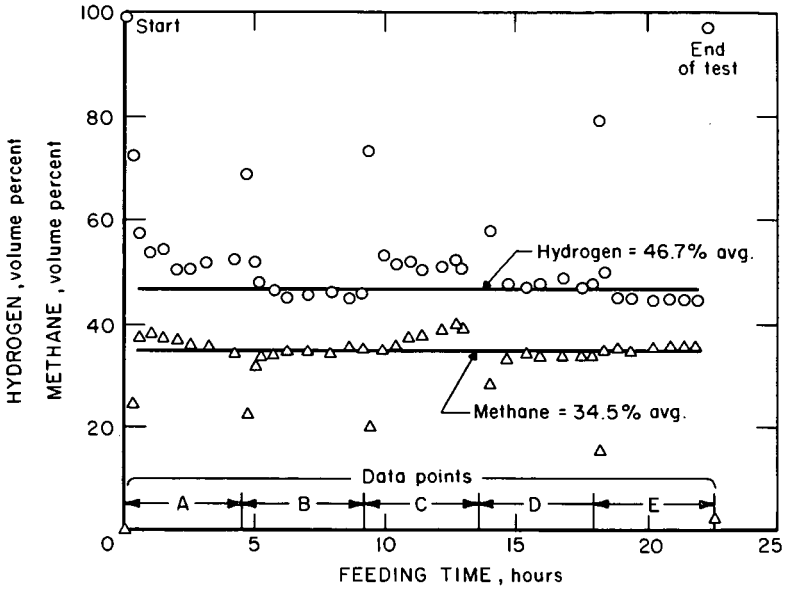

Figure 3 - Product gas composition vs time experiment #136 lignite feed, FDP reactor T=900°C P=1000 psig L=9ft.

Effects of Reaction Conditions on Gasification of Coal-Residual Oil Slurry

Hiroshi Miyadera, Mizuho Hirato, Shuntaro Koyama, Kenichi Gomi

Hitachi Reserach Laboratory, Hitachi Ltd., Ibaraki-ken, Japan

Introduction

In the face of energy crisis and environmental pollution, the technology for coal gasification is being developed as a part of "Sunshine Project" promoted by the Ministry of International Trade and Industry (MITI). Petroleum, however, will hold by far the largest share in Japan's primary energy supply for the next decades. While the utilization of heavy oil such as vacuum residue is limited from a point of view of the air pollution because of difficult desulfurization.

Therefore, in 1974 we have started the development of "Hybrid Gasification Process" in which coal and residual oil are simultaneously gasified to clean fuel gas. This report briefly describes the process and experimental results.

Process Description

A flow diagram of Hybrid Gasification Process is shown in Figure 1. Pulverized coal is mixed and stirred with residual oil to form a slurry, which is pumped to the pressurized fluidized bed gasifier with atomizing steam. The slurry is converted into gas and char by thermal cracking reactions in the upper zone of the fluidized bed. The char produced is further gasified with steam and oxygen.

The gas leaving the gasifier is scrubbed in oil and then in water quench to remove tar, dust and steam. A conventional gas clean up system is used to absorb carbon dioxide and hydrogen sulfide from the gas. If SNG is required, the product gas is shifted and methanated.

The advantages of the process are

(1) Almost all grades of coal and residual oil can be simultaneously converted to clean fuel gas.
(2) Raw materials are transported and fed to the pressurized gasifier without difficulty by means of slurry.
(3) The gasifier consists of a single fluidized bed and the gasification reactions proceed in two stages —— slurry thermal cracking and char partial oxidation. This simple structure of the gasifier achieves easy control and high thermal efficiency.

Experimental

In order to investigate the gasification characteristics and to improve the process, experiments were conducted in the pressurized gasification apparatus shown in Figure 2. The gasifier has the inner diameter of 120mm in the upper zone and 80mm in the lower zone. The height of each zone is 2000mm. The temperatures in the gasifier are controlled by the surrounding electric heaters.

At the beginning of each experiment, pulverized and sieved coal in the coal hopper is charged and fluidized with steam and oxygen. Then the 200°C pre-heated slurry with atomizing steam is fed to the middle part of the fluidized bed. The bed height above the slurry feeding point is 700mm. After dust, tar and steam in the product gas are removed in cyclones, scrubber and quencher, the gas pressure is reduced and its composition and its flow rate are measured.

Since a part of the gas is produced by the heat supplied from the external heaters, the gas yeilds of these experiments are somewhat different from the ones produced in the purely internally fired gasifier. Therefore, we have examined the characteristics of thermal cracking and partial oxidation separately. The gas produced in the thermal cracking zone is considered as follows.

$$G_S = G_T - G_C \qquad 1)$$

where G_S : gas production rate in the slurry thermal cracking zone,
G_C : gas production rate in the char partial oxidation zone,
G_T : total gas production rate in the gasifier when slurry thermal cracking and char partial oxidation occur simultaneously.

G_C can be measured when slurry feeding is stopped and only the char partial oxidation reaction takes place.

Feeding materials are shown in Table I. Taiheiyo coal, mined in Hokkaido, was chosen for this study because it is the most practicable for gasification use in domestic coals.

Table I. Raw materials

Taiheiyo coal		Gach Saran Vacuum Residue	
Proximate analysis (wt%)		Boiling point (°C)	>550
Moisture	5.3	Asphaltene (wt%)	10.4
Ash	14.4	Conradson carbon (wt%)	21.8
Fixed carbon	37.7	Metal content (ppm) V	318
Volatile matter	42.5	Metal content (ppm) Ni	112
Ultimate analysis (wt%, daf)		Ultimate analysis (wt%)	
C	76.6	C	85.0
H	6.5	H	10.8
N	1.0	N	0.1
O	15.3	O	-
S	0.6	S	3.5
Heating value (kcal/kg)	6580	Heating value (kcal/kg)	10090

(Note) Feed slurry ; Coal/Residual oil : 30/70 (wt. ratio)
Coal size : 40-140 mesh (0.105-0.42 mm)
Initially charged coal size : 25-40 mesh (0.42-0.71 mm)

Gasifier temperatures were controlled by oxygen feed rate and the surrounding electric heaters between 800 and 950°C in the lower partial oxidation zone and between 700 and 800°C in the upper thermal cracking zone. Reaction pressures were varied from 5 to 20 atm.

Results and Discussion

(1) Characteristics of Slurry Thermal Cracking Reaction.

Figure 3 shows the effects of temperature and pressure on the product yield of slurry thermal cracking. The main components produced are hydrogen, methane, carbon monoxide and carbon dioxide. The yields of these gases increase with temperature (T_S) and pressure, while yield of by-product tar decreases as pressure rises.

In this zone, following reactions take place.

$$\text{Slurry} \xrightarrow{\text{Heat}} \text{Gas} + \text{Tar} + \text{Char} \qquad 2)$$

$$\text{Slurry} \xrightarrow{H_2O} CO + CO_2 + H_2 \qquad 3)$$

$$\text{Slurry} \xrightarrow{H_2} CH_4 + C_2H_6 + \cdots \qquad 4)$$

Overall heat of reaction ΔH_R can be estimated by the next equation.

$$\Delta H_R = \sum_R N \Delta H_C - \sum_P N \Delta H_C \qquad 5)$$

where the first term on the right side refers to the summation of heats of combustion for the reactants and the second term for the products.

The overall heat of reaction estimated by the measured heats of combustion for

slurry, tar and char are shown in the upper columns of Figure 3. As shown in the fugure, ΔH_R increases with increasing temperatures and decreases with increasing pressures.

The characteristics stated above definitely show that endothermic reactions such as thermal cracking and steam reforming are dominant at higher temperatures and exothermic hydrogasification takes place at higher pressures.

(2) Characteristics of Char Partial Oxidation Reaction.

The main components in the gas produced in the partial oxidation zone are hydrogen, carbon monoxide and carbon dioxide. Therefore, the main reactions are supposedly as follows.

$$C\ (\text{char}) + O_2 = CO_2 \qquad 6)$$

$$C\ (\text{char}) + CO_2 = 2CO \qquad 7)$$

$$C\ (\text{char}) + H_2O = CO + H_2 \qquad 8)$$

$$CO + H_2O = CO_2 + H_2 \qquad 9)$$

The approach of these reactions toward equilibrium is indicated in Figure 4. Kp and Kp' are the equilibrium constant and the observed partial pressure ratio respectively. It is apparent from Figure 4 that the carbon - carbon dioxide reaction and the carbon-steam reaction are far from equilibrium for all of the run conditions tested, while the observed ratios for the shift reaction approach the equilibrium constant at pressures above 10 atm. in the range of 800 to 950°C.

(3) Heat and Material Balance in Gasifier.

Based on the results described above, the heat and material balance in the gasifier without external heating was investigated. As shown in Figure 5, following assumptions are made.

(i) Q_S, the heat required in the slurry thermal cracking zone, is represented by Equation A, where ΔH is the heat required to warm the reactants from the inlet temperature to the reaction temperature T_S.

(ii) In the char partial oxidation zone, Reaction 6 - 9 take place, Reaction 9 being in equilibrium. Overall heat of reaction in this zone raises the temperature of fluidizing char and gas, and this heat is released in the thermal cracking zone. Therefore, in the steady state, heat balance in the gasifier can be represented by Equation B, where Q_{RC} and Q_{GC} represent the quantities of heat transferred by char and gas, respectively.

(iii) In the steady state, the amount of char produced in the thermal cracking zone is equal to the amount of char gasified in the partial oxidation zone.

The conclusions from this investigation are summarized in Figure 6. It is indicated in Figure 6-a that the thermal efficiency, i.e., the ratio of the heating value of product gas to that of raw materials, has the maximum value at about 750°C. This is because the heat required in the thermal cracking zone is so large at higher temperatures that the amount of carbon dioxide increases. When pressures increase at constant temperature, as shown in Figure 6-b, both the product gas heating value and the thermal efficiency increase and oxygen feed rate decreases. This is because hydrogasification reactions play a more important role at higher pressures.

The typical heat and material balance is shown in Figure 7. The heating value of the raw gas is 4070 kcal/Nm^3(460 Btu/scf), and 5970 kcal/Nm^3(670 Btu/scf) after removal of carbon dioxide and hydrogen sulfide on the basis of dry gas. The thermal efficiency is about 75%.

The by-product tar yield is rather high (13-15 wt%) in this process. The tar can be either recycled to the gasifier or utilized as fuel oil, binder, raw materials for chemical industries and so on.

In addition to the study mentioned above, recently a low pressure (max. 3 atm) internally fired gasifier with a 300mm diameter has been operated to solve the possible mechanical and operational problems.

On the basis of these researches, a 12 t/D pilot plant is being designed, and it will be constructed in 1980.

Acknowledgement

This work was sponsored by the Agency of Industrial Science and Technology of MITI and is presented with their permission.

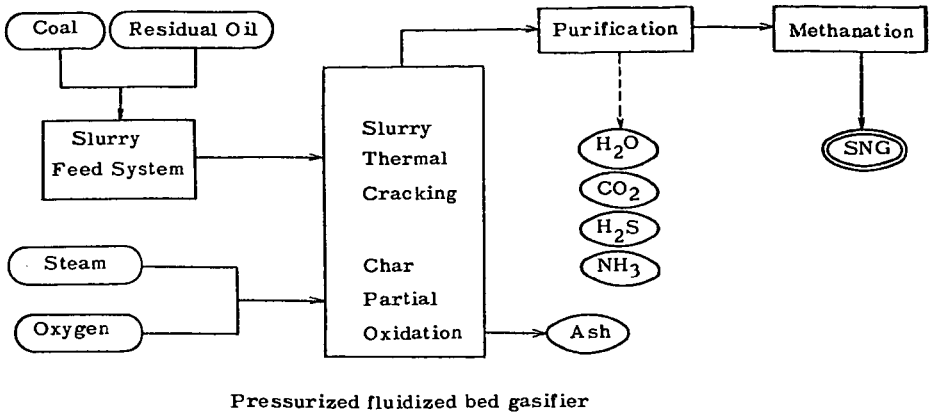

Figure 1. Coal-Residual Oil Hybrid Gasification Process

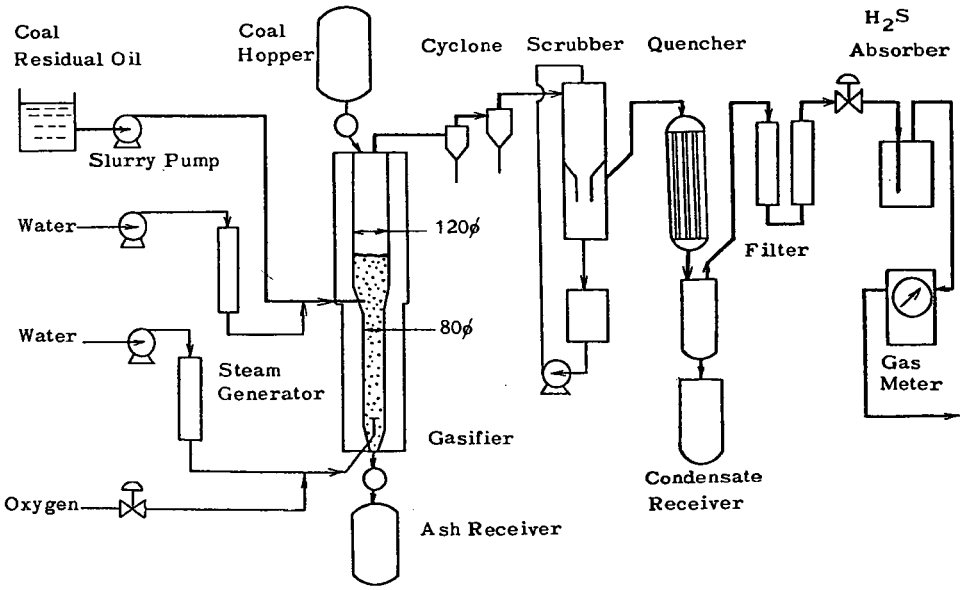

Figure 2. Pressurized fluidized bed gasification apparatus

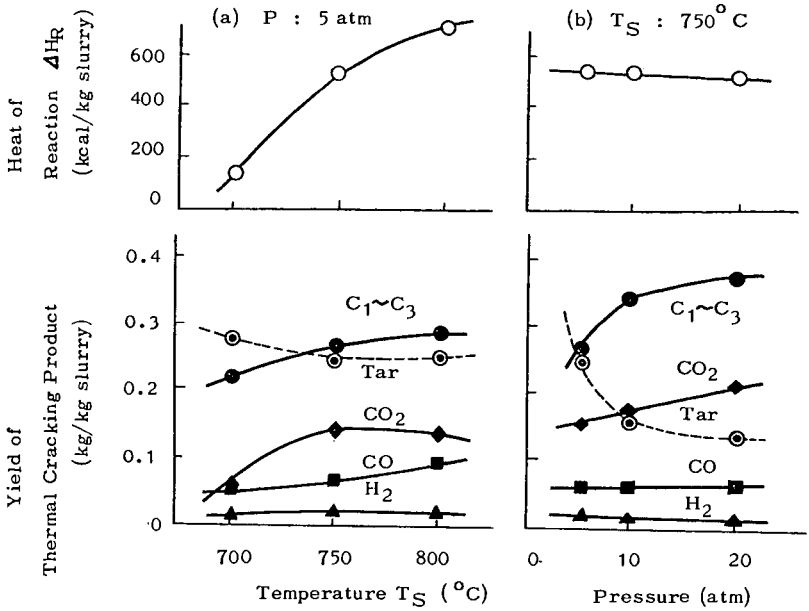

Figure 3. Effects of temperature and pressure on slurry thermal cracking

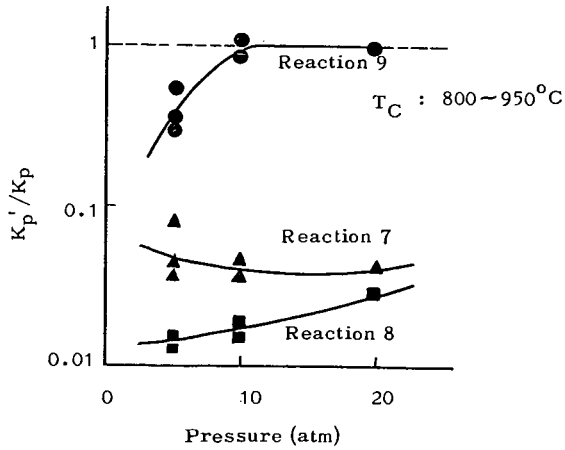

Figure 4. Comparison of observed partial pressure ratio of partial oxidation gas with equilibrium constant

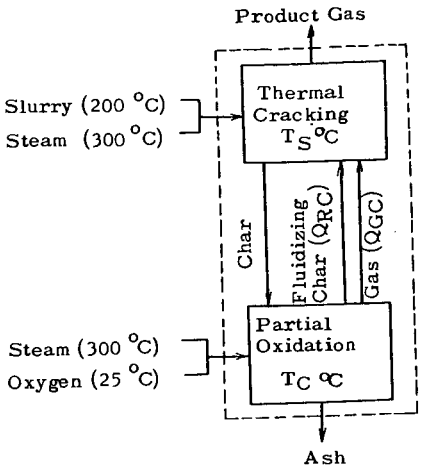

$$\text{Slurry} \xrightarrow{\Delta H_R} \text{Gas} + \text{Tar} + \text{Char} \quad 2)$$

$$\text{Slurry} \xrightarrow{\text{Heat}} CO + CO_2 + H_2 \quad 3)$$

$$\text{Slurry} \xrightarrow[H_2]{H_2O} CH_4 + C_2H_6 + \ldots \quad 4)$$

$$Q_S = \Delta H_R + \Delta H \quad A)$$

$$Q_S = Q_{RC} + Q_{GC} \quad B)$$

$$C + O_2 \longrightarrow CO_2 \quad 6)$$

$$C + CO_2 \longrightarrow 2CO \quad 7)$$

$$C + H_2O \longrightarrow CO + H_2 \quad 8)$$

$$CO + H_2O \rightleftharpoons CO_2 + H_2 \quad 9)$$

Figure 5. Reaction model in Hybrid Gasifier

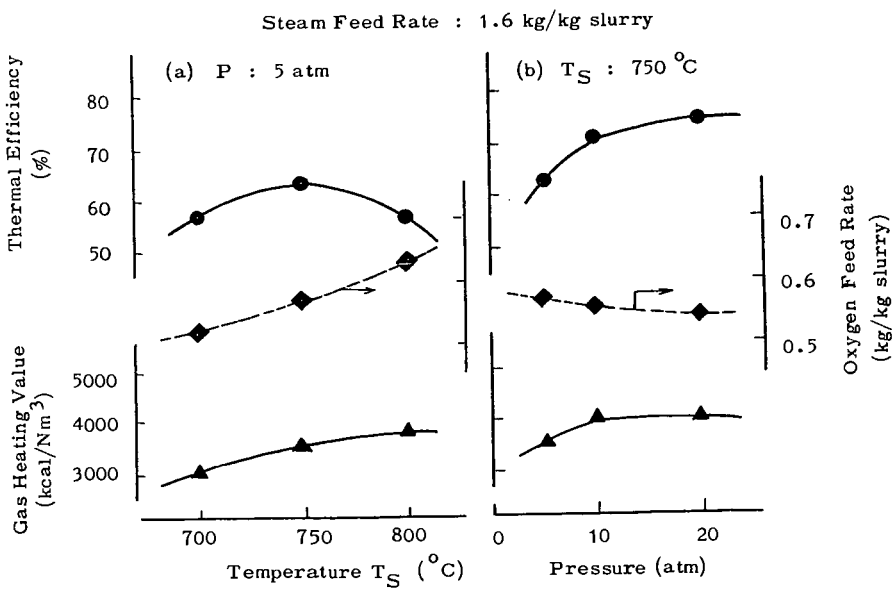

Figure 6. Effects of temperature and pressure on Hybrid Gasification Process

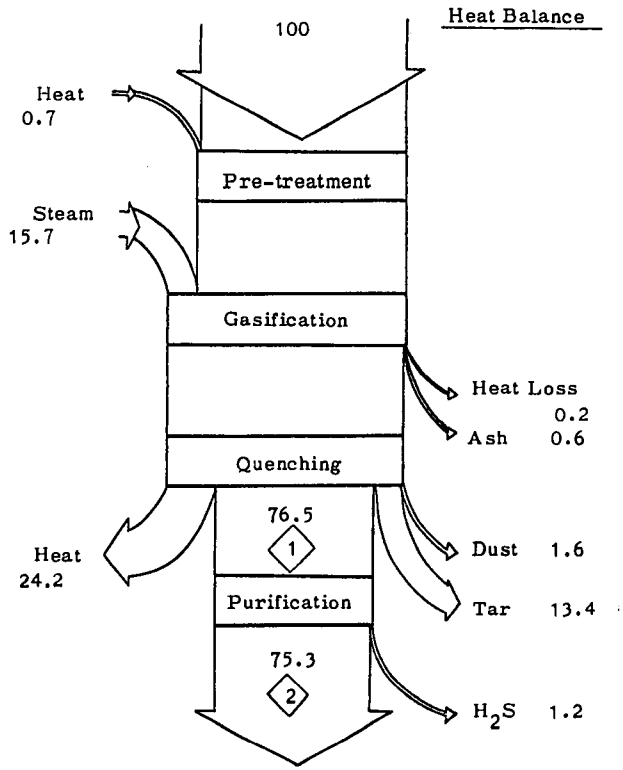

Material Balance

Feed	Slurry	1.0 kg	
	Steam	1.6 + 0.4 kg	
	Oxygen	0.54 kg	
Product Gas		1 Raw Gas	2 Purified Gas
Composition (vol%, dry)	H_2	33.0	49.5
	CO	10.1	15.1
	CO_2	32.1	-
	CH_4	17.6	26.4
	C_2's	5.5	8.1
	C_3's	0.6	0.9
	H_2S	1.1	-
Gas Heating Value ($kcal/Nm^3$) [Btu/scf]		4072 [457]	5974 [670]
Gas Volume (Nm^3/kg slurry)		1.698	1.135

Figure 7. Heat and material balance in Hybrid Gasification Process

Reactor Performance During Rapid-Rate Hydrogasification of Subbituminous Coal

Michael Epstein, Tan-Ping Chen, and Mohamed A. Ghaly

Bechtel National, Inc.
50 Beale Street
San Francisco, CA 94105

INTRODUCTION

In rapid-rate coal hydropyrolysis, pulverized coal particles are contacted with hot, high-pressure hydrogen for a short period of time. Typical conditions include temperatures of 1,000°F to 2,000°F, hydrogen partial pressures of 500 to 3,000 psi, and particle residence times of 0.05 to 5 seconds. Reaction products are primarily methane, with smaller amounts of ethane, benzene and its derivatives, light oils, and carbon-oxides. Agglomeration of caking coals is avoided by rapidly heating the coal particles at rates in excess of 50,000°F/sec to reaction temperature.

Rapid-rate coal hydropyrolysis involves a number of complex chemical and transport phenomena which are not well understood. These phenomena include devolatilization of the solid coal, hydrogenation of reactive volatile matter, hydrogenation of char, diffusion of volatile matter from the coal particles, and intrusion of hydrogen to stabilize the reactive volatiles or react with the active char.[1] Excellent reviews of the subject have been presented by Anthony and Howard[2] and by Pyrcioch et al.[3]

For the past several years, a number of studies have been conducted on the rapid-rate hydropyrolysis of various rank coals. These studies have included laboratory-scale experiments at CUNY;[4] bench-scale experiments at Pittsburgh Energy Research Center (PERC),[5] Cities Service,[6] and Brookhaven National Laboratory;[7] and small pilot-scale experiments at Rocketdyne.[8] Some of these studies have emphasized the production of both gas and liquid products (hydropyrolysis or hydrogenation); others have emphasized the production of only gas (hydrogasification).

Bechtel Corporation has conducted a program for the DOE (Contract EF-77-A-01-2565) to investigate the operability potential and scaleup feasibility of the Cities Service, Rocketdyne, PERC, and Brookhaven coal hydrogasification processes, relating to DOE plans for a hydrogasification process development unit (PDU). As part of the program objective, Bechtel has (1) collected bituminous, subbituminous, and lignite coal hydrogasification data from Rocketdyne, Cities Service, PERC, and Brookhaven, (2) performed a reactor model study for each of the processes, and (3) developed a conceptual full-scale hydrogasification reactor design for converting subbituminous coal to SNG. As part of the reactor model study, semiempirical correlations for predicting overall carbon conversion and carbon conversion to gaseous products have been fitted to the data. Results of the Bechtel program will be presented in a future publication.[9]

This paper presents (1) results of the reactor model study for the hydrogasification of subbituminous coal in the Rocketdyne and Cities Service reactor systems and (2) the design basis for a full-scale subbituminous coal hydrogasifier.

ROCKETDYNE AND CITIES SERVICE SUBBITUMINOUS COAL DATA

Bechtel has collected data from 12 Rocketdyne and 42 Cities Service hydrogasification tests using Montana Rosebud subbituminous coal feed. The data have been entered into a computerized data base for ease of evaluation and tabulation. A computer listing of all of the data contained in the data base will be presented in a future publication.[9] The Rocketdyne and Cities Service test programs were sponsored by the DOE under Contract EX-77-C-01-2518.

The Rocketdyne tests were conducted in an entrained-downflow tubular reactor system designed to feed coal at up to 1/4-ton/hr with coal fluxes to 20,000 lb/hr/ft^2. Coal particles and hot (1,500°F to 3,000°F) hydrogen gas are mixed inside a high-efficiency injector element, which produces coal heatup rates in excess of 200,000°F/sec. The hydrogen gas is heated first in a fired heat exchanger, then by partial combustion through oxygen addition in a preburner. A more detailed description of the reactor system has been given by Oberg, et al.[8]

The Rocketdyne tests were conducted at reactor outlet gas temperatures of 1,420°F to 1,900°F, particle (or gas)* residence times of 530 to 1,730 milliseconds, reactor pressures of 1,000 to 1,500 psig, and hydrogen-to-coal ratios of 0.33 to 0.71 lb/lb. The mass median coal particle size was approximately 45 microns. Overall carbon conversion for the tests ranged from 28 to 47 percent; carbon selectivity to gas ranged from 50 to 100 percent; and carbon selectivity to methane ranged from 25 to 87 percent. The maximum carbon conversion of 47 percent, carbon selectivity to gas of 100 percent, and carbon selectivity to methane of 87 percent were obtained at a reactor temperature of 1,760°F, a particle residence time of 1,420 milliseconds, and a hydrogen partial pressure of 1,390 psig.

The Cities Service bench-scale system incorporates an entrained-downflow tubular reactor system that is designed to feed coal at up to 5 lb/hr with coal fluxes to 15,000 lb/hr/ft^2. Preheated hydrogen and coal are mixed inside a high-velocity coaxial injector nozzle to produce coal heating rates in excess of 100,000°F/sec. The mixture then passes through the reactor tube, which is electrically heated through the walls to maintain adiabatic operation. An injected stream of cryogenically cooled hydrogen at the reactor outlet quenches the reaction. The tests employed a number of helical and vertical reactor tubes designed to accommodate the desired residence times and feed flow rates. A more detailed description of the reactor system has been given by Greene.[6]

The Cities Service subbituminous tests were conducted at reactor outlet gas temperatures of 1,500°F to 1,750°F, particle (or gas) residence times of 303 to 3,510 milliseconds, reactor pressures of 500 to 1,600 psig, and hydrogen-to-coal ratios of 0.74 to 1.4 lb/lb. The mass median coal particle size was approximately 45 microns. Overall carbon conversion ranged from 26 to 55 percent; carbon selectivity to gas ranged from 59 to 84 percent; and carbon selectivity to methane ranged from 18 to 59 percent. The maximum carbon conversion of 55 percent was obtained at a gas temperature of 1,610°F, a residence time of 3,160 milliseconds, and a pressure of 1,600 psig.

Greene[10] has presented a series of plots for the Cities Service subbituminous data. These plots revealed that at larger residence times carbon conversion increases with increasing pressure, and at smaller residence times carbon conversion decreases with increasing pressure. The plots also showed that temperature and pressure interacted in the same manner as residence time and pressure. Greene has postulated that this reversal effect of pressure with residence time suggests a two-step mechanism for carbon conversion: pyrolysis-controlled devolatilization at short residence time, and pressure-controlled hydrogenation of char at longer residence time.

PROPOSED REACTOR MODEL

Rapid hydropyrolysis of coal is an extremely complex process, which involves a number of reversible heterogeneous and homogeneous reactions.[2,3] Coal (or carbon) conversion kinetics during rapid devolatilization and subsequent hydrogenation are not well understood, and a majority of the models developed to correlate carbon conversion data have been more or less empirical. The principal correlative tool in most

---

* For a majority of the Rocketdyne and Cities Service entrained-downflow reactor tests, particle and gas residence times are nearly identical.

studies has been a simple first-order kinetic model for the irreversible reaction $C + 2H_2 \rightarrow CH_4$. An integration of this simple model, assuming the Arrhenius form for the reaction rate constant, gives:

$$X = 1 - \exp\left[-k_o \exp(-E/RT) P_{H_2} t_R\right] \quad (1)$$

where,

X = weight fraction overall carbon conversion
k_o = forward reaction rate frequency factor
E = activation energy
R = gas constant
T = reaction temperature
P_{H_2} = hydrogen partial pressure
t_R = particle (or gas) residence time

The above model, however, has not satisfactorily correlated data from different sources, where pressure, residence time, hydrogen-to-coal ratio, coal particle size, or coal type have differed markedly.[2]

Bechtel has proposed the following model for correlating overall carbon conversion to the operating variables:

$$X = X^* \left[1 - \exp(-\psi)\right] \quad (2)$$

with

$$\psi = \alpha_1 (t_R)^{\alpha 2} \exp(\alpha_3 P_{H_2}) \exp(\alpha_4 P_{H_2}/t_R) \exp(\alpha_5 P)$$
$$\exp(\alpha_6 H/C) \exp(-\alpha_7/T_G) \exp(-\alpha_8 P_{H_2}/T_G) (X^*)^{\alpha 9} \quad (3)$$

where,

X^* = weight fraction overall carbon conversion at equilibrium, i.e., at infinite residence time
ψ = fitted function of independent (operating) variables
$\alpha_1, \alpha_2, \ldots \alpha_9$ = fitted coefficients
P = total pressure
H/C = hydrogen-to-coal ratio
T_G = maximum reactor gas temperature

The coefficients, α_1 through α_9, have been fitted to the data using a computerized multiple-regression statistical analysis. The interaction terms, P_{H_2}/t_R and P_{H_2}/T_G, have been included in the model to account for the reversal effect of pressure with residence time and temperature reported by Greene.[10] Mean coal particle diameter was not included in the model, since particle size was not varied during the testing.

The proposed model, which consists of an equilibrium component, X^*, and a kinetic component, $[1-\exp(-\psi)]$, satisfies a number of boundary constraints. For example, as residence time or temperature approaches zero, conversion approaches zero, and as residence time approaches infinity, conversion approaches the equilibrium conversion limit, X^*.

The form of Equations 2 and 3 has been influenced by the similar form of an integrated, first-order kinetic model for the reversible homogeneous reaction $A \rightleftarrows B$, where one mole of reactant produces one mole of product. The analytical expression for conversion of A to B for this reaction, assuming the Arrhenius form for the forward rate constant, is:

$$X_A = X_A^* \left\{ 1 - \exp\left[-(k_o/X_A^*) \exp(-E/RT) t_R \right] \right\} \quad (4)$$

with

$$X_A^* = k_1/(k_1 + k_2) = K/(1 + K) \quad (5)$$

where,

X_A = weight fraction carbon conversion of species A
X_A^* = weight fraction carbon conversion of species A at equilibrium
k_1 = forward reaction rate constant
k_2 = reverse reaction rate constant
K = equilibrium constant

The proposed model has also been used to correlate the available data for carbon conversion to gas and methane, as follows:

$$X_G = X_G^* \left[1 - \exp(-\psi_G) \right] \quad (6)$$

$$X_M = X_M^* \left[1 - \exp(-\psi_M) \right] \quad (7)$$

where,

X_G, X_M = weight fraction carbon conversion to gas and to methane, respectively
X_G^*, X_M^* = weight fraction carbon conversion to gas and to methane at equilibrium, respectively
ψ_G, ψ_M = fitted functions of independent variables (assumed to have same form as ψ in Equation 3).

PREDICTION OF EQUILIBRIUM CARBON CONVERSION

Owing to the complexity of coal hydropyrolysis, a thermodynamic equilibrium computer model, PEP[11] (Propellant Evaluation Program), has been used to predict the thermodynamic equilibria for the test data. PEP considers a reaction system of carbon (β-graphite), hydrogen, oxygen, and hydrocarbon gases within a temperature and pressure range normally encountered in coal hydropyrolysis.

At a given temperature, pressure, and relative weights of initial reactants, PEP predicts the concentration of species that appear in significant amounts at equilibrium. For the operating range used in the hydrogasification reactor systems, the results from PEP indicate that methane is the major hydrocarbon product present at equilibrium. Higher hydrocarbon products, such as ethane, ethylene, or benzene, are present only in trace amounts. PEP also predicts that significant quantities of CO and CO_2 can be present in the gas phase at equilibrium. Note that for these conditions the equilibrium overall carbon conversion, X^*, and the equilibrium conversion to gas, X_G^*, are equal.

In Figure 1, predicted equilibrium conversions for the subbituminous coal are shown as a function of reaction temperature and hydrogen-to-coal ratio, at a reactor pressure of 1,500 psig. As expected, X^* increases with decreasing temperature (the overall reaction is exothermic) and with increasing hydrogen-to-coal ratio. Since there are fewer product gas moles than reactant gas moles during hydropyrolysis, X^* (or X_G^*) will increase with increasing pressure. Similarly, predicted values for equilibrium conversion to methane for the subbituminous coal are shown in Figure 2 as a function of temperature and hydrogen-to-coal ratio at 1,500 psig.

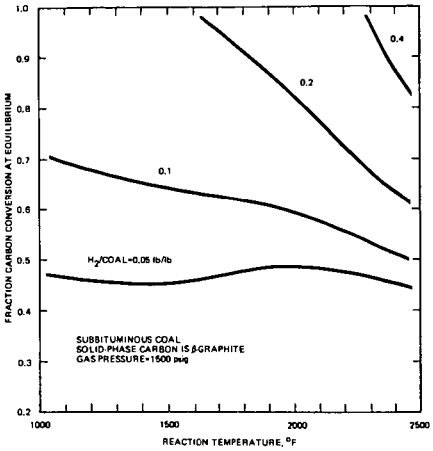

Figure 1. Predicted Fraction Carbon Conversion at Equilibrium for Subbituminous Coal

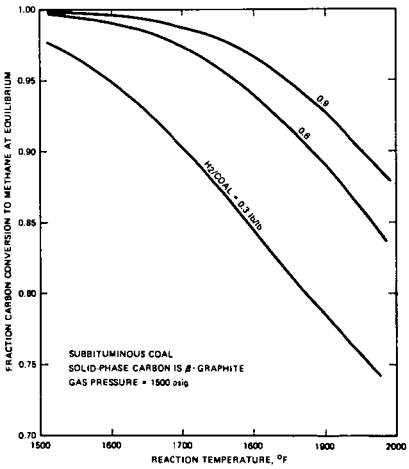

Figure 2. Predicted Fraction Carbon Conversion to Methane at Equilibrium for Subbituminous Coal

PEP predicts an equilibrium overall fraction carbon conversion and conversion to gas of unity for all of the Rocketdyne and Cities Service subbituminous tests; i.e., at infinite residence time, all of the carbon in the coal would be converted to methane and carbon-oxides. This is due primarily to the high levels of hydrogen-to-coal ratio, which varied from about 0.33 to 1.4 lb/lb (see Figure 1). PEP also predicts that the equilibrium fraction of carbon converted to methane is nearly unity for a majority of the Rocketdyne and Cities Service subbituminous tests (see Figure 2). For these conditions, Equations 2, 3, 6, and 7 simplify, with $X^* = X_G^* = X_M^* = 1$. The subbituminous data, therefore, were generated within a regime that is completely controlled by the kinetics of carbon conversion to products.

As mentioned previously, PEP assumes that the carbon present is β-graphite. Other studies[12,13] have indicated that the carbon present at equilibrium may be amorphous carbon, which has a higher reactivity than β-graphite. Therefore, the predictions of X^* and X_M^* shown in Figures 1 and 2 should be considered as approximate, and possibly on the low side.

FITTED CORRELATIONS

A statistical analysis of the fitted Rocketdyne and Cities Service subbituminous coal data showed that overall carbon conversion and carbon conversion to gas and methane were significant functions of gas temperature, particle (or gas) residence time, and hydrogen partial pressure. Carbon conversion was not significantly affected by reactor size or hydrogen-to-coal ratio within the region investigated.

As mentioned previously, the equilibrium computer model predicts that X^*, X_G^*, and X_M^* have values of unity for all of the subbituminous tests. Therefore, the effect of equilibrium conversion on the kinetic components of Equation 2, 6, or 7 could not be obtained from the data; i.e., the value for the fitted coefficient α_9 in Equation 3 could not be determined. Similarly, it was not possible to verify the predicted effect (illustrated in Figures 1 and 2) of hydrogen-to-coal ratio on the equilibrium conversions. Additional data are required at reduced hydrogen-to-coal ratio (0.1 to 0.3 lb/lb) to determine these effects.

It was also not possible to determine separately the effects of both hydrogen partial pressure, P_{H_2}, and reactor pressure, P, on carbon conversion for the subbituminous tests. This is because P_{H_2} was nearly equal to P for a majority of the tests; i.e., P_{H_2} and P are confounded. For convenience, the pressure variable is referred to as pressure or hydrogen partial pressure in this report. It should be noted that the separate effects of P_{H_2} and P could be determined by adding an inert gas (e.g., helium) and/or methane to the reactor recycle (feed) gas.

Overall Carbon Conversion

The correlation fitted to the Rocketdyne and Cities Service subbituminous coal carbon conversion data is:

$$X = 1 - \exp\left[-2.53 \exp(-0.175\, P_{H_2}/t_R) \exp(0.000393\, P_{H_2}) \exp(-3{,}820/T_G)\right] \quad (8)$$

where P_{H_2} is in psig, t_R is in milliseconds, and T_G is in $^{\circ}R$.

As Equation 8 indicates, X increases with increasing coal particle residence time and gas temperature. At high particle residence times, X increases with increasing hydrogen partial pressure; at low particle residence times, X decreases with increasing hydrogen partial pressure. In addition, the effect of residence time on carbon conversion increases as pressure increases. The fact that overall carbon conversion

increases with residence time suggests that conversion of carbon to products occurs throughout the length of the reactor.

Equation 8 has a standard error of estimate of 3.3 percent in the predicted percent carbon conversion. The measured and predicted carbon conversions are shown in Figure 3. The statistics and Figure 3 indicate that within the experimental error, the Cities Service bench-scale reactor and the Rocketdyne 1/4-ton/hr reactor achieve similar carbon conversions under comparable operating conditions.

As can be seen in Figure 3, the predictions of carbon conversion for the Rocketdyne reactor are, on the average, slightly higher than the measured values, whereas the predictions for the Cities Service reactor are, on the average, slightly lower than the measured values. With the data currently on hand, it is not possible to determine whether or not this discrepancy can be accounted for by (1) differences in the reactor sizes, (2) differences in the reactor operating conditions (e.g., the Rocketdyne feed gas contains water vapor), (3) differences in the accuracy of the values for maximum gas temperature, or (4) differences in the average levels of the hydrogen-to-coal ratio employed in the reactor systems.

In Figure 4, predicted overall carbon conversion from Equation 8 is plotted as a function of maximum gas temperature for selected levels of residence time and hydrogen partial pressure.

Carbon Conversion and Selectivity to Gas

The correlation fitted to the data for carbon conversion to gas is:

$$X_G = 1 - \exp\left[-0.277 \exp(-0.178\, P_{H_2}/t_R) \exp(0.00358\, P_{H_2}) \exp(-6.57\, P_{H_2}/T_G)\right] \quad (9)$$

where P_{H_2} is in psig, t_R is in milliseconds, and T_G is in ^{o}R.

As can be seen from Equation 9, X_G increases with increasing residence time and gas temperature. At high residence time and/or at high temperature, X_G increases with increasing hydrogen partial pressure; at low residence time and/or at low temperature, X_G decreases with increasing hydrogen partial pressure. In addition, the effects of residence time and gas temperature on conversion increase as hydrogen partial pressure increases.

Equation 9 has a standard error of estimate of 3.0 percent in the predicted percent carbon conversion to gas. The measured and predicted conversions are shown in Figure 5. The statistics and Figure 5 indicate that the Cities Service bench-scale reactor and the Rocketdyne 1/4-ton/hr reactor achieve similar carbon conversions to gaseous products under comparable operation conditions within the region investigated.

In Figure 6, predicted values for carbon selectivity to gas, Φ_G, obtained from Equations 8 and 9 (i.e., $\Phi_G = X_G/X$) are shown as a function of gas temperature, for selected values of hydrogen partial pressure at a residence time of 1,000 milliseconds. Selectivity to gas is very insensitive to residence time for the subbituminous coal data. Note that a selectivity to gas of 100 percent is predicted at 1,900°F and 1,500 psig.

Carbon Conversion and Selectivity to Methane

The correlation fitted to the data for carbon conversion to methane is:

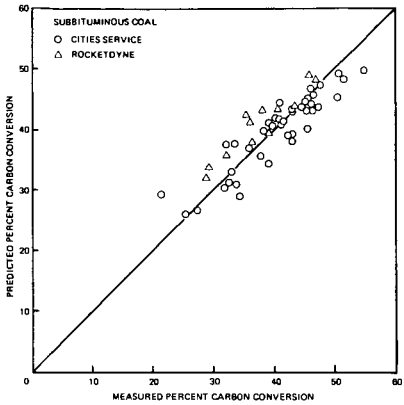

Figure 3. Comparison of Measured and Predicted Overall Carbon Conversion for Subbituminous Coal

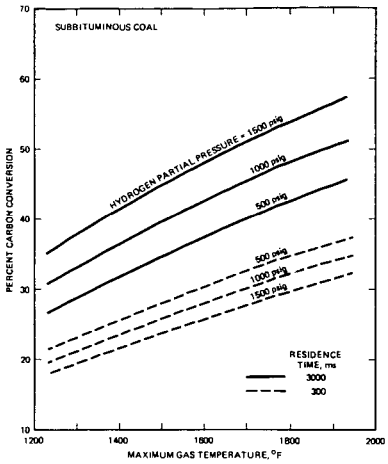

Figure 4. Predicted Overall Carbon Conversion for Subbituminous Coal

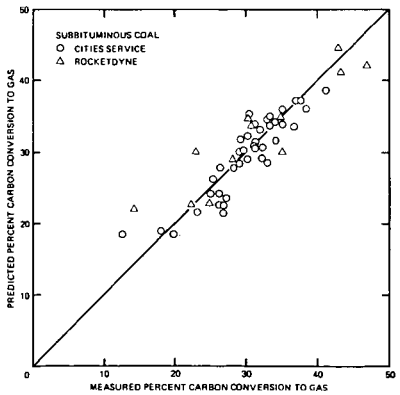

Figure 5. Comparison of Measured and Predicted Carbon Conversion to Gas for Subbituminous Coal

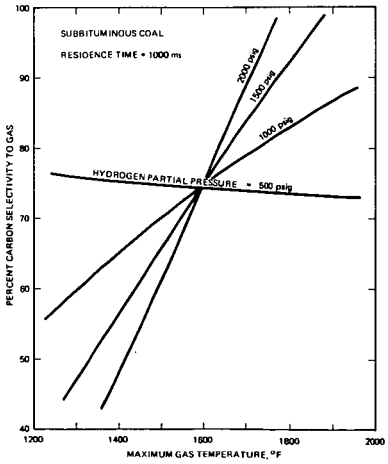

Figure 6. Predicted Carbon Selectivity to Gas for Subbituminous Coal

$$X_M = 1 - \exp\left[-0.125 \exp(-0.286\ P_{H_2}/t_R) \exp(0.00735\ P_{H_2}) \exp(-13.9\ P_{H_2}/T_G)\right] \quad (10)$$

where P_{H_2} is in psig, t_R is in milliseconds, and T_G is in ^{o}R.

As can be seen from Equation 10, X_M increases with increasing particle residence time and reaction temperature. At high residence time and/or at high temperature, X_M increases with increasing hydrogen partial pressure; at low residence time and/or at low temperature, X_M decreases with increasing hydrogen partial pressure. In addition, the effects of residence time and gas temperature on conversion increase as hydrogen partial pressure increases.

Equation 10 has a standard error of estimate of 2.6 percent in the predicted percent conversion. The measured and predicted conversions are shown in Figure 7. The statistics and Figure 7 indicate that the Cities Service bench-scale reactor and the Rocketdyne 1/4-ton/hr reactor achieve similar carbon conversions to methane under comparable operating conditions within the region investigated.

In Figure 8, predicted values for carbon selectivity to methane, Φ_M, obtained from Equations 8 and 10 (i.e., $\Phi_M = X_M/X$) are shown as a function of gas temperature for different levels of residence time and hydrogen partial pressure. The fact that carbon selectivity to methane increases with increasing residence time suggests that the initial higher hydrocarbon products of devolatilization and, perhaps, products of direct char hydrogenation are cracked down to methane as gas residence time increases.

Comparison Between Predicted Values for Carbon Conversion and Carbon Selectivity to Products

In Figures 9 and 10, predicted carbon conversion to products and predicted carbon selectivity to products are shown, respectively, as functions of gas temperature for a particle residence time of 1,000 milliseconds, a hydrogen partial pressure of 1,500 psig, and a hydrogen-to-coal ratio of 0.7 lb/lb. It should be noted that above about 1,700°F, the predicted value for X_M^* drops below unity at the selected operating variable levels (see Figure 2). Above 1,700°F, therefore, the values for X_M shown in Figures 9 and 10 were obtained from Equation 7 using the calculated kinetic component from Equation 10 and the predicted equilibrium component from Figure 2.

DESIGN BASIS FOR CONCEPTUAL FULL-SCALE HYDROGASIFICATION REACTOR

This section presents the conceptual design basis for the hydrogasification stage of a proposed full-scale reactor facility for converting subbituminous coal to SNG. As currently envisioned, the reactor facility will consist of a hydrogasification stage to produce methane-rich product gas from the coal, and a hydrogen production stage to produce hydrogen-rich product gas from unreacted char and coal.

The conceptual full-scale hydrogasification stage will have a configuration similar to the Rocketdyne and Cities Service reactor assemblies, which incorporate entrained-flow tubular reactor chambers. The operating levels for temperature, pressure, and residence time have been based on predictions from the semiempirical correlations, which have been fitted to the Rocketdyne and Cities Service subbituminous coal data. The selected and calculated operating parameters are:

Overall carbon conversion	50 percent
Carbon selectivity to gas	100 percent
Reactor pressure	1,500 psig
Maximum reactor gas temperature	1,875°F
Particle (or gas) residence time	1,100 milliseconds
Carbon selectivity to methane	86 percent

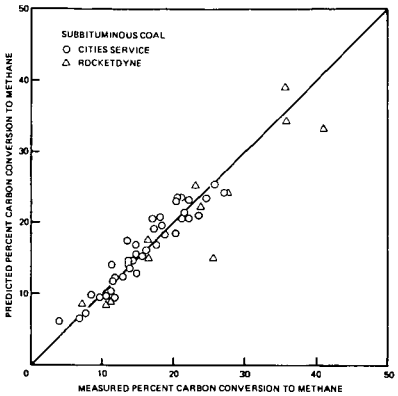

Figure 7. Comparison of Measured and Predicted Carbon Conversion to Methane for Subbituminous Coal

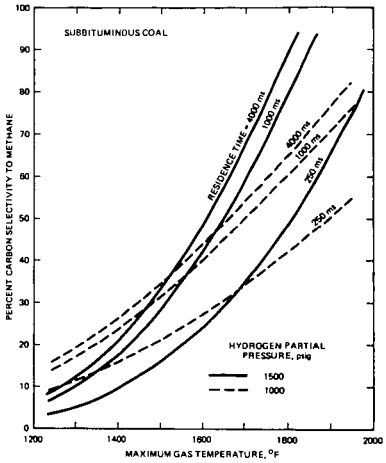

Figure 8. Predicted Carbon Selectivity to Methane for Subbituminous Coal

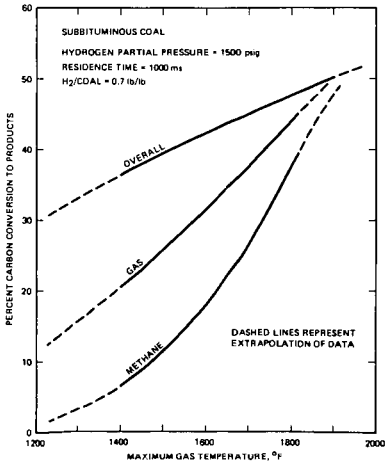

Figure 9. Predicted Carbon Conversion to Products for Subbituminous Coal

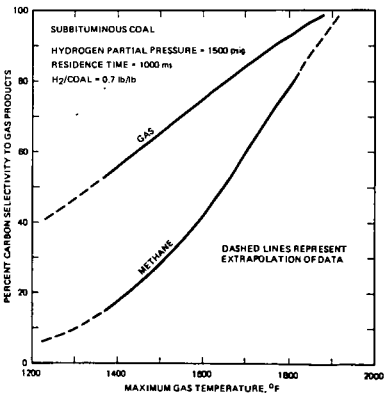

Figure 10. Predicted Carbon Selectivity to Gas Products for Subbituminous Coal

Greene[14] has shown that the cost of SNG produced from the reactor facility decreases as carbon conversion in the hydrogasification stage increases past the char balance point. (At the char balance point, the quantity of unreacted char from the hydrogasification stage is just sufficient to produce the required process hydrogen in the hydrogen production stages.) An overall carbon conversion of 50 percent was selected as the reactor design basis, since that value is close to the maximum conversion obtained to date in the Cities Service and Rocketdyne subbituminous coal testing, and is above the char balance point.

A carbon selectivity to gas of 100 percent was selected as the reactor design basis by the DOE. A reactor design pressure of 1,500 psig was chosen because at pressures less than 1,500 psig, the predicted maximum reaction temperature required for 100 percent carbon selectivity to gas is greater than 1,900°F (see Figure 6 and Equations 8 and 9). Temperatures greater than 1,900°F are considered excessive and are outside the range of the Cities Services and Rocketdyne subbituminous coal testing.

The selected hydrogen-to-coal ratio of 0.4 lb/lb is within the lower range investigated by Rocketdyne. A maximum gas temperature, T_G, of 1,875°F was calculated for the condition of 100 percent carbon selectivity to gas at a pressure of 1,500 psig. For the calculation, the predicted value for overall conversion (Equation 8) was equated to the predicted value for conversion to gas (Equation 9). Note that selectivity to gas is insensitive to residence time (see Figure 6).

A particle (or gas) residence time, t_R, of 1,100 milliseconds was computed, using Equation 8, for the condition of 50 percent overall carbon conversion, at a pressure of 1,500 psig and a temperature of 1,875°F.

The value of carbon selectivity to methane of 86 percent was obtained by dividing the predicted value for conversion to methane, X_M, by the predicted value for overall conversion, X, at a gas temperature of 1,875°F, a residence time of 1,100 milliseconds, and a pressure of 1,500 psig. The predicted value of X was obtained from Equation 8 and the predicted value of X_M from Equation 7. The kinetic component of Equation 7 was obtained from Equation 10 and the equilibrium component, X_M^*, is from Figure 2. It should be noted that for this relatively low hydrogen-to-coal ratio and relatively high temperature, X_M^* is approximately 0.86.

Bechtel has fitted carbon conversion to CO and CO_2 to the Rocketdyne and Cities Service data.[9] At the specified levels of the operating variables, the predicted values for carbon selectivity to CO and CO_2 were 13 and 0 percent, respectively.

CONCLUSIONS

The developed subbituminous coal correlations show that the Cities Service bench-scale reactor and the Rocketdyne 1/4-ton/hr reactor achieve similar values of overall carbon conversion and carbon selectivity to gaseous products under comparable operating conditions. Therefore, the results of testing at Rocketdyne and Cities Service should be scalable to a PDU or commercial-size reactor, within the region investigated.

The fitted correlations indicate that overall carbon conversion increases with increasing coal particle residence time and gas temperature. At high particle residence times, conversion increases with increasing hydrogen partial pressure; at low particle residence times, conversion decreases with increasing hydrogen partial pressure. This increase in overall carbon conversion with residence time suggests that conversion of carbon to products occurs throughout the length of the reactor. The reversal effects of pressure on carbon conversion suggests a two-step mechanism for hydrogasification: pyrolysis-controlled devolatilization at short residence time, and pressure-controlled hydrogenation of char at longer residence time.

The fitted correlations also indicate that carbon selectivity to methane increases with increasing temperature and particle residence time. The increase in selectivity to methane with increasing residence time suggests that the initial higher hydrocarbon products of devolatilization and, perhaps, the products of direct char hydrogenation are cracked down to methane as residence time increases.

The Rocketdyne and Cities Service subbituminous data were generated within a regime that is controlled by the kinetics of carbon conversion to products. This is due primarily to the relatively large hydrogen-to-coal ratios (0.3 to 1.4 lb/lb) used in the testing. For these hydrogen-to-coal ratios, the predicted carbon conversion at equilibrium is 100 percent for all tests; i.e., at infinite residence time, all of the carbon in the coal would be converted to methane and carbon-oxides.

REFERENCES

1. Russel, W. B., Saville, D. A., and Greene, M. I. "The Cities Service Model for Short Residence Time Hydropyrolysis of Coal," presented at the AIChE 70th Annual Meeting, New York City (November 1977).
2. Anthony, D. B. and Howard, J. B. "Coal Devolatilization and Hydrogasification," AIChE J., Vol. 22, No. 4, p. 625 (1976).
3. Pyrcioch, E. J., et al. "Production of Pipeline Gas by Hydrogasification of Coal," Research Bulletin No. 39, Vol. 1, Inst. Gas Tech., Chicago, Ill. (December 1972).
4. Graff, R. A., Dobner, S., and Squires, A. M. "Flash Hydrogenation of Coal," Fuel, Vol. 55, p. 109 (April 1976).
5. Feldman, H. F., Mima, J. A., and Yavorsky, P. M. "Pressurized Hydrogasification of Raw Coal in a Dilute-Phase Reactor," ACS Adv. Chem. Ser. No. 131, p. 108 (1974).
6. Greene, M. I. "Engineering Development of the Cities Service, Short Residence Time (CS-SRT) Process," presented at the ACS 174th National Meeting, Chicago (September 1977).
7. Fallon, P., and Steinberg, M. "Flash Hydropyrolysis of Coal," presented at the ACS 173rd National Meeting, New Orleans (March 1977).
8. Oberg, C. L., Falk, A. Y., Hood, G. A., and Gray, J. A. "Coal Liquefaction Under High-Mass Flux and Short-Residence Time Conditions," Ibid.
9. Bechtel Corporation, "An Analysis of Coal Hydrogasification Processes," Final Report, DOE Contract EF-77-A-01-2565 (to be published).
10. Combs, L. P. and Greene, M. I. "Hydrogasifier Development for the Hydrane Process," Monthly Progress Report, January 1978, DOE Contract EX-77-C-01-2518 (February 1978).
11. Cruise, D. R. "Notes on the Rapid Computation of Chemical Equilibria," Propulsion Development Department, U.S. Naval Ordnance Test Station, China Lake, California (1964).
12. Moseley, F. and Paterson, D. "The Rapid High-Temperature Hydrogenation of Coal Chars — Part 2: Hydrogen Pressures Up to 1000 Atmospheres," J. Inst. Fuel, Vol. 38, No. 296, p. 378 (September 1965).
13. Stephens, D. R. and Miller, D. C. "Thermodynamic Equilibrium for Wyoming Coal: New Calculations," Lawrence Livermore Laboratory, UCID-17044 (February 24, 1976).
14. Combs, L. P. and Greene, M. I. "Hydrogasifier Development for the Hydrane Process," Monthly Progress Report, March 1978, DOE Contract EX-77-C-01-2518 (April 1978).

ACKNOWLEDGMENT

The work presented in this paper was sponsored by the DOE, Washington, D.C., under Contract No. EF-77-A-01-2565. The authors wish to express appreciation for technical support provided by L. Jablansky (DOE Technical Project Officer), M. I. Greene (Cities Service), J. A. Gray (PERC), and J. Friedman and L. P. Combs (Rocketdyne).